

DEVELOPMENT OF MICELLAR PHASES AND
CAPILLARY COLUMNS FOR HIGH
PERFORMANCE CAPILLARY
ELECTROPHORESIS

By

JOEL TIMOTHY SMITH

Bachelor of Science

Southeastern Oklahoma State University

Durant, Oklahoma

1990

Submitted to the Faculty of the
Graduate College of the
Oklahoma State University
in partial fulfillment of
the requirements for
the Degree of
DOCTOR OF PHILOSOPHY
July, 1994

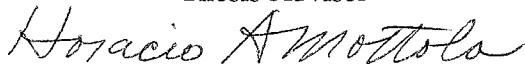
Thesis
1994D
5651d

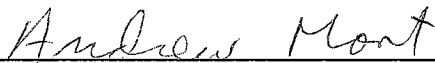
DEVELOPMENT OF MICELLAR PHASES AND
CAPILLARY COLUMNS FOR HIGH
PERFORMANCE CAPILLARY
ELECTROPHORESIS

Thesis Approved:

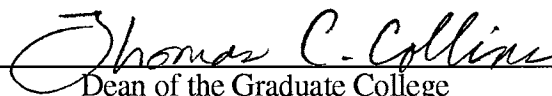


Thesis Adviser








Dean of the Graduate College

ACKNOWLEDGEMENTS

Completion of this work was made possible by the contributing efforts of several people to whom I am deeply indebted. First, I wish to thank my thesis advisor, Dr. Ziad El Rassi, for his guidance and encouragement offered generously through out this study. Through his leadership, I truly have learned that hard work pays off in the end. I would also like to extend my sincere appreciation to my committee members, Dr. Horacio A. Mottola, Dr. K. Darrell Berlin and Dr. Andrew Mort for their support and valuable suggestions.

I would like to thank the University Center for Water Research at OSU for supporting me with a fellowship over the last three years. I could not have finished in this time frame if it had not been for their continued financial support.

I appreciate the encouragement and support from the many close friends I have made at OSU over the years. Among these include: Lloyd Sumner, Paul West, Jeff Archer, Edralin Lucas, Shawn Childress, Curtis Schilling, Dr. Richard Bunce, Wassim Nashabeh, John Schemanaur, Greg Garrison, Shanker Subramanian and Matora Madler as well as many others. I will always remember the trips to Joe's, my attempts at golf, the racquetball games, and a few other things that made life more enjoyable at OSU. A special thank you goes out to Yehia Mechref for the for his help with my thesis, but more importantly for being a good friend. Yehia, I hope that you and Rita have a wonderful life together.

I would like to thank my wife, Gina, for being my best friend for the last four years. I greatly appreciate strength, love and understanding (for the long hours spent in the lab and so little time spent with her) which you have given to me. I will try my best to

make up for the lost time in the future. I thank the Lord every day for bringing us together. I love you now and always will. Thank you so much.

I would like to dedicate this small portion of my life's work to my parents, Bobby and LaWanda Smith. Thank you for the love and support that you have given me over the years. I will always be thankful for the values that you have instilled in me. I am honored to be your son and will always remember where home is, no matter where I am.

Finally, I would like to thank the Lord for the opportunities he has given. I pray that I will use my education to best serve you throughout this life.

TABLE OF CONTENTS

Chapter	Page
I. INTRODUCTION TO HIGH PERFORMANCE CAPILLARY ELECTROPHORESIS	
Introduction	1
Historical Background	3
Instrumentation	5
Modes of CE	9
Basic Concepts of CE	11
References	19
 II. SOME ASPECTS OF CAPILLARY ZONE ELECTROPHORESIS OF BIOPOLYMERS	
Introduction	22
Analytical Parameters in CZE	23
Solute-wall Interactions	26
Elimination of Solute-wall Interactions.....	28
Extreme pH Buffers	28
High Concentration Buffers	29
Amine Modifiers	30
Dynamically Coated Capillaries	30
Functionalized Capillaries	32
Objective and Rationale of Part I of the Dissertation	36
References	38
 III. CAPILLARY ZONE ELECTROPHORESIS OF BIOLOGICAL SUBSTANCES WITH SURFACE MODIFIED FUSED SILICA CAPILLARIES HAVING SWITCHABLE ELECTROOSMOTIC FLOW	
Abstract	41
Introduction	42
Experimental	44
Instrumental	44
Materials	44
Sugar Derivatization	45
Capillary Modification	45
Results and Discussion	46
Surface Modification	46
Electroosmotic Flow.....	48
Evaluation of the Surface Modification with Charged Species	51

Chapter	Page
Nucleotides	51
Proteins	53
Acidic Oligosaccharides	56
References	60

IV. CAPILLARY ZONE ELECTROPHORESIS OF BIOLOGICAL SUBSTANCES WITH FUSED SILICA CAPILLARIES HAVING ZERO OR CONSTANT ELECTROOSMOTIC FLOW

Abstract	62
Introduction	63
Experimental	65
Reagents and Materials	65
Capillary Electrophoresis Instrument	66
Alkylation of Polyethyleneimine Hydroxyethylated	67
Modification of the Capillary Surface	67
Zero Flow Coatings	67
Variable Anodal Flow Coating of	
Type VAF-1	69
Constant Anodal Flow Coating of	
Type CAF-1	69
Anodal Flow Coatings of Types	
VAF-2 and CAF-2	70
Results and Discussion	70
Alkylation of PEIHE	70
Surface Modifications	71
ZF Capillaries	73
Capillaries with Anodal Flow of	
Type VAF-1	73
Capillaries with Anodal Flow of	
Type CAF-1	74
Capillaries with Anodal Flow of	
Types VAF-1 and CAF-2	75
Electroosmotic Flow	75
Evaluation of Surface Modified Capillaries in CZE	
of Biological Substances	80
ZF Capillaries	81
Capillaries with Variable Anodal Flow of	
Type VAF-1	84
Capillaries with Constant Anodal Flow of	
Type CAF-1	91
Capillaries with Variable Anodal Flow of	
Type VAF-2	91
Capillaries with Constant Anodal Flow of	
Type CAF-2	94
Conclusion	94
References	96

V. SOME BASIC ASPECTS OF MICELLAR ELECTROKINETIC CAPILLARY CHROMATOGRAPHY

Chapter	Page
Introduction	98
Basic Concepts	98
Fundamental Equations	99
Operational Aspects of MECC	104
Manipulation of the Capacity Factor and Selectivity	105
Manipulation of the Migration Time Window	109
Chiral Separations in MECC	110
Rationale and Scope of Part II of the Dissertation	111
References	113

VI. MICELLAR ELECTROKINETIC CAPILLARY
 CHROMATOGRAPHY WITH *IN SITU* CHARGED
 MICELLES I. EVALUATION OF *N-D-GLUCO-N-*
 METHYLALKANAMIDE SURFACTANTS AS ANIONIC
 BORATE COMPLEXES

Abstract	116
Introduction	117
Principles of <i>In Situ</i> Charged Micelles and Some Aspects of Polyol-Borate Complexation	119
Experimental	126
Reagents and Materials	126
Instrument and Capillaries	126
Mass Spectrometry Measurements	127
NMR Measurements	128
Procedures	128
Results and Discussion	129
Evaluation of MEGA-Borate Complex Formation by Boron NMR and CF-LSIMS	129
Variable Migration Time Window	135
pH of the Running Electrolyte	135
Borate Concentration	137
Carbon Number in the Alkyl Tail of MEGA Surfactants	137
Retention Behavior of Neutral Solutes	140
Correlation Between Capacity Factor and Carbon Number of Homologous Series	140
Comparison of the Energetics of Retention on the Various Surfactants	143
Correlation Between Capacity Factor and Carbon Number of Surfactant	146
Dependence of Capacity Factor on Borate Concentration	147
Dependence of Capacity Factor on pH	149
Selected Separations	149
Herbicides	149
Aromatics	155
Barbiturates	155
Amino Acids	158
References	162

Chapter		Page
VII.	MICELLAR ELECTROKINETIC CAPILLARY CHROMATOGRAPHY WITH <i>IN SITU</i> CHARGED MICELLES II. EVALUATION AND COMPARISON OF OCTYLMALTOSIDE AND OCTANOYLSUCROSE SURFACTANTS AS ANIONIC BORATE COMPLEXES IN THE SEPARATION OF HERBICIDES	
	Abstract	166
	Introduction	167
	Experimental	169
	Reagents and Materials	169
	Instrument and Capillaries	170
	NMR Measurements	170
	Procedures	171
	Results and Discussion	172
	Evaluation of OS, OM and OG-Borate Complexation by Boron NMR	172
	Effect of pH	174
	Effect of Borate Concentration	177
	Effect of Surfactant Concentration	180
	Comparison of Retention Energetics	182
	Reproducibility	183
	Limits of Detection	184
	Applications of OS and OM	186
	Conclusions	192
	References	195
VIII.	MICELLAR ELECTROKINETIC CAPILLARY CHROMATOGRAPHY WITH <i>IN SITU</i> CHARGED MICELLES III. EVALUATION OF ALKYLGLUCOSIDE SURFACTANTS AS ANIONIC BUTYLBORONATE COMPLEXES	
	Abstract	197
	Introduction	198
	Some Aspects of Alkylglucoside-Boronate Micellar Phases	199
	Experimental	205
	Reagents and Materials	205
	Instrument and Capillaries	205
	NMR Measurements	206
	Procedures	206
	Results and Discussion	207
	Boron NMR Studies	207
	Electrochromatographic Behavior	210
	Influence of pH	210
	Effects of BBA Concentration	212
	Effects of BBA Concentration on the Electrochromatographic Behavior of Alkylglucoside-Borate Micelles	214
	Influence of the Surfactant Tail	220

Chapter		Page
	Effects of the Surfactant Concentration	223
	Applications	226
	Conclusions	231
	References	235
IX.	MICELLAR ELECTROKINETIC CAPILLARY CHROMATOGRAPHY WITH <i>IN SITU</i> CHARGED MICELLES IV. INFLUENCE OF THE NATURE OF THE ALKYLGLYCOSIDE SURFACTANT	
	Abstract	237
	Introduction	238
	Experimental	243
	Instrument	243
	Reagents	244
	Methods	244
	Results and Discussion	245
	Migration Time Window	245
	Efficiency and Peak Capacity	248
	Retention Energetics	249
	Selectivity	255
	Conclusions	262
	References	264

LIST OF TABLES

Table		Page
	Chapter II	
I.	Coated Capillaries for CZE	36
	Chapter IV	
I.	Summary of the EOF properties, coding and composition of the capillary coatings developed in this study	68
	Chapter V	
I.	Surfactants used in MECC	107
	Chapter VI	
I.	Correlation between Capacity Factor and Carbon Number of Homologous Series obtained on the various MEGA-Borate Micellar Phases	141
II.	Correlation between Capacity Factor and Carbon Number of Homologous Series at Various pHs	142
III.	Correlation between Capacity Factor and Carbon Number of Homologous Series at Various Borate Concentration	142
IV.	Slopes, Intercepts, <i>R</i> Values and Antilog of Intercepts of <i>logk'</i> – <i>logk'</i> Plots of Phenylalkyl alcohol and Alkylbenzene Homologous Series obtained on MEGA-Borate Surfactants	144
V.	Slopes, Intercepts, and <i>R</i> Values of Plots of <i>k'</i> vs <i>n_{c,surf}</i> for Alkylbenzenes, Phenylalkyl alcohols and Herbicides obtained with the Various MEGA Micellar Phases	147
	Chapter VII	
I.	<i>t₀</i> / <i>t_{mc}</i> , and <i>k'</i> as a Function of Electrolyte pH	176
II.	<i>n</i> , <i>N_{av}</i> and <i>k'</i> as a Function of Borate Concentration.	179
III.	<i>t₀</i> / <i>t_{mc}</i> , <i>n</i> and <i>N_{av}</i> as a Function of Concentration of OM	182

Table	Chapter VIII	Page
I.	$\mu_{ep(mc)}$, t_0/t_{mc} and N_{av} as a Function of BBA Concentration	212
II.	$\mu_{ep(mc)}$, t_0/t_{mc} and k' as a Function of BBA Concentration	215
III.	Correlation between $\log k'$ and n_c of Homologous Series at various BBA Concentration as an Additive	216
IV.	Slopes, Intercepts and Antilog of Intercepts of $\log k' - \log k'$ Plots for PAA and APK Homologous Series obtained with various Concentrations of the Additive BBA	219
V.	Slopes, Intercepts and Antilog of Intercepts of $\log k' - \log k'$ Plots for AB Homologous Series obtained with various Concentrations of BBA	219
VI.	Slopes, Intercepts and Antilog of Intercepts of $\log k' - \log k'$ Plots for PAA and APK Homologous Series obtained with different Alkylglucoside-borate Micelles	221
VII.	Slopes, Intercepts and Antilog of Intercepts of $\log k' - \log k'$ Plots for PAA and APK Homologous Series obtained with different Alkylglucoside-BBA Micelles	222
VIII.	t_0/t_{mc} and N_{av} as Function of OG Concentration	225
CHAPTER IX		
I.	Structures and CMCs of Surfactants used in our Studies	241
II.	Comparison of Migration Time Window, Mobility, Efficiency and Peak Capacity for the various Micellar Phases	246
III.	Comparison of Capacity Factors obtained with the various Micellar Phases	249
IV.	Correlation between $\log k'$ and n_c of APK Homologous Series for various Micellar Phases	252
V.	Slopes, Intercepts and Antilog of Intercepts of $\log k' - \log k'$ Plots for APK Homologous Series obtained with different Micellar Phases	253

LIST OF FIGURES

Figure	Page
Chapter I	
1. Instrument Set-up for Capillary Electrophoresis	6
2. Cross-sectional View of a Fused-silica Capillary	8
3. Illustrations of the Electrical Double Layer at the Surface of a Fused-Silica Capillary	14
4. Illustration of an Electrophoretic Separation in CE	17
Chapter II	
1. Schematic Representation of a Separation in CZE	25
2. Pictorial Representation of the Solute-wall Interactions	27
Chapter III	
1. Schematic Illustration of the Idealized Structure of the Coating of Switchable Flow Capillary	47
2. Plot of the Electroosmotic Flow obtained with the Switchable Flow Capillary versus pH	49
3. Electropherograms of Mono- and Diphosphate Nucleosides obtained with the Switchable Flow Capillary	52
4. Electropherograms of Basic Proteins obtained with the Switchable Flow Capillary	54
5. Plot of Migration Time versus Electrolyte pH for Basic Proteins obtained with the Switchable Flow Capillary	55
6. Electropherogram of 2-Aminopyridyl Derivatives of Oligogalacturonide Homologous Series obtained with the Switchable Flow Capillary	57
7. Plot of the logarithmic Migration Time of 2AP-(GalA) _n versus the logarithmic Degree of Polymerization	58

Chapter IV

1. Schematic Illustration of the Idealized Structures of the ZF, VAF-1 and CAF-2 coatings	72
2. Plots of Electroosmotic Mobility obtained with the VAF-1 and CAF-1 capillaries versus the pH	77
3. Plots of Electroosmotic Mobility obtained with the VAF-2 and CAF-2 capillaries versus the pH	79
4. Electropherograms of Basic Proteins obtained on ZF-1 and ZF-2 Capillaries	82
5. Plots of the Migration Time and average Plate Count in of Basic Proteins against pH obtained on the ZF-2 Capillary	83
6. Electropherograms of Acidic Proteins obtained on ZF-2 and CAF-2 Capillaries	85
7. Electropherograms of 2-Aminopyridyl Derivatives of Oligogalacturonic Acid Homologous Series obtained with ZF-1 and VAF-1 Capillaries	86
8. Plots of the Logarithm of Migration Time of 2AP-(GalA) _n against the Logarithm of the Degree of Polymerization obtained on the ZF-1 and VAF-1 capillaries	87
9. Electropherograms of Basic Proteins obtained on the VAF-1 and CAF-1 Capillaries	88
10. Electropherogram of Mono- and Diphosphate Nucleosides obtained on the VAF-1 capillary	90
11. Electropherogram of Crude Trypsin Inhibitor obtained on the VAF-2 capillary	92
12. Electropherogram of Acidic Peptides obtained on the CAF-2 Capillary	93

Chapter V

1. Schematic Illustration of the Separation Principle in MECC	100
2. Schematic of Zone Separation and the Resulting Chromatogram in MECC	101
3. Distribution of the Capacity Factor over the Migration Time Window	103

Figure	Page
--------	------

Chapter VI

1. Boron NMR Spectra of Surfactant-Borate Systems	130
2. Plots of Percentage of ^{11}B present in the MEGA 8-borate Mixtures versus MEGA:borate Molar Ratio	132
3. Plots of Percentage of ^{11}B present in the MEGA 8-borate and OG- borate Mixtures versus Surfactant:borate Molar Ratio	134
4. Effect of pH on the Magnitude of the Migration Time Window	136
5. Effect of Borate on the magnitude of the Migration Time Window	138
6. Effect of Alkyl Chain Length of the Surfactant on the Magnitude of the Migration Time Window	139
7. Plots of $\log k' - \log k''$ of Phenylalkyl alcohols Homologous Series	145
8. Capacity factor versus Borate Concentration in the Running Electrolyte	148
9. Capacity factor versus pH of the Running Electrolyte	151
10. Electropherogram of Herbicides	152
11. Electropherograms of Urea Herbicides	153
12. Electropherogram of some Aromatics	156
13. Electropherograms of some Barbiturates	157
14. Electropherograms of Dansyl Amino Acids	159
15. Electropherogram of D and L Dansyl Amino Acids	161

Chapter VII

1. Plots of Percentage of ^{11}B present in the Free and Complexed Forms for OM-borate, OS-borate and OG-borate Mixtures versus Surfactant:[borate] Molar Ratio	173
2. Effect of pH on the Migration Time Window and Electrophoretic Mobility	175
3. Effect of Borate Concentration on the Migration Time Window, Electrophoretic Mobility and the Elution Range Parameter for OM and OS	178

Figure	Page
4. Effect of OM concentration on the Migration Time Window, Electrophoretic Mobility and Capacity Factor	181
5. Electropherograms of three Consecutive Injections of Urea Herbicides	185
6. Electropherograms obtained with a "bubble" cell capillary and regular capillary	188
7. Electropherograms of Herbicides obtained OS and OM	189
8. Electropherograms of Urea Herbicides	191
9. Electropherograms of Aromatic Compounds obtained with OM and OS	193

Chapter VIII

1. Idealized Structure of the Alkylglucoside-Butyl Boronate Micelle	204
2. Plots of Percentage of ¹¹ B present in the Free and Complexed Forms for HG-borate and HG-boronate Mixtures versus Surfactant:[borate] or Surfactant:[boronate] Molar Ratio	209
3. Effect of pH on the Migration Time Window and Electrophoretic Mobility for HG and NG Micellar Phases	211
4. Effect of BBA Concentration on the Migration Time Window and Capacity Factor	213
5. Plots of log <i>k'</i> - log <i>k'</i> of Phenylalkyl Alcohols and Alkyl Phenyl Ketones Homologous Series	218
6. (a) Plots of the Capacity Factors of PAA versus Concentration of OG, (b) Plots of log <i>k'</i> versus Carbon Number of Homologous Series at various OG Concentration, and (c) Plots of log <i>k'</i> - log <i>k'</i> for PAA series	224
7. Electropherograms of Neutral and Acidic Herbicides obtained with Alkylglucoside-BBA Micellar Phases	228
8. Electropherograms of Urea Herbicides obtained with Alkylglucoside-BBA Micellar Phases	230
9. Electropherograms of Medicarpins and Precursors obtained with Alkylglucoside-BBA Micellar Phases	232
10. Electropherogram of D and L Dansyl Amino Acids	233

Figure	Page
Chapter IX	
1. Idealized Structure of Alkylglycoside-Borate Micelle	242
2. Electropherograms of APK Homologous Series	250
3. Plots of $\log k' - \log k'$ of APK Homologous Series	254
4. Electropherograms of Urea Herbicides	256
5. Bar Graphs of the Selectivity Factor for the Urea Herbicides	257
6. Electropherograms of Neutral and Acidic Herbicides	259
7. Bar Graphs of the Selectivity Factor for Neutral Herbicides	260
8. Electropherograms of Aromatic Species	261

LIST OF SYMBOLS AND ABBREVIATIONS

F_d	drag force
l	effective length of the capillary column
F_e	electrical force
ΔG^o	Gibbs free energy
$\log \alpha$	methylene group selectivity
n_c	number of carbon atoms
\bar{v}	partial specific volume of micelle
$\log \beta$	specific interaction between micellar and aqueous phases
ρ_{mc}	surface charge density of the micelle
V_{aq}	volume of aqueous phase
V_{mc}	volume of micellar phase
w_b	width of peak at base
w_h	width of peak at half height
w_i	width of peak at inflection point
2-AP	2-aminopyridine
2AP-(GalA) _n	2-aminopyridyl derivatives of oligogalacturonides
α	selectivity
AB	alkylbenzenes
APK	alkyl phenyl ketones
BBA	1-butaneboronic acid
CAF	constant anodal flow
CE	capillary electrophoresis

CF-LSIMS	continuous flow-liquid secondary ion mass spectrometry
CGE	capillary gel electrophoresis
CIEF	capillary isoelectric focusing
CITP	capillary isotachopheresis
CMC	critical micelle concentration
cps	centipoise
CTAB	cetyltrimethylammonium bromide
CZE	capillary zone electrophoresis
δ	thickness of the double layer
DBTD	disodium 5,12-bis(dodecyloxymethyl)-4,7,10,13-tetraoxa-1,16-hexadecanedesulphonate
DG	decyl- β -D-glucopyranoside
Δh	difference in height between reservoirs
DMF	N,N-dimethylformamide
E	electric field
ϵ	dielectric constant
EOF	electroosmotic flow
ϕ	logarithmic phase ratio
GC	gas chromatography
η	viscosity
HG	heptyl- β -D-glucopyranoside
HPC	hydroxypropyl cellulose
HPCE	high performance capillary electrophoresis
I	current or ionic strength
I.D.	internal diameter
φ	phase ratio
K	distribution coefficient

κ	Debye-Hückel constant
k'	capacity factor
L	total length of capillary
LSIMS	liquid secondary ion mass spectrometry
μ_{app}	apparent mobility
MECC	micellar electrokinetic capillary chromatography
MEGA 8	octanoyl- <i>N</i> -methylglucamide
MEGA 9	nonanoyl- <i>N</i> -methylglucamide
MEGA 10	decanoyl- <i>N</i> -methylglucamide
μ_{eo}	electroosmotic mobility
μ_{ep}	electrophoretic mobility
$\mu_{ep(eff)}$	effective electrophoretic mobility
$\mu_{ep(mc)}$	electrophoretic mobility of micelle
MPEIHE	methylated polyethyleneimine hydroxyethylated
MS	mass spectrometry
N	separation efficiency
n	peak capacity
v_{app}	apparent velocity
v_{eff}	effective velocity
v_{eo}	electroosmotic velocity
v_{ep}	electrophoretic velocity
NG	nonyl- β -D-glucopyranoside
v_{mc}	micelle velocity
v_s	solute velocity
OG	octyl- β -D-glucopyranoside
OM	octyl- β -D-maltopyranoside
OS	octanoylsucrose

PAA	phenylalkyl alcohols
PEG	polyethylene glycol
PEI	polyethyleneimine
PEIHE	polyethyleneimine hydroxyethylated
PEIHED	polyethyleneimine hydroxyethylated derivative
pI	isoelectric point
PVA	polyvinyl alcohol
q	net charge
R	resistance
r	radius
ρ	surface charge density
R_s	resolution
RSD	relative standard deviation
SDS	sodium dodecyl sulfate
TEA	triethanolamine
TEA	triethylamine
t_M	migration time
t_{mc}	migration time of micelle
t_0	migration time of bulk flow
t_r	retention time of solute in MECC
V	applied voltage
VAF	variable anodal flow
ψ_d	electric potential at the interface of the mobile and immobile parts of the double layer
ψ_0	electric potential at surface of the solid-liquid interface
ζ	zeta potential
ZF	zero flow

CHAPTER I

INTRODUCTION TO HIGH PERFORMANCE CAPILLARY ELECTROPHORESIS

Introduction

Capillary electrophoresis (CE), also called high performance capillary electrophoresis (HPCE), is a modern analytical technique which permits rapid and efficient separations. In many ways, CE is simply a miniaturized instrumental version of traditional electrophoresis. Electrophoresis is a process for separating charged molecules based on their differential movement through a fluid under the influence of an applied electric field.

The evolution of chromatographic methods over the last 30 years has produced a systematic and rational trend towards miniaturizing the given technique. The most significant example is that of gas chromatography (GC), where the advantages of open-tubular capillaries have virtually displaced the use of packed columns for almost every application. As in GC, miniaturization of electrophoresis calls for the separation to be performed in small capillaries. The justification of miniaturizing electrophoresis will be discussed later in this chapter.

During separation, there are two major transport processes that are occurring, separative and dispersive. Separative transport arises from the differences in free-energy encountered by molecules with their physico-chemical environment. The basis of separation may be dependent on equilibria processes such as adsorption, extraction or ion exchange. Alternatively, kinetic processes such as electrophoresis or dialysis may

provide the basis of separation. Whatever the mechanism of separation, each component of a mixture must have unique transport properties for separation to occur. Dispersive transport, or bandbroadening, is the sum of processes that contribute independently to the dispersing of zones about their center of gravity. Dispersive transport include diffusion, convection and mass transfer as well as other. Even under optimum conditions that offer excellent separative transport, dispersive transport, if not controlled, can merge peaks together. According to Giddings [1], "Separation is the art and science of maximizing separative transport relative to dispersive transport." In this regard, modern HPCE is perhaps the finest example of optimizing both transport mechanisms to yield efficient separations.

It should be noted that this dissertation consists of two major parts. The first part encompasses three chapters, which provide an introduction to capillary zone electrophoresis (CZE) of biopolymers (Chapter 2) as well as the development of novel capillary coatings for the CZE of proteins and other important biological species (Chapters 3 and 4). The second part consists of a series of five chapters related to micellar electrokinetic capillary chromatography (MECC). The first chapter of the second part (Chapter 5) overviews the basic principles of MECC, while the remaining chapters (Chapters 6-9) are focused on the development and characterization of novel micellar phases for use in MECC.

The goal of this chapter is to provide (i) a historical background of the introduction of electrophoresis and its development into high performance capillary electrophoresis as it stands today and (ii) review the fundamental concepts of electrophoretic separations in fused-silica capillaries.

Historical Background

The development of electrophoresis can be traced back to more than a century ago [2]. In the late 1800s, electrophoretic separations were attempted in solutions as well as various gels. Many of these early experiments were performed using glass U tubes with electrodes connected to each of the tubes arms. The experiments were performed using direct current of up to several hundred volts. The first reported separative experiments involved the fractionation of toxin/antitoxin solutions [2, 3]. Michaelis, who coined the name electrophoresis, used it to determine the isoelectric points of proteins [4]. In the 1930s, Tiselius [5, 6] performed studies involving moving boundaries of proteins using electrophoresis. In the following 10 years, many electrophoretic separations were reported involving amino acids, peptides and proteins [7, 8]. In order to overcome problems of convective mixing which were encountered in electrophoretic separations performed in free solutions, various stabilizing media were employed, such as agar [3], cellulose powder [9], glass wool [8], paper [10], silica gel [7] and acrylamide [11] with some success.

The direct forerunner of CE was developed as an alternative approach to alleviate thermal convection problems in free solution by the use of tubes with small internal diameters. These small tubes or capillaries allowed for better dissipation of heat and a more uniform thermal cross-section of the sample within the tube. Free zone electrophoresis in open tubes was first demonstrated by Hjertén in 1967 [12]. Hjertén's work was performed in rotating tubes with 3 mm internal diameter (I.D.) using high electrical field strength and on-column UV detection for sensing the separated zones as they pass across the detection point and is the first example of modern CE. In 1974, Virtanen described the advantages of using smaller I.D. glass capillaries (200-500 μm) using potentiometric methods of detection [13]. Mikkers *et al.* [14] performed zone electrophoresis in instrumentation adapted from isotachopheresis employing 200 μm I.D. PTFE capillaries. While these earlier studies with smaller I.D. tubing were improvements

over what could be obtained in traditional electrophoresis, they were unable to demonstrate high separation efficiencies because of sample overloading, a condition induced by the poor sensitivity of detectors available at that time and large injection volumes.

In 1981, Jorgenson and Lukacs [15] solved the intricate problems of injection and detection using 75 μm I.D. fused-silica capillaries for the separation of amino acids and peptides with on-column fluorescence detection. Their work was a major breakthrough in CE in terms of resolution and separation efficiency and clearly marked the start of the era of HPCE.

The 1980s brought about the introduction of several separation modes to capillary electrophoresis. Gel electrophoresis was adapted to the capillary format [16] as well as isoelectric focusing [17]. The first high resolution sieving separation by capillary gel electrophoresis was demonstrated by Karger and Cohen [18]. In 1984, Terabe *et al.* [19] described a new form of electrophoresis called micellar electrokinetic capillary chromatography (MECC). This new technique allowed the chromatographic separation of neutral as well as charged molecules *via* their differential partitioning into a charged micelle acting as a "pseudo-stationary" phase. Other new electrokinetic capillary techniques include the use of cyclodextrins [20], ligand exchange [21] and ion exchange [22] media. Almost every conceivable molecule could be analyzed in some form of HPCE.

Other great advances in HPCE in the 1980s came in the area of detection. Walbroehl *et al.* [23] introduced an improved UV detector that helped overcome some of the serious limitations of the short path length as dictated by the I.D. of the capillary. One of the most significant steps in terms of detection came with the introduction of laser-induced fluorescence [24] which improved detectability to the attomole range. Interfacing HPCE with the mass spectrometer for on-line detection proved to be another powerful addition [25]. This was of practical importance because of the difficulty of carrying out fraction collection. Electrochemical detectors that were sensitive enough to measure catecholamines in a single snail neuron were also introduced [26]. The adaptation of

indirect detection to CE allowed for the monitoring of solutes that neither absorbed nor fluoresced [27].

One significant problem was that of protein interaction with the capillary wall which was addressed from several fronts. The use of treated capillaries was described by Hjertén [28] in 1985. Others approached the problem by adjusting the buffer conditions, e.g., pH and composition, that diminish the electrostatic interactions between the solute and capillary wall and allow the separation of proteins on untreated capillaries [29]. Based on these and related developments, solute-wall interaction have been drastically reduced allowing for highly efficient separation of charged proteins.

These successive original works, as well as others, have transformed HPCE into a powerful new microseparation technique for the determination of both neutral and ionic species. As a result of increased interest in HPCE towards the late 80's, the first commercial instrument was introduced in 1988. Presently, more than six companies produce fully automated HPCE instruments while some others produce modular component systems to be assembled in-house. The development of commercial instrumentation has lead to the increasing popularity of CE as a analytical tool for routine separation.

Instrumentation

One of the key advantages of HPCE is the simplicity of the instrumental configuration. A schematic illustration of an in-house assembled HPCE instrument, similar to that used in our studies, is shown in Figure 1. It is comprised of 5 major components: (i) a high voltage power supply of single or dual polarity capable of delivering up to 30 kV, (ii) a buffer filled fused-silica capillary with an inner diameter ranging from 10 to 100 μm , (iii) a plexiglass safety box to protect the operator from high voltages, (iv) an on-column detection system and (v) a data storage and processing device.

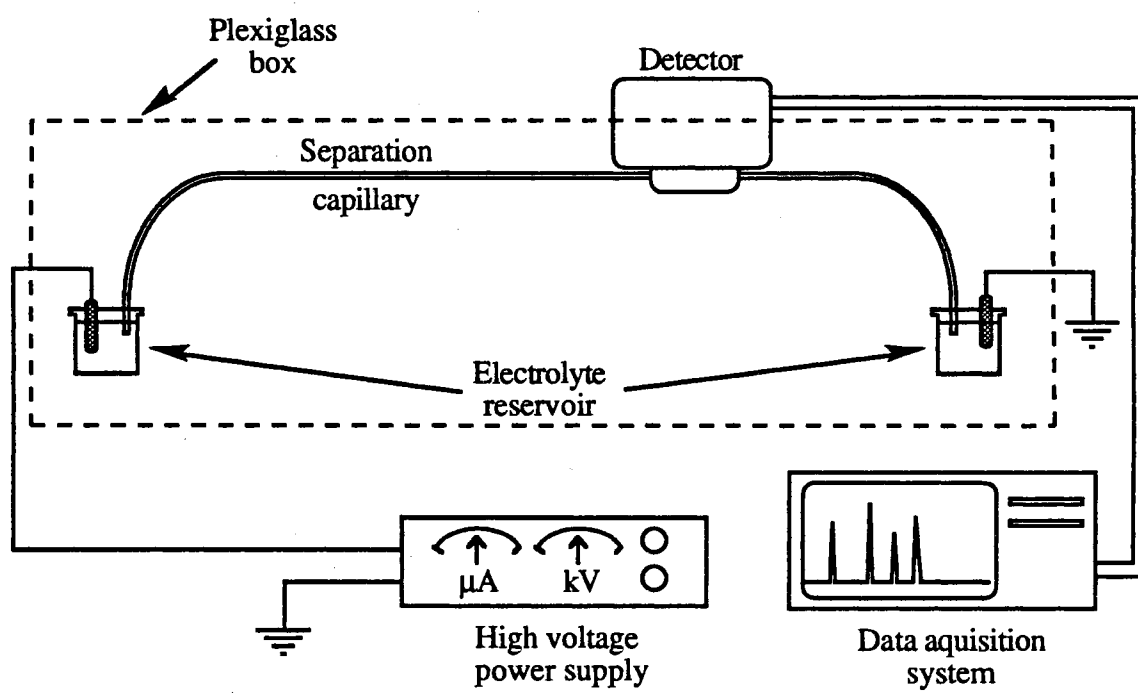


Figure 1. Instrumentation set-up for capillary electrophoresis

As a safety precaution, the high voltage power supply is wired into a switch that will automatically turn off the power supply upon opening the plexiglass box. The capillary is rinsed and refilled with a microsyringe whose needle is inserted into a teflon tube of an inner diameter that matches the outer diameter of the fused-silica capillary. Many commercial instruments are automated in the sense that they will complete all necessary steps during and between runs once programmed properly.

Fused-silica is a material to be used in CE because of its UV transparency and availability in uniform and flexible tubing. The fused-silica capillary is protected from moist air or dust particles that promote the growth of fissures and cracks making the capillary more fragile by coating it with a protective polyimide film. Internal diameters can range from 10 to 100 μm depending on the requirements of the separation. Figure 2 illustrates a cross-sectional view of the fused-silica capillaries used in these studies. Solute-capillary wall interactions is the most important limitation of the material, but can be overcome by the use of functionalized capillaries and buffer additives. Many commercial instruments have the capillary placed in a temperature controlled environment. This feature has proven to be a valuable tool in terms of improving reproducibility and adjusting selectivity.

Sample injection in CE can be performed by one of two major approaches, hydrodynamic and electromigration [30]. The most widely used approach is hydrodynamic injection because it is nondiscriminative in nature, i.e., it allows the introduction of all sample components into the capillary without bias. There are three different types of hydrodynamic injection: (i) head-space pressurization; (ii) vacuum injection (to the end of the capillary opposite to injection); and (iii) gravimetric (siphoning). The gravimetric technique was used throughout this study and is performed by raising the inlet reservoir above the outlet reservoir for a given height differential (e.g., 10 cm) and specific amount of time (e.g., 5 seconds).

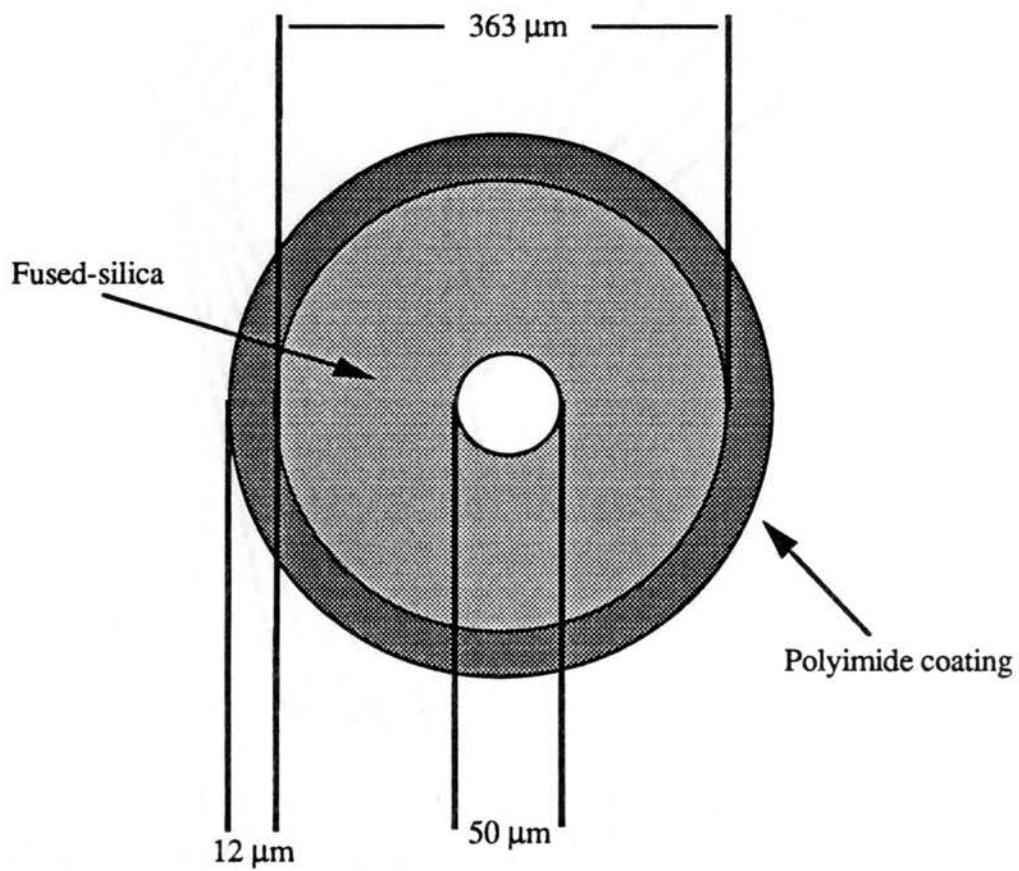


Figure 2. Cross-sectional view of a fused-silica capillary.

The sample can also be introduced electrophoretically into the capillary using electrokinetic injection. With electrophoretic injection the sample loading is a function of both electroosmotic flow of the capillary and the electrophoretic mobility of the analyte (these concepts are described in the following section). Because sample loading is a function of the electrophoretic mobility of the solute, discriminative injection will occur when the solute have different mobilities. This problem is most significant when injecting solutes that have opposite electrophoretic mobility. However, sample injection by electrokinetic injection can also be useful for concentrating the sample on-column [31]. This concentration step is achieved with sample solutions having a lower conductivity than the separation buffer. Under these conditions, the electric field in the sample zone is greater than that in the capillary which causes the solutes to move through the sample zone at an accelerated velocity until they enter the capillary where they slow down and "stack" into a narrow zone. It should be noted that quantification with "sample stacking" can be difficult if the sample composition is not accurately known.

Modes of CE

Capillary electrophoresis encompasses a series of branches or modes that have distinctly different operative and separative characteristics. These different branches can all be performed using the same basic instrumentation. The various modes of CE are capillary zone electrophoresis (CZE), capillary isoelectric focusing (CIEF), capillary gel electrophoresis (CGE), capillary isotachopheresis (CITP) and micellar electrokinetic capillary chromatography (MECC). The origins of the different modes of separation may be attributed to the fact that CE has developed from a combination of many electrophoresis and chromatographic techniques.

Capillary zone electrophoresis, also known as free solution capillary electrophoresis, is currently the most commonly used technique in CE. The separation in

CZE is based on the differences in the electrophoretic mobilities resulting in different migration velocities for ionic species in the electrophoretic buffer contained in the capillary. The separation mechanism is mainly based on differences in solutes size and charge at a given pH.

In CIEF, substances are separated on the basis of their isoelectric points or pI values [32]. In this mode, a mixture of zwitterionic chemicals, known as carrier ampholytes, form a pH gradient inside the capillary. The fundamental premise of CIEF is that a molecule will migrate so long as it is charged. Should it become neutral, it will stop migrating in the electric field. Charged species will migrate in the electrical field until they reach the point in the pH gradient where the pH equals the pI; this is known as the focusing step. Once the analytes have been focused, a mobilization step is required to pass the focused analytes in front of the detector.

Capillary gel electrophoresis has proven to be a powerful extension of CE, especially in the separation of large molecular weight biopolymers. The main separation mechanism in CGE is based on differences in solute size as analytes migrate through the pores of gel-filled capillary column. The gel, e.g., polyacrylamide, provides an anticonvective medium, which serves to minimize solute diffusion. Due to this nature, CGE has recorded efficiencies up to 30 million theoretical plates per meter [18].

The separation mechanism of CITP is based on distribution of the solutes into continuous but discretely sharp zones in a discontinuous buffer system. Sample components condense between leading and terminating buffers, producing a steady-state migrating configuration composed of consecutive sample zones. An isotachopherogram contains a series of steps, with each step representing an analyte zone where the amount of sample present can be determined from the zone length.

In MECC, the separation medium consists of an electrolyte containing an ionic surfactant in an amount above its critical micelle concentration. Upon formation of the micelle, there are two phases inside the capillary, an aqueous mobile phase and a micellar

"pseudo-stationary" phase. When a sample is injected, it will distribute between the two phases with the more hydrophilic solutes spending most of their time in the aqueous phase, while the more hydrophobic solutes spend most of their time in the micellar phase. Under the influence of an electrical field the micellar phase will have an electrophoretic mobility. By associating with micelles, neutral solutes will acquire an effective electrophoretic mobility that is a function of their affinity for the micellar phase.

Basic Concepts of CE

To have a clear understanding of the basic physical processes that occur upon passage of an electrical current through an ionic solution, a few simple concepts are reviewed here. These processes are far more complex when compared to the passage of current through a metal or a solid-state conductor. In metals, current is carried by electrons which are uniform and weightless. In solution, the current is carried by cations and anions. The formula weight of these ions ranges from one for a simple proton to tens of thousands for large complex ions such as proteins.

Conduction of a fluid is described by Ohm's Law,

$$V = IR \quad (1)$$

where V is the applied voltage, I is the current that passes through the solution, and R is the resistance of the fluid medium. Conductance is the reciprocal of resistance. When current passes through an ionic solution, anions migrate towards the anode (positively charged electrode) while cations migrate towards the cathode (negatively charged electrode) in equal quantities. The conductance of a solution is determined by the concentration of the ionic species and the mobility of the ionic species in an electric field.

The mobility of ions in fluid solutions is governed by their charge/size ratio. The size of the molecule is based on its molecular weight, three-dimensional structure and its

degree of hydration. When considering simple alkali metals (i.e., Li^+ , Na^+ and K^+), their mobilities are reversed of what would be expected based on the crystal radii data [33]. The smallest ion, Li^+ , is more hydrated than its larger counterparts, i.e., Na^+ or K^+ . As a result of hydration the largest ion, K^+ , has the greatest mobility, almost twice that of Li^+ . The current generated by a running electrolyte is proportional to the ionic mobility of the anions and cations. This feature becomes important when selecting the appropriate counterion for preparing buffer solutions.

Under the influence of any electrical field, a charged species experiences a force F_e which is equal to the product of its net charge q and the electrical field strength E :

$$F_e = q \times E \quad (2)$$

Where E is given by:

$$E = \frac{V}{L} \quad (3)$$

where L is the total length of the capillary. The F_e force is positive for positively charged ions such that this force pushes them in the direction of the more negative electrode; the opposite applies to negative ions. The electrical force acting on a charged species accelerates it, but as the species begins to move through the background buffer, it experiences a viscous drag force that is opposite to the electrical force. The drag force F_d is proportional to the species electrophoretic velocity v and is given by:

$$F_d = f \times v \quad (4)$$

where f is translational frictional resistance. The frictional resistance for small spherical ions can be expressed by Stokes' Law,

$$f = 6\pi\eta r \quad (5)$$

where η = viscosity and r = radius. The frictional drag is directly proportional to viscosity, size and electrophoretic velocity. Due to the presence of the frictional drag a charged species is accelerated to a limiting velocity, which is dependent on both F_e and F_d . This limiting velocity is called drift velocity, steady-state velocity or electrophoretic velocity (v_{ep}) and is achieved when the acceleration force is balanced by the retarding forces as follows:

$$v_{ep} = \frac{qE}{f} \quad (6)$$

These terms can be combined as an expression for the electrophoretic mobility, μ_{ep} , by:

$$\mu_{ep} = \frac{v_{ep}}{E} = \frac{q}{6\pi\eta r} \quad (7)$$

The electrophoretic mobility is defined as the steady-state velocity of a species per unit field strength. The magnitude of μ_{ep} depends on the net charge on a molecule and its frictional properties (size and shape) as well as the dielectric constant ϵ and the viscosity η of the running buffer. This relationship for large molecules or colloids is given by [34]:

$$\mu_{ep} = \frac{2\epsilon\zeta}{3\eta} f(\kappa a) \quad (8)$$

where ζ is the zeta potential of the charged particle, κ is the Debye-Hückel constant and a is the radius of the ionic species. The parameter $f(\kappa a)$ is a constant whose value varies between 1 and 1.5 depending on the shape of the migrating species.

Separations in HPCE have been performed almost exclusively on fused-silica capillaries. Fused-silica is a highly crosslinked polymer of silicon dioxide with tremendous tensile strength. The surface of fused-silica capillaries is composed of silanol groups which ionize under most conditions leaving a negatively charged surface. Because of this charged surface, ionic species with similar charge sign (co-ion) are repelled from the surface, while ionic species with opposite sign (counterions) are attracted to the

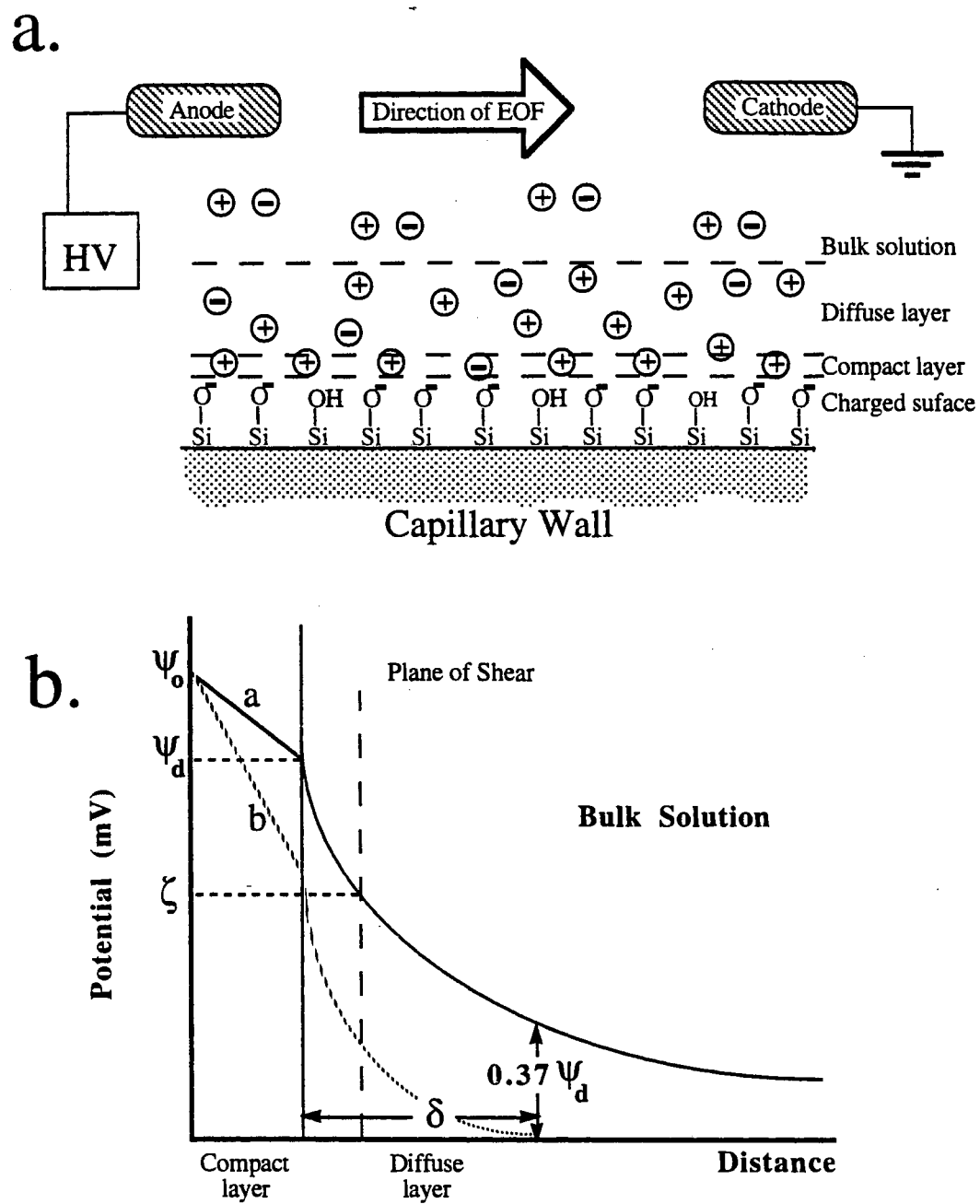


Figure 3. Illustrations of (a) the electrical double layer at the surface of a fused-silica capillary and (b) the point potential as a function of the distance from the capillary wall.

capillary wall. The anionic charge on the capillary surface in combination with counterions from the running electrolyte result in the formation of an electrical double layer at the silica-solution interface. Figure 3a illustrates the idealized surface of a bare fused-silica capillary. Part of these counterions are immobilized by electrostatic forces in a region next to the surface forming what is known as the compact layer, while others (due to thermal motion) reach further into the liquid forming the mobile or diffuse layer. Because of the spatial distribution of ions within the electrical double layer, an electric potential gradient arises as described by the Stern-Gouy-Chapman theory [34].

Figure 3b illustrates the electric potential gradient at the capillary wall-liquid interface inside the capillary. The electric potential Ψ_0 is greatest at the capillary surface. The electric potential first decreases linearly in the compact layer and then exponentially in the diffuse region and then diminishes in the bulk solution. The electric potential at certain intangible planes in the liquid is used to characterize the double layer. Ψ_d is the electric potential at the interface between the compact and diffuse layers, i.e., immobile and mobile parts of the double layer. The thickness of the double layer δ is defined as the distance between the two planes where the electric potential is $(1/e)\Psi_d$ and Ψ_d , respectively. The zeta potential ζ is another descriptive characteristic used to define a given interface and is the potential at the plane of shear occurring when the liquid is forced to move by an external force, which is the electrical field.

When an electric field is applied across the length of the capillary, the mobile positive charges in the diffuse layer migrate in the direction of the cathode. Since these ions are solvated by water, the fluid in the buffer is mobilized as well and dragged along by the migrating cations. Even though the thickness of the double layer is on the order of 100-300 Å, the flow is transmitted throughout the diameter of the capillary. This flow or pumping action is known as the electroosmotic flow (EOF) and is the driving force for many modes of CE. The EOF always migrates in the direction of the counterions in the double layer. The linear velocity of the electroosmotic flow v_{e0} is given by [35]:

$$v_{eo} = \mu_{eo} E = \frac{\epsilon \zeta}{4\pi\eta} E \quad (9)$$

where μ_{eo} is the electroosmotic mobility. The zeta potential is expressed as [36]:

$$\zeta = \frac{4\pi\delta\rho}{\epsilon} \quad (10)$$

where ρ is the surface charge density of the capillary surface. By implementing modern electrolyte theory which states that δ equals $1/\kappa$, equation 10 can be rearranged to:

$$\zeta = \frac{4\pi\rho}{\kappa\epsilon} \propto \frac{1}{\sqrt{I}} \quad (11)$$

where κ is the Debye-Hückel parameter and I is the ionic strength of the medium. It follows that increasing the ionic strength of the running electrolyte decreases the ζ potential as well as the EOF. The influence of the electrolyte's ionic strength is illustrated in Figure 3b where curve (a) is for a lower ionic strength and curve (b) is for a higher ionic strength.

Since the EOF originates at the wall of the capillary, a flat or plug flow profile is obtained as opposed to the parabolic flow profile observed with pressure driven flow, thus enhancing separation efficiencies by reducing the linear distribution for a sample zone. The EOF in most cases is faster than the electrophoretic mobilities of most species. This is advantageous in the sense that all solutes in the capillary will travel toward one end regardless of their net charge with the positively charged species being detected first, followed by the neutral and then the negatively charged solutes. As illustrated in Figure 4, positively charged species are attracted towards the cathode and their velocity is the sum of both v_{ep} and v_{eo} . Because their charge-to-mass ratio is zero, species with a net charge of zero will not separate but will migrate with the EOF and pass the detector after the positively charged species. Finally, the negatively charged species which are electrophoretically attracted towards the anode, are carried towards the cathode by the EOF. The EOF will add the same velocity component, v_{eo} , to all species regardless of

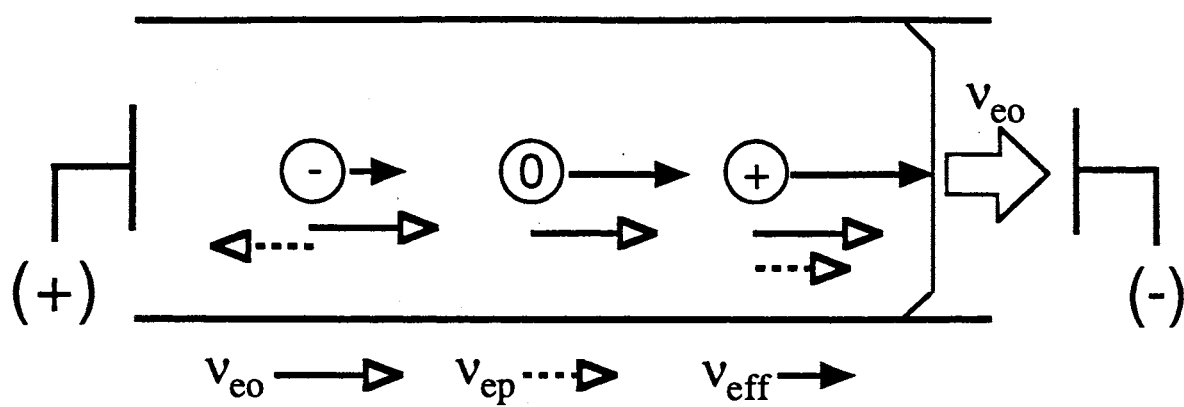


Figure 4. Illustration of an electrophoretic separation in CE.

their radial position and charge. In other words, the observed velocity or effective velocity, v_{eff} , is always additive of the EOF and the solute's electrophoretic velocity. A relatively strong EOF is needed for the simultaneous determination of oppositely charged solutes in a single electrophoretic run. With some modes of CE, e.g., CIEF, it is necessary to completely eliminate the EOF. A significant amount of work has been carried out to introduce ways for manipulating the EOF in order to improve a given separation [37-39]. The control of the EOF is topic of discussion in chapters 3 and 4 as well as the various methods introduced by other laboratories.

The efficiency in CE can be readily estimated from the electropherogram by the following equation which is the same as that used in liquid chromatography [40]:

$$N = 4 \left(\frac{t_r}{w_i} \right)^2 = 5.54 \left(\frac{t_r}{w_h} \right)^2 = 16 \left(\frac{t_r}{w_b} \right)^2 \quad (12)$$

where w_i , w_h and w_b are the peak widths at the inflection point, half-height and base, respectively, for a Gaussian peak.

In summary, this chapter provided a classification and a historical background of electrophoresis and its miniaturized version, capillary electrophoresis. It also discussed the instrumentation used in CE, overviewed the various modes of CE and gave an account to the basic concepts of CE including the definitions of electrophoretic mobility, electroosmotic mobility and the influence of the variables that affect the migration of ionic species.

References

1. J. C. Giddings, *Unified Separation Science*, John Wiley and Son, New York, 1991.
2. I. Smirnow, *Berl. Klin. Woch.*, 32 (1892) 645.
3. C. W. Field and O. Teague, *J. Exp. Med.*, 9 (1907) 86.
4. L. Michaelis, *Biochem. Z.*, 16 (1909) 81.
5. A. Tiselius, *Trans. Faraday Soc.*, 33 (1937) 524.
6. A. Tiselius, University of Upsala, Sweden, 1930.
7. R. A. Consden, A. H. Gordon and A. J. P. Martin, *Biochem. J.*, 40 (1946) 33.
8. T. B. Coolidge, *J. Biol. Chem.*, 127 (1939) 551.
9. J. Porath, *Biochem. Biophys. Acta.*, 22 (1956) 151.
10. A. Tiselius and P. Flodin, *Advances in Protein Chem.*, 8 (1953) 461.
11. S. Hjertén, S. Jerstedt and A. Tiselius, *Anal. Chem.*, 11 (1965) 211.
12. S. Hjertén, *Chromatogr. Rev.*, 9 (1967) 122.
13. R. Virtanen, *Acta Polytech. Scand.*, 123 (1974) 1.
14. F. E. P. Mikkers, F. M. Everaerts and T. P. E. M. Verheggen, *J. Chromatogr.*, 270 (1979) 11.
15. J. Jorgenson and K. D. Lukacs, *Anal. Chem.*, 53 (1981) 1298.
16. S. Hjertén, *J. Chromatogr.*, 270 (1983) 1.
17. S. Hjertén and M. D. Zhu, *J. Chromatogr.*, 346 (1985) 265.
18. A. S. Cohen and B. L. Karger, *J. Chromatogr.*, 397 (1987) 409.
19. S. Terabe, K. Otsuka, K. Ichikama, A. Tsuchiya and T. Ando, *Anal. Chem.*, 56 (1984) 111.
20. S. Terabe, H. Ozaki, K. Otsuka and T. Ando, *J. Chromatogr.*, 332 (1985) 211.
21. P. Gozel, E. Gossman, H. Michelsen and R. N. Zare, *Anal. Chem.*, 59 (1987) 44.

22. S. Terabe and T. Isemura, *Anal. Chem.*, 62 (1990) 650.
23. Y. Walbroehl and J. W. Jorgenson, *J. Chromatogr.*, 315 (1984) 135.
24. E. Gassman, J. E. Kuo and R. N. Zare, *Science*, 230 (1985) 813.
25. R. D. Smith, J. A. Olivares and N. T. Nguyen, *Anal. Chem.*, 60 (1988) 436.
26. R. A. Wallingford and A. G. Ewing, *Anal. Chem.*, 60 (1988) 258.
27. W. G. Kuhr and E. S. Yeung, *Anal. Chem.*, 60 (1988) 1832.
28. S. Hjerten, *J. Chromatogr.*, 347 (1985) 191.
29. H. Lauer and D. McManigill, *Anal. Chem.*, 58 (1986) 166.
30. P. D. Grossman and J. C. Colburn (Editors), *Capillary Electrophoresis Theory & Practice*, Academic Press, 1992.
31. R. Chien and D. S. Burgi, *Anal. Chem.*, 64 (1992) 489.
32. S. Hjerten and M. Zhu, *J. Chromatogr.*, 346 (1985) 265.
33. P. W. Atkins, *Physical Chemistry*, Oxford University Press, Oxford, 1986.
34. R. J. Hunter, *Zeta Potential in Colloid Science*, Academic Press, London, 1981.
35. C. L. Rice and R. Whitehead, *J. Phys. Chem.*, 69 (1965) 4017.
36. A. Adamson, in *Physical Chemistry of Surfaces*, Interscience, New York, 1967, Chapter 4.
37. W. Nashabeh and Z. El Rassi, *J. Chromatogr.*, 599 (1991) 367.
38. M. Hayes and A. Ewing, *Anal. Chem.*, 64 (1992) 512.
39. C. Wu, T. Lopes, B. Patel and C. S. Lee, *Anal. Chem.*, 64 (1992) 886.
40. B. L. Karger, L. R. Snyder and C. Horváth, *An Introduction to Separation Science*, Wiley, 1973.

PART I

CHAPTER II

SOME ASPECTS OF CAPILLARY ZONE ELECTROPHORESIS OF BIOPOLYMERS

Introduction

Capillary zone electrophoresis, thus far, is the most popular branch of CE because of its extremely high resolving power and the simplicity of the experimental approaches for carrying out separations. Separations in CZE are performed in a homogeneous carrier electrolyte or running buffer, and the selectivity can easily be adjusted by simply changing the composition of the running electrolyte.

Capillary zone electrophoresis has found applications in many areas of the life sciences and biotechnology, which have recently been reviewed by Kuhr and Monnig [1]. While the separation of many biological samples can be performed with relative ease using untreated fused silica capillaries in CZE, some biopolymers, such as proteins, require coated capillaries in order to minimize solute-wall adsorption and in turn achieve efficient separations. In any event, even samples that can be easily resolved in simple buffer systems such as most carbohydrates, amino acids and small peptides, the use of coated capillaries is advantageous as far as the reproducibility of separations is concerned. In fact, uncoated fused-silica capillaries yield pH hysteresis and consequently poor reproducibility [2].

The aim of this chapter is to provide an overview of the fundamental aspects of the separation of biopolymers in CZE. First, the analytical parameters of separation are briefly discussed. Second, an overview of approaches that have been used

to increase the selectivity and efficiency in the separation of various biopolymers are illustrated. Finally, a description of the objective and rationale of our studies in part I of this dissertation is provided at the end of the chapter. For clarity, additional background on the various research aspects of the thesis can be found in introductory parts of the following two chapters.

Analytical Parameters in CZE

The separation mechanism of CZE, which was briefly described in Chapter 1, involves the separation of the ionic components into discrete bands based on each solute's individual mobility. As shown in Fig. 1, after sample introduction, the solutes start migrating under the influence of the electrical field as well as being carried along by the EOF. For separation to occur, each solute must have a unique apparent mobility that contains both an electrophoretic and electroosmotic component. The relationship for apparent mobility, μ_{app} , is given by:

$$\mu_{app} = \mu_{ep} + \mu_{eo} \quad (1)$$

and similarly the apparent velocity is given by:

$$v_{app} = v_{ep} + v_{eo} = (\mu_{ep} + \mu_{eo})E \quad (2)$$

The migration time t_M , i.e., the time for a solute to migrate from the point of injection to the detection point, is given by [3]:

$$t_M = \frac{l}{v_{app}} = \frac{lL}{(\mu_{ep} + \mu_{eo})V} \quad (3)$$

where l is the length from the inlet of the capillary to the detection point, L is the total length of the capillary and V is the applied voltage. The electroosmotic mobility, μ_{eo} , which affects all solutes to the same extent is given by:

$$\mu_{eo} = \frac{v_{eo}}{E} = \frac{IL}{t_o V} \quad (4)$$

where t_o is the migration time of a neutral species such as phenol, acetone or mesityl oxide. The electrophoretic mobility, μ_{ep} , is given by:

$$\mu_{ep} = \mu_{app} - \mu_{eo} = \frac{v_{ep}}{E} = \frac{IL}{(t_M - t_o)V} \quad (5)$$

where μ_{app} is calculated using the observed migration time of the solute:

$$\mu_{app} = \frac{IL}{t_M V} \quad (6)$$

The μ_{ep} can be either positive or negative in sign depending on the solutes charge and the polarity of the applied field.

The ability to predict the migration behavior of biopolymers (e.g., proteins, peptides and oligosaccharides) under different experimental conditions would be extremely desirable as it would allow the optimization of separation conditions. Researchers could choose conditions such that a native protein could be distinguished from closely related variants or degradation products. Predictive models could be useful in the characterization of unknown species as well as purity analysis.

In general, *small* biopolymers (e.g., peptides with a few amino acids or oligonucleotides with less than 10 units) are well behaved in CZE and their electrophoretic mobility can be accurately predicted based on their mass (size) and charge characteristics. The charge of small biopolymers can be estimated from the pK_a values of the individual monomers making up the polymer [4]. For example, the migration of small peptides in a particular electrophoretic buffer can be easily calculated from commercially available computer software. However, with larger biopolymers, e.g., proteins and DNA, the calculation of charge based on ionization constants is not trivial. Aside from the mass-to-charge ratio, other factors may affect μ_{ep} of biopolymers including hydrophobicity,

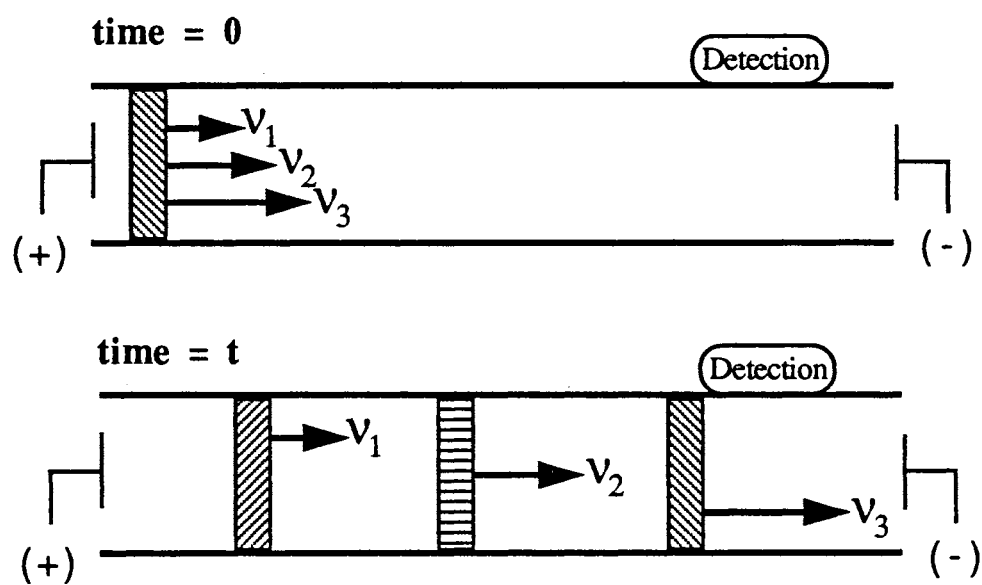


Figure 1. Schematic representation of a three-component separation in CZE at (a) the moment of injection and (b) after a given time frame.

conformation, primary sequence or even the chirality of amino acids [5]. The most significant problem in predicting the mobility of most biopolymers involves solute-wall interactions.

Solute-wall Interactions

Many biopolymers, especially proteins, have the unfortunate property of sticking to different surfaces, including metals, plastics and glass. One key advantage of HPCE when compared to HPLC is the absence of the chromatographic packing or support. The vast surface area of the packing material is responsible in part for irreversible adsorption of many solutes, particularly proteins. While the open tubular format used in CZE has been shown, in principle, to reduce the adsorption problem, the composition of the capillary surface, i.e., fused-silica, still provides sites for biopolymer adsorption. Binding of solutes to the capillary wall leads to bandbroadening, tailing, and irreproducibility of separations. If the kinetics of adsorption-desorption are slow, broadened, tailed peaks are observed with low efficiencies. Irreversible adsorption leads to modification of the capillary surface, resulting in changes in EOF, irreproducible separations and no elution of some components of the sample.

Figure 2 illustrates the electrostatic binding of a protein to the wall of an untreated fused-silica capillary. At most pH values, the capillary wall has a net negative charge due to the ionization of surface silanols. Separation of proteins at a pH below their pI produces cationic solutes that are electrostatically attracted to the capillary wall. Some proteins may have a net negative charge but isolated regions of positive charge, i.e., point charges, may still be susceptible to solute-wall electrostatic interactions. Hydrophobic interactions between the siloxane moiety of fused-silica and a hydrophobic solute can also affect the binding kinetics of biopolymers. Since separations in CZE are typically performed in

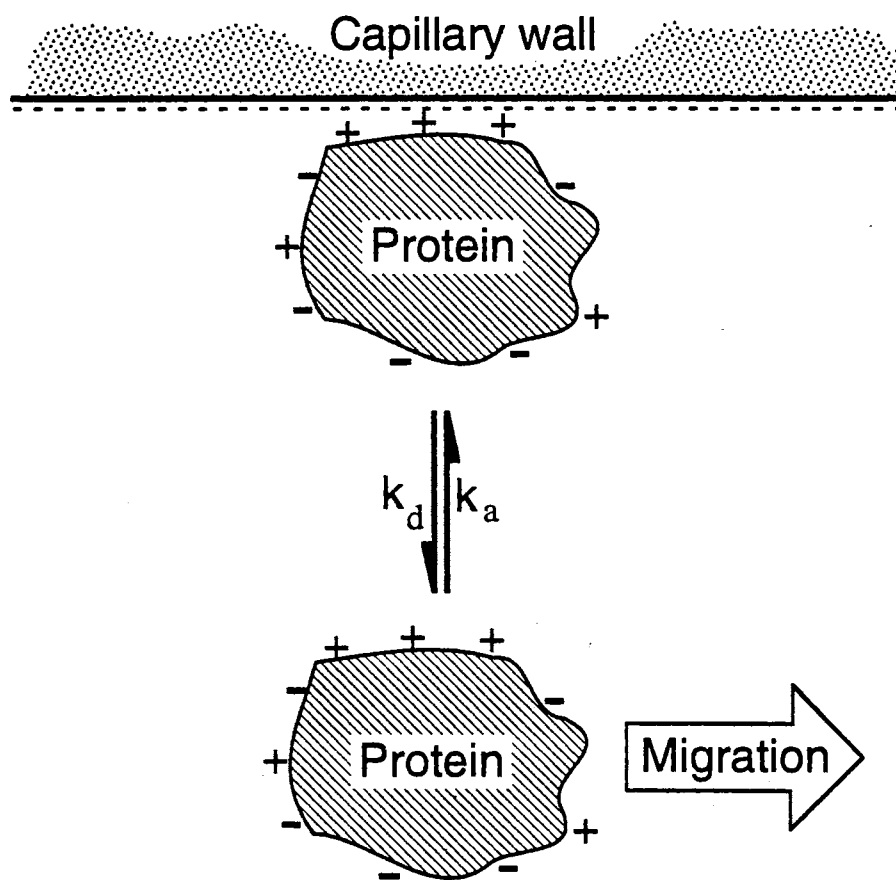


Figure 2. Pictorial representation of the electrostatic interaction of a protein with an untreated fused-silica capillary.

aqueous media, hydrophobic solutes are not well solvated, further enhancing the potential binding mechanism.

Elimination of Solute-wall Interactions

Solute-wall interactions have proven to be a difficult problem in the separation of biopolymers since the beginning of HPCE [6]. To solve this problem several strategies have been proposed, including the use of (i) extreme pH buffers, (ii) high-concentration buffers, (iii) amine modifiers, (iv) dynamically coated capillaries and (v) treated or functionalized capillaries. The following sections provide an overview of the various approaches introduced to alleviate solute adsorption to the capillary wall.

Extreme pH Buffers

If the pH of the running electrolyte is 1-2 units above the *pI* of a given biopolymer, the solute should be in an anionic form such that it is repelled from the anionic capillary wall. This approach was used by Lauer and McManigill [7] in 1986 for the separation of proteins. There are several limitations to this approach: (i) hydrophobic binding to the capillary wall is not eliminated, (ii) many basic proteins, whose *pI* > 7 are not anionic until pH 13 is reached, a condition that requires the use of 100 mM sodium hydroxide which is too conductive to be a useful running electrolyte due to Joule heating and (iii) alkaline pH are not usually optimal media for the separation of many proteins.

Soon after the work of Lauer and McManigill, the use of extremely low pH was explored. The silanol groups of the capillary wall are not ionized at pH < 2.0 and since most proteins are cationic at that pH, electrostatic interactions should be eliminated. McCormick [8] used a phosphate buffer, which further decreased the activity of the surface silanols, at low pH for the separation of basic proteins. Zhu *et al.* [9] used a phosphate buffer at pH 2.5 to prevent adsorption of hemoglobin on both bare and polyacrylamide-

coated capillaries. Attempts that used borate-phosphate (pH 7), and especially acetate, yielded significant protein adsorption and low efficiencies [10]. The low pH approach works well with some proteins but also has several limitations including: (i) poor selectivity, (ii) increased hydrophobic binding and (iii) the tendency of some proteins to precipitate in low-pH buffers.

High-Concentration Buffers

Buffers with high concentrations of salts were found to decrease adsorption of proteins on the capillary wall and increase the separation efficiency [7, 11]. Under these conditions, the counterions from the salt compete with protein for adsorption sites. One key issue with this approach is to choose a buffer based on its performance and UV absorption as the background electrolyte. Based on these characteristics, potassium sulfate was the additive of choice and was used at concentrations exceeding 200 mM [12]. This approach has a major drawback in that these buffers have a high ionic strength. The increased ionic strength required the use of low field strengths and narrow I.D. capillaries to prevent excessive Joule heating. Prolonged run times resulted as a combination of the low field strengths and low EOF.

To avoid the use of high ionic strength buffers, Bushey and Jorgenson proposed the use of zwitterionic salts as buffer additives [13]. Zwitterions such as betaine, sarcosine, and triglycine do not contribute to the conductivity and consequently can be used at high concentrations, i.e., up to 2.0 M. Zwitterionic salts are effective over a wide range but are limited by the pK_a 's of the ionizable groups.

Although the use of high salt concentrations, i.e., > 200 mM, is not a widely used approach due to its severe limitation, however, modest salt concentrations are widely used in combination with other approaches, e.g., functionalized capillaries or extreme pH. Increasing the buffer concentration from 10 mM tricine to 100 mM tricine at the same pH

can yield dramatic improvement in the separation efficiency of a tryptic digest while still allowing the use of moderate field strength for acceptable separation times [14].

Amine Modifiers

Several amine derivatives, e.g., trimethylamine, have been employed for years to suppress silanophilic interactions in HPLC. Lauer and McManigill [15] explored the use of 5 mM putrescine (1,4-diaminobutane) to improve the resolution and peak shape of myoglobin, but it was not effective at this concentration for strongly basic proteins such as lysozyme and cytochrome *c*. The separation of basic proteins required the use of divalent amines at much higher concentrations, such as 1,5-diaminopentane [16] or 1,3-diaminopropane [17] in the range of 40-60 mM. These approaches separated basic proteins at pH below their *pI*. One significant drawback in the use of polyamines is their effect on the EOF. Polyamines can significantly reduce the EOF and in many cases reverse its direction upon adsorption onto the capillary wall, but this in some cases may be an advantage as is discussed in the following section. Thus, the effect on the EOF must be taken into consideration when using polyamines as buffer additives.

Dynamically Coated Capillaries

The approach of dynamically coating capillaries involves the use of buffer additives to reduce solute/wall interactions. Several different types of dynamic coatings have been introduced including charge reversal additives, non-ionic surfactants and zeta potential suppressers.

Several investigators have used the approach of reversing the charge of the capillary surface from negative to positive by the addition of cationic additives to the running electrolyte to reduce protein adsorption [18-22]. Charge reversal can be accomplished by using either a cationic surfactant such as cetyltrimethylammonium bromide (CTAB) or a polyamine additive such as hexadimethrine bromide (polybrene).

The mechanism of charge reversal is based on ion-pair formation between a cationic group of the additive and the anionic silanol group. It should be stressed that the direction and magnitude of the EOF are dependent on the net charge of the capillary surface. If an additive possesses multiple positive charges it may ion-pair to the surface with one or more charges while the remaining charges making contributions towards the net charge of the surface. Once the zeta potential of the surface is reversed in sign from negative to positive, positively charged biopolymers are no longer attracted to the surface, but repelled electrostatically. The reversal of the EOF may also be beneficial in terms of shortening analysis time.

Non-ionic surfactants have proven useful in the separation of hydrophobic proteins which may interact with the capillary wall, particularly if the surface has been modified by a hydrophobic bonded-phase. It has been shown that non-ionic surfactants such as Brij35 and Tween20 can be used to dynamically coat deactivated capillaries, allowing high separation efficiencies with hydrophobic proteins [23]. This approach can be used with commercially available coated capillaries designed for use in capillary gas chromatography. In fact, little difference in performance was observed between C1, C8 and C18 bonded phases when using Brij35 [24]. The detergent coating makes the capillary wall less hydrophobic and therefore more suitable for the analysis of hydrophobic biopolymers.

The most widely explored dynamic coating involves the use of zeta potential suppressors. The suppression of the zeta potential is achieved by adding small amounts of a non-ionic polymeric species, e.g., hydroxypropylmethylcellulose or polyvinyl alcohol, to the running electrolyte [25-27]. These large polymers are adsorbed to the surface of the capillary where they serve two principle functions. First, they increase the viscosity in the electrical double layer which drastically decreases or even eliminates the EOF. Secondly, they "shield" large molecules by reducing access to the charged surface thus preventing undesirable adsorption. The most significant disadvantage of this approach is increasing the viscosity of the running electrolyte will produce longer analysis time especially in the

absence of the EOF. Because the solutes are migrating only by their own electrophoretic mobility, they must possess significant charge. This eliminates the ability to separate oppositely charged species in the same run and the pH of the running electrolyte must be removed from the pI value of solutes in order to induce the necessary charge for their migration. At higher concentrations, these soluble polymers may cause a molecular sieving effect through the formation of an entangled polymer network [28].

A variety of dynamically coated capillary systems have been introduced. Some of these dynamic systems provide high separation efficiencies and have proven quite useful for a particular separation. Nevertheless, all of the dynamic coated capillaries have one major disadvantage: poor reproducibility, because the coating is only adsorbed on the surface and is continuously changing.

Functionalized Capillaries

In their pioneering work on CE, Jorgenson and Lukacs concluded that the separation of many proteins would require a more inert and nonadsorptive surface than fused-silica [29]. These early studies prompted the development of a variety of functionalized fused-silica capillaries. There are two major types of functionalized capillaries, covalently bonded functional groups and adsorbed functional groups. With covalent attachment, the surface modifier or coating is chemically attached to the capillary surface by a covalent bond. Whereas the adsorbed coating is not covalently attached, but stabilized by crosslinking and/or adsorption phenomena such as electrostatic interactions, hydrophobic interactions, dipole interactions, van der Waals interactions or hydrogen bonding. Functionalized capillaries of both types have been designed to perform a variety of functions. Some of these coatings reduce or eliminate the EOF while others reverse the EOF. All surface modifications should be designed to minimize the adsorption of biopolymers to the surface.

To be an applicable coating, the surface modification procedure should meet several requirements, including: (i) the coating should shield sensitive biopolymers from direct contact with the surface proper of the capillary and itself be nonreactive with the biopolymer solutes over a wide range of operating conditions, (ii) the coating should be chemically stable and resist hydrolytic degradation when in contact with aqueous solutions, (iii) the surface modification should produce the desired EOF and (iv) the coating procedure should be reproducible so that constancy in terms of efficiency and migration times are observed from a run-to-run, day-to-day and batch-to-batch operation. Several coatings, both covalently bonded and adsorptive, have been reported and have shown significant improvements in separations of almost every conceivable biopolymers. The nature of these coatings are characterized by being either charged or neutral.

One of the first attempts at surface modifications was performed by Jorgenson and Lukacs [29]. They prepared a silylated capillary to reduce the EOF and improved the resolution of dansyl amino acids. But this coating technique was not designed to reduce solute-wall interactions for proteins.

In 1985 Hjertén [26] attached methylacryl groups to the surface of the capillary which were subsequently cross-linked with polyacrylamide to produce a fairly inert surface that did not yield an EOF. This coating technique allowed the separation of human serum samples and nucleotides, but was characterized by a limited column lifetime [45].

The weakest point with many polymeric coatings was a single bond attachment of the polymer entity. In addition, this single bond was typically a siloxane bond which is susceptible to cleavage at alkaline pH. To increase the stability of the coating, Cobb *et al.* [46] reported the use of a polyacrylamide-coated capillary similar to that described previously by Hjertén, except that the coating was bonded to the silica wall through a Si-C bond, rather than a Si-O-Si bond. The Si-C bond is hydrolytically more stable than the siloxane bond, which yields an improvement in the coating stability. While this coating proved to be stable over a wide pH range (2-10.5) and practically eliminated the EOF, the

formation of the Si-C bond is by no means a simple task. The reaction scheme involved three separate stages: (1) the silica surface is chlorinated using thionyl chloride, (2) the chlorinated silica is reacted with a Grignard reagent containing a terminal double bond and (3) the acrylamide is polymerized on the surface. Due to the reactivity of the chlorinated surface and the use of a Grignard reaction, this scheme is very difficult to reproduce, especially inside a 50 μm capillary.

Several groups have studied the use of polyethylene glycol (PEG) coatings and its effects on the control of the EOF and the reduction of protein adsorption. Bruin *et al.* [36] bonded PEG 600 to the capillary surface using γ -glycidoxypropyltrimethoxysilane. The PEG capillaries were stable for several months but showed a substantial decrease in the adsorption of proteins when the capillary was operated at pH 3-5. However, the capillary performance decreased rapidly at pH greater than 5 as well as the stability of the coating.

Our laboratory recently introduced two surface modification schemes that yielded stable and inert capillaries having moderate EOF [35]. In one approach, the hydrophilic coatings consisted of two layers; a glyceropropylpolysiloxane sublayer covalently attached to the inner surface and a polyether top layer. In a second approach, the capillary wall was coated with polysiloxane polyether chains whose monomeric units at both ends were covalently attached to the capillary inner surface with possible interconnection. These coatings yielded capillaries with different electroosmotic flow characteristics. The relatively long polyether chains of the various coatings were effective in shielding the unreacted surface silanols, thus minimizing solute-wall adsorption. As a consequence, high separation efficiencies were obtained in the pH range 4.0 to 7.5, which allowed the separation of widely differing proteins, the characterization of heterogeneous proteins and the fingerprinting of crude protein mixtures.

The idea behind charged coatings is to induce coulombic repulsive forces between the biopolymers and the capillary surface, i.e., both have the same charge sign. Towns and Regnier [44] developed capillaries having positively charged polyethyleneimine (PEI)

layers adsorbed to the capillary surface which were later crosslinked together. These capillaries produce a strong EOF in the direction of the anode, which is the reversal of that observed with a bare fused-silica capillary. The major disadvantages of these capillaries lie in the fact that they were only useful for the separation of positively charged biopolymers, which were repulsed from the surface. Negatively charged biopolymers were not shielded in any way and showed pronounced adsorption to the capillary surface.

Other investigators have introduced coatings that adsorb strongly on the fused-silica surface. In Hjertén's pioneering work in CZE [6], biopolymer adsorption was reduced by coating the capillary surface with methylcellulose. His procedure called for methylcellulose to first be adsorbed to the capillary surface and then crosslinked by baking the capillary in the presence of formaldehyde. This coating eliminated the EOF, but was characterized by a very limited lifetime. Similarly, Schomburg and co-workers [47] used polyvinyl alcohol (PVA) as an adsorbed coating. In their coating procedure, PVA was adsorbed on the surface, then heated to remove water, producing a highly organized network of PVA. This coating worked well with basic proteins, but the capillaries suffered from a limited lifetime.

The above mentioned coating procedures are only a representative sample of the massive quantity of work that has been devoted to the control of the EOF and minimization of biopolymer adsorption. Table I illustrates a more comprehensive listing of the various coated capillaries that have been developed for CZE as well as the resulting effects on the EOF. Very little data have been published on most of these coatings. Without going into exhaustive details, it should be noted that stability and reproducibility plague many of these new surface treatments. Most of these functionalized capillaries resulted in reducing or eliminating the EOF and yielded a surface on which biopolymer adsorption was reduced. Only a few investigations have introduced capillaries in which the EOF is reversed in order to enhance the selectivity of separation.

TABLE I. Coated Capillaries for CZE.

Coating	Resulting EOF	Reference
Polyacryamide	Eliminated	[26, 30-32]
Polyvinylpyrrolidone	Eliminated	[8]
Methylcellulose	Eliminated	[33]
Polymethylglutamate	Reduced	[34]
Polyethylene glycol	Reduced	[35-38]
Arylpentafluoro	Reduced	[39]
Epoxydiol	Reduced	[36, 40, 41]
Maltose	Reduced	[36]
Trimethylsilane	Reduced	[3, 42]
Octyl	Reduced	[43]
Octadecyl	Reduced	[23, 43]
Polyethyleneimine	Reversed	[37, 44]

Objective and Rationale of Part I of the Dissertation

As indicated above, capillary zone electrophoresis has developed into an important microseparation technique. While progress has certainly been made in the functionalization of fused-silica capillaries for the analysis of biopolymers, capillaries with different surface properties are badly needed to fully exploit the potential of CZE. Thus, the broad objective of this research was to contribute to the advancement of CZE methodology by providing (i) improved functionalized fused-silica capillaries for the separation of important biological species (e.g., proteins, peptides, oligosaccharides and nucleic acids) and (ii) a better understanding of the underlying phenomena. In pursuing this goal, a variety of surface modifications were developed to enhance the selectivity of CZE in the separation of biopolymers.

In one approach, the surface modification was controlled to yield hydrophilic capillaries with switchable (anodal/cathodal) EOF. The characterization and the utility of these capillaries are discussed in chapter 3. In a second approach, the surface modifications were devised to produce multilayered coatings having zero or constant (pH independent) anodal EOF. Studies involving the characterization and application of the constant and zero EOF coatings are the subject of chapter 4.

References

1. W. G. Kuhr and C. A. Monnig, *Anal. Chem.*, 64 (1992) 389.
2. W. J. Lambert and D. L. Middleton, *Anal. Chem.*, 62 (1990) 1585.
3. J. W. Jorgenson and K. D. Lukacs, *J. High Resolut. Chromatogr. Chromatogr. Commun.*, 4 (1981) 230.
4. H. J. Issaq, I. Z. Atamna, G. M. Muschik and G. M. Janini, *Chromatographia*, 32 (1991) 155.
5. H. J. Issaq, G. M. Janini, I. Z. Atamna, G. M. Muschik and J. Lukszo, *J. Liq. Chromatogr.*, 15 (1992) 1129.
6. S. Hjertén, *Chromatogr. Rev.*, 9 (1967) 122.
7. H. Lauer and D. McManigill, *Anal. Chem.*, 58 (1986) 166.
8. R. McCormick, *Anal. Chem.*, 60 (1988) 2322.
9. M. Zhu, R. Rodriguez, D. Hansen and T. Wehr, *J. Chromatogr.*, 516 (1990) 123.
10. B. J. Compton and E. A. O'Grady, *Anal. Chem.*, 63 (1991) 2597.
11. J. S. Green and J. W. Jorgenson, *J. Chromatogr.*, 478 (1989) 63.
12. G. O. Roberts, P. H. Rhodes and R. S. Snyder, *J. Chromatogr.*, 480 (1989) 35.
13. M. M. Bushey and J. W. Jorgenson, *J. Chromatogr.*, 480 (1989) 301.
14. R. G. Nielsen and E. C. Rickard, *J. Chromatogr.*, 516 (1990) 99.
15. H. H. Lauer and D. McManigill, *Anal. Chem.*, 58 (1986) 166.
16. V. Rohlicek and Z. Deyl, *J. Chromatogr.*, 494 (1989) 87.
17. J. A. Bullock and L. C. Yuan, *J. Microcol. Sep.*, 3 (1991) 241.
18. A. Emmer, M. Jansson and J. Roeraade, *HRC & CC*, 14 (1991) 738.
19. A. Emmer, M. Jansson and J. Roeraade, *J. Chromatogr.*, 547 (1991) 544.
20. R. L. Cunico, V. Gruhn, L. Kresin, D. E. Nitecki and J. E. Wiktorowicz, *J. Chromatogr.*, 559 (1991) 467.
21. K. Tsuji and R. Little, *J. Chromatogr.*, 594 (1992) 317.

22. J. E. Wiktorowicz and J. C. Colburn, *Electrophoresis*, 11 (1990) 769.
23. J. Towns and F. Regnier, *Anal. Chem.*, 63 (1991) 1126.
24. R. Dougherty, *Supelco Reporter*, 10 (1991) 4.
25. M. Gilges, H. Husmann, M.-H. Kleemib, S. R. Motsch and G. Schomburg, *High Res. Chromatogr.*, 15 (1992) 452.
26. S. Hjerten, *J. Chromatogr.*, 347 (1985) 191.
27. M. J. Gordon, K.-J. Lee and R. N. Zare, *Anal. Chem.*, 63 (1991) 69.
28. S. Hjertén, L. Valtcheva, K. Elenbring and D. Eaker, *J. Liq. Chromatogr.*, 12 (1989) 2471.
29. J. Jorgenson and K. D. Lukacs, *Anal. Chem.*, 53 (1981) 1298.
30. J. Kohr and H. Engelhardt, *J. Microcol. Sep.*, 3 (1991) 491.
31. M. A. Strege and A. L. Lagu, *J. Chromatogr.*, 630 (1993) 337.
32. M. Huang, W. P. Vorkink and M. L. Lee, *J. Microcol. Sep.*, 4 (1992) 233.
33. S. Hjertén and K. Kubo, *Electrophoresis*, 14 (1993) 390.
34. D. Bontrop, J. Kohr and H. Engelhardt, *Chromatographia*, 32 (1991) 171.
35. W. Nashabeh and Z. El Rassi, *J. Chromatogr.*, 599 (1991) 367.
36. G. J. M. Bruin, J. P. Chang, R. H. Kuhlman, K. Zegers, J. C. Kraak and H. Poppe, *J. Chromatogr.*, 471 (1989) 429.
37. M. Huang, W. P. Vorkink and M. L. Lee, *J. Microcol. Sep.*, 4 (1992) 135.
38. J. A. Lux, H. Yin and G. Schomburg, *HRC & CC*, 13 (1990) 145.
39. S. A. Swedberg, *Anal. Biochem.*, 185 (1990) 51.
40. M. Bacolod and Z. El Rassi, *J. Chromatogr.*, 512 (1990) 237.
41. J. K. Towns, J. Bao and F. E. Regnier, *J. Chromatogr.*, 599 (1992) 227.
42. A. T. Balchunas and M. J. Sepaniak, *Anal. Chem.*, 59 (1987) 1466.
43. A. M. Dougherty, C. L. Woolley, D. L. Williams, D. F. Swaile, R. O. Cole and M. J. Sepaniak, *J. Liq. Chromatogr.*, 14 (1991) 907.
44. J. Towns and F. Regnier, *J. Chromatogr.*, 516 (1990) 69.

45. S. Hjertén and M. Kiesling-Johansson, *J. Chromatogr.*, 550 (1991) 811.
46. K. Cobb, V. Dolnik and M. Novotny, *Anal. Chem.*, 62 (1990) 2478.
47. D. Belder and G. Schomburg, *J. High Resolut. Chromatogr.*, 15 (1992) 686.

CHAPTER III

CAPILLARY ZONE ELECTROPHORESIS OF BIOLOGICAL
SUBSTANCES WITH SURFACE MODIFIED FUSED
SILICA CAPILLARIES HAVING SWITCHABLE
ELECTROOSMOTIC FLOW*

Abstract

A surface modification yielding fused-silica capillaries with switchable electroosmotic flow (anodal/cathodal) was developed. The capillary surface is a composite material consisting of unreacted silanol groups, a layer of positively charged quaternary ammonium functions, and a hydrophilic layer of long polyether chains. Due to the presence of positively and negatively charged groups, the net charge of the capillary surface can be varied from positive to negative by changing the pH of the running electrolyte, thus allowing the manipulation of the magnitude and direction of the electroosmotic flow. The long polyether chains were effective in shielding the charged inner surface of the capillary toward biomacromolecules, thus minimizing the electrostatic interactions of the solutes with the unreacted silanols and the introduced quaternary ammonium groups. As a consequence, high separation efficiencies were achieved with proteins, nucleotides and a series of acidic oligosaccharides.

* *J. T. Smith and Z. El Rassi, J. High Resolut. Chromatogr., 15 (1992) 573. Presented in part as a poster at the 4th International Symposium on Capillary Electrophoresis (HPCE'92), Amsterdam, The Netherlands, February 9-13, 1992.*

Introduction

One of the important features of capillary zone electrophoresis (CZE) with fused-silica tubes is its ability to separate oppositely charged solutes in a single run. This is facilitated by the phenomenon of electroosmosis, which is the bulk flow of the liquid through the capillary in the presence of an electric field. This flow can cause the migration of anionic, cationic and neutral species in one direction passing the detection point. When an electric field is applied to the capillary, solvated counterions in the diffuse region of the electric double layer at the silica-electrolyte solution interface migrate to the electrode of opposite sign and drag solvent with them, thus producing an electroosmotic flow (EOF) across the capillary tube [1]. The spatial distribution of ions in the electric double layer causes an electric potential to develop across the diffuse region, and is referred to as the ζ potential [2]. Under a given set of conditions, the flow-rate and direction of electroosmosis is dictated by the value and sign of the ζ potential of the capillary, respectively [3]. The magnitude of the ζ potential is influenced among other things by the charge density of the solid surface, whereas the polarity of this potential is determined by the net charge of the capillary surface [4]. It follows then that the velocity and direction of the EOF can be conveniently manipulated by varying the charge density and the sign of the net charge of the capillary surface, respectively.

Bare fused-silica capillaries possess a negative ζ potential. Thus, at a given applied voltage the EOF is in the direction of the cathode and its magnitude can be adjusted by the electrolyte pH. Although this feature is useful for certain applications, bare fused-silica capillaries are inadequate for the separation of positively charged species and especially proteins due to solute adsorption onto the negatively charged walls. This adsorptivity leads to band broadening and in some cases to irreversible adsorption of the solutes. Several approaches have been introduced to circumvent this undesirable property of bare fused-silica capillaries including (i) the use of buffers at high [5, 6] or low pH [7], i.e.,

above or below the isoelectric points of proteins, (ii) the inclusion of surface-active species in the running electrolyte [8], (iii) the addition of relatively high salt concentrations to the separation medium [9], (iv) the use of zwitterionic buffers with high salt concentrations [10] and (v) the chemical modification of the capillary surface [7, 11-18]. Among all these approaches, capillary surface modification by permanent attachment of hydrophilic coatings to the surface is the most desirable as far as the adjustment of selectivity with electrolyte pH is concerned.

For CZE, an ideal surface modification should minimize solute-wall interactions, maintain a moderate EOF and allow a systematic tuning of the velocity and direction of the flow while keeping the electric field strength relatively low. Under these conditions, the separations can be carried out at low current and consequently band broadening arising from Joule heating is minimized. In addition, a moderate EOF in the opposite direction to the electrophoretic mobility of the separated analytes would benefit the separations due to the fact that the charge on the solutes and on the capillary surface is of the same sign, which would minimize sorptive interactions [2].

Recently, a few approaches for the manipulation of EOF have been reported. Typical examples include the use of an additional electric field applied from outside of the capillary [19-21] and the coupling in series of capillaries with different magnitude of ζ potentials [22, 23].

The aim of this chapter is to provide surface modified capillaries with moderate EOF, the magnitude and direction of which can be readily manipulated in order to facilitate the separation of various species by CZE. The surface modification reported here involves the covalent bonding of quaternary ammonium functionalities to the inner surface of fused-silica capillaries via siloxane bonds and the subsequent attachment of a top hydrophilic layer of polyether chains. While the top polyether layer is to reduce electrostatic interactions of the separated analytes with the quaternary ammonium sublayer and the surface proper of the fused-silica, the charged sublayer is to change the charge density and

net charge of the capillary wall. At a given applied voltage, this surface modification yielded capillaries with an EOF whose direction and velocity can be varied by the pH of the running electrolyte, thus they are referred to as switchable flow capillaries. These capillaries were evaluated with proteins, small nucleic acids and acidic oligosaccharides, and characterized in terms of flow and separation efficiencies over a wide range of pH.

Experimental

Instrument

The instrument for capillary zone electrophoresis was assembled in-house from commercially available components, and resembles that previously reported [24]. It was constructed from a Spellman (Plainview, NY, USA) Model CZE1000/PN/R high-voltage power supply with positive and negative polarity and a Linear (Reno, NV, USA) Model 200 UV-VIS variable-wavelength detector equipped with a cell for on column detection. The electropherograms were recorded with a Shimadzu (Columbia, MD, USA) Model CR601 computing integrator.

Samples were introduced hydrodynamically, i.e., by gravity-driven flow, for a given period of time. The electroosmotic flow was determined from the migration time of phenol.

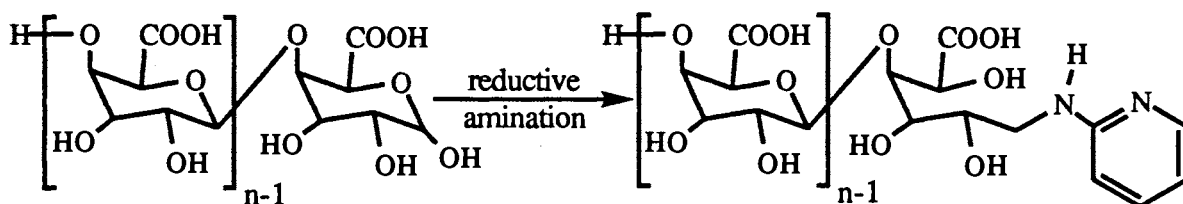
Materials

All proteins and nucleotides were purchased from Sigma (St. Louis, MO, USA). The galacturonic acid homooligosaccharides were a gift from Dr. Mort from the Department of Biochemistry at Oklahoma State University. Bis(2-hydroxyethyl)-aminopropyltriethoxysilane and trimethylethoxysilane were purchased from Hüls America Inc. (Bristol, PA, USA). Polyethylene glycol diglycidyl ether of M.W. 600 (diepoxy PEG

600) was purchased from Polysciences (Warrington, PA, USA). Polyethylene glycol of M.W. 200 (PEG 200), boron trifluoride etherate, phenol, sodium cyanoborohydride, 2-aminopyridine (2-AP), and iodomethane were obtained from Aldrich (Milwaukee, WI, USA). Reagent-grade sodium phosphate monobasic, sodium hydroxide, dioxane, and toluene were obtained from Fisher Scientific (Pittsburgh, PA, USA). Fused-silica capillaries with 50 μm I.D. and 375 μm O.D. were purchased from Polymicro Technology (Phoenix, AZ, USA). Deionized water was used to prepare the running electrolyte.

Sugar Derivatization

A series of galacturonic acid homooligosaccharides ranging from the dimer to the octadecamer were derivatized with 2-aminopyridine by reductive amination using a previously described method [25].



This labeling procedure allows sensitive UV and fluorescence detection of carbohydrates. Samples of the derivatized oligosaccharides were applied directly to CZE without the removal of excess 2-AP since only the acidic sugars migrated into the capillary in a negative polarity mode of separation.

Capillary Modification

A fused-silica capillary was first filled with an aqueous solution of 10% (v/v) bis(2-hydroxyethyl)-aminopropyltriethoxysilane and allowed to react at 90 °C for one hour. This treatment was repeated twice. After washing with water and methanol, the capillary was flushed with a methanolic solution at 30% (v/v) iodomethane and allowed to

react for 3 hours at 40 °C. Subsequently, the capillary was washed with methanol, and dioxane. Then the capillary was filled with a solution of dioxane containing 10% (v/v) diepoxy PEG 600 and 0.5% (v/v) boron trifluoride. This solution was allowed to react at 90 °C for 2 hrs. After washing with dioxane, the capillary was filled with 1% (v/v) boron trifluoride in dioxane, which was allowed to stay inside the capillary for 5 min. Thereafter, 5% (v/v) PEG 200 in dioxane was introduced into the capillary and allowed to stay twenty-five minutes at room temperature. These two-steps were repeated twice. Finally, after washing the capillary with dioxane and toluene, it was filled with a 10% (v/v) solution of trimethylethoxysilane in toluene and allowed to react overnight at room temperature. The capillaries were stored in HPLC-grade methanol.

Results and Discussion

Surface Modification

Figure 1 represents the idealized structure of the hydrophilic coating which yielded capillaries with switchable flow characteristics, i.e., anodal/cathodal. The modified surface is a composite material containing (i) quaternary ammonium functional groups sandwiched between a propylsilyl layer (i.e., sublayer) covalently attached to the surface of the capillary and a hydroxylated polyether top layer, (ii) end-capped silanol groups and (iii) unreacted silanol groups. The hydrophilic top layer is a network of polyether chains resulting from the reactions of diepoxy PEG 600 with the sublayer as well as with PEG 200. The diepoxy PEG 600 are attached to the sublayer through the hydroxyl groups of the quaternary ammonium functional groups. To open the remaining glycidyl group, the diepoxy PEG 600, after reacting at one end with the hydroxyl groups of the sublayer, would yield polyether chains having diol groups or would form longer polyether chains by either reacting with another diepoxy PEG 600 molecule or with PEG 200. These long

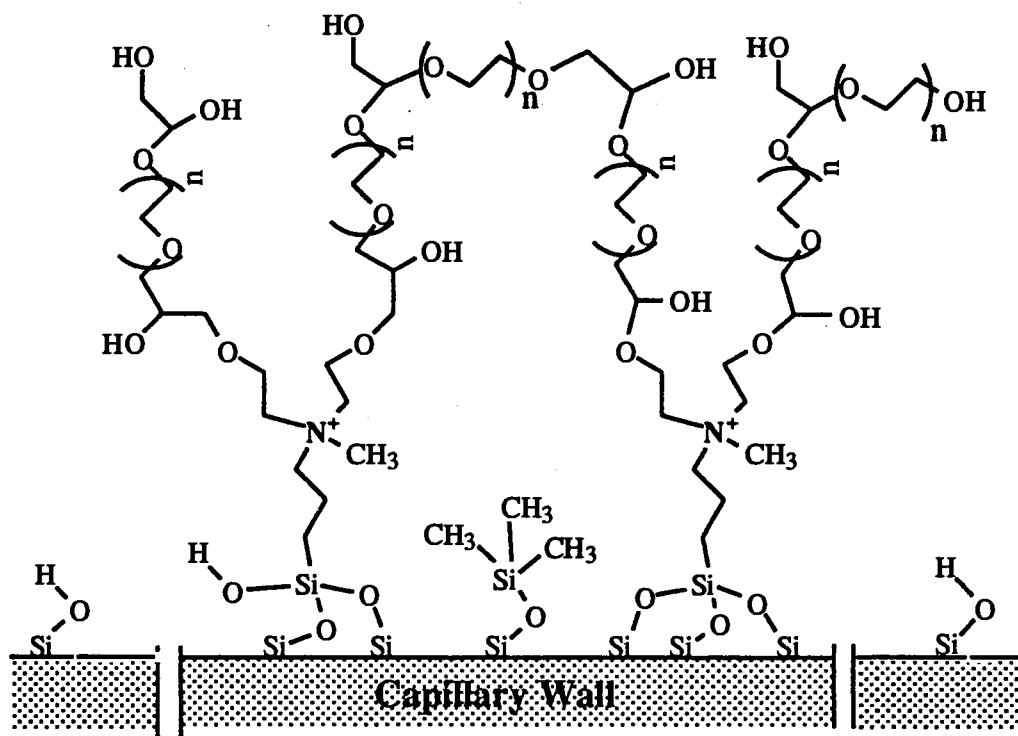


Figure 1. Schematic illustration of the idealized structure of the coating of switchable flow capillary.

polyether chains can either attach to an epoxy group already on the surface or stay unbound at the other end. Thus, a fuzzy polar top layer of polyether chains is formed.

The fuzzy top layer is to reduce electrostatic interactions of the solutes with either the quaternary ammonium functional groups or the unreacted silanols on the surface of the fused-silica capillary. In a recent report from our laboratory [17], this type of fuzzy polyether network has been shown to effectively shield the fused-silica surface toward proteins. The positively charged groups and the unreacted silanols are to keep certain electroosmotic flow across the capillary, and to change the direction of this flow.

It should be mentioned that the coating was quite reproducible, and after an initial 2 hours break-in period (i.e., preconditioning), the coated columns exhibited constant performance in terms of solute migration time, electroosmotic flow characteristics and separation efficiency for over 50-60 runs, in the pH range investigated (i.e., 3.5-7.0) using 0.10 M phosphate solutions as the running electrolytes.

Electroosmotic Flow

The above scheme of surface modification yielded hydrophilic capillaries with significantly different EOF characteristics than those obtained on untreated fused-silica capillary tubes. Figure 2 illustrates the results obtained at 20 kV in terms of plot of EOF versus pH over the range 3.5-7.0 using phenol as the inert tracer. As can be seen in Figure 2, the direction of the EOF changed from anodal to cathodal with increasing the pH of the running electrolyte. Inversion of EOF direction was also observed with capillaries having short chain polyethyleneimine coating [14] as well as on capillaries with surface immobilized proteins [16] or enzymes [26].

Anodal flow refers to the movement of the bulk solution towards the anode. This EOF occurs when the net charge on the surface of the capillary is positive (i.e., positive ζ potential). Under this condition, the diffuse region of the electric double layer is populated by negatively charged counter-ions which under the influence of an applied electric field

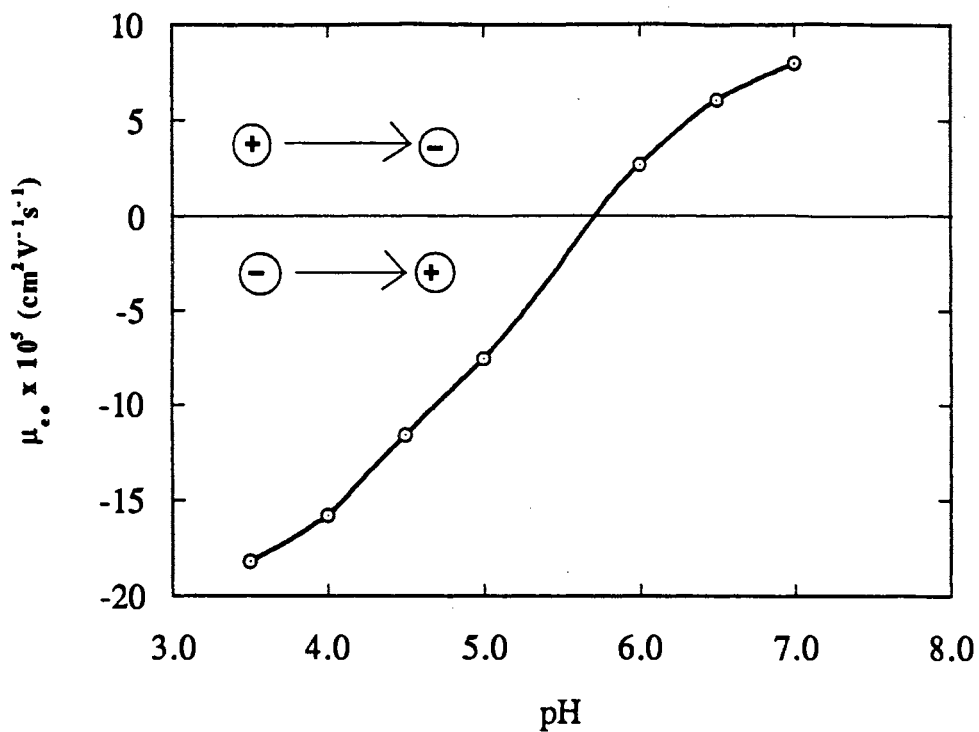


Figure 2. Plot of the electroosmotic flow obtained with the switchable flow capillary versus pH of the running electrolyte. Capillary, 80 cm total length x 50 μm I.D. (50 cm to detection point). Running electrolyte, 0.10 M phosphate solutions at different pH; applied voltage, 20 kV; detection, UV at 210 nm; inert tracer, phenol.

will migrate to the anode dragging with them the solvent. Cathodal EOF refers to an electroosmotic pumping in the direction of the cathode. The surface of the capillary is negatively charged (i.e., negative ζ potential), and therefore the diffuse layer is rich in positively charged counter-ions. When an electric field is applied, these solvated counter-ions will carry the solvent with them and migrate to the cathode.

The quaternary ammonium functional groups are fully ionized over a wide range of pH, whereas the silanol groups [14] start ionizing at pH 3.0 and at pH above 8.0 they are fully deprotonated. Therefore, at any pH, the flow-rate and polarity of EOF is determined by the relative concentration of both functional groups and by their degree of ionization. As expected, the net charge of the surface changed from positive at low pH to negative at high pH passing through neutral at an intermediate pH. At pH below 5.7, the capillary exhibited anodal electroosmotic flow, and the rate of this flow increased steadily as pH decreased. At pH above 5.7, a cathodal EOF was obtained the magnitude of which increased with pH. At approximately pH 5.7, the capillary exhibited no electroosmotic flow, thus indicating that the surface of the capillary has a net zero charge. This point in pH, i.e., pH 5.7, is referred to as the isoelectric point of the surface of the modified capillary.

Under a given set of conditions, the magnitude of the EOF is an inverse function of the viscosity of the medium [4]. In addition, the EOF originates near the location of the charges [2-4]. Although the local viscosity at the capillary wall is relatively high due to the presence of the cross linked network of polyether chains, a relatively strong electroosmotic flow has been obtained. With naked fused-silica capillaries, and in the absence of buffer additives, the EOF is negligible at pH below 4.0 and approaches zero at pH 3.5 [17]. With the switchable flow capillary, the magnitude of EOF at pH 3.5 using an applied voltage of 20 kV is relatively high (ca. 54 nL/min), and is nearly one third but opposite in direction to that obtained on naked fused-silica at pH 7.0. At pH 7.0, the EOF obtained on the switchable flow capillary is still relatively moderate (ca. 24 nL/min) and is

about 6 times less than that obtained on naked tubes. The switchable flow capillary has the virtue of allowing the tuning of the direction of EOF as well as permitting the operation at zero flow. These features would allow the separation of a wider range of species with a single capillary column.

Evaluation of the Surface Modification with Charged Species

Nucleotides. To assess the accessibility of the charged surface to small solutes, the switchable flow capillaries were evaluated with a mixture of mono-, and diphosphate nucleosides. As shown in Figure 3A and B, these acidic species were eluted as relatively sharp peaks using 0.10 M phosphate at pH 2.0 and 3.5 even though the net charge of the hydrophilic capillary is positive in this pH range. However, at pH above 5.0, the electrostatic interactions between the acidic solutes and the quaternary ammonium groups of the surface increased, and as a result excessive band broadening was observed at high pH. The pK_a values of the amino groups of guanine, adenine and cytidine moieties of the nucleotides are 2.1, 3.5 and 4.2, respectively, and the corresponding pK_a values of their primary and secondary phosphoric acids are ca. 0.7-0.9 and 5.8-6.6 [27]. Therefore, increasing the pH of the electrolyte increased the net negative charge of the nucleotides and concomitantly the magnitude of their electrostatic interactions with the charged coating of the capillary. These interactions were greatly reduced when 0.20 M instead of 0.10 M phosphate solutions were used as the running electrolytes. However, the trade-off was longer separation time since higher ionic strength increased the current and necessitated the use of 12 kV instead of 18 kV.

Nevertheless, these switchable flow capillaries were useful for the separation of nucleotides at low pH yielding relatively high separation efficiencies, see Figure 3A and B. It has to be noted that at pH 2.0 and an applied voltage of -18 kV, the current was relatively high due to the increase in the concentration of hydronium ions. To minimize Joule heating, the running voltage was dropped to -15 kV. This was not the case at pH

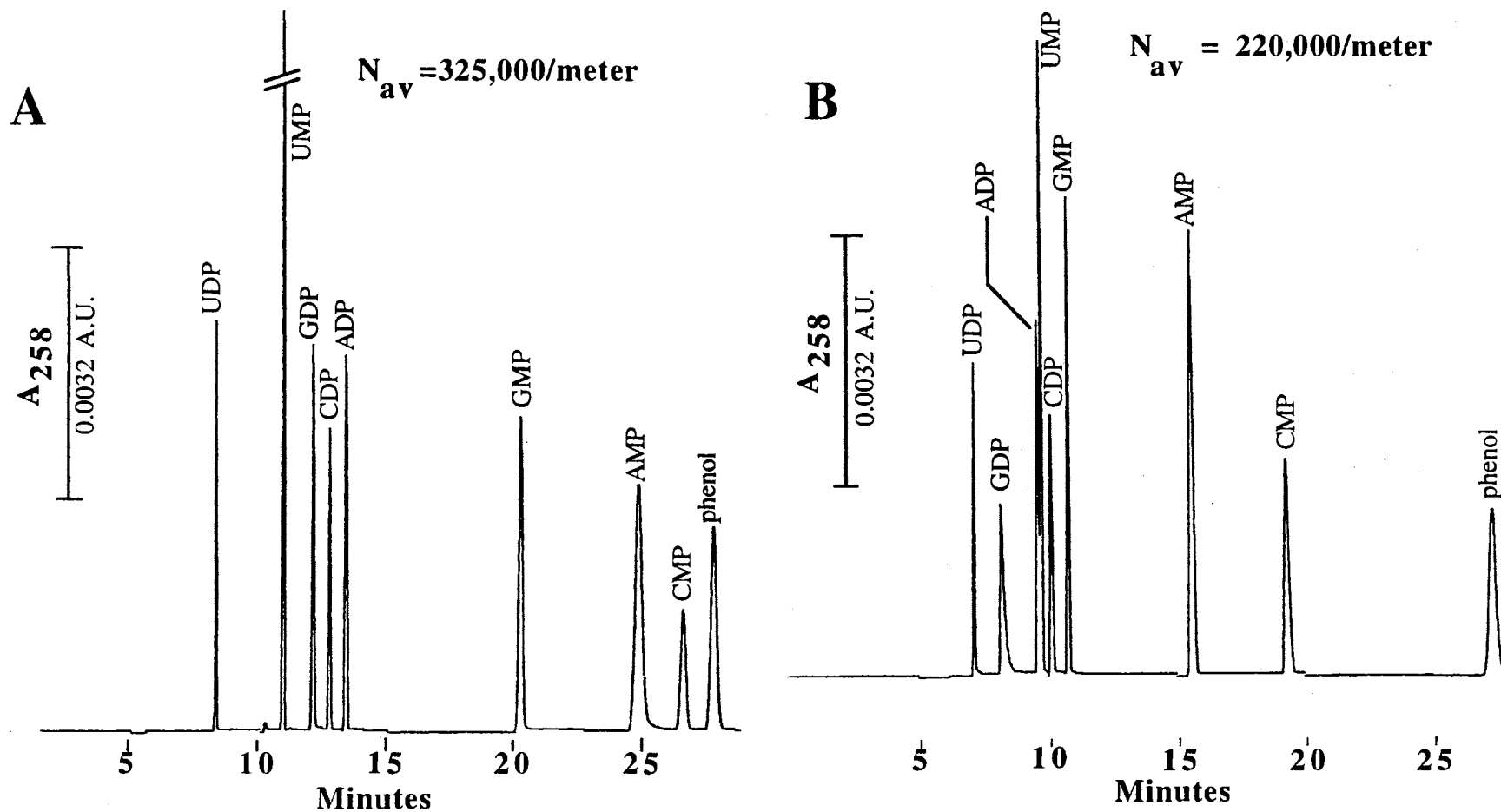


Figure 3. Electropherograms of mono- and diphosphate nucleosides obtained with the switchable flow capillary at pH 2.0 (A) and pH 3.5 (B). Running electrolyte, 0.10 M phosphate; hydrodynamic injection, 5 sec, 15 cm differential height; applied voltage, -15 kV in (A) and -18 kV in (B). Sample: UDP, uridine-5'-diphosphate; UMP, uridine-5'-monophosphate; GDP, guanosine-5'-diphosphate; GMP, guanosine-5'-monophosphate; ADP, adenosine-5'-diphosphate; AMP, adenosine-5'-monophosphate; CDP, cytidine-5'-diphosphate; CMP, cytidine-5'-monophosphate. Other conditions are the same as in Fig. 2.

3.5 and the electropherogram in Figure 3B was performed at -18 kV. Due to different currents at the two pH values, it was necessary to obtain the electropherograms in Figure 3A and B at different applied voltages and that may have led to changes in the observed separation efficiencies.

Although useful for the separations of small charged solutes under certain conditions, these capillaries were developed for large biomacromolecules.

Proteins. Figure 4A and B illustrates typical electropherograms of model basic proteins obtained on the switchable flow capillaries at +18 kV using 0.10 M phosphate solutions as the running electrolyte at pH 4.0 and 7.0, respectively. The average plate count per meter, N_{av} , is indicated on each electropherogram. These high separation efficiencies suggest that electrostatic interactions between the positively charged solutes and the inner surface of the capillaries, i.e., untreated silanol groups, are greatly reduced. At pH 4.0, the positively charged groups introduced by the coating may have promoted coulombic repulsion between the capillary surface and the positively charged proteins. At pH 7.0, the capillary surface has a net negative charge as indicated by the direction of the EOF, see Figure 2. However, at this pH the theoretical plate number was as high as that obtained at pH 4.0, a fact that may indicate that the electrostatic field above the capillary surface was only accessible for the binding of small charged solutes (see above) and electrolyte counterions, whereas the larger positively charged solutes (i.e., proteins) were effectively hindered by the long polyether chains from undergoing any significant interactions with the negatively charged electrostatic field.

Figure 5 represents the plots of migration time versus electrolyte pH for the basic proteins. The "U" shaped curves may be explained as follows. At pH < 5.0, the fact that the electroosmotic mobility is in the opposite direction to the electrophoretic mobility, and the magnitude of EOF increased with decreasing pH may have resulted in reducing the net mobility of the proteins, i.e., longer migration time. At pH of ca. 5.0, the migration time

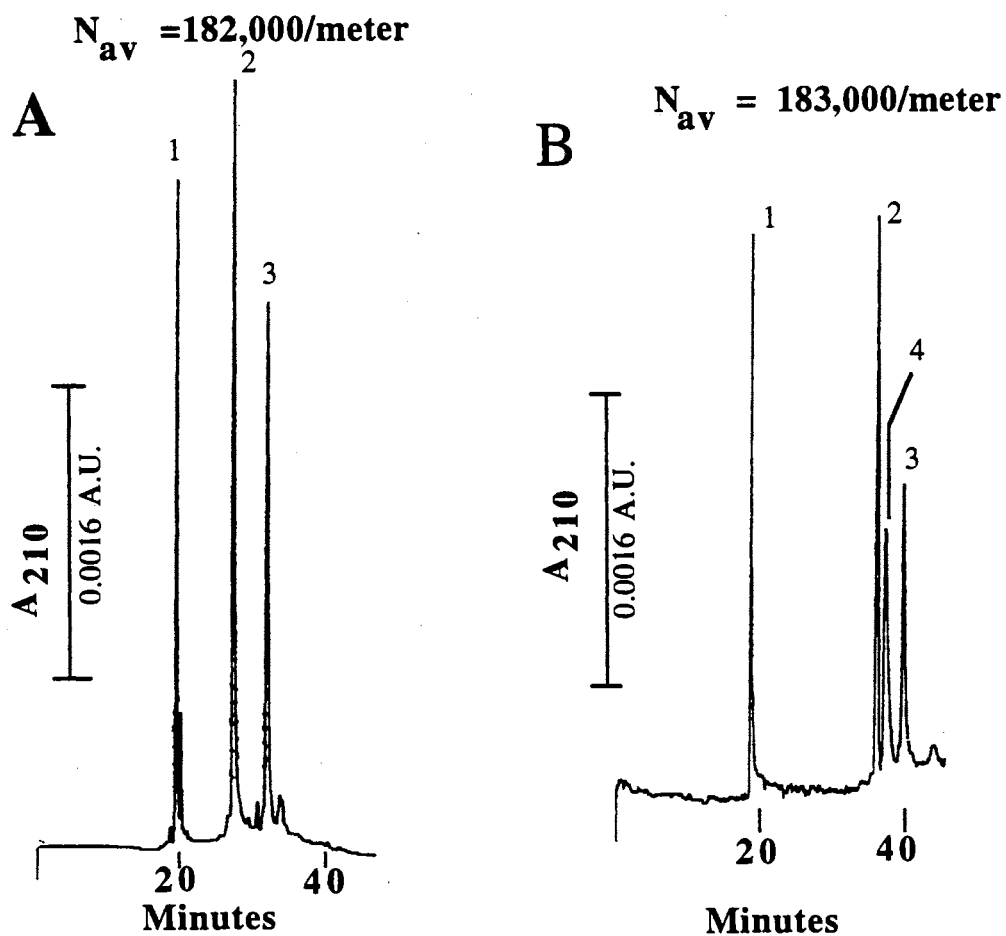


Figure 4. Typical electropherograms of basic proteins obtained with the switchable flow capillary at pH 4.0 (A) and pH 7.0 (B). Capillary, 80 cm total length x 50 μm I.D. (50 cm to detection point). Running electrolyte, 0.10 M phosphate; hydrodynamic injection, 5 sec, 20 cm differential height; applied voltage, +18 kV; detection, UV at 210 nm. Proteins: 1, lysozyme, $pI = 11.0$; 2, ribonuclease A, $pI = 9.4$; 3, α -chymotrypsinogen A, $pI = 9.5$; 4, ribonuclease S, $pI \leq 9.4$.

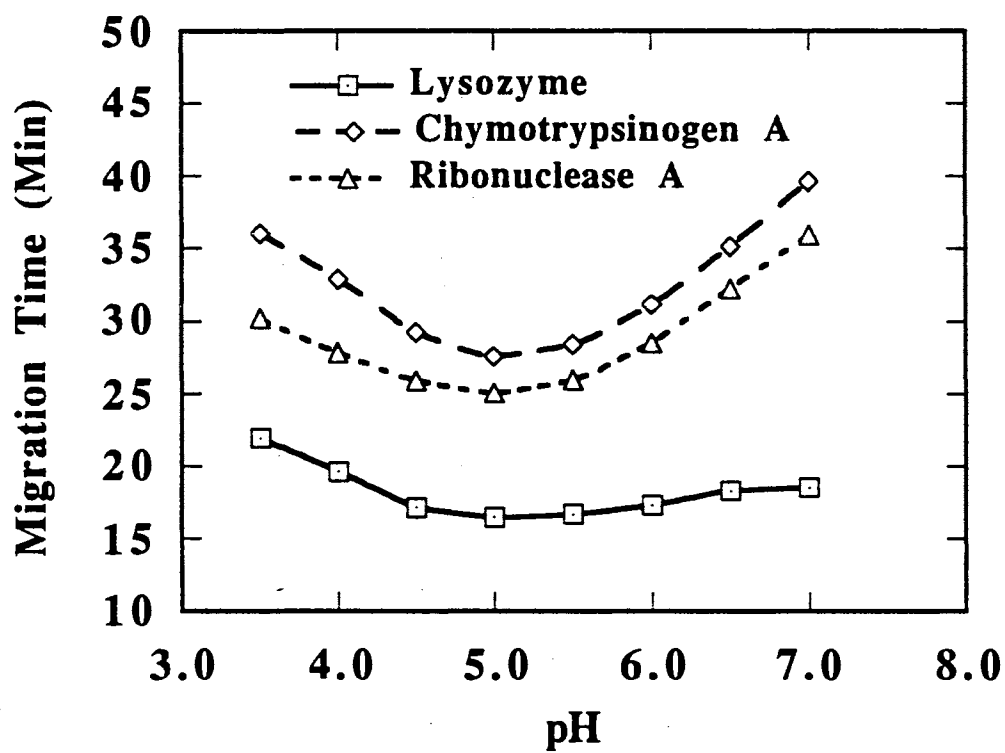


Figure 5. Plot of migration time versus electrolyte pH for basic proteins obtained with the switchable flow capillary. Conditions are the same as in Fig. 4.

has reached a minimum because at this pH the EOF approached zero but the proteins still retained a relatively high net positive charge. At higher pH, both the electroosmotic and electrophoretic mobilities are in the same direction but are lower in magnitude which would explain the increase in migration time at pH 6.0 and 7.0. It should be noted that due to its higher pI value, lysozyme had a migration time which was less affected by the pH than for the other two proteins .

Unlike the control of EOF by an external field [20, 21], the approach of switchable flow capillaries for tuning the EOF involves the manipulation of the electrolyte pH, a parameter that can also affect the electrophoretic mobilities of the analytes. As can be seen in Figs 4 and 5, this unique feature of switchable flow capillaries can bring about the modulation of the relative migration time of the analytes.

Acidic Oligosaccharides. To demonstrate their usefulness for medium molecular weight solutes, the switchable flow capillaries were evaluated with a mixture of 2-aminopyridyl derivatives of galacturonic acid homooligosaccharides (2AP-(GalA)_n). A typical electropherogram obtained at pH 6.5 is portrayed in Figure 6. The tentative identity of the peaks was determined from the migration times of authentic samples of pentamer and undecamer, and from graphical extrapolation using the linear plot of the logarithmic migration time versus the logarithmic degree of polymerization shown in Figure 7. This linear relationship is in agreement with data reported by Liu *et al.* [28] on the CZE of oligogalacturonide homologous series in open-tubular capillaries. As can be seen in Fig. 6, the resolution between the homologues decreased with increasing number of recurring units because of the unfavorable mass-to-charge ratio at high degree of polymerization.

The acidic homooligosaccharides did not show significant electrostatic interactions with the coating over the pH range 3.0-7.0. The carboxyl groups of these oligosaccharides are rather weak acids, and as the degree of polymerization increases the accessibility of the charges of the capillary to these solutes would decrease. The separation

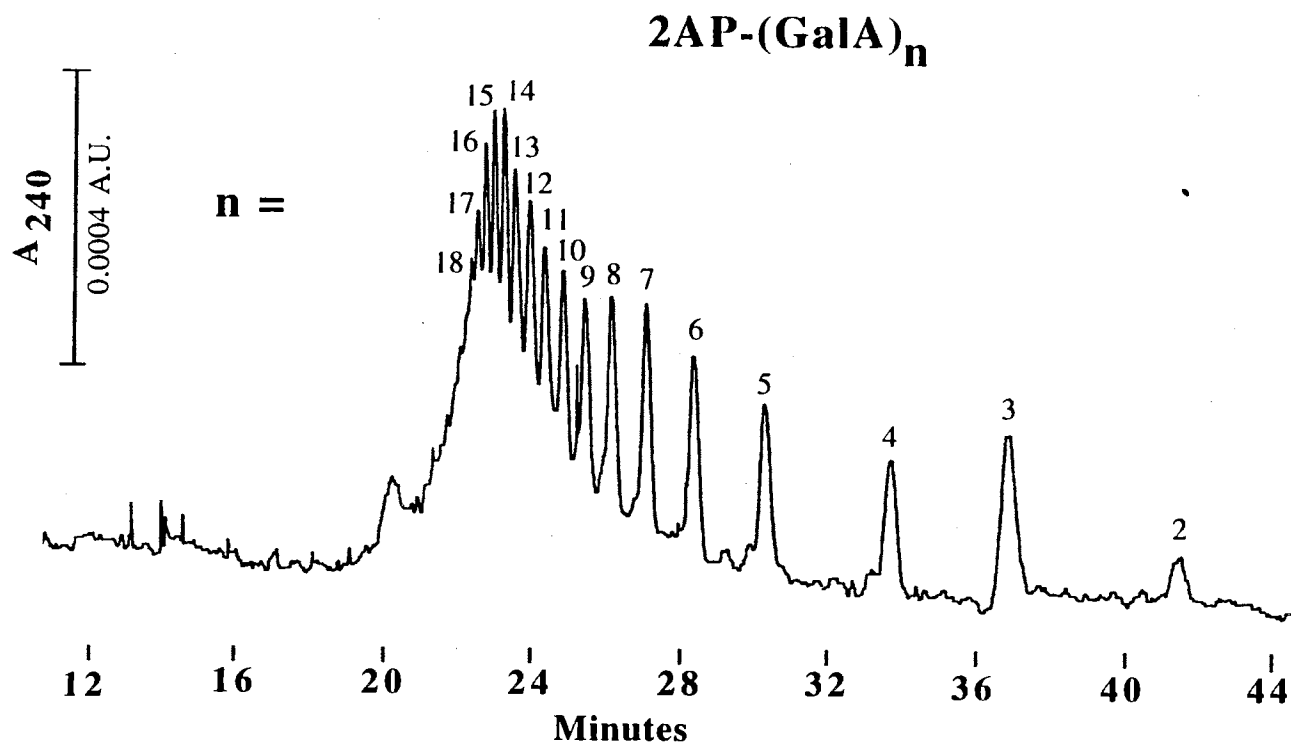


Figure 6. Electropherogram of 2-aminopyridyl derivatives of oligogalacturonide homologous series obtained with the switchable flow capillary at pH 6.5. Running electrolyte, 0.10 M phosphate; hydrodynamic injection, 10 sec, 20 cm differential height; applied voltage, -15 kV; detection, UV at 240 nm. Other conditions are the same as in Fig. 2.

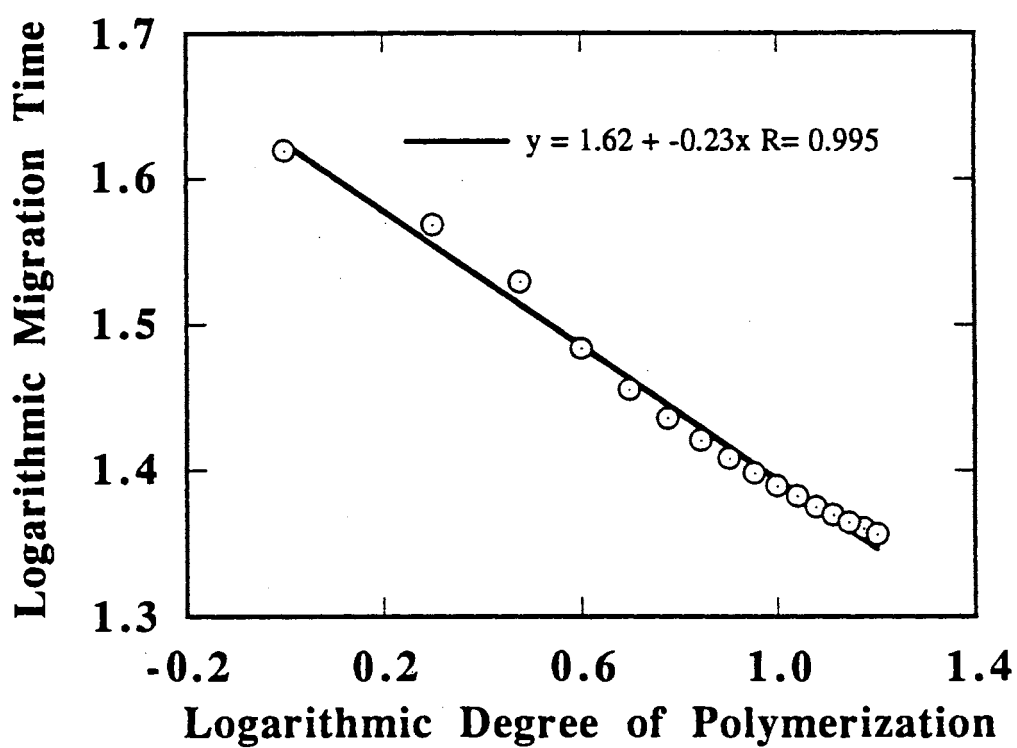


Figure 7. Plot of the logarithmic migration time of 2AP-(GalA)_n versus the logarithmic degree of polymerization. Conditions are the same as in Fig. 6.

of these oligosaccharides was best achieved at pH 6.5, since at this pH the EOF is low and is in opposite direction to the electrophoretic mobility of the solutes.

Acknowledgement

This work was supported in part by the Dean Incentive Grant program at Oklahoma State University. J. T. Smith is the recipient of a Water Resources Presidential Fellowship from the University Center for Water Research at Oklahoma State University.

References

1. T. S. Stevens and H. J. Cortes, *Anal. Chem.*, 55 (1983) 1365.
2. E. Heftmann, "*Chromatography*", 2nd ed., Reinhold, New York, 1976, pp. 210-251.
3. R. J. Hunter, "*Zeta Potential in Colloid Science: Principles and Applications*", Academic Press, New York, 1981.
4. C. J. O. R. Morris and P. Morris, "*Separation Methods in Biochemistry*", 2nd ed., Wiley, New York, 1976, pp. 703-760.
5. H. H. Lauer and D. McManigill, *Anal. Chem.*, 58 (1986) 166.
6. Y. Walbroehl and J. W. Jorgenson, *J. Microcol. Sep.*, 1 (1989) 41.
7. R. M. McCormick, *Anal. Chem.*, 60 (1988) 2322.
8. A. Emmer, M. Jansson and J. Roeraade, *J. Chromatogr.*, 547 (1991) 544.
9. J. S. Green and J. W. Jorgenson, *J. Chromatogr.*, 478 (1989) 63.
10. M. M. Bushey and J. W. Jorgenson, *J. Chromatogr.*, 480 (1989) 301.
11. S. Hjertén, *J. Chromatogr.*, 347 (1985) 191.
12. G. J. M. Bruin, J. P. Chang, R. M. Kuhlman, K. Zegers, J. C. Kraak and H. Poppe, *J. Chromatogr.*, 471 (1989) 429.
13. S. A. Swedberg, *Anal. Biochem.*, 185 (1990) 51.
14. J. K. Towns and F. E. Regnier, *J. Chromatogr.*, 516 (1990) 69.
15. K. A. Cobb, V. Dolnik and M. Novotny, *Anal. Chem.*, 62 (1990) 2478.
16. Y.-F. Maa, K. J. Hyver and S. A. Swedberg, *J. High Resolut. Chromatogr.*, 14 (1991) 65.
17. W. Nashabeh and Z. El Rassi, *J. Chromatogr.*, 559 (1991) 367.
18. A. M. Dougherty, C. L. Woolley, D. L. Williams, D. F. Swaile, R. O. Cole and M. J. Sepaniak, *J. Liq. Chromatogr.*, 14 (1991) 907.

19. C. S. Lee, W. C. Blanchard and C.-T. Wu, *Anal. Chem.*, 62 (1990) 1550.
20. C.-T. Wu, T. Lopes, B. Patet and C. S. Lee, *Anal. Chem.*, 64 (1992) 886.
21. M. A. Hayes and A. G. Ewing, *Anal. Chem.*, 64 (1992) 512.
22. W. Nashabeh and Z. El Rassi, *J. High Resolut. Chromatogr.*, 15 (1992) 289.
23. W. Nashabeh and Z. El Rassi, *J. Chromatogr.*, 632 (1993) 157.
24. J. Cai, J. T. Smith and Z. El Rassi, *J. High Resolut. Chromatogr.*, 15 (1992) 30.
25. N. A. Maness, E. T. Miranda and A.J. Mort, *J. Chromatogr.*, 587 (1991) 177.
26. W. Nashabeh and Z. El Rassi, *J. Chromatogr.*, 596 (1992) 251.
27. D. O. Jordan, "*The Chemistry of Nucleic Acids*", Butterworths & Co., Ltd., London, 1960, p. 137.
28. J. Liu, O. Shirota and M. Novotny, *J. Chromatogr.*, 559 (1991) 223.

CHAPTER IV

CAPILLARY ZONE ELECTROPHORESIS OF BIOLOGICAL
SUBSTANCES WITH FUSED SILICA CAPILLARIES
HAVING ZERO OR CONSTANT
ELECTROOSMOTIC FLOW*

Abstract

A series of capillary surface modifications entailing multilayered coatings were introduced and evaluated in capillary zone electrophoresis of biological substances, e.g., proteins, peptides, oligosaccharides and nucleotides. In one set of surface modifications, a high molecular weight hydroxypropyl cellulose coating afforded "zero" flow capillaries, which were used as precursors for developing anodal flow capillaries. When "zero" flow capillaries were further functionalized with a charged polyethyleneimine layer, to which a top polyether layer was covalently attached, the resulting anodal electroosmotic flow was relatively weak due to the high viscosity of the coated wall imparted by the hydroxypropyl cellulose layer. Capillaries with relatively strong and constant anodal electroosmotic flow were best achieved when the inner capillary surface was first chemically derivatized with methylated (i.e., quaternized) polyethyleneimine hydroxyethylated. This hydroxylated and permanently charged polymeric coating yielded constant anodal flow regardless of electrolyte pH. The hydroxyl groups of the charged polymeric coating permitted the covalent attachment of polyether chains, which minimized electrostatic interaction between

* J. T. Smith and Z. El Rassi, *Electrophoresis*, 14 (1993) 396. Presented as a part of a poster at the 4th International Symposium on High Performance Capillary Electrophoresis (HPCE'92), Amsterdam, The Netherlands, February 9-13, 1992.

the positive charges of the polymeric layer and oppositely charged biopolymers. Under these conditions, rapid transport of acidic biopolymers past the detection point in the separation capillary could be achieved, and relatively high plate counts were obtained.

Introduction

Capillary surface modification has been an area of active research since the introduction of capillary electrophoresis. This has been prompted by the fact that basic solutes, and especially proteins, undergo adsorption onto the surface of bare fused silica capillaries. The solute-silanol interactions lead to band broadening and in some instances to irreversible adsorption.

Thus far, various capillary surface modifications have been reported. While some of these modifications inhibited the electroosmotic flow (EOF) [1-3], other coatings have been designed to keep a certain levels of EOF in order to permit the analysis of oppositely charged species in a single run [4-7]. Our laboratory has focused on the second aspect, and introduced capillaries with polyether coatings [5] at various level of EOF as well as capillaries with ionic-polyether coatings having switchable anodal/cathodal EOF [8].

In capillary zone electrophoresis, solutes can be rapidly transported past the detection point when the net charge of the migrating species is opposite in sign to the ζ potential of the capillary wall. This is because, under these circumstances, the EOF is in the same direction as the electrophoretic migration of the analytes. Thus, capillaries with inert hydrophilic coatings having moderate cathodal EOF are not sufficient to bring about the rapid analysis of acidic proteins unless they are coupled in series with untreated fused silica tubes as shown elsewhere [9-11], whereby the average EOF of the coupled capillaries becomes relatively strong and pulls acidic proteins toward the detection end of the capillary. Alternatively, with coated capillaries having cathodal EOF, the rapid transport of acidic proteins past the detection point can be only achieved at relatively high

pH and high voltage. However, these conditions can lead to denaturation of proteins, system overheating and hydrolytic degradation of the coatings.

Thus far, few reports have appeared describing ways to provide an anodal EOF. Typically, the anodal EOF was achieved by coating the capillary surface with a crosslinked layer of PEI [7] and *in situ* by adding a cationic fluorosurfactant [12], or cationic spermine [13] or an amphiphatic polymer [14] to the running electrolyte. However, these coatings were limited to the analysis of basic proteins that were repulsed electrostatically from the positively charged coating. While the PEI and spermine coated capillaries were shown to provide an anodal EOF the magnitude of which was pH dependent, there was no data on how the magnitude of EOF generated by the fluorosurfactant or the amphiphatic polymer varied with electrolyte pH.

To our knowledge, no attempt has been made to provide capillary coatings with constant anodal EOF, which can be used in the analysis of acidic species. In this chapter, which represents an extension of our recent work on ionic-hydrophilic coatings [8], our goal is to provide a better understanding of the impact of chemical modifications on the properties of the silica surface and, consequently, on the magnitude and polarity of the EOF. In this regard, we have performed some preliminary studies with capillaries having multilayered coatings. In these attempts, our primary goal was to produce capillaries with constant anodal EOF (i.e., the magnitude of EOF is independent of electrolyte pH) the positive charge of which are sufficiently shielded toward proteins. Coated capillaries with constant EOF would permit the modulation of the relative migration (i.e., separative transport) of solutes with electrolyte pH while providing a constant flow transport across the separation channel.

To achieve a constant anodal flow while minimizing solute-surface interactions, the following criteria must be met: (i) the contribution of silanols to the net charge of the coating must be eliminated, (ii) the net positive charge of the coating must be independent of pH and (iii) the electrostatic field of the surface must be shielded towards proteins but

accessible to the binding of the electrolyte anionic counterions. The last criterion is essential in order to reduce protein-coating interaction and to allow an EOF to develop. In this study, the first and second criteria were met by two different routes. In the first approach, the surface silanols were sealed off with an inert polymeric network that also generated a viscous wall, and then a positively charged layer was attached to the inert polymeric coating. In the second approach, a branched polymeric network containing quaternary ammonium groups was covalently attached to the capillary inner wall. While the quaternary ammonium groups located at the side of the branched polymeric network facing the capillary wall have canceled the charges of surface silanols by an ion-pair mechanism, the solvent exposed quaternary ammonium groups provided the sites for bindings of small electrolyte counterions, thus producing the anodal EOF. In both approaches, the third criterion was met by covalently attaching a hydrophilic layer to the positively charged network. This bulky layer hindered proteins from coming into close contact with the positively charged layer. As will be shown below, the second approach was more effective in terms of allowing a higher anodal EOF to be realized, and it involved less chemical reaction steps.

Experimental

Reagents and Materials

Lysozyme from chicken egg white, ribonuclease A from bovine pancreas, albumin and iron saturated transferrin both from human serum, α -lactalbumin and β -lactoglobulin A both from bovine milk, soybean trypsin inhibitor, glutamine, bradykinin potentiator C, Val-Gly-Ser-Glu, and Phe-Leu-Glu-Glu-Val, adenosine-5'-, guanosine-5'-, cytidine-5'- and uridine-5'-mono- and diphosphate were purchased from Sigma (St. Louis, MO, U.S.A.). Galacturonic acid homooligosaccharides were derivatized with 2-aminopyridine using well established procedures [8]. Polyethyleneimine hydroxyethylated (PEIHE) with

a molecular weight of 60,000-80,000, polyethyleneimine (PEI) with a molecular weight of 1,800, polyethylene glycol 200 diglycidyl ether (diepoxy PEG 200), polyethylene glycol 600 diglycidyl ether (diepoxy PEG 600) and triglycidoxyglycerol were purchased from Polysciences Inc (Warrington, PA, U.S.A.). Hydroxypropyl cellulose (HPC) 3-6 cps, 150-400 cps and 1,000-4,000 cps, which correspond to molecular weights of 30,000-50,000, 150,000 and 400,000, respectively, were purchased from TCI America (Portland, OR, U.S.A.). γ -Glycidoxypropyltrimethoxysilane was a gift from Dow Corning (Midland, MI, U.S.A.). *N,N*-Dimethylformamide (DMF), triethylamine (TEA), boron trifluoride etherate (BF₃), formaldehyde, formic acid, chloroform, polyethylene glycol (PEG) of molecular weight 2000, 1,4-butanediol diglycidyl ether and iodomethane were purchased from Aldrich (Milwaukee, WI, U.S.A.). Reagent grade sodium phosphate monobasic, phosphoric acid and sodium hydroxide were purchased from Fisher Scientific (Pittsburgh, PA, U.S.A.). Phenol which was used as an inert tracer for measuring the EOF was obtained from J. T. Baker Inc. (Phillipsburg, NJ, U.S.A.). Fused silica capillaries of 50 μ m i.d. and 375 μ m o.d. were purchased from Polymicro Technology (Phoenix, AZ, U.S.A.). Deionized water was used to prepare the running electrolyte.

Capillary Electrophoresis Instrument

Capillary zone electrophoresis was performed on instrumentation assembled in-house from commercially available components: a Spellman (Plainview, NY, U.S.A.) Model CZE1000/PN/R high voltage power supply with positive and negative polarities and a Linear (Reno, NV, U.S.A.) Model 200 UV/Vis variable wavelength detector equipped with a cell for on-column detection. The equipment resembles that previously reported [8,15]. Electropherograms were recorded with a Shimadzu (Columbia, MD, U.S.A.) Model CR601 computing integrator. Samples were introduced hydrodynamically, i.e., by gravity-driven flow, for an appropriate period of time.

Alkylation of Polyethyleneimine Hydroxyethylated

The aqueous solution of PEIHE was rotary evaporated under reduced pressure (6 mm Hg) to remove as much of the water from the commercial product as possible. A mixture of 50 mL of DMF, 1.0 g of PEIHE and 3 mL of iodomethane was stirred at room temperature for 10 h, then an additional 3 mL of iodomethane were added and the solution was allowed to stir for another 10 h at room temperature. Next, the reaction mixture was rotary evaporated to remove unreacted iodomethane and DMF. The resulting mixture was washed with methanol (3 x 30 mL). The methanol soluble product was rotary evaporated, and named polyethyleneimine hydroxyethylated derivative (PEIHED). On the other hand, the methanol insoluble residue was dried to remove residual solvents. The semi-solid material thus obtained is referred to as methylated polyethyleneimine hydroxyethylated (MPEIHE). ^1H and ^{13}C NMR data of both PEIHED and MPEIHE were acquired by the Departmental 400 MHz Varian instrument.

Modification of the Capillary Surface

The various surface modifications developed in this study are summarized in Table I. This table lists the EOF properties, the acronyms and the composition of the different capillary coatings.

Zero Flow (ZF) Coatings. Fused silica capillaries were first filled with an aqueous solution of 5 % (v/v) γ -glycidoxypropyltrimethoxysilane and then allowed to react for 30 min at 95 °C. This treatment was repeated twice. After washing with water and then DMF, the capillary was flushed with a solution of 1% (v/v) BF_3 in DMF. After 5 min, the capillary was filled with a 3% (w/v) solution of HPC 6-10 cps in DMF and allowed to react for 20 min at room temperature. This treatment was repeated twice. Thereafter, the capillary was flushed with water for 30 min using a syringe pump. The capillary was then filled with a solution composed of the following: 20 mL of water, 0.10 g of HPC 150-400

Table 1. Summary of the EOF properties, coding and composition of the capillary coatings developed in this study.

EOF Properties of Capillary Coatings	Capillary Code	Coating Composition				
		First layer of the coating	Second layer of the coating	Third layer of the coating	Fourth layer of the coating	Fifth layer of the coating
Zero flow	ZF-1	γ -Glycidoxypropyl-siloxane	HPC 6-10 cps	HPC 150-400 cps crosslinked with formic acid/formaldehyde	None	None
	ZF-2	γ -Glycidoxypropyl-siloxane	HPC 6-10 cps	HPC 1,000-4,000 cps crosslinked with formic acid/formaldehyde	None	None
Variable anodal flow	VAF-1	γ -Glycidoxypropyl-siloxane	HPC 6-10 cps	HPC 150-400 cps crosslinked with formic acid/formaldehyde	PEI-triglycidoxy-glycerol	PEG 2000-diepoxy PEG 600
	VAF-2	γ -Glycidoxypropyl-siloxane	PEIHED	Diepoxy PEG 200-diepoxy PEG 600	None	None
Constant anodal flow	CAF-1	γ -Glycidoxypropyl-siloxane	MPEIHE crosslinked with 1,4-butanediol-diglycidyl ether	None	None	None
	CAF-2	γ -Glycidoxypropyl-siloxane	MPEIHE	Diepoxy PEG 200-diepoxy PEG 600	None	None

cps or 1,000-4,000 cps, 2.0 mL of formic acid and 10 mL of formaldehyde. This acidified HPC solution was allowed to adsorb onto the capillary surface for 5 min, and subsequently the capillary was purged with nitrogen gas. Thereafter, the capillary was baked at 140 °C for 40 min [1]. The last two steps were repeated 4 times. Finally, the capillary was flushed with water for 3 h and then stored in methanol. The capillaries having surface-bound HPC 150-400 cps are referred to as ZF-1, while the capillaries coated with HPC 1,000-4,000 cps are denoted ZF-2.

Variable Anodal Flow Coating of Type VAF-1. The ZF-1 capillary prepared according to the above procedure was filled with a 10% (w/v) methanolic solution of PEI, which was allowed to adsorb onto the capillary surface at room temperature for 4 hrs. Following, the capillary was purged with nitrogen gas for 30 min. Thereafter, a mixture composed of 15 % (v/v) triglycidoxylglycerol, 30 % (v/v) TEA and 55 % (v/v) chloroform was introduced into the column, and allowed to adsorb for 1 hr. Next, the capillary was flushed with nitrogen gas for 40 min and then baked at 80 °C for 30 min. After washing thoroughly with water followed by DMF, the capillary was filled with a solution of 1% (v/v) BF₃ in DMF. This solution was allowed to adsorb onto the capillary surface for 5 min. Subsequently, the capillary was filled with an equimolar mixture of diepoxy PEG 600 and PEG 2000 in DMF and allowed to react for 20 min. The last two steps were repeated twice. Finally, the capillary was washed with water, followed by methanol. The capillaries thus obtained are referred to as VAF-1.

Constant Anodal Flow Coating of Type CAF-1. Fused silica capillaries were first filled with an aqueous solution of 5 % (v/v) γ -glycidoxypropyltrimethoxysilane and then allowed to react at 95°C for 30 min. This treatment was repeated twice. Thereafter, the capillary was filled with a solution of 5% (w/v) MPEIHE in DMF, which was allowed to adsorb onto the capillary surface for 4 hrs. Next, the capillary was purged with nitrogen gas for 30 min. Following, a mixture composed of 60 % (v/v) 1,4-butanediol diglycidyl

ether and 40 % (v/v) TEA was introduced into the capillary and allowed to sit for 40 min. After flushing with nitrogen gas for 30 min, the capillary was baked at 85 °C . Finally, the capillary was washed with water for 1 h and then stored in methanol. These capillaries are referred to as CAF-1.

Anodal Flow Coatings of Types VAF-2 and CAF-2. Fused silica capillaries were first filled with an aqueous solution of 5 % (v/v) γ -glycidoxypropyltrimethoxysilane and then allowed to react at 95 °C for 30 min. This treatment was repeated twice. The capillaries were then filled with 5% (w/v) mixture of MPEIHE in DMF or a 5% (w/v) methanolic solution of PEIHED. In both cases, the solutions were allowed to adsorb onto the surface of the capillary columns at room temperature for 4 h. This was followed immediately by purging with nitrogen gas for 40 min. Next, the capillaries were filled with a mixture composed of 10% (v/v) diepoxy PEG 200, 10% (v/v) diepoxy PEG 600, 30% (v/v) TEA and 50% (v/v) DMF and allowed to sit at room temperature for 4 h. After purging with nitrogen gas for 40 min, the capillaries were baked at 85°C for 40 min. Subsequently, the capillaries were washed with water for 1 h and then stored in methanol. The capillaries treated with PEIHED are denoted as VAF-2, while those coated with MPEIHE are referred to as CAF-2.

Results and Discussion

Alkylation of PEIHE

To generate hydrophilic-ionic coatings with constant EOF, a polymeric species with a constant charge density over a wide range of pH is needed. In this regard, we have attempted the alkylation of polyethyleneimine hydroxyethylated, which in principle should yield a polymeric network with quaternary ammonium functions. PEIHE is a highly branched polymer derived from the parent polymer PEI. Because it is hydroxyethylated,

PEIHE contains primarily tertiary amines. The hydroxyl functions are needed for further attachment of other functionalities to the polymer or for crosslinking. Due to charge repulsion and geometrical constraints, it is unlikely that the methylation of PEIHE would be complete. In fact, upon dissolving the methylation reaction mixture in methanol (see Materials and methods) two products were readily identified. One set of products dissolved in methanol and is referred to as PEIHED. It is believed to be composed primarily of lower molecular weight fragments that resulted from cleavage of the polymer as well as remaining underivatized or partially methylated PEIHE. The other product (MPEIHE) was insoluble in methanol and precipitated out, which is consistent with the formation of an ammonium salt. NMR data (spectra not shown) for MPEIHE showed significant deshielding and an up field shift of ethylene protons as well as the presence of methyl groups. These shifts correspond to those found in Ref. 16. Due to the high molecular weight and the resulting reduction in symmetry of the polymer, NMR signals were very broad and individual signal assignments could not be made.

Surface Modifications

Figure 1 represents the idealized structures of a series of hydrophilic or hydrophilic-ionic coatings, which yielded ZF or anodal flow capillaries, respectively. For clarity the coatings are also summarized in Table I. In all cases, the capillaries were designed to meet the following criteria: (i) to reduce biopolymer interactions with the capillary wall and/or the deliberately introduced charges, (ii) to be chemically stable over a wide pH range and (iii) to yield constant performance so that reproducible separations can be achieved.

The ZF capillaries were developed for potential use as precursors for anodal flow tubes. In addition, we were interested in assessing their usefulness in CZE of proteins and other biological substances.

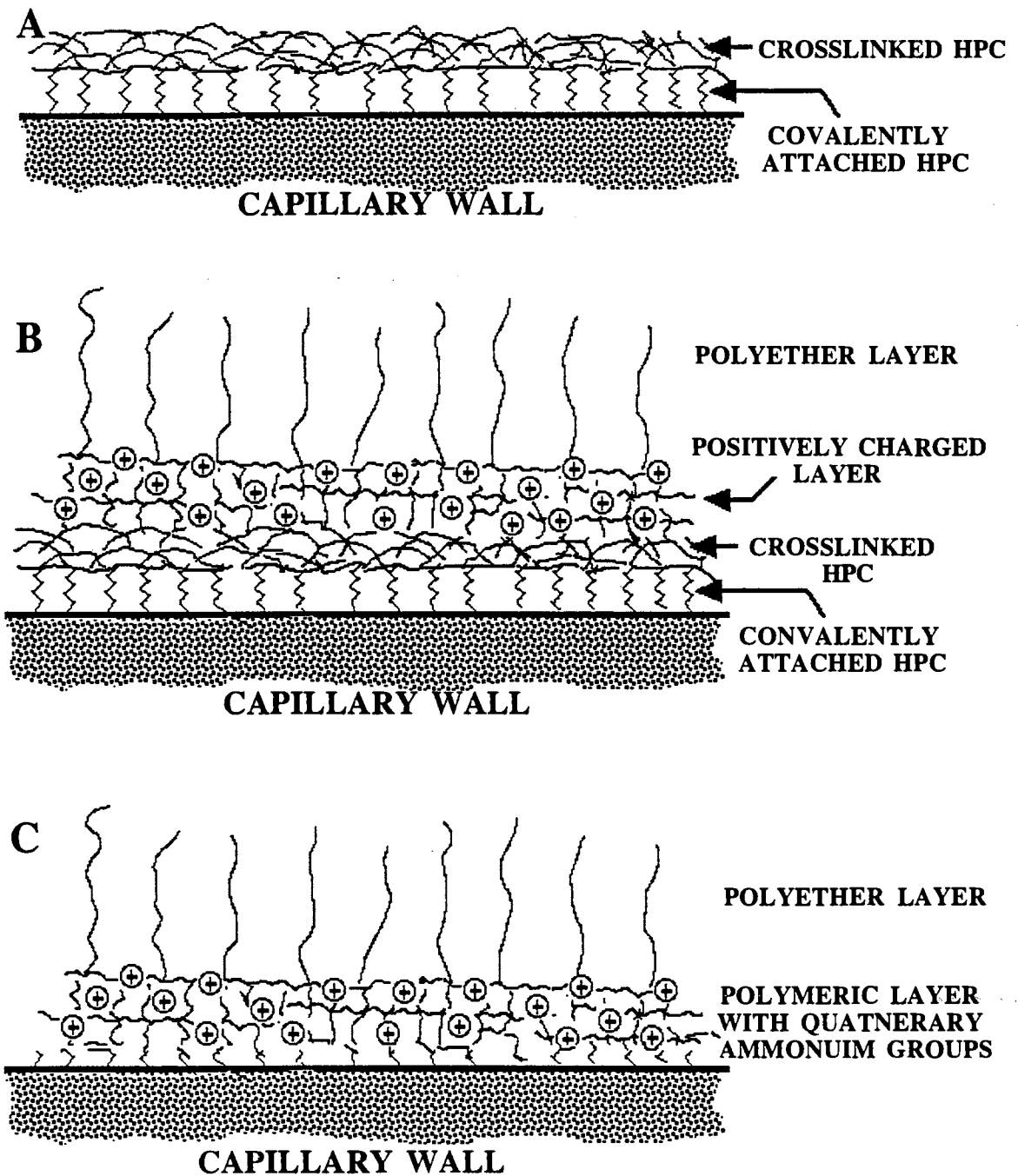
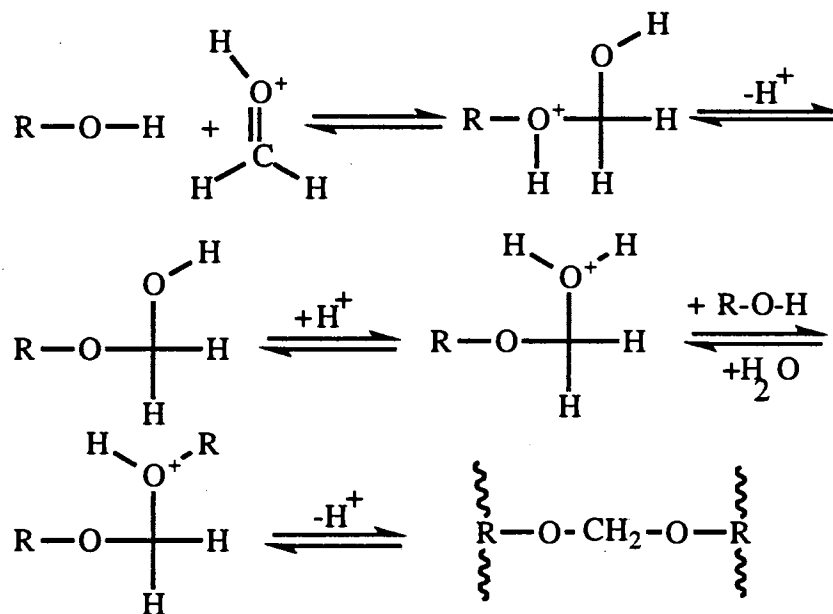


Figure 1. Schematic illustration of the idealized structures of the ZF coatings in (A), VAF-1 coatings in (B) and VAF-2 or CAF-2 coatings in (C).

ZF Capillaries. In 1967, Hjertén applied the procedure of crosslinking methylcellulose to produce hydrophilic coating on quartz tubing [1]. The procedure was effective in reducing the EOF as well as solute-wall interactions. As described in Materials and Methods, we have introduced and evaluated a series of reaction schemes that allowed both the covalent attachment and crosslinking of large polymeric HPC moieties. As illustrated in Fig. 1A, the surface is composed of two different HPC layers: the first layer is made up primarily of covalently attached medium molecular weight HPC (30,000-50,000) while the second layer contains highly crosslinked large molecular weight HPC (150,000 or 400,000). The γ -glycidoxypropyltrimethoxysilane provided the spacer arm for the covalent attachment of the lower molecular weight HPC to the capillary surface. The crosslinking of the HPC is thought to proceed through the reaction of the primary alcohol groups of the HPC with the acidified formaldehyde according to the following reaction scheme:



where R-O-H designates HPC.

Capillaries with Anodal Flow of Type VAF-1. Figure 1B is a schematic illustration of the capillary coating having variable anodal flow (VAF-1). As can be seen in Fig. 1B,

the modified capillary surface is a composite material containing: (i) a covalently attached low molecular weight HPC, (ii) a crosslinked layer of higher molecular weight HPC, (iii) relatively low molecular weight positively charged PEI moieties and (iv) a layer of hydrophilic polyether chains on the outer most surface. The cellulose bilayer is to cancel the contribution of the surface silanols to the net charge of the coating, while the PEI layer supplies the charge necessary for anodal EOF. The triepoxide (i.e., triglycidoxyglycerol) used in the reaction ensured the crosslinking of the PEI layer as well as its covalent linkage to the cellulosic bilayer. The hydrophilic top layer is a network of polyether chains resulting from the reaction of the diepoxy PEG 600 with both the sublayer and PEG 2000, see Materials and Methods. The diepoxy PEG 600 are attached to the sublayer through the remaining primary or secondary amines of the PEI and also to any exposed part of the HPC inner layer. The PEG 2000 can attach to an unopened epoxide of the diepoxy PEG 600 or to a triepoxide used to crosslink the PEI. This procedure led to the formation of a fuzzy polar network of polyether chains, which has been shown to reduce electrostatic interactions of the solute with a charged capillary surface [5]. In total, the VAF-1 is composed of presumably four distinct polymeric layers each of which plays a certain role in the properties of the capillaries.

Capillaries with Anodal Flow of Type CAF-1. The constant anodal flow (CAF-1) coating consisted basically of a positively charged layer of MPEIHE. As can be seen in Materials and Methods, the charged polymeric layer was covalently attached to the capillary surface through the base catalyzed reaction between the epoxides of γ -glycidoxypropylsilyl layer and the hydroxyethyl groups of the polymeric "quaternary" amine compound, i.e., MPEIHE. The MPEIHE was crosslinked with a short chain diepoxide (i.e., 1,4-butanediol diglycidyl ether), that proved ineffective in linking MPEIHE together as a stable network as was manifested by the relatively short life time of the coating using relatively high salt concentration as the running electrolyte, i.e., 10 h at

100 mM phosphate, pH 7.0, see below. Nevertheless, this coating proved that a permanently charged polymeric unit (i.e., polymeric unit with quaternary ammonium functions) is essential to totally cancel the silanol contribution to the net charge of the capillary coating. This strategy forms the basis of the constant anodal EOF design.

Capillaries with Anodal Flow of Types VAF-2 and CAF-2. Figure 1C illustrates the idealized structures of VAF-2 and CAF-2 capillaries having variable and constant anodal flow, respectively. Both capillaries are composed of the methylated products of PEIHE covalently attached to the capillary wall through γ -glycidoxypropyltrimethoxysilane. VAF-2 capillaries have the smaller and slightly methylated PEIHE (i.e., methanol soluble fraction or PEIHED) immobilized to the surface, while CAF-2 capillaries were coated with the larger and highly charged polymeric unit, MPEIHE. Both coatings were crosslinked with diepoxy PEG 600 and diepoxy PEG 200. These long chains of diepoxides can attach to the hydroxyethyl groups and to the primary or secondary amines of the PEIHE. Besides shielding the charged surface from biopolymers, it is believed that the long diepoxy PEG chains through crosslinking can impart an increased stability to the coating, see below.

Electroosmotic Flow

Both ZF-1 and ZF-2 capillaries exhibited virtually "zero flow" over a wide range of pH. As expected, even with very dilute buffers (i.e., 10 mM phosphate), the EOF could not be detected at pH 3.5 when 22 kV were applied to these capillaries. However, at pH 8.5 a negligible EOF developed and was determined to be $2.70 \times 10^{-5} \text{ cm}^2\text{V}^{-1}\text{s}^{-1}$ on the ZF-2 capillaries. At this pH, the disturbance peak of methanol was used as an EOF marker instead of phenol peak. This represents more than 15 fold decrease over what is observed with untreated fused silica capillaries. We believe that it will be impossible to totally eliminate the EOF with any hydrophilic coating approach since ions from the bulk

electrolyte may be trapped in or adsorbed to the polymeric coatings. Under these circumstances, the adsorbed or trapped ions become the potential determining ions. As has been shown by Hjertén, it is the high viscosity of the polymeric coating that "inhibits" the EOF. Furthermore, the conditions used in measuring the EOF are also important. In fact, at higher ionic strength, i.e., 0.10 *M* buffer concentration, the EOF could not be detected at any pH with the cellulosic capillaries. The flow characteristics of ZF-1 and ZF-2 were virtually identical. The ZF capillaries exhibited constant performance for over 80 h when operated in the pH range of 3-8 and proved to be stable for up to 40 h at pH 10. It should be noted that acetal bonds are not very stable at pH below 7.0 and siloxane bonds undergo hydrolytic degradation at high pH. In the event of cleavage of a small percent of the coating due to hydrolytic degradation of either the acetal or siloxane bonds, the integrity of the capillary coating remains almost unchanged for a certain period of time due to the thick polymeric layers resulting from five repetitive treatments with HPC.

As illustrated in Fig. 2 (curve a), the VAF-1 capillaries yielded an anodal EOF when using 100 mM phosphate in the pH range 3.5-6.5 at an applied voltage of -18 kV. As can be seen in Fig. 2, these coatings provided a quasi-constant anodal EOF over the pH range studied. The HPC bilayer has drastically minimized the contribution of the surface silanols to the observed EOF. As mentioned above, the positively charged PEI layer is to provide the charges necessary to affect an anodal EOF. PEI of molecular weight 1800 has been described to have a ratio of primary: secondary: tertiary amines of approximately 1:2:1 [17]. It is known that the ionization of primary, secondary, and tertiary amino groups are almost linearly related between pH 4-10, a fact that may explain the shallow decrease in the EOF. The hydrophilic polyether top layer whose primary function is to shield the positively charged amino groups towards oppositely charged biomacromolecules, still allowed access to the binding of electrolyte anionic counterions. This ionic binding is responsible for the anodal flow. The polyether chains would also lead to the formation of viscous wall, which may explain the relatively low EOF that could

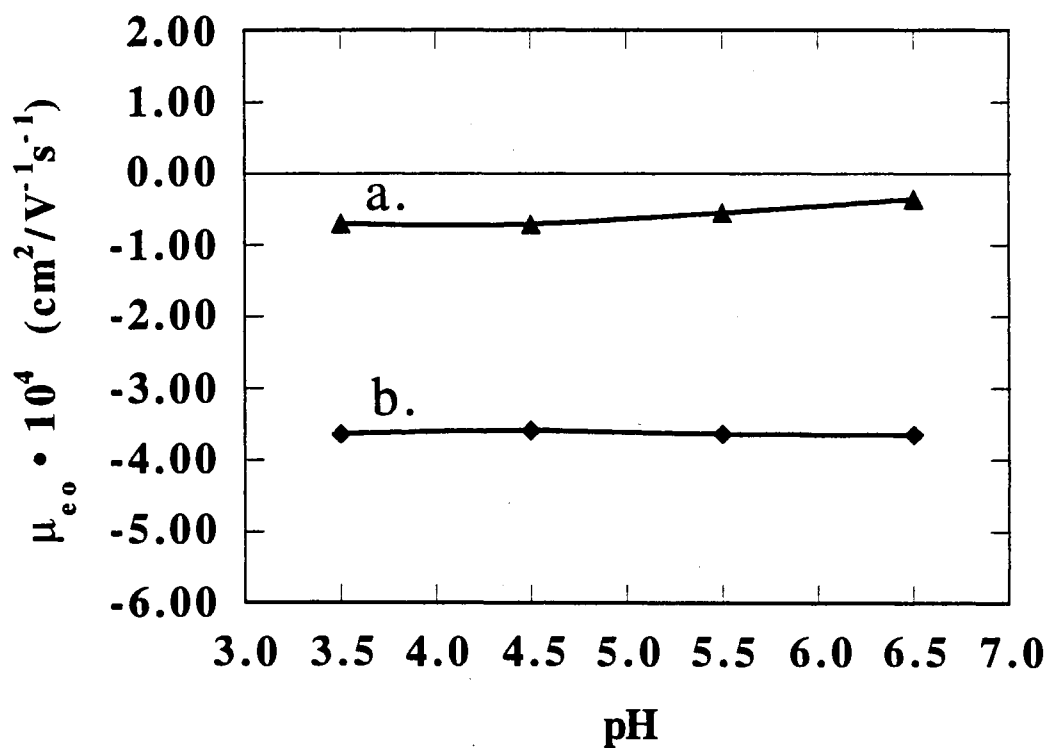


Figure 2. Plots of electroosmotic mobility, μ_{eo} , obtained with the VAF-1 (curve a) and CAF-1 capillaries (curve b) against the pH of the running electrolyte. Capillary, 80 cm total length (50 cm to detection point) x 50 μm i.d.; running electrolytes, 100 mM and 25 mM phosphate solutions in curve a and b, respectively, at different pH; applied voltage, -18 kV; detection, UV at 210 nm; inert tracer, phenol.

be achieved under the conditions of the experiments. But in return the polyether chains provided high separation efficiencies for biopolymers with a net charge opposite in sign to that of the capillary coating, see below.

The surface modifications described for CAF-1 produced capillaries possessing constant anodal EOF. As can be seen in Fig. 2 (curve b), the EOF is not a function of pH and remained constant at $-3.6 \times 10^{-4} \text{ cm}^2\text{V}^{-1}\text{s}^{-1}$ when using 25 mM phosphate and an applied voltage of -18 kV. With these capillaries, the charges of the silanol groups may have been overshadowed by the highly, permanently charged polymeric layer. Although, the high molecular weight charged coating would yield a viscous wall, the observed EOF was relatively strong, may be due to the fact that the ionic strength of the running electrolyte was low, i.e., 25 mM phosphate. At this ionic strength, the capillaries exhibited good stability, and provided 30 or more h of reproducible performance in the pH range of 3.0-7.0. The electrostatic interactions between the positively charged polymer and the silanols may have stabilized the coating. Unfortunately, this coating was not stable when the ionic strength was increased when going from 25 to 100 mM phosphate, and the lifetime was only 10 h under these conditions. This instability at higher ionic strength may be attributed to the short diepoxides used in the crosslinking step, since the same behavior was observed with a similar coating in which the MPEIHE was only covalently attached (i.e., not crosslinked). This may indicate that the crosslinking is mainly occurring within the individual polymeric units.

The VAF-2 capillaries, which have the small and partially methylated PEIHE product (i.e., PEIHED) covalently bound to the surface, exhibited a relatively moderate anodal EOF. This EOF decreased by a factor of two when going from pH 3.5 to 6.5, as illustrated in Fig. 3, curve a. This means that either the surface silanols are still contributing to the net charge of the capillary surface or the net charge on the PEIHED moieties is a function of pH. Even though the ionic strength of the running electrolyte was 2.5 times less than with the CAF-1 capillary, the EOF obtained with VAF-2 at pH 3.5 was

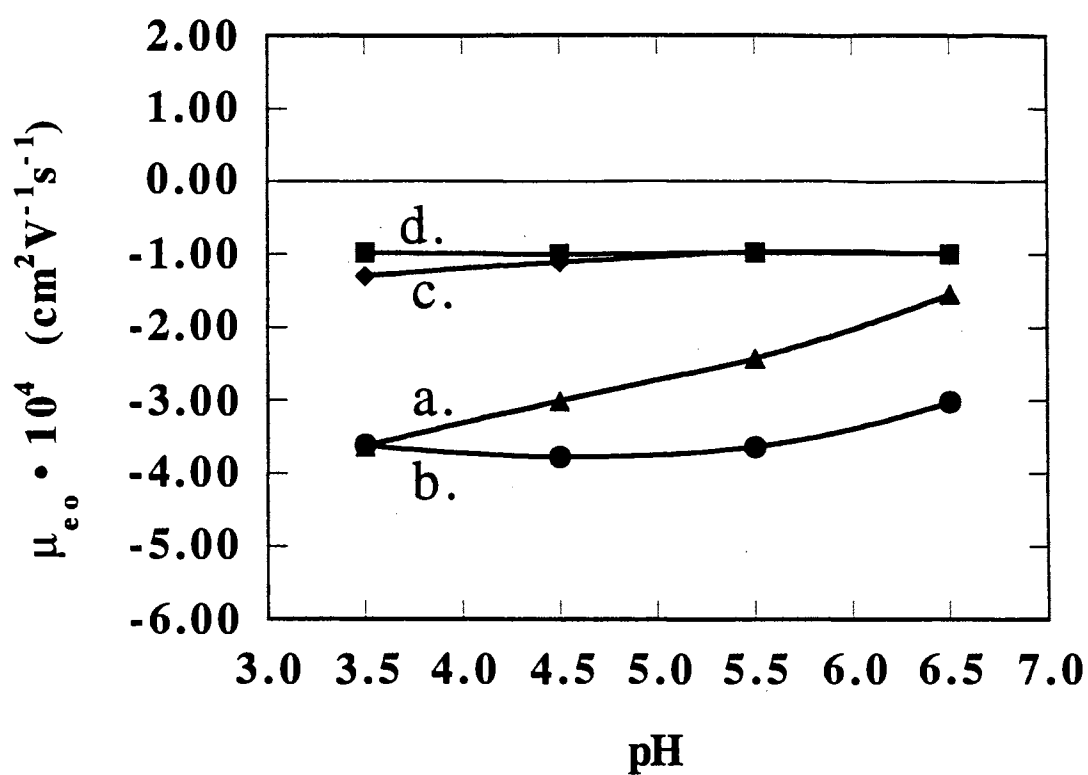


Figure 3. Plots of electroosmotic mobility, μ_{eo} , obtained with the VAF-2 capillary (curve a) and CAF-2 capillary (curves b, c and d) against the pH of the running electrolyte. Capillary, 80 cm total length (50 cm to detection point) x 50 μm i.d.; running electrolyte, 10 mM phosphate in curve a, 10 mM phosphate in curve b, 100 mM phosphate in curve c, and 5 mM phosphate/100 mM NaCl in curve d at different pH; applied voltage, -20 kV in curves a and b, -18 kV in curves c and d; detection, UV at 210 nm; inert tracer, phenol.

almost of the same magnitude. This may be attributed to the fact that the polymeric surface is crosslinked with a fairly large substance (i.e. diepoxy PEG 200 and 600), which may have increased the local viscosity of the modified surface, thus producing a relatively moderate EOF. The polyether top layer whose primary function is to shield the charged layer towards biopolymers, still allowed access to the binding of small electrolyte ions, thus yielding the observed EOF. These capillaries proved to be stable at both low and high ionic strength. Typically the EOF was reproducible for over 60 hours of use at relatively high ionic strength, i.e., 0.10 M.

The capillary modifications described for CAF-2 yielded capillaries with constant anodal EOF over the indicated pH range. Figure 3 (curves b, c and d) illustrates the observed EOF with three different electrolyte solutions. First, at an applied voltage of -20 kV using 10 mM phosphate (curve b), the EOF remained quite constant, averaging ca. $-3.6 \times 10^{-4} \text{ cm}^2\text{V}^{-1}\text{s}^{-1}$. The small fluctuations observed in the EOF, may be due to variations in the ionic strength of the buffer with changing the pH. Using 100 mM phosphate at an applied voltage of -18 kV, there is a slight change in the EOF as the electrolyte pH varies, again due to the change in the ionic strength of the running electrolyte, see Fig. 3, curve c. When using 5 mM phosphate with 100 mM NaCl as the running electrolyte, which provided a relatively constant ionic strength, a constant EOF is observed (Fig. 3, curve d). The constancy in EOF is due to the invariability of the charge density of the modified surface with the electrolyte pH. Again, the polymeric network is crosslinked with the diepoxy PEG 200 and 600 to provide shielding towards macromolecules. The modification schemes designed for the CAF-2 capillaries yielded quiet stable coating. The CAF-2 capillaries showed reproducible EOF and separation performance for more than 60 hours of use in the pH range of 3.0 to 7.0.

Evaluation of Surface Modified Capillaries in CZE of Biological Substances

ZF capillaries. The ZF capillaries were first evaluated with a mixture of basic proteins in order to assess the shielding ability of the cellulose network towards positively charged proteins that would normally exhibit strong electrostatic interactions with unmodified fused silica. Figure 4A illustrates a typical electropherogram of 3 basic proteins obtained at pH 3.0 on the ZF-1 capillary. The average plate count per meter approached 550,000 while individual plate count for lysozyme exceeded 700,000 plates/m. Figure 4B portrays an electropherogram of the same protein mixture obtained on the ZF-2 capillary at pH 4.5. The average plate count was greater than 700,000 plates/m, while the individual plate count for lysozyme was over 1,000,000 plates/m. With both ZF capillaries, the high separation efficiencies may indicate that electrostatic interaction with the silica matrix is insignificant. As expected, in the absence of EOF, the migration time of the basic proteins under investigation increased with the electrolyte pH due to decreasing the net positive charge of these solutes, Fig. 5A. As a result, the separation efficiency started to decrease at pH above 4.5 due to an increase in the magnitude of longitudinal molecular diffusion at extended analysis times. This is shown in Fig. 5B by plots of the average plate number per meter ($n = 3$) *versus* the electrolyte pH. The average plate count is typically 200,000 plates/m higher for the ZF-2 capillaries than for the ZF-1 tubes. This may be attributed to the thicker HPC coating in the ZF-2 capillaries. The HPC top layer in ZF-1 capillaries has an average molecular weight of 150,000, while that in the ZF-2 capillaries was on the average 400,000. Thus, increasing the thickness of the polymeric layer is a definite advantage. The only disadvantage of the ZF capillaries, and especially with amphoteric solutes such as proteins, is that the analyte must be sufficiently charged either positively or negatively, i.e., the running electrolyte pH must be significantly different from the pI value of the solute, to achieve the separation in reasonable time.

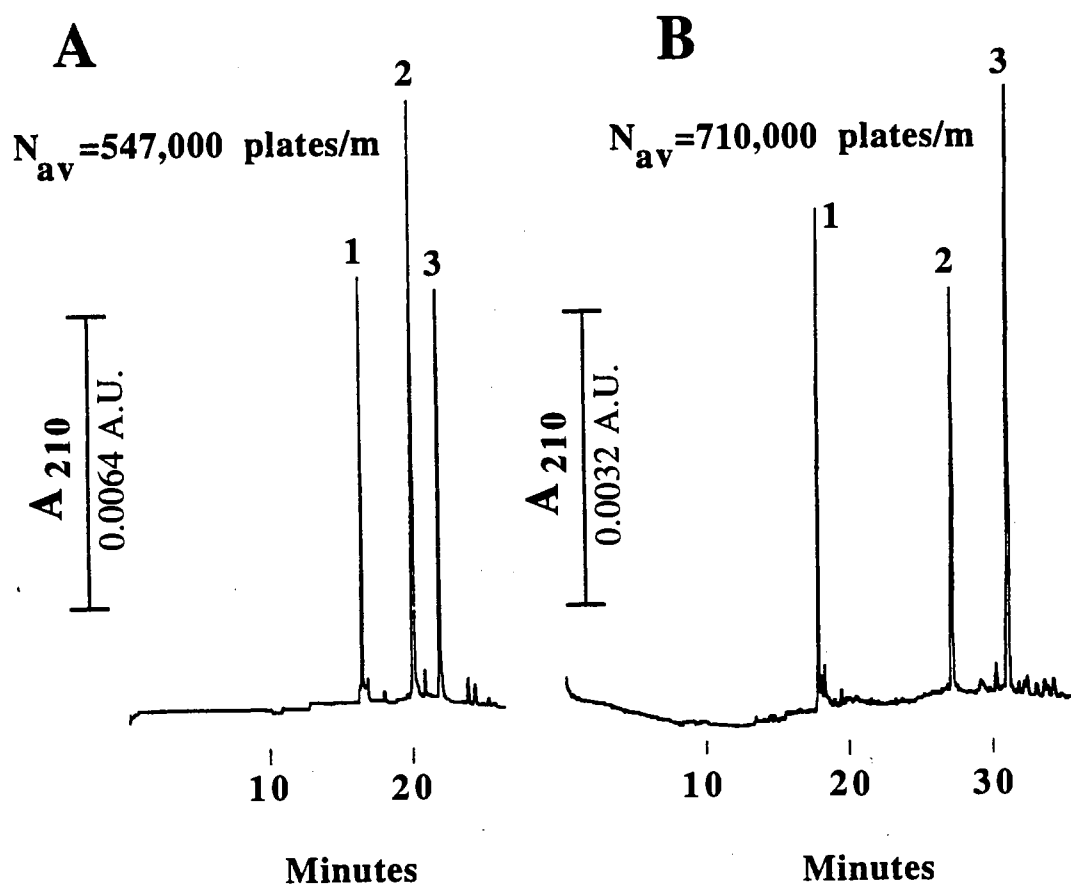


Figure 4. Electropherograms of basic proteins obtained on ZF-1 and ZF-2 capillaries in (A) and (B), respectively, at pH 3.0 in (A) and 4.5 in (B). Capillary, 80 cm total length (50 cm to detection point) x 50 μ m i.d.; running electrolyte, 100 mM phosphate; hydrodynamic injection, 5 s, 15 cm differential height; applied voltage, +18 kV; detection, UV at 210 nm; 1, lysozyme, $pI = 11.0$; 2, ribonuclease A, $pI = 9.4$; 3, α -chymotrypsinogen A, $pI = 9.5$.

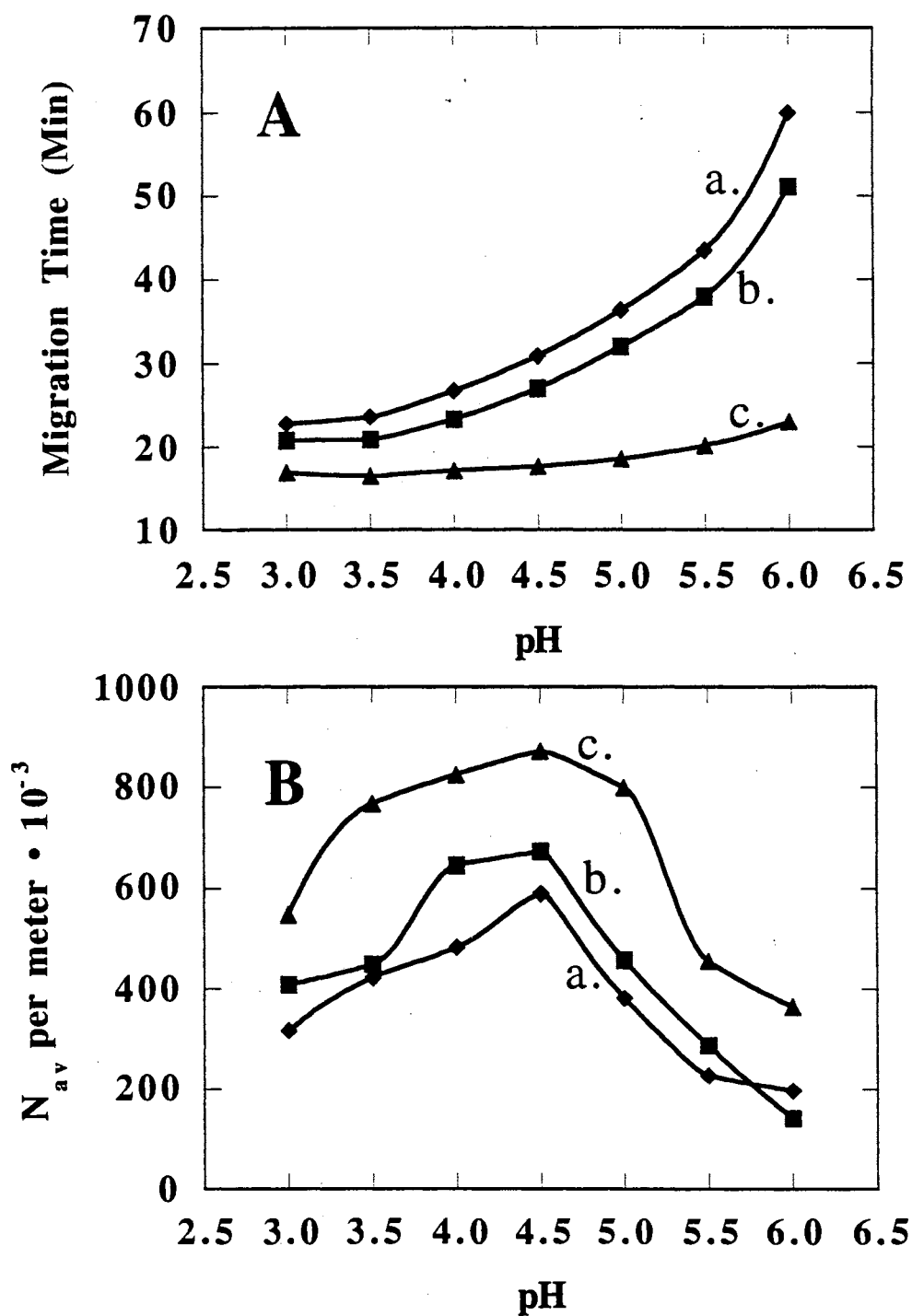


Figure 5. Plots of the migration time in (A) and average plate count in (B) of basic proteins against electrolyte pH obtained on the ZF-2 capillary. a, α -Chymotrypsinogen A; b, ribonuclease A; c, lysozyme. Conditions as for Fig. 4B.

The ZF-2 capillaries were next evaluated with a mixture of acidic proteins. Figure 6A illustrates a typical electropherogram obtained using 50 mM glutamine, pH 10.5, with an applied voltage of -22 kV. The mixture of the four acidic proteins was well resolved, yielding on the average over 85,000 plates/m. This separation efficiency is considerably lower than that observed with basic proteins. But, this plate count may be regarded as acceptable for most applications. The relatively low plate count may be attributed to hydrophobic interaction with the cellulosic layer at this high pH. At elevated pH the amount of uncharged groups on the surface of the biomolecule (i.e., deprotonation of side chains amino groups) is increased, thus increasing the hydrophobic character of the protein molecule. As mentioned above, an extreme pH (i.e., greater than 9.0) was required to increase the net negative charge of the analytes and to bring about the elution of acidic proteins in reasonable time.

To demonstrate the usefulness of ZF capillaries with medium molecular weight analytes, a series of acidic oligosaccharides (i.e., 2AP-(GalA)_n) was electrophoresed using 100 mM phosphate with an applied voltage of -18 kV. Figure 7A shows an electropherogram obtained at pH 6.5 on the ZF-1 capillary, in which the tetramer through the decamer are well resolved. The smaller peaks are believed to represent the addition of nonacidic sugars to the homologous series. The tentative identities of the peaks were determined from the migration times of standards and by graphical extrapolation. As shown in Fig. 8 (curve a), a linear relationship is obtained when the logarithm of the migration time is plotted against the logarithm of the degree of polymerization.

Capillaries with Variable Anodal Flow of Type VAF-1. The VAF-1 capillaries were evaluated with model basic proteins, a series of acidic oligosaccharides, and a mixture of mono- and diphosphate nucleosides. With the VAF-1 capillary, the EOF is not as strong as with the other anodal flow capillaries. The relatively low EOF makes the VAF-1 capillary ideal for the separation of positively charged species the electrophoretic

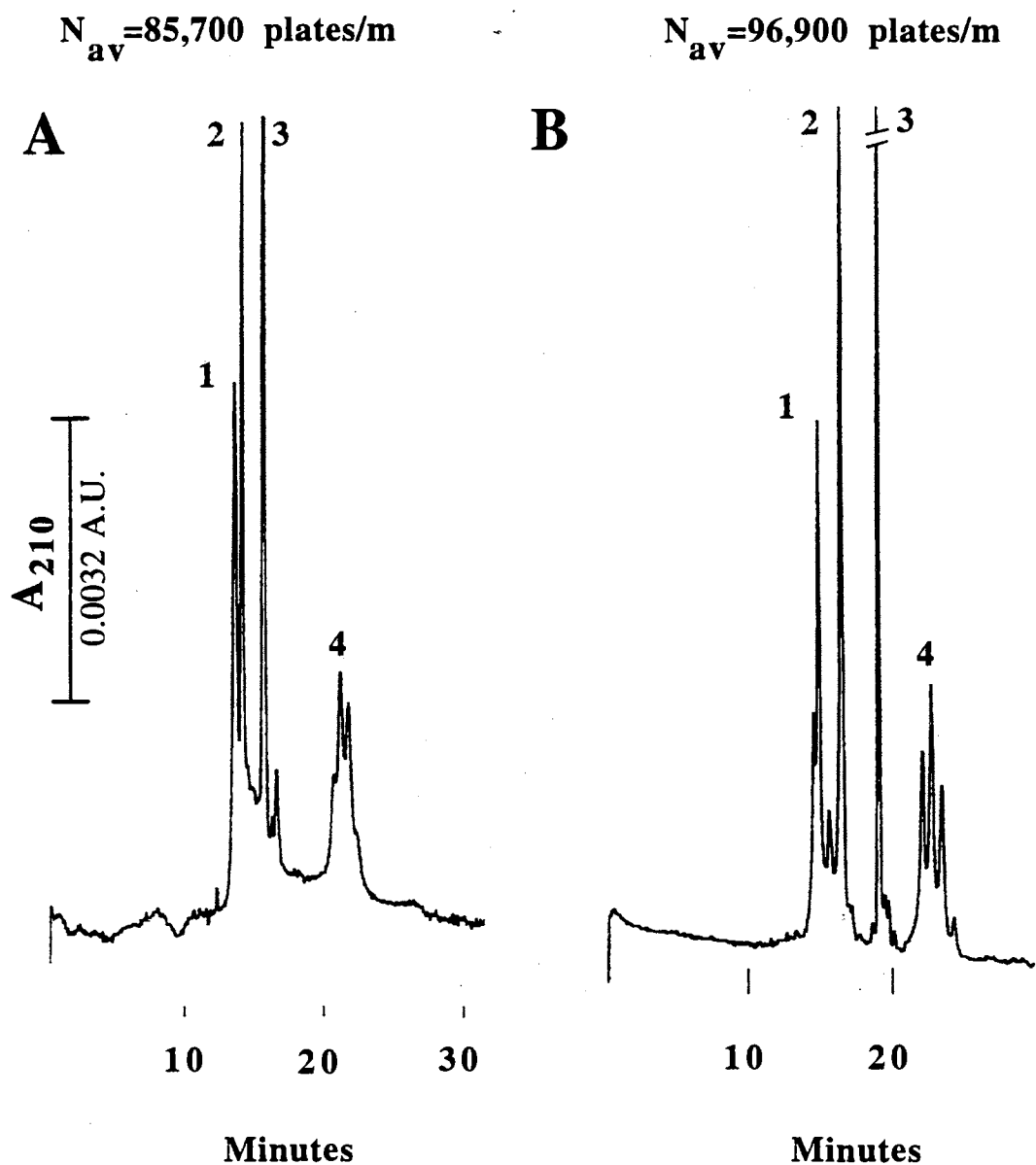


Figure 6. Typical electropherograms of acidic proteins obtained on ZF-2 and CAF-2 capillaries in (A) and (B), respectively, at pH 10.5 in (A) and 6.5 in (B). Capillary, 80 cm total length (50 cm to detection point) x 50 μ m i.d.; running electrolytes, 50 mM glutamine in (A), 100 mM phosphate in (B); hydrodynamic injection, 5 s, 15 cm differential height; applied voltage, -22 kV in (A), -18 kV in (B); detection, UV at 210 nm; 1, human serum albumin, $pI = 4.7$; 2, β -lactoglobulin A, $pI = 5.2$; 3, α -lactalbumin, $pI = 4.8$; 4, human serum transferrin, $pI = 5.2-6.1$.

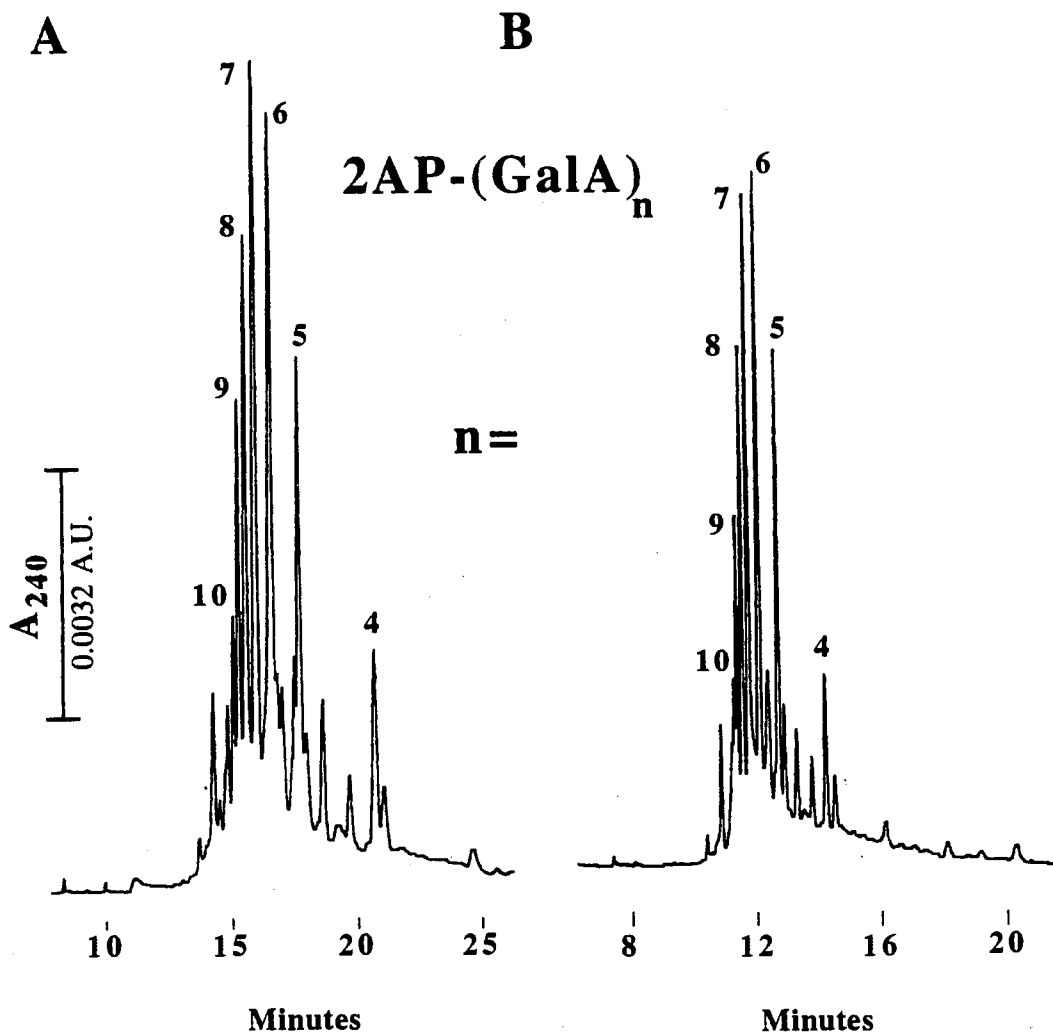


Figure 7. Electropherograms of 2-aminopyridyl derivatives of oligogalacturonic acid homologous series obtained with ZF-1 and VAF-1 capillaries in (A) and (B), respectively. Capillary, 80 cm total length (50 cm to detection point) x 50 μm i.d.; running electrolyte, 100 mM phosphate, pH 6.5; hydrodynamic injection, 5 s, 20 cm differential height; applied voltage, -18 kV; detection, UV at 240 nm.

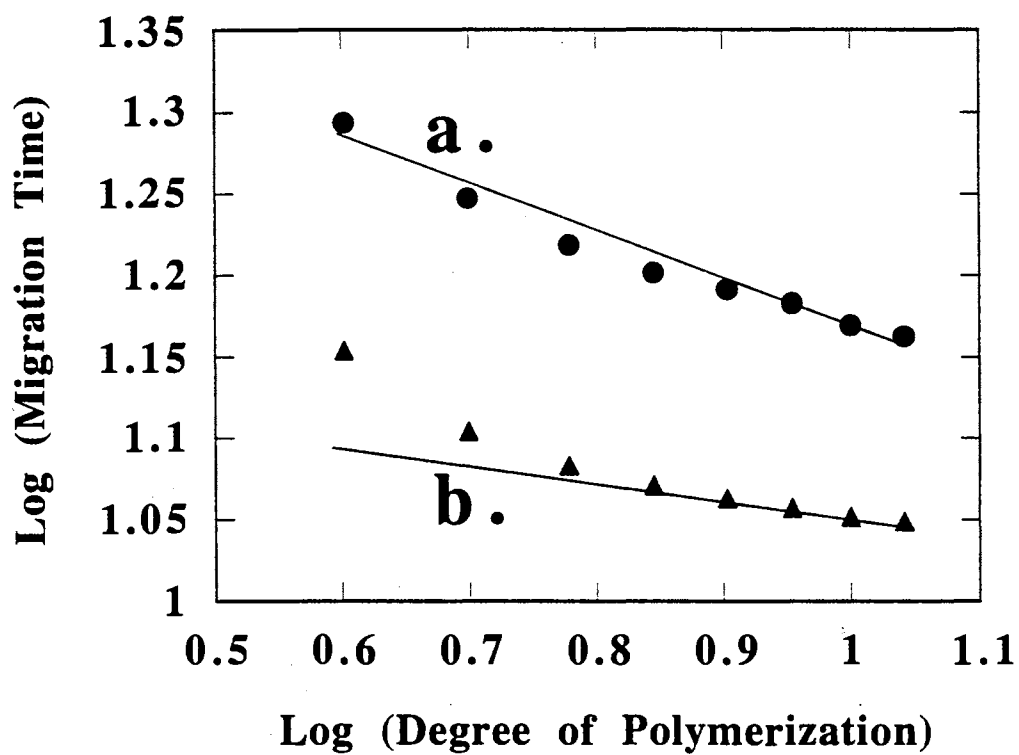


Figure 8. Plots of the logarithm of migration time of 2AP-(GalA)_n against the logarithm of the degree of polymerization obtained on the ZF-1 capillary in curve a and VAF-1 capillary in curve b. Conditions as for Fig. 7A and B.

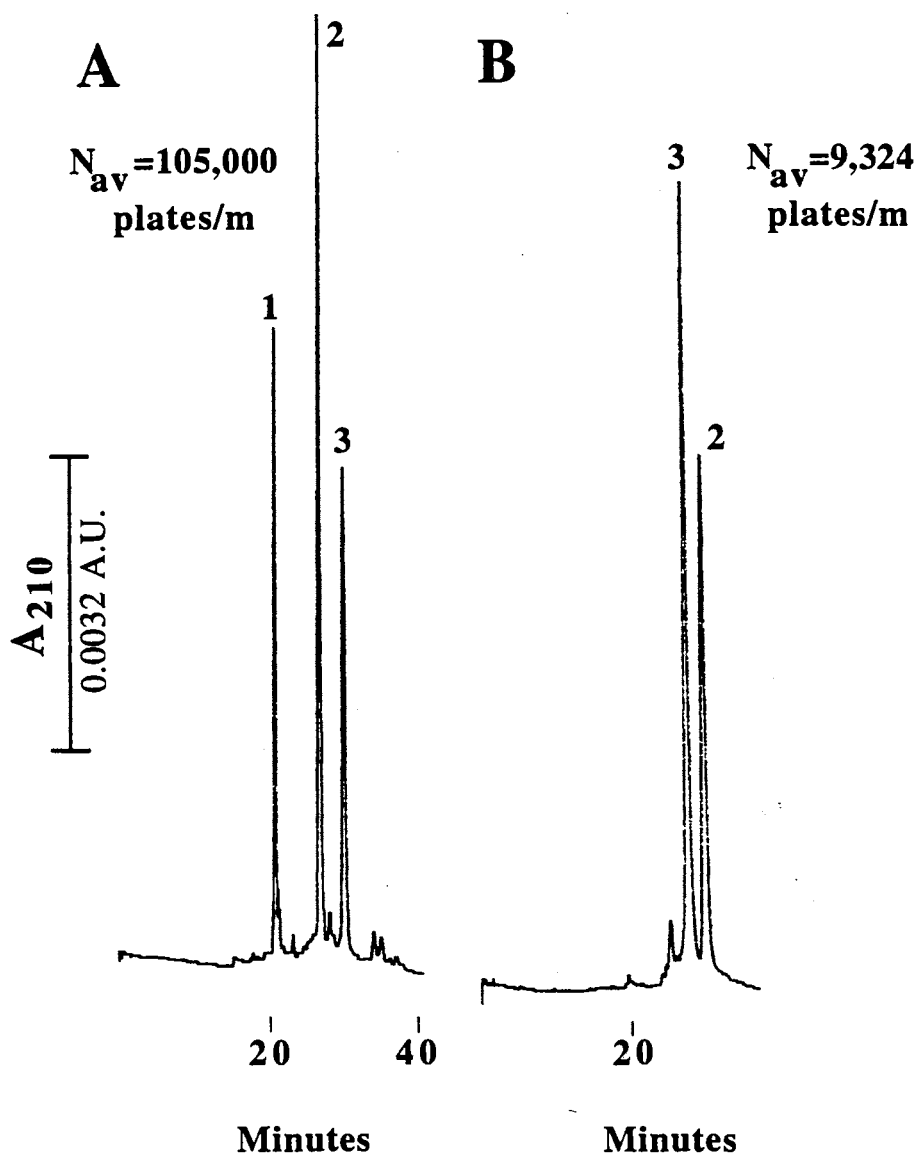


Figure 9. Electropherograms of basic proteins obtained on the VAF-1 and CAF-1 capillaries in (A) and (B), respectively, at pH 3.0 in (A) and 6.5 in (B). Capillary, 80 cm total length (50 cm to detection point) x 50 μm i.d.; running electrolyte, 100 mM phosphate; hydrodynamic injection, 5 s, 15 cm differential height; applied voltage, +18 kV in (A), -18 kV in (B); detection; UV at 210 nm; 1, lysozyme, $pI = 11.0$; 2, ribonuclease A, $pI = 9.4$; 3, α -chymotrypsinogen A, $pI = 9.5$.

mobilities of which is in the opposite direction to the EOF, i.e., migrating towards the cathode. A good application would be the separation of basic proteins. In this system, however, low pH is required to give sufficient charge to the proteins, i.e., pH 3.0-5.0, so that their electrophoretic mobilities will overcome the EOF which travels in the opposite direction. Figure 9A shows an electropherogram obtained with the VAF-1 capillary at pH 3.0 and an applied voltage of 18 kV. Under these conditions, the average plate count was 105,000 plates/m. This represents a significant decrease in separation efficiency when compared to the ZF capillaries.

Next, the VAF-1 capillary was evaluated with 2AP-(GalA)_n mixture, Fig. 7B. The electrophoretic mobility of these negatively charged species is in the same direction as the EOF. This yielded shorter analysis times as compared to ZF capillaries, compare Fig. 7A and 7B. The plot of the logarithm of migration time versus the logarithm of the degree of polymerization is shown in Fig. 8, curve b. The log-log plot was linear for up to the hexamer. This indicates that the polyether chains effectively reduced electrostatic interactions with the positively charged PEI layer for the larger, i.e., $n > 5$, negatively charged oligosaccharides. On the other hand, the charged layer was accessible for the bindings of the smaller oligosaccharides, thus producing a deviation from linearity of the aforementioned log-log plot, see Fig. 8, curve b. This provides evidence that the polyether chains are effective in hindering the accessibility of charged solutes to the PEI layer when the molecular weight of the biopolymer molecule is greater than ca. 1,000.

Finally, the VAF-1 capillary was tested with a mixture of nucleotides. As shown in Fig. 10, even though the capillary surface is positively charged, these acidic species were eluted as sharp peaks with an average plate count of 240,000 plates/m when using 100 mM phosphate, pH 7.0. These small molecules had access to the charged surface, but the presence of 100 mM phosphate in the running electrolyte was enough to diminish electrostatic interactions. These interactions were further reduced when 200 mM phosphate solution was used instead of 100 mM, but the trade off was a longer separation

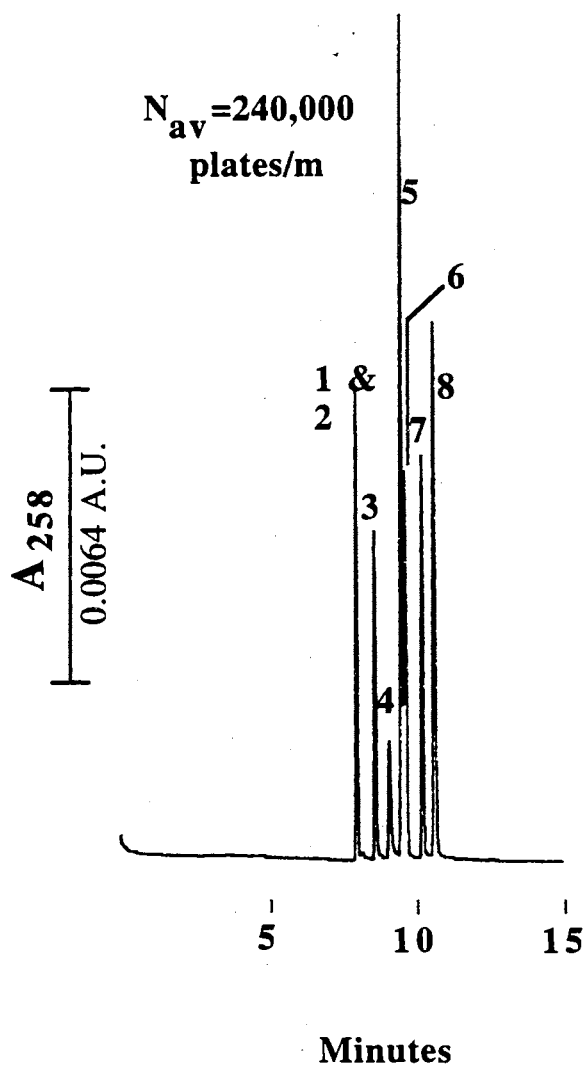


Figure 10. Typical electropherogram of mono- and diphosphate nucleosides obtained at pH 7.0 with the VAF-1 capillary. Capillary, 80 cm total length (50 cm to detection point) x 50 μm i.d.; running electrolyte, 100 mM phosphate; hydrodynamic injection, 5 s, 15 cm differential height; applied voltage, -18 kV; detection, UV at 258 nm; 1, uridine-5'-diphosphate; 2, cytidine-5'-diphosphate; 3, adenosine-5'-diphosphate; 4, guanosine-5'-diphosphate; 5, uridine-5'-monophosphate; 6, cytidine-5'-monophosphate; 7, adenosine-5'-monophosphate; 8, guanosine-5'-monophosphate.

time since a lower separation voltage was required to avoid system overheating at high ionic strength. Furthermore, the magnitude of these interactions can be controlled by the pH since the degree of ionization of the PEI is a function of pH. Such separations on the other anodal flow capillaries with higher positive charge densities, i.e., VAF-2 or CAF-2, yielded much lower separation efficiencies.

Capillaries with Constant Anodal Flow of Type CAF-1. The CAF-1 capillary provided a moderate and constant EOF, but was of little value as far as the quality of separation is concerned. This is because the charged layer was not shielded enough from the incoming solutes. Due to Coulombic repulsion, these capillaries would only work well with species with net positive charge. However, since positively charged solutes migrate against the EOF, the analytes must not be overly positively charged to allow their transport past the detector, when a negative potential drop is applied across the separation capillary. Figure 9B shows the separation of two basic proteins at pH 6.5 and an applied voltage of -18 kV. The two proteins are clearly resolved, but the separation efficiencies (9,320 plates/m) are much lower than in the case of VAF-1 capillaries. Even though the proteins carry a net positive charge there will be negatively charged regions present on the surface of the analyte, which may undergo slight interaction with the positively charged layer, thus reducing the column separation efficiency. This clearly underscores the necessity of a hydrophilic polyether top layer to provide reduced solute-coating interactions.

Capillaries with Variable Anodal Flow of Type VAF-2. These capillaries generated an anodal EOF the magnitude of which decreased as the pH increased. The VAF-2 capillaries had sufficiently long PEG chains to prevent large biomolecules from coming into direct contact with the electrostatic field of the charged PEIHED layer. These capillaries were evaluated in the analysis of a crude soybean trypsin inhibitor, a relatively strong acidic protein. Figure 11 shows an electropherogram of this protein at pH 6.5 using 100 mM phosphate and an applied voltage of -18 kV. The protein exhibited only

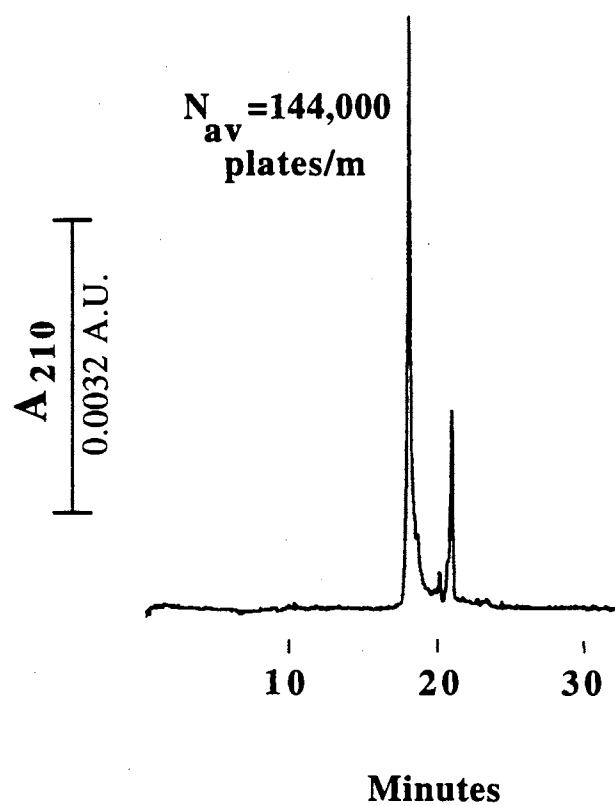


Figure 11. Typical electropherogram of crude trypsin inhibitor ($pI = 4.5$) obtained on the VAF-2 capillary at pH 6.5. Capillary, 80 cm total length (50 cm to detection point) x 50 μm i.d.; running electrolyte, 100 mM phosphate; hydrodynamic injection, 5 s, 15 cm differential height; applied voltage, -18 kV; detection, UV at 210 nm.

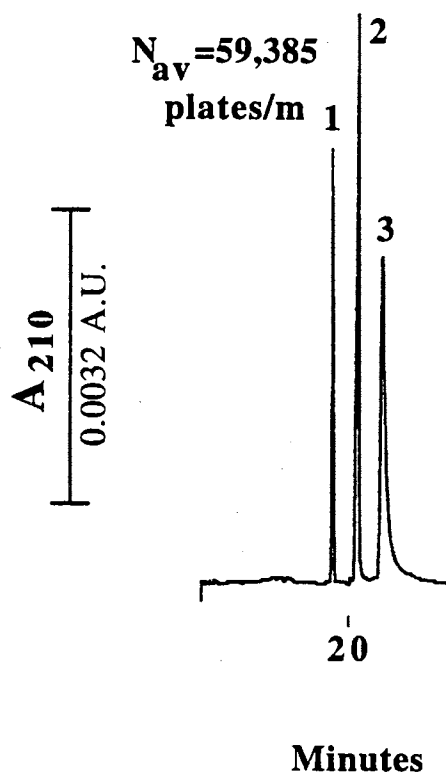


Figure 12. Electropherogram of acidic peptides obtained on the CAF-2 capillary at pH 5.5. Capillary, 80 cm total length (50 cm to detection point) x 50 μ m i.d.; running electrolyte, 10 mM phosphate; hydrodynamic injection, 5 s, 15 cm differential height; applied voltage, -20 kV; detection, UV at 210 nm; 1, bradykinin potentiator C; 2, Val-Gly-Ser-Glu; 3, Phe-Leu-Glu-Glu-Val.

slight interaction with the charged layer, as manifested by a plate count greater than 140,000 plates/m. The VAF-2 capillaries allowed a somewhat tunable EOF by varying the electrolyte pH, while still providing high separation efficiencies.

Capillaries with Constant Anodal Flow of Type CAF-2. The CAF-2 capillary which contain a polymeric network of highly charged quaternary amine that is topped by a hydrophilic polyether layer, provided a constant anodal EOF in the pH range studied. A mixture of acidic proteins was used to evaluate their performance. Figure 6B portrays an electropherogram of the acidic proteins, which was performed using 100 mM phosphate, pH 6.5, and an applied voltage of -18 kV. At this pH, all the proteins under investigation carry a net negative charge, and therefore they migrated towards the anode, i.e., in the same direction of the EOF, the reason for which their rapid separation was achieved. When compared to the electropherogram of an identical mixture (see Fig. 6A) obtained on ZF-2 capillaries, the CAF-2 modification yielded superior resolving power. The average plate count approached 100,000 plates/m, while the analysis time did not exceed 25 min. The multiple peaks observed for transferrin (i.e., the various glycoforms) demonstrates the resolving power of the CAF-2 capillary. The CAF-2 capillary provided rapid and highly efficient separation of acidic proteins without the need of extreme pH.

Finally, a mixture of short acidic peptides was chosen to evaluate the CAF-2 capillary. To allow the rapid separation of these peptides, 10 mM phosphate was used as the running electrolyte. Figure 12 shows an electropherogram obtained at pH 5.5 and an applied voltage of -20 kV. The electrophoretic mobility of the analytes and the EOF are in the same direction, thus permitting short analysis times. As can be seen in Fig. 12 some interaction between the charged MPEIHE layer and the solutes could be detected, but the peptides were fully resolved. Higher salt concentration can greatly reduce the magnitude of these interactions, but at the expenses of a longer analysis time.

Conclusions

In summary, we have developed and evaluated a series of surface modifications for fused silica capillaries for use in capillary zone electrophoresis of biological substances. Capillaries with "zero" EOF were obtained through the covalent attachment of a relatively thick cellulosic network on the inner capillary surface. These ZF capillaries yielded more than 1,000,000 plates/m with positively charged proteins. Because of the absence of EOF, the analytes must be highly charged in order to bring about their elution past the detection point. This requirement necessitated the use of extreme pH. Other surface modifications were developed to generate capillaries with quasi-constant anodal EOF. This was achieved *via* ZF capillary precursors the surface of which were covered with a cellulosic network in order to minimize the magnitude of the negative ζ potential of the silica surface. Following, a crosslinked network of PEI was covalently attached to inner cellulose bilayer, and a hydrophilic layer of polyether chains was then bonded to the PEI moieties. These polyether chains have markedly reduced solute-coating interactions. Still other capillary modifications that provided tubes with constant anodal EOF (i.e., the EOF is not a function of electrolyte pH) were also developed. These capillaries were coated with a polymer layer containing a high density of quaternary ammonium groups. The ammonium groups provided constant positive charge density to the capillary surface, and therefore a constant positive ζ potential. This led to a constant EOF. When the highly charged polymeric coating was covered with long polyether chains, both acidic and basic proteins as well as other biopolymers could be resolved with high separation efficiencies.

Acknowledgement

J. T. Smith is the recipient of a Water Resources Presidential Fellowship from the University Center for Water Research at Oklahoma State University.

References

1. S. Hjertén, *Chromatogr. Rev.*, 9 (1967) 122.
2. S. Hjertén, *J. Chromatogr.*, 347 (1985) 191.
3. K. A. Cobb, V. Dolnik and M. Novotny, *Anal. Chem.*, 63 (1990) 2478.
4. G. Bruin, J.-P. Chang, R. Kuhlman, K. Zegers, J. Kraak and H. Poppe, *J. Chromatogr.*, 471 (1989) 429.
5. W. Nashabeh and Z. El Rassi, *J. Chromatogr.*, 559 (1991) 367.
6. S.A. Swedberg, *Anal. Biochem.*, 185 (1990) 51.
7. J. K. Towns and F. E. Regnier, *J. Chromatogr.*, 516 (1990) 69.
8. J. T. Smith and Z. El Rassi, *J. High Resolut. Chromatogr.*, 15 (1992) 573.
9. W. Nashabeh, J. T. Smith and Z. El Rassi, *Electrophoresis*, 14 (1993) 407.
10. W. Nashabeh and Z. El Rassi, *J. High Resolut. Chromatogr.*, 15 (1992) 289.
11. W. Nashabeh and Z. El Rassi, *J. Chromatogr.*, 632 (1993) 157.
12. A. Emmer, M. Jansson and J. Roeraade, *J. Chromatogr.*, 547 (1991) 544.
13. W. Nashabeh and Z. El Rassi, *J. Chromatogr.*, 596 (1992) 251.
14. J. E. Wiktorowicz and J. C. Colburn, *Electrophoresis*, 11 (1990) 769.
15. J. Cai, J. T. Smith and Z. El Rassi, *J. High Resolut. Chromatogr.*, 15 (1992) 30.
16. "Standard Proton NMR Collection", Sadtler Research Laboratories, Philadelphia, PA, Vol. 5, spectra 2870 and 2832; Vol. 12, spectrum 7690; Vol. 14, spectrum, 8892 M.
17. R. E. Chicz, Z. Shi and F. E. Regnier, *J. Chromatogr.*, 359 (1986) 121.

PART II

CHAPTER V

SOME BASIC ASPECTS OF MICELLAR ELECTROKINETIC
CAPILLARY CHROMATOGRAPHY

Introduction

The applicability of HPCE was greatly extended by the introduction of micellar electrokinetic capillary chromatography (MECC) by Terabe *et al.* [1] in 1984. MECC allows the high resolution separation of uncharged species. Although designed for the separation of neutral species, MECC has proven to have unique selectivities, different from CZE, in the separation of charged species as well. Micellar electrokinetic capillary chromatography involves the use of a charged surfactant above its critical micelle concentration in the running electrolyte.

The goal of this chapter is to (i) summarize the basic concepts of MECC, (ii) provide an insight into the operational aspects of MECC and (iii) give the rationale for the studies of the second part of the dissertation.

Basic Concepts

Much like liquid chromatography, the mechanism of separation in MECC is based on the distribution of a solute between two distinct phases, a pseudo-stationary or micellar phase and an aqueous phase. Upon application of an electric field, the EOF transports the bulk solution towards the cathode due to the ionization of the silanol groups on the fused silica capillary surface. An anionic micelle migrates towards the anode by its

electrophoretic mobility that is a function of the micelle's size and charge as described in chapter 1 by equation 8. The EOF, under neutral or alkaline conditions, is usually much stronger than the electrophoretic mobility of the micelle, $\mu_{ep(mc)}$, which results in the micelles being swept in the direction of the EOF but at a much slower velocity as illustrated in Figure 1. Solutes are then separated according to their differential partitioning between both phases. Very polar solutes that do not partition into the micellar phase are carried by the EOF and elute at time t_0 . On the other hand, very hydrophobic solutes that are completely solubilized by the micelle, i.e., insoluble in the aqueous phase, will elute last at time t_{mc} (migration time of the micelle). When a neutral solute is injected into the capillary, a fraction of it is incorporated into the micelle and migrates at the velocity of the micelle while the remaining fraction of that solute stays in the aqueous phase and migrates with the EOF. Thus, the migration velocity of a solute is dependent on the distribution between the micellar and aqueous phases. Solutes with a greater hydrophobic character will migrate with a lower velocity than more hydrophilic solutes as illustrated in Figure 2a. Any neutral species will elute in the migration time window that extends from t_0 to t_{mc} , see Figure 2b.

Fundamental Equations

The fundamental characteristics of MECC are well understood and have been described by Terabe and co-workers [2]. The retention and resolution in MECC are related to the electrokinetic velocities of both the aqueous phase (i.e., EOF) and the micellar phase as well as the solute distribution between the two phases. The apparent velocity of the micelle, v_{mc} , is the sum of the electroosmotic velocity of the aqueous phase, v_{eo} , and the electrophoretic velocity of the micelle, v_{ep} , [2]:

$$v_{mc} = v_{eo} + v_{ep} \quad (1)$$

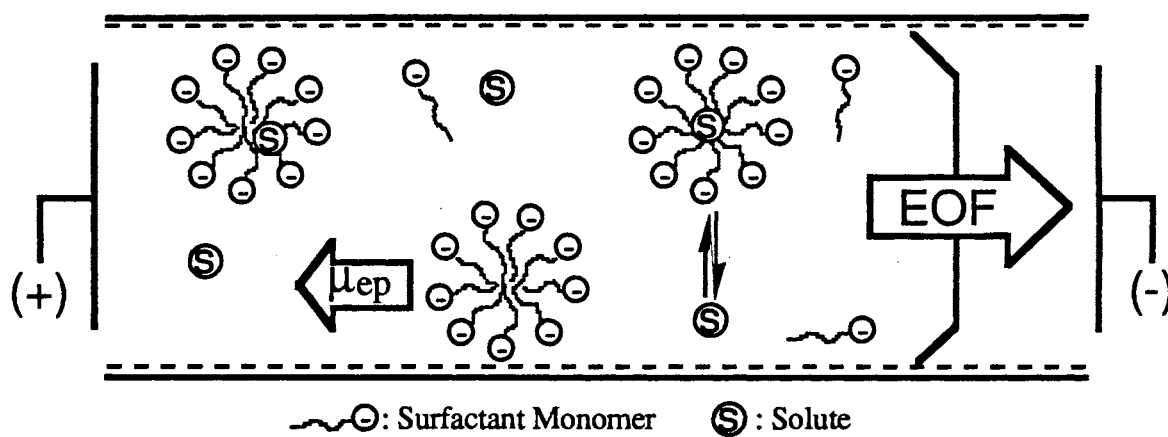


Figure 1. Schematic illustration of the separation principle in MECC.

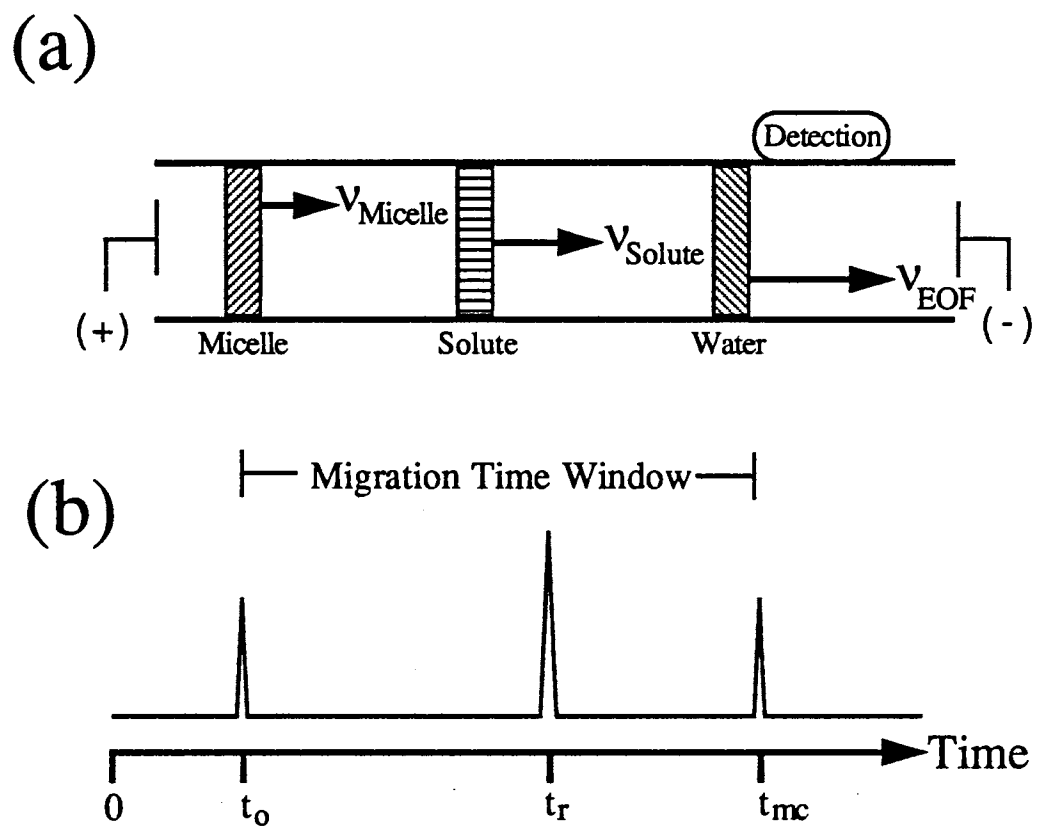


Figure 2. Schematic of (a) the zone separation in MECC and (b) the resulting chromatogram.

The v_{eo} and v_{ep} , described in equations 8 and 9 of Chapter 1, can be combined in the form:

$$v_{mc} = -\frac{\epsilon E \zeta_c}{\eta} + \frac{2\epsilon E \zeta_{mc}}{3\eta} f(\kappa a) = -\frac{\epsilon E}{\eta} \left(\zeta_c - \frac{2\zeta_{mc}}{3} f(\kappa a) \right) \quad (2)$$

where ζ_{mc} and ζ_c are the zeta potentials of the micelle and the capillary, respectively. The negative sign in equation 2 indicates that the zeta potential of the capillary is negative, i.e., the EOF is towards the cathode. Similar to CZE, the velocity of a neutral solutes in MECC is given by [3]:

$$v_s = [\mu_{eo} + \mu_{ep(\text{eff})}]E \quad (3)$$

where $\mu_{ep(\text{eff})}$ is the effective electrophoretic mobility of the solute obtained upon partitioning in the micelle.

The capacity factor or retention factor, k' , is a fundamental term in chromatography and is defined in MECC as [3]:

$$k' = \frac{n_{mc}}{n_{aq}} \quad (4)$$

where n_{mc} and n_{aq} are the amounts of the solute incorporated into the micelle and that dissolved in the aqueous phase, respectively. We can obtain the relationship between k' and measurable migration times by the equation [3]:

$$k' = \frac{(t_r - t_o)}{t_o \left(1 - \frac{t_r}{t_{mc}} \right)} \quad (5)$$

where t_r is the retention time of the solute. Figure 3 illustrates the distribution of k' over the migration time window.

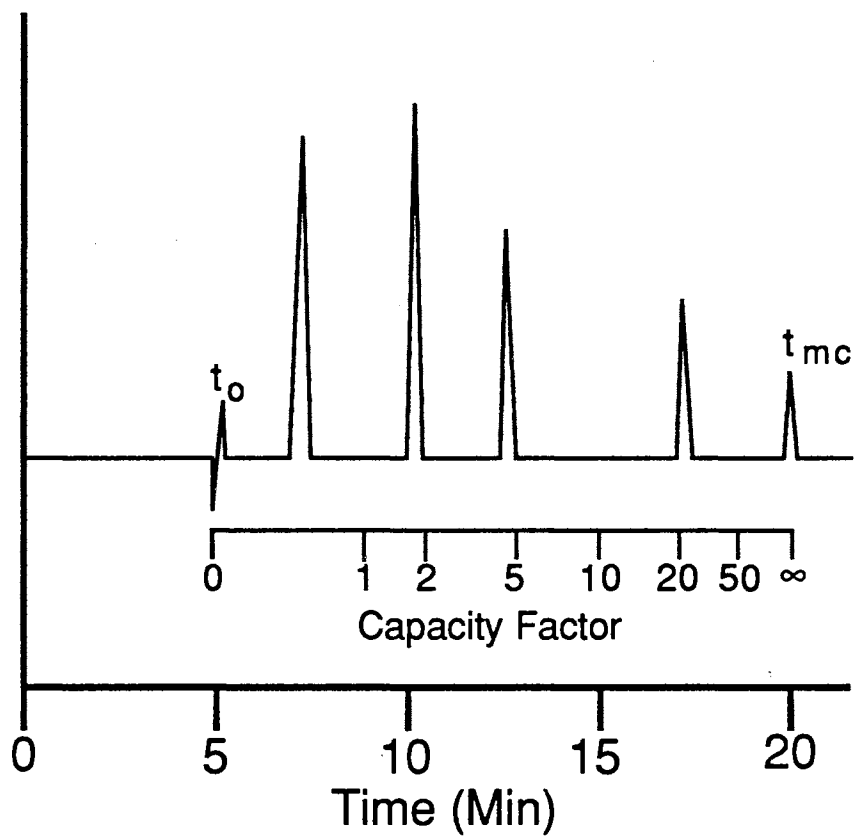


Figure 3. Distribution of the capacity factor over the migration time window.

The selectivity factor, α , can be readily estimated from the electropherogram by the following equation which is the same as that used in liquid chromatography [4]:

$$\alpha = \frac{k'_2}{k'_1} \quad (6)$$

The resolution, R_s , between any two peaks is a function of several parameters and is described by [2]:

$$R_s = \underbrace{\left(\frac{\sqrt{N}}{4} \right)}_{\text{Efficiency}} \underbrace{\left(\frac{k'_2}{k'_2 + 1} \right) \left(\frac{1 - t_o / t_{mc}}{1 + (t_o / t_{mc}) k'_1} \right)}_{\text{Retention}} \underbrace{\left(\frac{\alpha - 1}{\alpha} \right)}_{\text{Selectivity}} \quad (7)$$

The ratio of t_o/t_{mc} is defined as the elution range parameter, which is a reflection of the migration time window. A more general measure of the resolution of a given system is the peak capacity. The peak capacity, n , is defined as the number of peaks that can be separated in a given time interval with a resolution of unity. In MECC, n is calculated by [2]:

$$n = 1 + \frac{\sqrt{N}}{4} \ln \frac{t_{mc}}{t_o} \quad (8)$$

Based on these fundamental equations, several operational parameters can be adjusted to provide the optimum separation conditions.

Operational Aspects of MECC

The goal of any separation is to completely separate all of the sample components in a minimum amount of time. Referring to equation 7, resolution is related to three fundamental parameters: efficiency, selectivity and retention. For two adjacent peaks with capacity factors of k'_1 and k'_2 , a convenient approximation to equation 7 is given by:

$$R_s = \left(\frac{\sqrt{N}}{4} \right) \left(\frac{\alpha - 1}{\alpha} \right) f(k') \quad (9)$$

where $f(k')$ is equivalent to:

$$f(k') = \left(\frac{k'_2}{k'_2 + 1} \right) \left(\frac{1 - t_o / t_{mc}}{1 + (t_o / t_{mc})k'_1} \right) \quad (10)$$

In MECC, all three parameters (i.e., efficiency, selectivity and retention) can be manipulated to optimize a given separation. Resolution can be increased by increasing retention, but there is a limit beyond which increasing retention will cause R_s to drop. Terabe and co-workers [2] evaluated $f(k')$ as a function of k' and found that bell-shaped curves are obtained. Each bell-shaped curve is unique for a given t_o/t_{mc} or migration time window. It has been shown by differentiating equation 10 with respect to k' and setting the resulting expression to zero, that the optimum k' for maximum resolution between two neighboring peaks is given by [5]:

$$k'_{opt} = \left(\frac{t_{mc}}{t_o} \right)^{1/2} \quad (11)$$

According to equation 7, resolution increases with the square root of N , but the value of N is usually fixed for a given micellar phase. Thus, increasing the selectivity has proven to be the most useful approach for maximizing resolution.

Manipulation of the Capacity Factor and Selectivity

Since the useful range for k' is very narrow in terms of resolution, it is beneficial to adjust the capacity factor of the solutes of interest into the optimal range to provide better separation. Usually, the capacity factor is changed by adding an organic modifier [6], changing the surfactant concentration [2], or by selecting a micellar phase with a different hydrophobic character [7].

Similar to liquid chromatography, the capacity factor is related to the distribution coefficient, K , by

$$k' = K \frac{V_{mc}}{V_{aq}} = K\phi \quad (12)$$

where V_{mc} and V_{aq} are the volumes of the micellar and aqueous phases, respectively, and ϕ is the phase ratio. The capacity factor is approximately related to the surfactant concentration, $[S]$, by [2]:

$$k' = K\bar{v}([S] - CMC) \quad (13)$$

where \bar{v} is the partial specific volume of the micelle and CMC is the critical micelle concentration. Accordingly, it is apparent that k' will increase linearly with the concentration of surfactant. Therefore, we can easily vary k' by adjusting the surfactant concentration, provided the CMC is known. It should be mentioned that due to increasing viscosity and ionic strength with increasing surfactant concentration, there is an upper limit for the amount of surfactant that can be added to the running electrolyte.

Organic modifiers can also be added to the running electrolyte to change the selectivity. These modifiers can be classified under two general classes. Class I modifiers which modify the micelle itself and class II modifiers which modify the surrounding aqueous phase. Class I modifiers, such as 1-heptanol, modify the structure of the micelle or the micelle's interaction with the surrounding aqueous phase at low concentrations (i.e., $< 300 \text{ mM}$). Class I modifiers usually result in an increase of k' by increasing the partition coefficient [8]. Class II modifiers are used at much higher concentrations (i.e., 5 - 40 % v/v) where they change the manner of interaction of the solutes with the surrounding aqueous phase, typically resulting in a decrease in k' [9]. Examples of class II modifiers include organic solvents, urea, glucose and ion-pairing agents. Class II modifiers usually result in an increase in t_0 and t_{mc} by reducing the zeta potential of the capillary and the micelle.

The k' can also be altered by selecting micellar phases with different hydrophobic character. To be suitable for MECC, the surfactant should meet the following criteria: (i) the surfactant must have a CMC in the workable range; (ii) the micellar solution must be homogeneous and UV transparent; and (iii) the viscosity of the micellar phase must be low. There are dozens of micellar phases that have been applied to MECC for the separation of various solutes. Table I summarizes some of the micellar phases that have been explored. Surfactants have a hydrophobic tail and a hydrophilic head group. Surfactants with alkyl chains of less than six carbons are typically not useful since their CMCs are far too high; however, they can be used as ion-pairing reagents [10]. Alkyl tails of greater than 14 carbons pose solubility problems in aqueous solutions [11].

TABLE I. Surfactants used in MECC.

Surfactant	Abbreviation	Reference
Anionic		
Sodium dodecyl sulfate	SDS	[1, 2, 16]
Sodium decyl sulfate	STS	[2]
Sodium taurocholate	STC	[17]
Sodium cholate	SC	[18]
Sodium taurodeoxycholate	-	[17]
Sodium lauroyl methyltaurate	SLMT	[17]
Sodium dodecanoyl valinate	SDVal	[19]
Cationic		
Dodecyltrimethyl-ammonium chloride	DTAC	[11]
Dodecyltrimethyl-ammonium bromide	DTAB	[11]
Tetradecyltrimethyl-ammonium bromide	TTAB	[20]
Cetyltrimethyl-ammonium bromide	CTAB	[21]
Cetyltrimethyl-ammonium chloride	CTAC	[11]

Solutes can interact with the micelle in its different regions. Solutes may partition (i) in the hydrophobic core that is completely removed from the aqueous media, (ii) between the hydrophobic tails of the surfactant, (iii) in the outer hydrophilic head groups, or (iv) adsorb on the micelle surface [12]. Polar solutes interact with the two outermost regions of the micelle (i.e., at the surface or with the hydrophilic head groups). Due to this nature of interaction, the hydrophilic head group is more important than the hydrophobic tail in terms of selectivity for polar solutes. Studies by Terabe and co-workers [13], showed that exchanging sodium dodecyl sulfate (SDS) with sodium tetradecyl sulfate (STS) will increase the hydrophobic nature of the micellar phase yielding an increase in k' , but the selectivity was practically unaltered. But by replacing SDS with *N*-lauroyl-*N*-methyltaurate (SLMT), a significant change in selectivity was observed [13]. Even changing the counterion to the ionic head group of the micelle can alter the selectivity in some cases [14].

Some surfactants have very specific selectivities. Surfactants with perfluorinated alkyl chains show an enhanced selectivity for fluorinated solutes. Bile salts, e.g., sodium cholate, which are naturally occurring steroidal surfactants that form helical as opposed to spherical micelles, have proven to have unique selectivities for steroidal-like compounds [15].

Besides changing the surfactant type, the properties of a micellar phase can be changed by adding a co-surfactant. Mixed micelle systems have been explored recently by several groups [22-24]. The mixing of cationic surfactants of various alkyl chain lengths was recently explored in our laboratory to change selectivity [25]. Other groups have added nonionic surfactants to ionic micellar phases to alter the selectivity of the system [23]. It should be mentioned that the addition of a nonionic co-surfactant lowers the surface charge density of the micelle, and correspondingly, results in a shorter migration time window.

Manipulation of the Migration Time Window

The manipulation of the migration time window (see Fig. 2b) has proven a valuable tool in MECC. In some cases, an extended migration time window is required for the separation of a complex sample. Other times, a shorter migration time window will be beneficial to maximize sample throughput. Most ionic surfactants form micelles with a constant surface charge density and are characterized by a fixed migration time window in the useful pH range, i.e., $\text{pH} > 6.0$. According to equations 1-3, the migration time window can be varied by changing: (i) the surface charge density of the micelle and/or the capillary, (ii) the zeta potential of the micelle or capillary, or (iii) the viscosity of the medium.

Several approaches have been taken to achieve this goal. Most commonly, the migration time window is extended by the addition of an organic modifier. Many organic modifiers, including methanol [26, 27], 2-propanol [24] and acetonitrile [26, 28], have proven useful in MECC. Organic modifiers interact with the capillary wall producing a lower zeta potential for the capillary surface, and in turn, a slower EOF. However, the percent modifier that can be added is limited by the impact of the solvent on the micelle. Micellar physico-chemical properties such as the CMC, aggregation number, and micellar dissociation (rate of exchange of surfactant between the micelle and bulk solution) are affected by the percent organic modifier. Generally, the use of less than 25% (v/v) organic modifier does not totally disrupt micelle formation. However, the major disadvantage of organic modifiers lies in a significant decrease in efficiency. Because of this characteristic, the peak capacity may decrease even though the migration time window has increased.

Metal salts [29] and ion-pairing agents [30] have been added to anionic micellar phases to decrease the migration time window. These counter-ions are attached to the micelle's surface *via* electrostatic interactions. Thus, upon complex formation, the zeta potential of the micelle is reduced, resulting in a lower $\mu_{\text{ep}(\text{mc})}$. Additionally, the use of

such agents is beneficial in reducing electrostatic repulsion between the micelle and a solute possessing the same charge. This technique has proven useful for the separation of oligonucleotides in MECC [31].

As mentioned in the previous section, nonionic surfactants can be added to a micellar phase to reduce the surface charge density of the micelle. This results in a reduction in the migration time window and bring about a change in selectivity. This technique can be useful in speeding up the separation without increasing the field strength provided the resolution is adequate.

A novel concept introduced recently by our laboratory involves the use of *in situ* charged micelles [32]. This micellar system uses nonionic surfactants which are converted *in situ* to form charged micelles. Due to the nature of these systems, the surface charge density of the micelles can be conveniently adjusted by a number of operational parameters. As a result of the adjustable surface charge density, the migration time window can be tuned over a wide range without significant losses in separation efficiency or changes in selectivity.

Chiral Separations in MECC

One of the most powerful extensions of MECC has been the ability to perform chiral separations. Chiral selectivity in MECC can be obtained in one of two ways: (i) by the addition of chiral selector additives to the running electrolyte or (ii) the use of a micellar phase possessing chiral recognition sites, i.e., chiral surfactant. Upon the addition of chiral selectors to the electrolyte, the solute is distributed between three phases, i.e., the aqueous, micellar and chiral selector phases, while the use of chiral micelles involves only two phases. In either case, the affinity of the selector towards one enantiomer must be increased to achieve separation. In any event, the chiral selector can be changed by simply changing the running electrolyte, which greatly enhances the potential of this technique.

The use of both native and derivatized cyclodextrins has been successfully employed for the chiral separations of a wide variety of aromatic species [33-36]. Cyclodextrins are macrocyclic oligosaccharides that are synthesized by bacterial enzymatic digestion of starch. The basic structure comprise 6, 7 or 8 glucopyranose units attached by α -1,4 linkages and are referred to as α -, β - and γ -cyclodextrins, respectively. These compounds are shaped like a torus and have a hydrophobic interior that is optically active. The mechanism of chiral selectivity is based on differences in the solute-cyclodextrin complex stability with each enantiomer.

The first example of chiral selectivity in CE involved the addition of Cu(II) and *L*-histidine to the running electrolyte to resolve dansyl amino acids *via* a trimolecular complex [37]. A similar system has been employed in MECC using a Cu(II)-aspartame complex for the resolution of 18 chiral dansyl amino acids [38].

Separations have been reported employing a mixture of SDS and optically active surfactants such as *N,N*-dodecyl-*L*-alanine [29] or *N*-dodecyl-*L*-valinate [19]. However these separations have been limited to derivatized amino acids. Certain bile salts, which are naturally optically active, have been shown to be useful in the chiral resolution of certain hydrophobic species [17, 39, 40].

Rationale and Scope of Part II of the Dissertation

Micellar electrokinetic capillary chromatography has developed into an extremely powerful branch of CE. The application of MECC has extended the intrinsic high resolving power of HPCE to the separation of neutral solutes which cannot otherwise be resolved by an electrophoretic technique. As an analytical technique, MECC offers several advantages over other competing separation techniques (e.g., HPLC) for a wide variety of neutral and charged species. The combination of chiral selectivity and MECC has greatly enhanced the potential of this technique. Although significant advances have been made,

many aspects of MECC require further development before the full potential of the technique can be realized.

Further improvements of the technique must include the expansion of its ability to separate hydrophobic solutes and the realization of lower detection limits. One of the unique features of MECC is the ease with which the nature of the micellar pseudo-stationary phase can be altered and/or changed simply by rinsing the capillary and filling it with a new micellar solution. Despite this characteristic, most reported MECC separations to date have utilized aqueous solutions of sodium dodecyl sulfate (SDS) as the micellar phase. Only a limited number of other ionic surfactants have been explored. To provide alternative selectivities, novel surfactant systems must be introduced and characterized so that a wider range of species can be effectively resolved.

The broad objective of this research was to contribute to the advancement of MECC methodology by providing (i) novel *in situ* charged micellar phases for the separation of a variety of both neutral and charged species and (ii) developing a better understanding of the underlying phenomena involving *in situ* charged micellar phases. Systematic studies which involved characterization of the electrokinetic and chromatographic properties of these novel phases over a wide range of operating conditions were pursued in order to achieve this objective. The characterization and demonstration of these novel micellar phases are discussed in Chapters 6-9.

Overall, this work has contributed to the understanding of the electrokinetic behavior of *in situ* charged micelles and provided a systematic evaluation of the influence of both the alkyl tail length of the surfactant and the hydrophilic head group on the selectivity for a variety of environmentally important species.

References

1. S. Terabe, K. Otsuka, K. Ichikama, A. Tsuchiya and T. Ando, *Anal. Chem.*, 56 (1984) 111.
2. S. Terabe, K. Otsuka and T. Ando, *Anal. Chem.*, 57 (1985) 834.
3. S. Terabe, H. Ozaki, K. Otsuka and T. Ando, *J. Chromatogr.*, 332 (1985) 211.
4. B. L. Karger, L. R. Snyder and C. Horvath, *An Introduction to Separation Science*, Wiley, 1973.
5. J. P. Foley, *Anal. Chem.*, 62 (1990) 1302.
6. A. T. Balchunas and M. J. Sepaniak, *Anal. Chem.*, 59 (1987) 1466.
7. G. M. Janini and H. J. Issaq, *J. Liq. Chromatogr.*, 15 (1992) 927.
8. J. H. Aiken and C. W. Huie, *J. Microcol. Sep.*, 5 (1993) 95.
9. M. J. Sepaniak, *J. High Resolut. Chromatogr.*, 13 (1990) 679.
10. H. Nishi, N. Tsumagari, T. Kakumoto and S. Terabe, *J. Chromatogr.*, 465 (1989) 331.
11. D. E. Burton, M. J. Sepaniak and M. P. Maskarinec, *J. Chromatogr. Sci.*, 25 (1987) 514.
12. M. J. Rosen, *Surfactants and Interfacial Phenomena*, John Wiley and Sons, New York, 1988.
13. H. Nishi, T. Fukuyama, M. Matsuo and S. Terabe, *J. Pharm. Sci.*, 79 (1990) 519.
14. D. Crosby and Z. El Rassi, *J. Liq. Chromatogr.*, 16 (1993) 2161.
15. S. Terabe, M. Shibata and Y. Miyashita, *J. Chromatogr.*, 480 (1989) 403.
16. S. Takasaki and A. Kobata, in V. Ginsburg (V. Ginsburgs), *Methods in Enzymology*, Academic Press, New York, 1978, 51.

17. H. Nishi, T. Fukuyama, M. Matsuo and S. Terabe, *J. Microcol. Sep.*, 1 (1989) 234.
18. R. O. Cole, M. J. Sepaniak, W. L. Hinze, J. Gorse and K. Oldiges, *J. Chromatogr.*, 557 (1991) 113.
19. A. Dobashi, T. Ono, S. Hara and J. Yamaguchi, *Anal. Chem.*, 61 (1989) 1984.
20. S. Terabe, H. Utsumii, K. Otsuka, T. Ando, T. Inomata, S. Kuze and H. Yanaoka, *J. High Resolut. Chromatogr.*, 9 (1986) 666.
21. K. Otsuka, S. Terabe and T. Ando, *J. Chromatogr.*, 348 (1987) 39.
22. R. A. Wallingford, P. D. Curry and A. G. Ewing, *J. Microcol. Sep.*, 1 (1989) 23.
23. H. T. Rasmussen, L. K. Goebel and H. M. McNair, *J. High Resolut. Chromatogr.*, 14 (1991) 25.
24. A. T. Balchunas and M. J. Sepaniak, *Anal. Chem.*, 60 (1988) 617.
25. D. L. Crosby, Ph.D. Thesis, Oklahoma State University, 1993.
26. J. Gorse, A. T. Balchunas, D. F. Swaile and M. J. Sepaniak, *J. High Resolut. Chromatogr. Chromatogr. Commun.*, 11 (1988) 554.
27. M. M. Bushey and J. W. Jorgenson, *J. Microcol. Sep.*, 1 (1989) 125.
28. J. Vindevogel and P. Sandra, *Anal. Chem.*, 63 (1991) 1530.
29. A. S. Cohen, A. Paulus and B. L. Karger, *Chromatographia*, 24 (1987) 15.
30. H. Nishi, N. Tsumagari and S. Terabe, *Anal. Chem.*, 61 (1989) 2434.
31. A. S. Cohen, S. Terabe, J. A. Smith and B. L. Karger, *Anal. Chem.*, 59 (1987) 1021.
32. J. Cai and Z. El Rassi, *J. Chromatogr.*, 608 (1992) 31.
33. S. Fanali, *J. Chromatogr.*, 545 (1991) 437.
34. S. Fanali and P. Bocek, *Electrophoresis*, 11 (1990) 757.
35. J. Snopek, H. Soini, M. Novotny and I. Jellinek, *J. Chromatogr.*, 559 (1991) 215.
36. A. Pluym, W. Van Ael and M. De Smet, *Trends Anal. Chem.*, 11 (1992) 27.

37. E. Gassman, J. E. Kuo and R. N. Zare, *Science*, 230 (1985) 813.
38. P. Gozel, E. Gossman, H. Michelsen and R. N. Zare, *Anal. Chem.*, 59 (1987) 44.
39. H. Nishi, T. Fukuyama, M. Matsuo and S. Terabe, *J. Chromatogr.*, 515 (1990) 233.
40. T. O. Cole, M. J. Sepaniak and W. L. Hinze, *J. High Resolut. Chromatogr.*, 13 (1990) 570.

CHAPTER VI

MICELLAR ELECTROKINETIC CAPILLARY CHROMATOGRAPHY
WITH *IN SITU* CHARGED MICELLES I. EVALUATION OF
N-D-GLUCO-*N*-METHYLALKANAMIDE
SURFACTANTS AS ANIONIC
BORATE COMPLEXES*

Abstract

A series of *N*-D-glucosyl-*N*-methylalkanamide (MEGA) surfactants was evaluated in micellar electrokinetic capillary chromatography (MECC) of neutral and charged species. The nonionic MEGA surfactants are readily converted *in situ* to anionic borate complexes through the association between their polyhydroxy head groups and borate ions at alkaline pH. The MEGA-borate complex surfactants yielded micelles with adjustable surface charge density, and consequently, the magnitude of the migration time window was readily altered by the pH and the concentration of borate in the running electrolyte. Studies by ¹¹B NMR and liquid secondary ion mass spectrometry on the borate complex formation with MEGA surfactants permitted the quantitative and qualitative determination of the various MEGA-borate complexes, respectively, and allowed the comparison of the MEGA-borate micelles to other *in situ* charged micelles recently introduced by this laboratory, i.e., the alkylglucopyranoside-borate micelles. The bulky polyhydroxy head group of the MEGA-borate surfactants yielded MECC systems with unique retention properties toward neutral

* J. T. Smith, W. Nashabeh and Z. El Rassi, *Anal. Chem.*, 66 (1994) 1119. Presented as a part of a poster at the 5th International Symposium on High Performance Capillary Electrophoresis (HPCE'93), Orlando, Florida, January 25-28, 1993.

and charged species. At constant micellized surfactant concentration, the methylene group selectivity of various homologous series, e.g., alkylbenzenes, phenylalkylalcohols and phenylalkylketones, was largely unaffected by the length of the alkyl tail of the surfactant indicating similar physico-chemical basis for retention on the various MEGA-borate micellar phases. Moreover, when the micellized surfactant concentration was held constant, the homologous solutes exhibited homoenergetic retention with the various *in situ* charged micellar phases. Under the same conditions, the capacity factors of neutral solutes increased linearly with the alkyl chain length of the MEGA surfactants indicating an increase in the hydrophobic phase ratio of the MECC systems. The MEGA-borate micellar phases were useful in the separation of a number of herbicides, polyaromatics, barbiturates and dansyl amino acids. In addition, in the presence of small amounts of γ -cyclodextrin, the MEGA-borate micelles allowed for the high resolution chiral separation of D,L dansyl amino acids.

Introduction

Micellar electrokinetic capillary chromatography (MECC), employing high electric field strengths and open tubular fused-silica capillaries filled with surfactant-rich electrolyte solutions, is well suited for the separations of neutral and charged species [1-8]. MECC is practiced with charged surfactants [1,3,6,9-11] including those with enantiomeric selectivity such as bile salts [12-14] and *N*-dodecanoyl-*L*-valinate [15]. The various micellar phases and their applications in MECC have been recently reviewed [16-18].

MECC is characterized by an elution range or migration time window that extends from the migration time of an unretained solute, t_0 , to the migration time of another solute completely solubilized by the micelle, t_{mc} . The magnitude of the migration time window largely influences peak capacity, resolution and analysis time, and therefore it is important that the migration time window stays as a freely adjustable parameter. Indeed, while for

some difficult separations a relatively large migration time window is needed (i.e., long separation time) in other cases a much narrower elution range would provide satisfactory separation. With surfactants that are charged in their natural environment, e.g., sodium alkyl sulfate, alkyltrimethylammonium halides, etc., the magnitude of the migration time window is usually predetermined and can not be varied systematically. In fact, with anionic surfactants such as sodium dodecyl sulfate, and in the useful pH range (i.e., pH > 7.0), the magnitude of the migration time window is largely unaffected by pH [19], i.e., the values of t_0 and t_{mc} are largely unaffected. Also, with cationic surfactants such as cetyltrimethylammonium halides, the magnitude of the migration time window remains unchanged (i.e., t_0 and t_{mc} are unchanged) over a wide range of pH (4.5 to 9.0) [20]. For both types of micellar phases, the concentration of the surfactant has little or no effect on the extent of the elution range [19,20]. The magnitude of the migration time window of MECC with ionic surfactants can be somewhat increased (t_{mc} increases) by using surfactants with short alkyl chains [20,21] or by surface modification of fused silica capillaries [19,21,22] (both t_0 and t_{mc} increase), but its width is still predetermined. Although several approaches have been described, the addition of organic solvents such as methanol or isopropanol to the electrolyte seems to be the most effective in altering the magnitude of the migration time window [8,23,24]. However, in the presence of organic modifiers both t_0 and t_{mc} increased, thus yielding long separation time [23]. Also, because organic modifiers (e.g., methanol, acetonitrile, isopropanol) disrupt the formation of the micelles, the separation efficiency was significantly reduced [24]. This is to say that for the same total concentration of surfactant, the number of micelles by unit column volume decreases in the presence of organic modifier leading to increased intermicellar distance, and consequently resistance to mass transfer in the aqueous phase increases [25].

Very recently, our laboratory has addressed the need for micellar phases having adjustable migration time window by introducing and evaluating *in situ* charged micelles [26]. In general, *in situ* charged micelles are based on the complexation of borate or

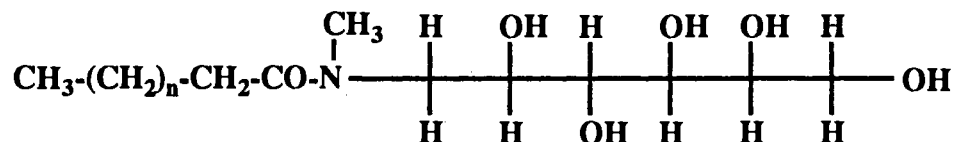
boronate ions with neutral surfactants having polyolic polar head groups. We have already described the electrokinetic and chromatographic behavior of octyl- β -D-glucopyranoside-borate micelles [26], and in an upcoming chapter we will introduce other *in situ* charged micelles which are based on the complexation of a series of alkyl- β -D-glucopyranoside surfactants with butylboronate ions [27]. In the present chapter, the MECC behavior of *N*-D-glucosyl-*N*-methylalkanamide (MEGA) surfactants in the presence of borate ions at alkaline pH is evaluated. With *in situ* charged micelles, the surface charge density of the micellar phases can be varied conveniently by changing the borate or boronate concentration and/or the pH of the running electrolyte. As a result, the migration time window of the micellar system can be varied systematically over a certain range, a feature that allows the optimization of resolution and peak capacity [26].

Thus, this chapter is an extension to our recent contribution to MECC, and entails the following objectives: (i) to further develop the concept of micelles with variable surface charge density, (ii) to shed light on the energetics of retention of neutral solutes with various MEGA-borate surfactants, (iii) to examine the correlation between solute retention and the hydrophobic character of the micellar systems, and (iv) to evaluate the usefulness of the new micellar phases in the separation of a wide range of species. Furthermore, and in order to understand the complexation of polyolic surfactants with borate, preliminary studies involving ^{11}B NMR analysis and liquid secondary ion mass spectrometry (LSIMS) were performed.

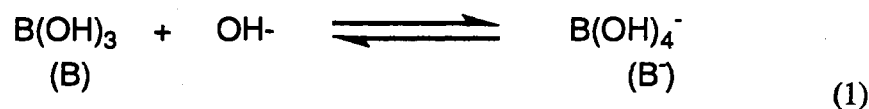
Principles of *In Situ* Charged Micelles and Some Aspects of Polyol-Borate Complexation

The chemical structure of the *N*-D-glucosyl-*N*-methylalkanamide surfactants is shown below, where $n = 5, 6$ and 7 for the octanoyl- (MEGA 8), nonanoyl- (MEGA 9) and decanoyl-*N*-methylglucamide (or MEGA 10), respectively [28]. These homologous

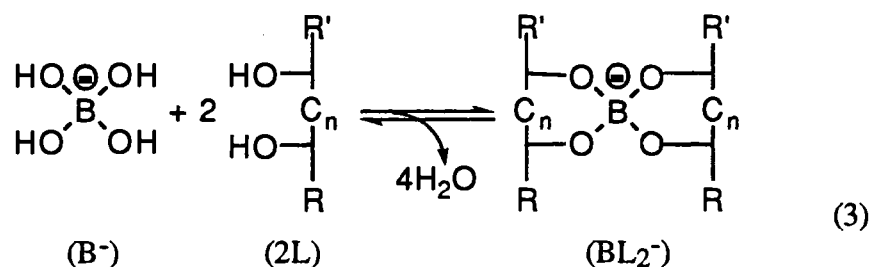
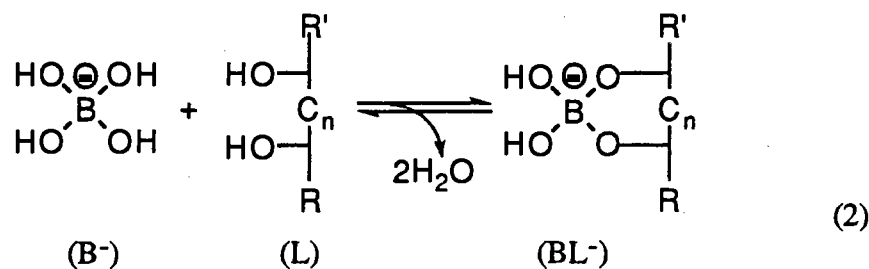
surfactants have in common a linear sugar head group, the *N*-methyl-D-glucamidyl moiety, which can be charged *in situ* through borate complexation.



The complex formation between borate ions and polyhydroxy compounds, i.e., polyols, is not a new topic [29-31], and this phenomenon has been widely exploited in the separation [30] as well as the determination of the configuration of carbohydrates [29]. In these complexation reactions, it is the tetrahydroxyborate ion, $\text{B}(\text{OH})_4^-$, that undergoes complexation with the polyols. At alkaline pH, i.e., pH 8-12, where the complexation is most effective, aqueous boric acid solutions ($\text{pK}_a = 9.24$) contain tetrahydroxyborate ions according to the following equilibrium:



In general, the complex formation can be described by the following equilibria [32,33]:



where BL^- and BL_2^- are the mono- and di-esters, respectively, L is the polyol and $n = 0$ or 1. Equilibrium 2 is situated very much to the right whereas 3 is dependent upon the position of the hydroxyl groups in the polyol.

According to the above equilibria, polyols with adjacent hydroxyl groups could form cyclic borate esters with either five or six atom rings when $n = 0$ or 1, respectively, i.e., for 1,2-diols or 1,3-diols, respectively. The monocomplexes, BL^- , are less commonly called bidentate mono-esters, whereas the dicomplexes or spiranes, BL_2^- , are less often referred to as tetradentate di-esters. Tridentate borate esters (also called cleisto complexes) are known to exist, and their formation in high yields require polyols with specific configurations such as *cis,cis*-cyclohexane-1,3,5-triol [34].

Borate complex formation is favored if the distance between the two hydroxyl groups in the polyol molecule is of the same magnitude as the O-O distance in the borate ion [35] (O-O = 2.4 Å). Such a distance is found in the *cis*-1,2-diols of five membered ring compounds (2.49 Å), which react more strongly with borate than do their *trans* isomers [36] (O-O, 3.40 Å). Moreover, on the basis of the O-O distance open chains (acyclic) of sugars react more strongly with borate ions than do the cyclic chains [37]. The stability of borate esters is enhanced upon increasing the number of hydroxyl groups in the polyol molecule [29,32].

The MEGA surfactants with their linear polyol moiety are by far the most suitable commercially available neutral surfactants that can be charged *in situ* with borate or boronate ions. When compared to alkyl- β -D-glucopyranoside surfactants, the extent of complexation of MEGA surfactants with borate or boronate ions should be much higher due to the presence of two consecutive *threo-threo* 1,2-diols [32] at C2/C3 and C3/C4 in the *N*-methyl-D-glucamidyl moiety of the MEGAs, whereas in the alkyl- β -D-glucopyranoside the complexation is found to occur at the C4 and C6 hydroxyl groups of the glucopyranoside moiety in chair conformation which is not very favorable [30]. The

difference between both types of surfactants is discussed later in more details on the basis of ^{11}B NMR studies, see Results and Discussion.

Mono- and dicomplex (or spirane) borate esters coexist in aqueous solutions [33,38], and their molar ratio is affected (i) by the relative concentration of borate ions and polyol molecules, (ii) by the position of the hydroxyl groups in the polyol and (iii) by the presence of substituents. The spirocyclic complex is favored at high polyol:borate ratio [33]. The quantity of spiranes is directly connected, under otherwise identical conditions, with the position of two of the 1,2 (sometimes 1,3) hydroxyl groups. The less favorable the position of the hydroxyl groups the smaller is the quantity of spiranes, and at large excess of borate:sugar ratio, the quantity of dicomplexes (i.e., spiranes) becomes negligible.

Thus, while the MEGA surfactants are expected to form dicomplexes as well as monocomplexes with borate ions, the alkylglucosides may yield dicomplexes in smaller amounts due to the unfavorable position of their hydroxyl groups. Since mono- and dicomplex formations are dynamic, all surfactant molecules will be associated with a negative charge the magnitude of which will be influenced by the position of the equilibrium and therefore by the stability of the complex. According to equilibria 1, 2 and 3, at constant surfactant concentration, the complex concentration increases with borate concentration according to the law of mass action and also with pH due to higher concentration of borate ions.

An important variable in MECC is the elution range parameter defined by the ratio [19]:

$$\frac{t_0}{t_{mc}} = \frac{v_{mc}}{v_{eo}} = 1 - \frac{2\zeta_{mc}}{3\zeta_c} f(\kappa a) \quad (4)$$

where v_{mc} is the net velocity of the micelle, v_{eo} is the electroosmotic velocity of the aqueous phase, ζ_c and ζ_{mc} are the zeta potentials of the inner surface of the capillary and of the outer surface of the micelle, respectively, $f(\kappa a)$ depends on the shape of the micelle

[39], a is the radius of the micelle and κ is the familiar Debye-Hückel constant. The value of $f(\kappa a)$ varies between 1.0 and 1.50 depending on the dimensions of κa . The ζ potentials can be expressed by the following relationship [40]:

$$\zeta = \frac{4\pi\delta\rho}{\epsilon} \quad (5)$$

where ρ is the surface charge density of either the capillary surface (ρ_c) or the micelle (ρ_{mc}), and δ is the thickness of the diffuse double layer adjacent to either the capillary wall (δ_c) or the micelle surface (δ_{mc}). Modern theory equates δ to $1/\kappa$, and therefore eqn 5 can be rearranged as follows:

$$\zeta = \frac{4\pi\rho}{\kappa\epsilon} \propto \frac{1}{\sqrt{I}} \quad (6)$$

where I is the ionic strength of the medium.

According to eqns 4 and 5, the elution range parameter can be varied conveniently by changing the charge density of the micelle and/or that of the capillary inner surface. As with the octylglucoside-borate micelles described previously [26], one of the characteristics of the MEGA-borate micellar systems is that the surface charge density of the micelle can be readily adjusted through pH, borate concentration and surfactant concentration, see below, while that of the capillary can be kept almost constant. In fact, at alkaline pH, the silanol groups of the fused silica surface are fully ionized, and as a result the charge density is practically constant.

The adjustment of the surface charge density of the MEGA surfactants, and consequently the elution range parameter is based on varying the extent of complexation between the MEGA surfactants and borate ions. The overall surface charge density of the micelle, ρ_{mc} , can be expressed as [26]:

$$\begin{aligned}\rho_{mc} &= \frac{[MEGA \cdot B]}{[MEGA \cdot B] + [MEGA]} \rho_{mc-c} \\ &= \frac{\rho_{mc-c}}{1 + \frac{[MEGA]}{[MEGA \cdot B]}}\end{aligned}\quad (7)$$

where ρ_{mc-c} is the limiting charge density of the MEGA-borate micelle, $[MEGA \cdot B]$ is the total concentration of the complexed MEGA (i.e., mono- and dicomplex), and $[MEGA]$ is the concentration of uncomplexed surfactant. The higher the charge density the more negative the micelle. At constant surfactant concentration, any increase in the borate concentration or pH will result in a decrease in the ratio $[MEGA]/[MEGA \cdot B]$, and therefore a larger ρ_{mc} , see eqn 7. At constant pH and borate concentration, an increase in the surfactant concentration will yield an increase in the ratio $[MEGA]/[MEGA \cdot B]$, and as a result, ρ_{mc} will decrease, see eqn 7. According to eq 4 and 5, these readily tuned features of the micelles would allow the tailoring of the elution range for a given separation problem. It should be noted that changing the charge of the micelles through borate complexation may produce small changes in the size of the micelles [26]. In a recent study involving octylglucoside surfactant [41], it was shown that increasing the ionic strength up to 0.20, the CMC of the surfactant was largely unaffected.

With MEGA-borate complexes at alkaline pH, the magnitude of the migration time window can be altered through t_{mc} without drastically affecting t_0 . This is because at alkaline pH (i.e., above pH 8.0) the surface silanols are fully ionized, and consequently ρ_c remains constant. In other words, with alkaline borate while ζ_c of the capillary will undergo small changes, ζ_{mc} of the micelle will be affected to a much larger extent through borate and surfactant concentrations and the pH of the running electrolyte.

A particular feature of the *in situ* charged micelles is that the elution range can be manipulated through t_{mc} while keeping the capacity factor, k' , of neutral solutes constant. This is readily achieved by varying the pH or the borate concentration at fixed surfactant

concentration. Under these conditions, and for a given value of k' (i.e., surfactant concentration), the wider the migration time window (i.e., the smaller the ratio t_0/t_{mc}), the better the resolution and peak capacity.

With the traditionally used micelles (i.e., fixed surface charge density), and in the useful pH range [19] (i.e., pH > 7.0), the migration time window is predetermined and can not be varied systematically by altering the pH or ionic strength of the running electrolyte. In this case, resolution optimization is achieved mainly through k' (i.e., surfactant concentration), and the optimum k' for maximum resolution is given by [42,43]:

$$k'_{opt} = (t_{mc}/t_0)^{1/2} \quad (8)$$

This means that there is a limit beyond which increasing the amount of the surfactant (i.e., increasing k') would cause resolution to decline. This represents a drawback as far as the optimization of resolution for a multicomponent mixture is concerned since the maximum resolution for each pair of adjacent solutes is obtained at different surfactant concentrations [26]. For instance, for a pair of solutes of low retention, the optimum k' for maximum resolution is obtained at relatively high surfactant concentration, whereas the maximum resolution for a pair of solutes of higher retention would be at lower surfactant concentration [26]. Thus, the optimization of resolution for various pairs of solutes in a multicomponent mixture can not be effectively achieved through k' , i.e., through surfactant concentration.

With the micellar systems under consideration, it is possible to affect simultaneously a double optimization of resolution through k' and t_{mc} [26]. With SDS and other ionic surfactants, window optimization is most often achieved through an increase in both t_0 and t_{mc} by adding methanol to the running electrolyte [24]. But increasing the concentration of organic modifier lead to a drastic increase in the separation time. In addition, SDS micellar systems can not tolerate a large amount of methanol

without disrupting the micellar formation, a phenomenon that usually leads to band broadening [24], see introduction for explanation.

Experimental

Reagents and Materials

Octanoyl-*N*-methylglucamide (MEGA 8), nonanoyl-*N*-methylglucamide (MEGA 9), decanoyl-*N*-methylglucamide (MEGA 10) and octyl- β -D-glucopyranoside were purchased from Calbiochem Corp. (La Jolla, CA, U.S.A.) or from Anatrace (Maumee, OH, U.S.A.). All the herbicides were purchased from Chem Service (West Chester, PA, U.S.A.). Sudan III, which was used for the determination of the migration time of the micelles, t_{mc} , phenylalkyl alcohols, alkylbenzenes, phenyl alkyl ketones and boron trifluoride etherate were obtained from Aldrich Chemical Co. (Milwaukee, WI, U.S.A.). Barbiturates and dansyl amino acids were purchased from Sigma Chemical Co. (St. Louis, MO, U.S.A.). All chemicals for the preparation of electrolyte were from Fisher Scientific (Pittsburgh, PA, U.S.A.). Methanol was purchased from EM Science (Cherry Hill, NJ, U.S.A.). Triethanolamine was purchased from Fluka Chemical Corp. (Ronkonkoma, NY, U.S.A.). Aniline, 1-naphthylamine, naphthalene, biphenyl and anthracene were from Eastman Kodak Co. (Rochester, NY, U.S.A.). γ -Cyclodextrin was a gift from American Maize-Products Co. (Hammond, IN, U.S.A.). All solutions were prepared with deionized water and filtered with 0.2 μ m Uniprep Syringeless filters from Fisher Scientific to avoid capillary plugging.

Instrument and Capillaries

The capillary electrophoresis instrument used in this study is the same as that described previously [44,45]. It consisted of two high-voltage power supplies of positive and negative polarity Models MJ30P400 and MJ30N400, respectively, from Glassman

High Voltage (Whitehouse Station, NJ, U.S.A.) and a UV-Vis variable wavelength detector Model 200 from Linear Instrument (Reno, NV, U.S.A.) equipped with a cell for on-column detection. The detection wavelength was set at 240 nm for the detection of herbicides, or 254 nm for the detection of phenylalkyl alcohols, alkylbenzenes, phenyl alkyl ketones, dansyl amino acids and barbiturates or at 340 nm for the detection of Sudan III. It should be noted that at wavelengths below 220 nm the background absorbance increases due to the amide bond in the MEGA surfactants. Unless otherwise indicated, in all experiments, the running voltage was 15.0 kV. The electropherograms were recorded with a computing integrator Model C-R4A from Shimadzu (Columbia, MD, U.S.A.)

Fused-silica capillaries having an inner diameter of 50 μm and an outer diameter of 375 μm were obtained from Polymicro Technology (Phoenix, AZ, U.S.A.). In all experiments, the total length of the capillary was 80.0 cm with 50.0 cm separation distance, i.e., from the injection end to the detection point.

Mass Spectrometry Measurements

All mass spectra were acquired with a VG ZAB2-SE instrument (VG Analytical Ltd., Manchester, UK). The instrument is equipped with a VG II-250 data acquisition system. Liquid secondary ion mass spectrometry (LSIMS) was performed with a cesium ion gun operated at 32 kV. The negative secondary ions were accelerated at 6 kV. The mass range scanned was 100 to 950 m/z at a rate of 10 seconds/decade. An instrument resolution of approximately 1000 was used in acquiring the spectra. Calibration was made using cesium iodine on the probe tip.

For continuous flow-liquid secondary ion mass spectrometry (CF-LSIMS), the spectra were obtained by a single scan, and no signal averaging was applied. The mobile phase was a 1:1 mixture of water and methanol containing 2% (w/v) triethanolamine (TEA) adjusted to pH 10.5 with ammonium hydroxide. Ammonium hydroxide was used instead of sodium hydroxide to avoid the formation of sodium adducts commonly observed in

LSIMS of sugars. A flow-rate of 4.5 $\mu\text{L}/\text{min}$ was supplied to the source by a μLC -500 syringe pump (ISCO, Inc., Lincoln, NE, USA). The mobile phase was delivered by a 50 μm fused silica capillary, that was approximately 80.0 cm in length from the microinjector to the source. A 1 μL loop was used in the microinjector (Valco, Houston, TX, U.S.A). Standard surfactant-borate solutions were adjusted to pH 10.5 with ammonium hydroxide to ensure ionization of the borate.

NMR Measurements

All ^{11}B NMR spectra were recorded at room temperature on a Varian XL-400 Fourier-transform spectrometer, using boron trifluoride etherate as an external standard. At this field strength, the ^{11}B resonance is at 128 MHz. Samples were prepared in H_2O , keeping the total borate concentration constant 100 mM. The concentration of surfactant was varied and the pH was adjusted to 9.5 and 12.0 with NaOH for octyl- β -D-glucopyranoside and MEGA 8, respectively.

Procedures

The running electrolyte was prepared by dissolving proper amounts of boric acid and MEGA surfactants in water, and adjusting the pH to the desired value with sodium hydroxide. Sample solutions were made by dissolving pure compounds in the running electrolyte (i.e., micellar solution) containing small amounts of methanol (maximum 20% (v/v)).

Hydrodynamic sample injection mode, i.e., gravity-driven flow, was used in this study. The sample reservoir was raised to a height of 20 cm above the outlet reservoir for 5 s. The capillary was rinsed between runs with running electrolyte and was equilibrated for 5 min before sample introduction. Under these conditions of rinsing and equilibration, the reproducibility of migration times expressed by %RSD ($n = 3$ repetitive measurements) ranged between 0.05 to 1.7% with most of the RSDs below 1%.

In all calculations involving plate count, N was estimated from peak standard deviation taken as the half peak width at 0.607 of peak height (i.e., the inflection point). In all cases, the reported plate count is the average of at least three runs.

Results and Discussion

Evaluation of MEGA-Borate Complex Formation by Boron NMR and CF-LSIMS

^{11}B NMR is a proven method for the calculation of stability constants for the complex formation between borate and polyols [32]. The reaction rate for the interconversion of boric acid and tetrahydroxyborate (i.e., borate) anions is rapid enough on the ^{11}B NMR time scale, such that only one peak is observed for the two forms. The peak's chemical shift is dependent on the pH of the solution [46]. The chemical shift varies from $\delta \approx 20$ ppm at pH below 4 where primarily boric acid is present to $\delta \approx 2$ ppm at pH above 12 where borate is the predominant species. On the other hand, the reaction rate between the borate complexes and free borate is sufficiently low on the ^{11}B NMR time scale so that sharp and well resolved resonances are usually observed for the different components of the complexation equilibria. The spectrum for the MEGA 8-borate system at pH 12.0 is shown in Fig. 1A. The peak due to the free $\text{B}(\text{OH})_4^-$ at $\delta = 1.7$ ppm decreased gradually as other peaks at $\delta = 5.0$, $\delta = 6.0$ and $\delta = 10.0$ ppm began to increase when the concentration of surfactant added to the sample was increased. The peaks at $\delta = 5.0$ and $\delta = 6.0$ ppm correspond to the formation of a five-membered ring monocomplex (BL^-). The two different peaks are likely to be due to the presence of two pairs of vicinal diols that are well positioned for the binding of borate ions to the surfactant molecule. The two pairs of hydroxyl groups may have been the *threo-threo* 1,2 diols at C2/C3 and C3/C4. The peak at $\delta = 10.0$ ppm corresponds to two five-membered rings in a spiro

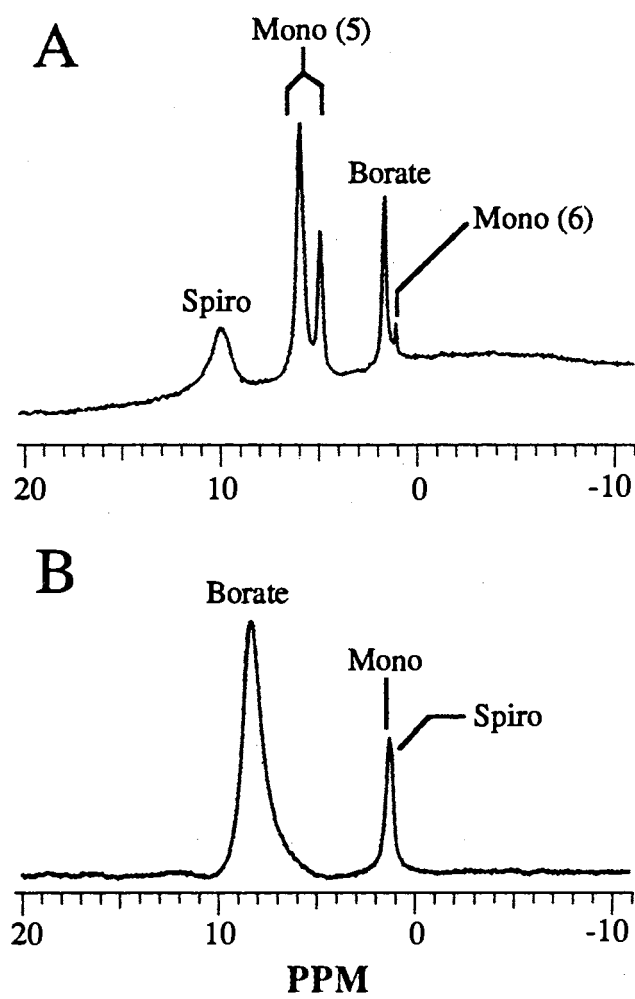


Figure 1. ^{11}B NMR spectra of surfactant-borate systems in H_2O . (A), 100 mM MEGA 8, 100 mM borate, pH 12.0; (B), 100 mM octyl- β -D-glucopyranoside, 100 mM borate, pH 9.5; external standard, BF_3 .

complex (BL_2^-). Finally, the minor peak at $\delta = 1.12$ ppm corresponds to a six-membered ring monocomplex (BL^-). These chemical shifts correspond very well to those reported in similar systems [47]. It should be noted that besides 1:1 (BL^-) complex formation, it is also possible to obtain 2:1 (B_2L^{2-}) but in relatively small amounts [47]. Unfortunately, NMR is unable to distinguish if more than one borate ion is attached to a single surfactant molecule (i.e., B_2L^{2-}), because the peaks for BL^- and B_2L^{2-} would have identical shifts.

The peaks of the various spectra were integrated in order to estimate the distribution of borate among the different species. The results of the integration are shown in Fig. 2 in terms of plots of the percentage of ^{11}B in free borate, monocomplex and dicomplex *versus* the surfactant:borate molar ratio. The plot for the monocomplex comprises all the 1:1 complexes and in addition the B_2L^{2-} since ^{11}B NMR can not distinguish BL^- from the B_2L^{2-} . Referring to Fig. 2, as the MEGA 8:borate molar ratio increased, the amount of monocomplex passed through a maximum in the region 0.5 to 1.0 while the spirane complex started to form at a molar ratio of 0.5 and became the predominant species at a molar ratio above 1.5.

In order to compare the borate-MEGA complex formation with similar systems previously developed in our laboratory [26], a comparative study was made using octyl- β -D-glucopyranoside. Octyl- β -D-glucopyranoside can form both six-membered mono- and spiro-complexes with borate. Literature reports six-membered monocomplexes (BL^-) at 1.6 ppm and spirocyclic complexes (BL_2^-) at 1.2 ppm for propane-1,3-diol [48]. At pH 12.0, the resonance for the complexed borate overlaps with the signal of free borate. In order to avoid complicated peak resolving methods, the pH was dropped to 9.5. At pH 9.5, the free borate has a chemical shift of $\delta = 8.4$, well shifted downfield of the complexed borate. Again, the borate was kept constant at 100 mM and the concentration of octyl- β -D-glucopyranoside was varied. With increasing the surfactant concentration, two peaks appeared at $\delta = 1.28$ and 1.16 ppm, which are believed to correspond to the

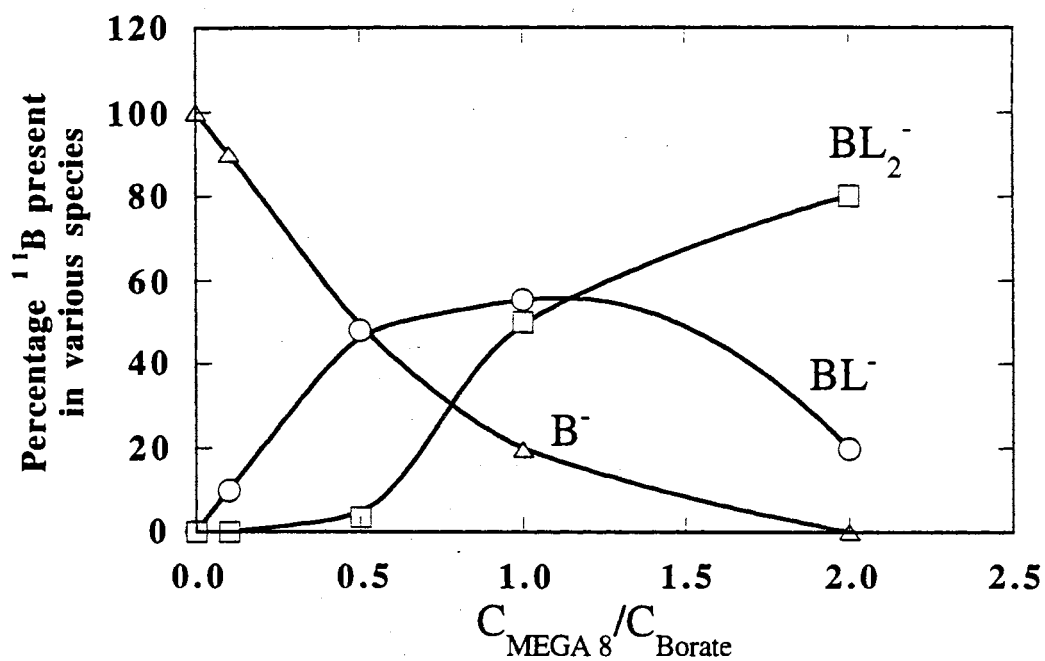


Figure 2. Plots of percentage of ^{11}B present in the various species of the MEGA 8-borate mixtures *versus* MEGA:borate molar ratio calculated using ^{11}B NMR integration data. Borate concentration, 100 mM ; pH 12.0; solvent, H_2O . At this pH $C_{\text{Borate}} \equiv [\text{Borate}]$.

mono- and spirocyclic complexes, respectively, see Fig. 1B. These two peaks are not resolved to an extent that separate integration values could be obtained. To compare the octyl- β -D-glucopyranoside-borate and MEGA 8-borate systems, the amount of free and complexed borate are shown in Fig. 3. At pH 9.5, approximately 65% of the borate is ionized as calculated from pK_a value. In Fig. 3, this partial ionization for boric acid is taken into account, by assuming that the analytical concentration of borate is 65 mM. In MECC, the typical operating conditions for these surfactant-borate systems lie between 0.5 to 1.0 $C_{\text{Surfactant}}/C_{\text{Borate}}$. As can be seen in Fig. 3, the MEGA surfactants have a 3-4 fold higher affinity for borate than the alkylglucoside surfactants. This would explain the wider migration time window obtained with MEGA even when using much lower borate concentration than with the alkylglucoside surfactant, thus allowing higher electric field strengths to be used.

To further gain insight into the complex formation reactions between the polyolic surfactants and borate, CF-LSIMS was applied in a similar study. The CF-LSIMS spectrum obtained by injecting a solution of 25 mM MEGA 8 and 250 mM borate (results not shown) yielded several peaks which were readily identified as corresponding to the free surfactant (MEGA 8 - H)⁻ at 320.5 m/z, the surfactant-borate tridentate monocomplex, also called cleisto, (MEGA 8 + Borate - 3 H₂O)⁻ at 346.5 m/z, the surfactant/matrix-borate spiro complex (MEGA 8 + TEA + Borate - 4 H₂O)⁻ at 477.9 m/z and the surfactant-borate spiro complex (2(MEGA 8) + Borate - 4 H₂O)⁻ at 649.8 m/z. However, a peak at 420.7 m/z corresponding to a 100 m/z adduct could not be identified, and was also detected in the octyl- β -D-glucopyranoside system. Interestingly, the BL^- observed was in the cleisto form (i.e., tridentate monocomplex), (MEGA 8 + Borate - 3 H₂O)⁻, instead of the bidentate monocomplex, (MEGA 8 + Borate - 2 H₂O)⁻. ¹¹B NMR showed no evidence of the cleisto complex which should have a chemical shift at $\delta = 0.76$ - 0.85 ppm [34]. The formation of cleisto complex in the mass spectrum is believed to be a gas phase anomaly [49]. In addition, all of the suitable matrices such as TEA undergo complexation with

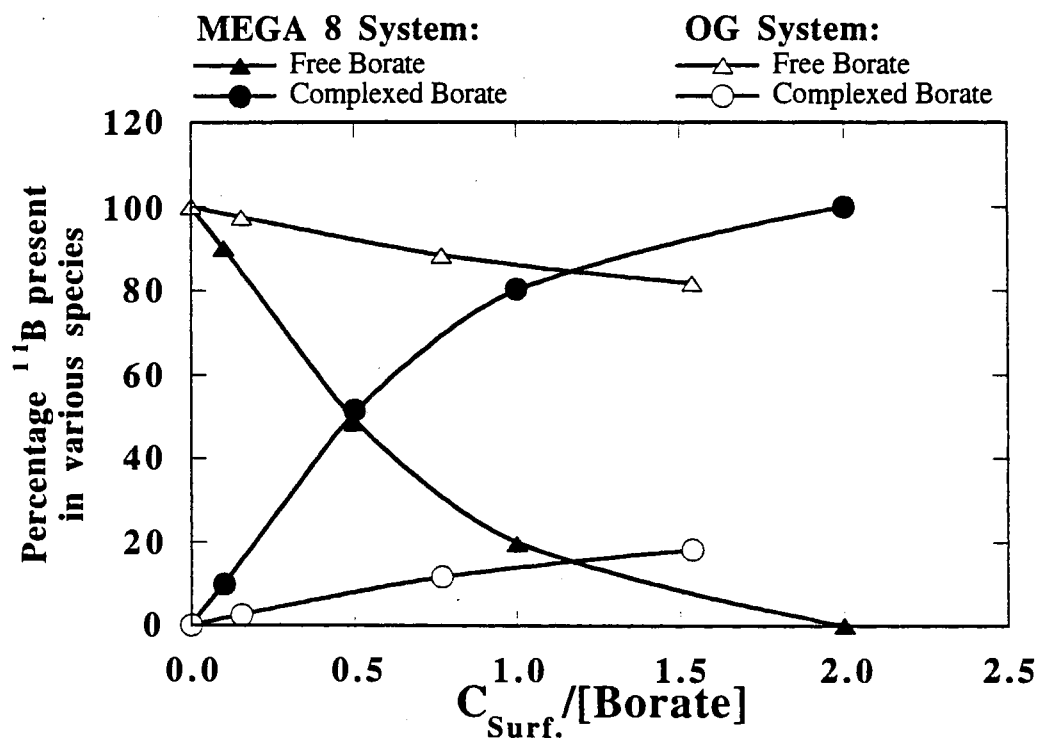


Figure 3. Plots of percentage of ¹¹B present in the various species of both MEGA 8-borate and Octyl- β -D-glucopyranoside-borate mixtures *versus* surfactant:borate molar ratio calculated using ¹¹B NMR integration data. MEGA 8 system: ionized borate concentration, 100 mM ; pH 12.0. Octyl- β -D-glucopyranoside system: ionized borate concentration, 65 mM ; pH 9.5. At pH 9.5, the species concentration of borate, [Borate], was used in the calculation.

borate thus changing the actual position of the equilibria involving the complex formation between borate and surfactant. Thus, LSIMS is not suitable to provide quantitative information about the species present in solution, but it does confirm the presence of some of the species identified by ^{11}B NMR.

CF-LSIMS was also performed on a solution of 25 mM octyl- β -D-glucopyranoside (OG) and 250 mM borate. Peaks identified in the resulting spectrum (results not shown) included the free surfactant $(\text{OG} - \text{H})^-$ at 291.3 m/z, $(\text{OG} + \text{Borate} - 3 \text{H}_2\text{O})^-$ at 317.2 m/z, $(\text{OG} + \text{Borate} - 2 \text{H}_2\text{O})^-$ at 335.2 m/z, $(\text{OG} + \text{Borate} + \text{TEA} - 4 \text{H}_2\text{O})^-$ at 448.5 m/z and $(2\text{OG} + \text{Borate} - 4 \text{H}_2\text{O})^-$ at 591.5 m/z. Again, there was an unidentified peak at 391.3 m/z corresponding to an adduct of 100 m/z to the surfactant. Three different forms of the borate complexes were identified, the monocomplex at 335.2 m/z, the cleisto complex at 317.2 m/z and the spiro complex at 591.5 m/z.

Variable Migration Time Window

The electrokinetic behavior of the various MEGA-borate micellar phases was evaluated at various pH and borate concentration. In these studies, methanol and Sudan III were used as the electroosmotic flow tracer and the micelle migration time indicator, respectively.

pH of the Running Electrolyte. Typical data pertaining to the relationship between the magnitude of the migration time window and the pH of the running electrolyte are presented in Fig. 4. These data were obtained with micellar solutions containing 100 mM MEGA 8 and 200 mM borate at various pH. As can be seen in Fig. 4, while t_{mc} increased sharply, t_0 increased only slightly over the pH range studied. At higher pH, the surface charge density of the micelle ρ_{mc} is increased as a result of increasing the concentration of MEGA-borate complexes (see eqns 1, 2, 3 and 7). This is accompanied by an increase in the electrophoretic velocity of the micelle in the opposite direction to the electroosmotic flow, and consequently t_{mc} is increased. The slight increase in t_0 , i.e., the

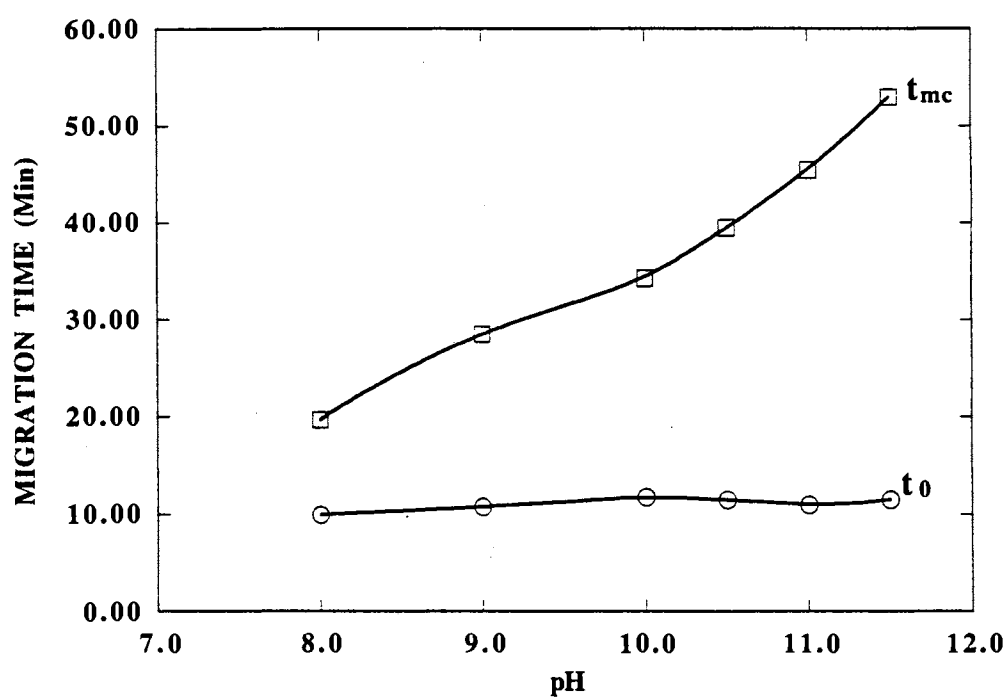


Figure 4. Effect of pH on the magnitude of the migration time window. Separation capillary, untreated fused-silica, 50.0 cm (to the detection point), 80.0 cm (total length) x 50 μm I.D.; running electrolytes, 100 mM MEGA 8, 200 mM borate at various pH; running voltage, 15.0 kV; tracers, Sudan III (for t_{mc}) and methanol (for t_0).

shallow decrease in electroosmotic flow, is caused by the increase in the ionic strength of the running electrolyte, see eq 6. In the pH range 8-12 the silanol groups of the siliceous wall are fully ionized, and consequently the charge density of the capillary inner surface is virtually constant. However, as the pH is raised from 8 to 12, the ζ potential of the capillary wall, which is inversely proportional to the square root of ionic strength, decreases causing the EOF to diminish.

Borate Concentration. The dependence of the breadth of the migration time window on borate concentration is shown in Fig. 5. These are typical plots of t_0 and t_{mc} *versus* the concentration of borate in the running electrolyte obtained with MEGA 10 at pH 10.0. As expected, the migration time window increased with borate concentration. While t_{mc} increased substantially, t_0 increased only slightly in the concentration range studied. The larger increase in t_{mc} is primarily due to an increase in the charge density of the micelles as a result of increasing MEGA-borate complex concentration and the predominance of MEGA-borate monocomplex, see Fig. 2. The slight increase in t_0 , i.e., the shallow decrease in the electroosmotic flow velocity, may be caused by the higher ionic strength and viscosity of the running electrolyte at elevated borate concentration, see eq 6.

Carbon Number in the Alkyl Tail of MEGA Surfactants. Figure 6A and B illustrates the magnitude of the migration time window obtained at constant micellized surfactant concentration (i.e., $[S] - CMC = \text{constant}$) *versus* the number of carbon atoms in the alkyl tails of the MEGA surfactants. These experiments were carried out at either constant borate concentration (Fig. 6A) or constant surfactant:borate (1:1) molar ratios (Fig. 6B), while keeping the voltage (or the current) and the pH constant. As can be seen in Fig. 6A, at constant borate concentration, the magnitude of the migration time window increased by a factor of 1.4 when the length of the alkyl tail of the surfactant increased from C₇ to C₉. This is due to the fact that for the same amount of borate in the running electrolyte and at constant micellized surfactant concentration, the molar ratio of

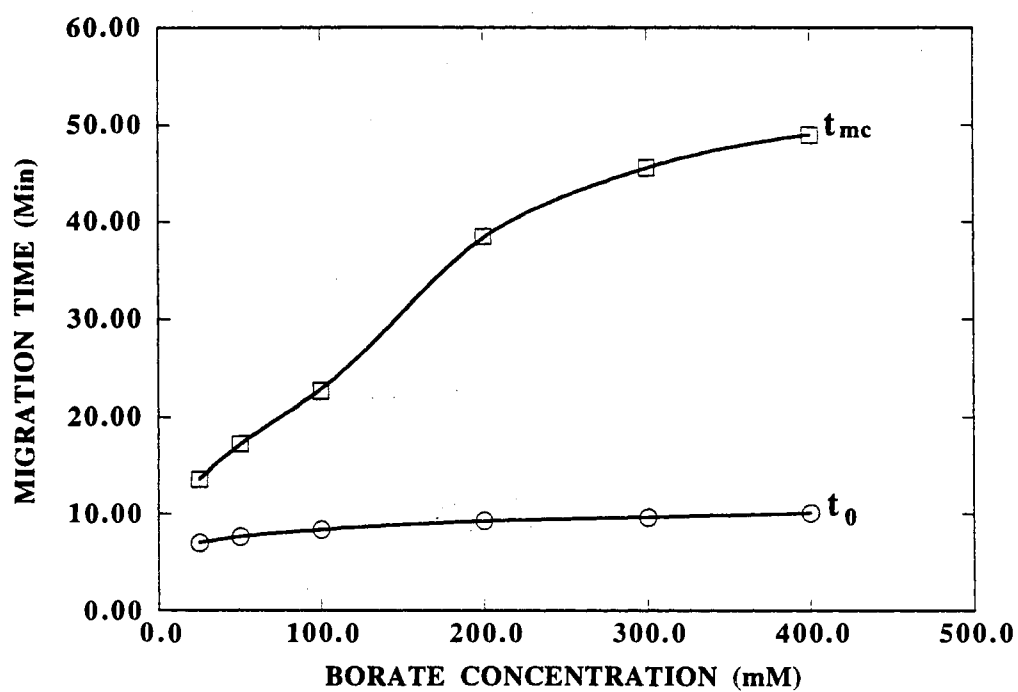


Figure 5. Effect of borate on the magnitude of the migration time window. Running electrolytes, 12.0 mM MEGA 10 at various concentration of borate, pH 10.0. Other conditions are as in Fig. 4.

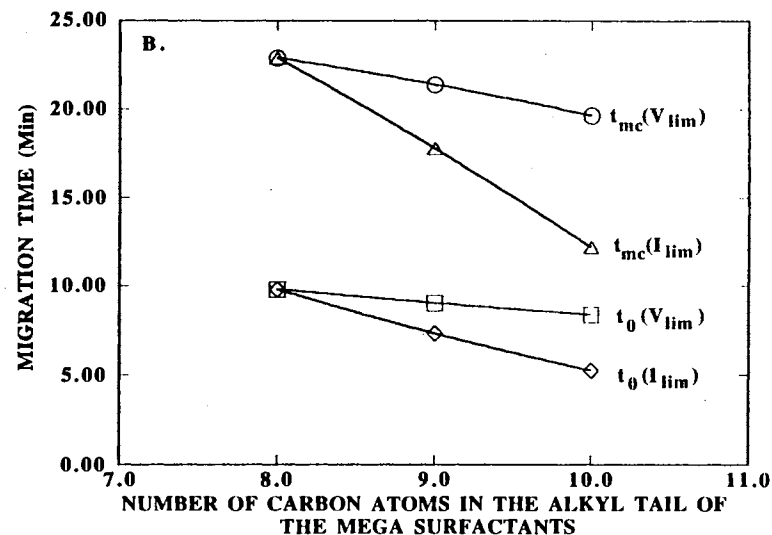
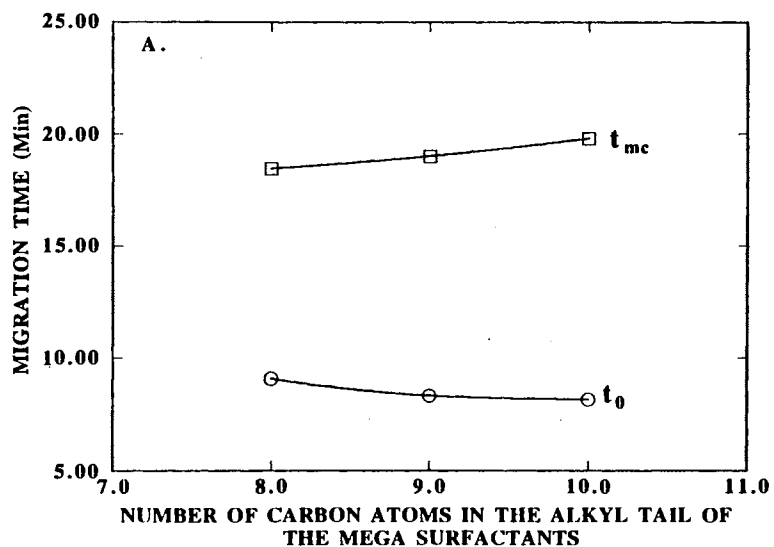


Figure 6. Effect of alkyl chain length of the surfactant on the magnitude of the migration time window. (A): electrolytes, 100 mM borate, pH 10.0 at constant micellized surfactant concentration (i.e., $[S] = CMC + 92.0 \text{ mM}$) which corresponds to 150 mM, 116 mM and 99 mM for MEGA 8, MEGA 9 and MEGA 10, respectively; running voltage, 15.0 kV. (B): electrolytes, surfactant concentration and pH were the same as in (A) except that the ratio of surfactant:borate was 1.0; in the case of voltage limiting regime (V_{lim}), running voltage was 15.0 kV; in case of current limiting regime (I_{lim}), running current was 30.3 μA .

surfactant:borate decreases from 1.51 to 0.99 when going from MEGA 8 to MEGA 10 micellar phases, a condition that favors the formation of BL^- over BL_2^- (see NMR studies). This procedure yields micelles with higher surface charge density, thus leading to a wider migration time window for MEGA 10. On the other hand, when the molar ratio of surfactant:borate was maintained the same (1:1) and the measurements were carried out at constant voltage (see Fig. 6B), the breadth of the migration time window remained constant as the length of the surfactant alkyl tail increased. This may be explained by the fact that under these conditions the surface charge density was the same for all the micellar phases and a difference in two carbon atoms in the alkyl tail of MEGA surfactants may not be sufficient to produce significant differences in their migration times. However, at constant surfactant:borate molar ratio and constant current, the breadth of the migration time window decreased by a factor of 1.95 with increasing the length of the surfactant tail from C₇ to C₉. Under these circumstances, as the length of the alkyl tail is increased the amount of borate in the running electrolyte decreases, thus permitting higher running voltages, and consequently both t_0 and t_{mc} are decreased.

Retention Behavior of Neutral Solutes

The MEGA-borate complex surfactants were characterized with neutral solutes, e.g., herbicides, phenylalkyl alcohols, phenyl alkyl ketones and alkylbenzenes at various pH and borate concentrations.

Correlation Between Capacity Factor and Carbon Number of Homologous Series.

The retention behaviors of three sets of homologous series, namely phenylalkyl alcohols ($n_c = 1$ to 6), phenyl alkyl ketones ($n_c = 1$ to 6) and alkylbenzenes ($n_c = 1$ to 4), were examined with the various MEGA-borate micellar phases. In all cases, plots of the logarithmic capacity factors *versus* the number of carbon atoms in the alkyl chains, n_c , of the homologous series yielded straight lines, and the results of the linear regression are listed in Tables I, II and III. From these results, and in accordance with recently published

data from our laboratory with cationic micellar phases [20], the relationship between $\log k'$ and n_c seems to follow the expression normally found in reversed-phase chromatography [50]:

$$\log k' = (\log \alpha)n_c + \log \beta \quad (9)$$

where the slope $\log \alpha$ is a measure of methylene group or hydrophobic selectivity which characterizes nonspecific interactions, while the intercept $\log \beta$ reflects the specific interactions between the residue of the molecule and the aqueous and micellar phases. This equation implies a constant contribution to the free energy of transfer of the solute between the aqueous phase and the micellar phase with each $-CH_2-$ increment in the chain length of the homologues.

The results in Table I were obtained at constant micellized surfactant concentration, i.e., $[S] - CMC = \text{constant}$. Under this condition, the $\log \alpha$ values remained almost the same when varying the length of the surfactant tail. These findings suggest similar physico-chemical basis for retention on the various MEGA micellar phases, and the only

TABLE I. Correlation between capacity factor, k' , and carbon number of homologous series obtained on the various MEGA-borate micellar phases at constant micellized surfactant concentration: $\log k' = (\log \alpha)n_c + \log \beta$; solutes, phenylalkyl alcohols; $[S] = CMC + 92 \text{ mM}$; $[\text{Borate}] = 100 \text{ mM}$; pH 10.0; 15.0 kV. CMCs of MEGA 8, MEGA 9 and MEGA 10 in pure water are 58, 24 and 7 mM, respectively.

Surfactant	$\log \beta$	$\log \alpha$	R
MEGA 8	-0.970	0.318	0.9997
MEGA 9	-0.897	0.338	0.9994
MEGA 10	-0.888	0.345	0.9995

difference is perhaps the phase ratio. These results corroborate earlier observations with a series of cationic surfactants [20]. Inspection of Table II reveals that there are no substantial differences between the $\log \alpha$ values for alkylbenzenes and phenylalkylalcohols

obtained on a MEGA 9 micellar phase at various pH. Moreover, the $\log\alpha$ values for phenylalkylketones and phenylalkylalcohols obtained on a MEGA 10 micellar phase at various borate concentration are about the same order of magnitude, see Table III. This may suggest that the contribution by a methylene group to the free energy transfer of the solute between the aqueous and micellar phases is largely independent of the rest of the molecule of the analyte.

TABLE II. Correlation between capacity factor, k' , and carbon number of homologous series at various pH: $\log k' = (\log\alpha)n_c + \log\beta$; solutes: phenylalkyl alcohols (PAA) or alkylbenzenes (AB); [MEGA 9] = 43 mM; [Borate] = 100 mM; 15.0 kV.

pH	$\log\beta$		$\log\alpha$		R	
	PAA	AB	PAA	AB	PAA	AB
9.0	-1.473	-0.398	0.343	0.390	0.9988	0.9947
10.0	-1.540	-0.602	0.364	0.436	0.9991	0.9993
11.0	-1.329	-0.634	0.322	0.448	0.9942	0.9992
12.0	-1.585	-0.427	0.365	0.395	0.9985	0.9936

TABLE III. Correlation between capacity factor, k' , and carbon number of homologous series at various borate concentration; $\log k' = (\log\alpha)n_c + \log\beta$; solutes: phenylalkylalcohols (PAA) or alkylphenylketones (APK); [MEGA 10] = 50 mM; pH 10.0; 15.0 kV.

[Borate]	$\log\beta$		$\log\alpha$		R	
	PAA	APK	PAA	APK	PAA	APK
25 mM	-1.035	-0.914	0.334	0.425	0.9949	0.9929
50 mM	-1.071	-0.951	0.336	0.431	0.9957	0.9933
100 mM	-1.121	-1.007	0.345	0.443	0.9950	0.9929
200 mM	-1.100	-1.025	0.342	0.455	0.9939	0.9926
300 mM	-1.086	-1.015	0.342	0.457	0.9939	0.9926

It should be noted that the value of $\log k'$ of benzyl alcohol solute did not align well with the rest of the homologues, and consequently it was not considered in the linear regression. Similarly, acetophenone, the first solute in the phenyl alkyl ketone homologous

series, did not fit well the linear relationship. This non-linearity is also observed in reversed phase chromatography for homologues below a "critical carbon number" and was attributed to functional groups in the homologous series [50]. Below the critical carbon number, the influence of a methylene group is overshadowed by the effect of an adjacent functional group. In this study, the functional groups are the hydroxyl and carbonyl groups in the phenylalkyl alcohols and phenyl alkyl ketones, respectively. Also, it should be mentioned that due to the stronger hydrophobic character of the alkylbenzene homologous series, these solutes could be resolved only for n_c up to 4 under the experimental conditions used in this study, i.e., at pH 9.0 and relatively low borate concentration.

Comparison of the Energetics of Retention on the Various Surfactants. Very recently, we have evaluated the energetics of retention of neutral solutes with a series of alkyltrimethylammonium halide micellar phases, and demonstrated that these cationic surfactants are quasi-homoenergetic toward neutral solutes and the major parameter that affected the retention of the analytes on the various micellar phases is the phase ratio [20]. In these studies, we have adapted the model of Horváth *et al.* [51,52] which proved useful in comparing the energetics of retention of various types of stationary phases, and more recently those of zirconia-based reversed phase packings introduced by Yu and El Rassi [53]. In this model, plots of $\log k'$ obtained on one micellar phase A *versus* those obtained on a reference micellar phase B can be utilized to compare the energetic of solute retention. If the Gibbs free energies for a given solute are identical in both micellar phases, the retention is termed homoenergetic. Under these circumstances, plots of $\log k'_A - \log k'_B$ obtained on the two micellar systems yield straight lines with unit slope and the antilog of the intercept is the quotient of the phase ratios of the two micellar systems according to the following equation:

$$\log k'_B = \log k'_A - \phi_A + \phi_B \quad (10)$$

where ϕ is the logarithmic phase ratio. If the corresponding Gibbs free energies for the two MECC systems are proportional, such that $\Delta G_A^0 = \alpha \Delta G_B^0$, where α is a constant, linear plots are still obtained with a slope different than unity as follows :

$$\log k'_A = \alpha \log k'_B + \phi_A - \alpha \phi_B \quad (11)$$

In this case, the retention is termed homeoenergetic. Equation 10 is a special case of eq 11 when α is unity.

Typical results obtained with phenylalkyl alcohols are depicted in Fig. 7, in terms of plots of $\log k'_B$ versus $\log k'_A$, which show a linear correlation. The values of the slopes and intercepts are summarized in Table IV. In all cases, the slopes are close to unity indicating quasi-homoenergetic retention on the various MEGA-borate micellar systems.

TABLE IV. Slopes, intercepts, R values and antilog of intercepts (i.e., quotient of phase ratios ϕ_B/ϕ_A) of $\log k' - \log k'$ plots of phenylalkyl alcohol (PAA) and alkylbenzene (AB) homologous series obtained on MEGA-borate surfactants. Experimental conditions are as in Table I.

Micellar Phase B/ Micellar Phase A	Slope		Intercept		R		ϕ_B/ϕ_A	
	PAA	AB	PAA	AB	PAA	AB	PAA	AB
	MEGA 8/MEGA 10	0.922	1.037	-0.179	-0.322	0.9997	0.9909	0.66
MEGA 9/MEGA 10	0.956	1.008	-0.055	-0.124	0.9999	0.9975	0.88	0.75
MEGA 10/MEGA 10	1.000	1.000	0.000	0.000	1.0000	1.0000	1.00	1.00

Both probe solute systems indicate that the MEGA 8 surfactant is on the average 0.6 as hydrophobic than MEGA 10, whereas the phase ratio of the MEGA 9 surfactant is 0.8 that of the MEGA 10. This means that adding a methylene group to the alkyl tail of the surfactant results in an increment of 0.2 in the quotient of the phase ratios with respect to the reference micellar phase, which is here the MEGA 10.

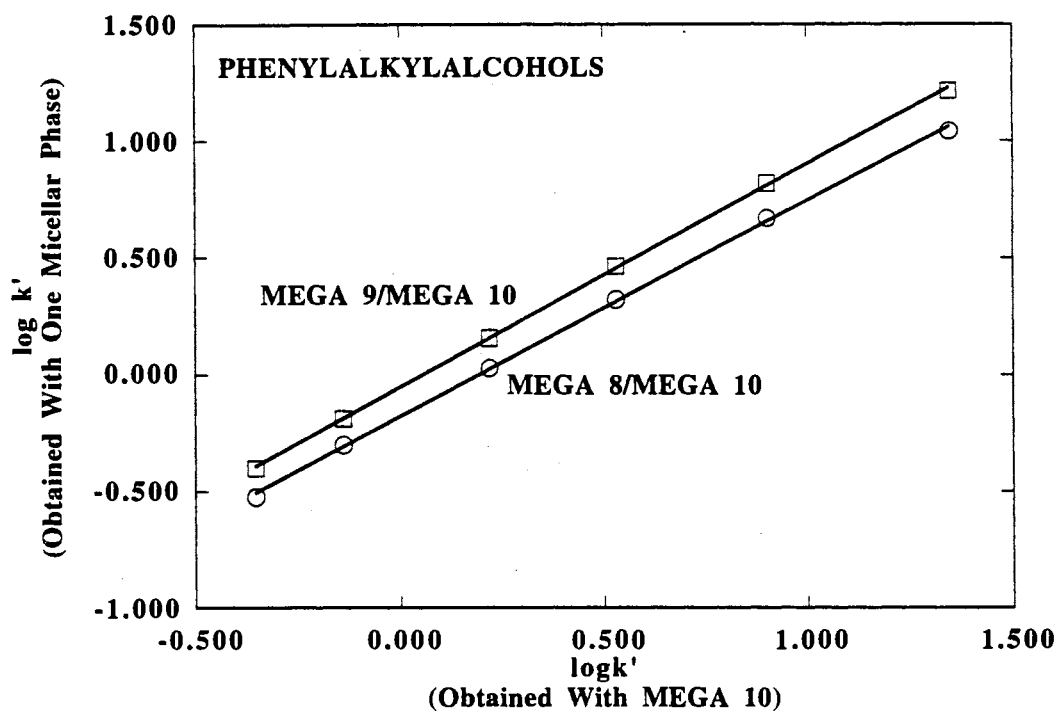


Figure 7. Plots of $\log k' - \log k'$ of phenylalkylalcohols homologous series obtained on one micellar phase versus another reference micellar at constant micellized surfactant concentration. Electrolytes, 100 mM borate, pH 10.0, at constant micellized surfactant concentration (i.e., $[S] = \text{CMC} + 92 \text{ mM}$) which corresponds to 150 mM, 116 mM and 99 mM for MEGA 8, MEGA 9 and MEGA 10, respectively. Other conditions are as in Fig. 4.

Correlation between Capacity Factor and Carbon Number of Surfactant. In a recent report from our laboratory [20] in which a series of cationic micellar phases was evaluated in MECC, we have shown that at constant micellized surfactant concentration, the capacity factor k' is given by

$$k' = \varphi K = (\text{Constant})K\vartheta \propto K.n_{c,surf} \quad (12)$$

where φ , K , ϑ and $n_{c,surf}$ are the phase ratio (i.e., ratio of the volume of the micellar phase to that of the aqueous phase), solute distribution coefficient between micellar and aqueous phases, the partial specific volume of the micelle and the number of carbon atoms in the alkyltail of the surfactant, respectively. According to eq 12, at constant micellized surfactant concentration, varying the length of the alkyl tail of the surfactant may affect the capacity factor through its effect on either the phase ratio (i.e., ϑ), the partition coefficient K , or both.

Table V summarizes the results of the linear regression for the plots of capacity factors of phenylalkyl alcohols, alkylbenzenes and herbicides versus the number of carbon atoms in the surfactant molecule. As can be seen in Table V, the R values are between 0.9759 and 0.9999 indicating that the plots of k' vs $n_{c,surf}$ are linear to quasi linear depending on the solute. This may suggest that the capacity factor depends on the size of the alkyl tail of the surfactant, i.e., $n_{c,surf}$, while the distribution coefficient K remains the same. Stated differently, at constant micellized surfactant concentration, the distribution coefficient of a given solute is largely unaffected by the length of the surfactant tail and the major contributor to retention is the phase ratio (i.e., ϑ or the size of the alkyl tail, $n_{c,surf}$). These findings corroborate earlier observations by Terabe *et al.* [2] in that the distribution coefficients of a series of neutral solutes were found to be almost the same with sodium dodecyl sulfate and sodium tetradecyl sulfate micellar phases. Also, these findings support our earlier observations with a series of cationic surfactants, whereby the capacity factors

of urea herbicides as well as that of phenylalkyl alcohol homologues were linear function of the alkyl tail of the surfactant [20].

TABLE V. Slopes, intercepts, and R values of plots of k' vs $n_{c,surf}$ for alkylbenzenes, phenylalkyl alcohols and herbicides obtained at constant micellized surfactant concentration with the various MEGA micellar phases. Experimental conditions are as in Table I.

Solutes	Slope	Intercept	R
<i>Alkylbenzenes:</i>			
Toluene	0.74	-3.13	0.9978
Ethylbenzene	2.83	-15.3	0.9998
Propylbenzene	8.96	-48.0	0.9985
Butylbenzene	12.12	-34.6	0.9940
<i>Phenylalkylalcohols:</i>			
2-Phenylethanol	0.11	-0.27	0.9848
3-Phenylpropanol	0.29	-0.98	0.9909
4-Phenylbutanol	0.65	-2.44	0.9910
5-Phenylpentanol	1.67	-6.97	0.9960
6-Phenylhexanol	5.56	-27.9	0.9999
<i>Herbicides:</i>			
Prometon	0.71	-3.17	0.9784
Propazine	1.48	-7.28	0.9759
Prometryne	2.85	-14.50	0.9780

Dependence of Capacity Factor on Borate Concentration. Figure 8A and B illustrates the dependence of the capacity factors of herbicides and phenylalkyl alcohols on borate concentration at constant pH and surfactant concentration. The capacity factor of the herbicides (i.e., prometryne, propazine and prometon) and the homologues showed little or no dependence on borate concentration in the range studied. The slight decrease in k' at low borate concentration may be due to the fact that the CMC of the MEGA surfactant increased first upon complexing with borate as a result of electrostatic repulsion between similarly charged head groups [54]. The shallow increase in k' at borate concentration higher than 100 mM may be explained by the fact that increasing the ionic strength would

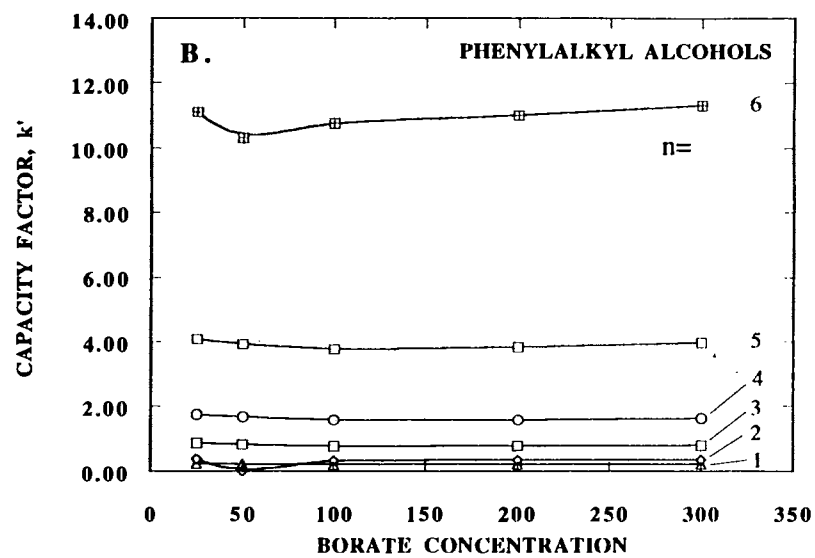
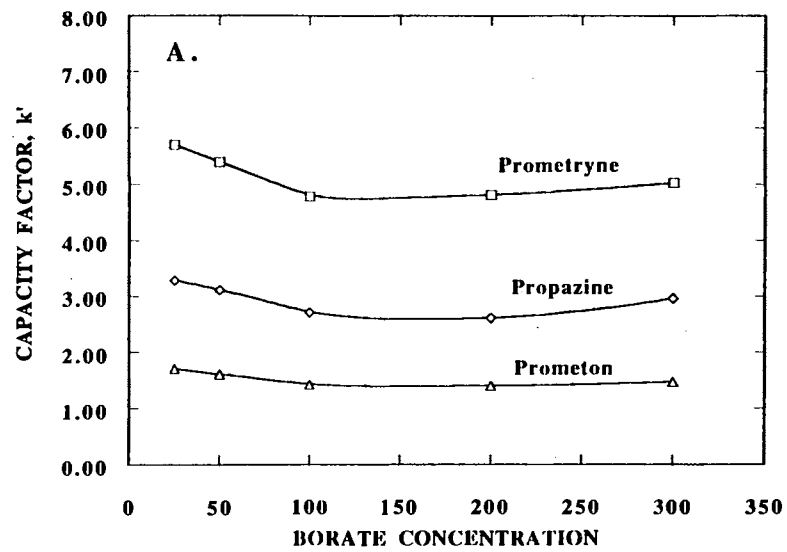


Figure 8. Capacity factor, k' , versus borate concentration in the running electrolyte. Electrolytes, 50 mM MEGA 10, pH 10.0, at various borate concentration; solutes: herbicides in (A) and phenylalkylalcohols in (B). Other conditions are as in Fig. 4.

decrease the repulsion between similarly charged groups of the MEGA-borate surfactant, thereby decreasing the CMC and increasing the aggregation number and volume of the micelles.

Dependence of Capacity Factor on pH. Figure 9A and B shows the dependence of the capacity factor on pH. As expected, since the borate and surfactant concentrations were kept constant, the k' values of the selected neutral solutes did not change significantly in the pH domain studied. The slight fluctuations in the k' values of the neutral solutes under investigation are within the range of experimental errors.

Selected Separations

Herbicides. Figure 10 illustrates the separation of a mixture of 8 herbicides consisting of three s-triazine herbicides (i.e., prometon, prometryne and propazine), one acetamide herbicide (i.e., butachlor), two chlorinated phenoxy acid herbicides (i.e., silvex and 2,4,5-T), one organophosphorus pesticide (i.e., diazinon) and one sulfur-carbamate herbicide (i.e., aldicarb). This separation was carried out at 15.0 kV using 100 mM MEGA 8 containing 100 mM borate, pH 10.0. Under these conditions, Silvex and 2,4,5-T are fully ionized and experience little or no interaction with the negatively charged micelles. The weak bases, namely prometon, propazine and prometryne having pK_a values of 4.20, 1.85 and 4.05, respectively, are neutral at this pH and elute in the order of increasing hydrophobic character. Diazinon and butachlor having less nitrogen groups in their molecules and carrying methyl and ethyl groups in their structures, respectively, eluted well resolved last just before Sudan III. The average plate count is about 452,000 plates/m.

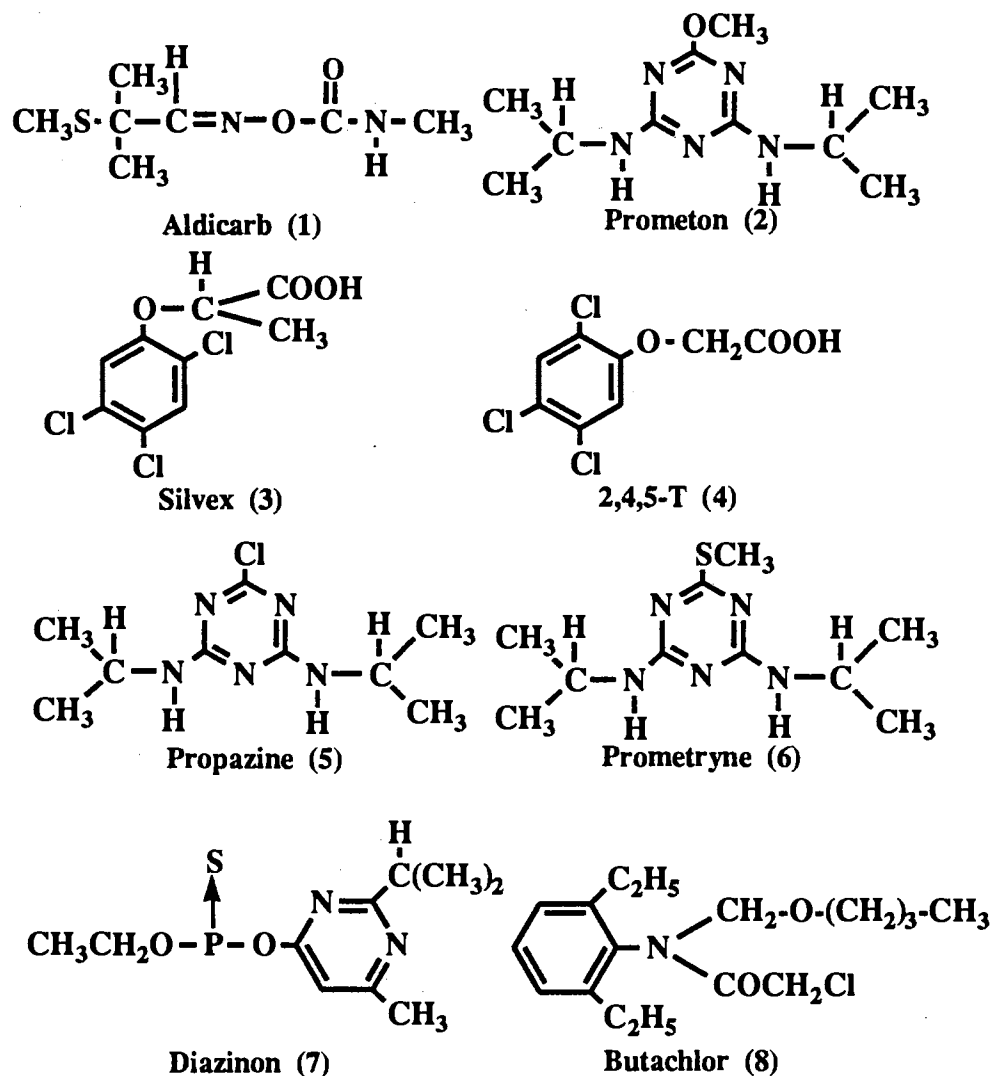


Figure 11A and B illustrates the separation of 9 urea herbicides on MEGA 8 and MEGA 10, respectively. Both micellar phases afforded excellent resolution between the individual herbicides, and the plate counts were 554,000 and 845,000 on MEGA 8 and MEGA 10, respectively. The higher separation efficiency obtained with MEGA 10 is due to the fact that the solutes associate more strongly with this micellar phase than with the MEGA 8-borate micellar system, a phenomenon that leads to decreased longitudinal molecular diffusion since the micelle has a smaller diffusion coefficient. As expected, the monohalogenated compounds eluted before the dihalogenated ones, thus indicating that the

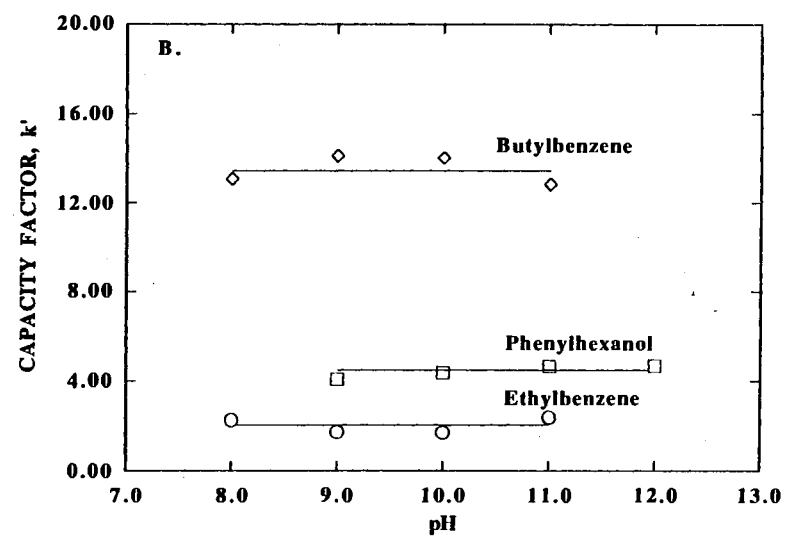
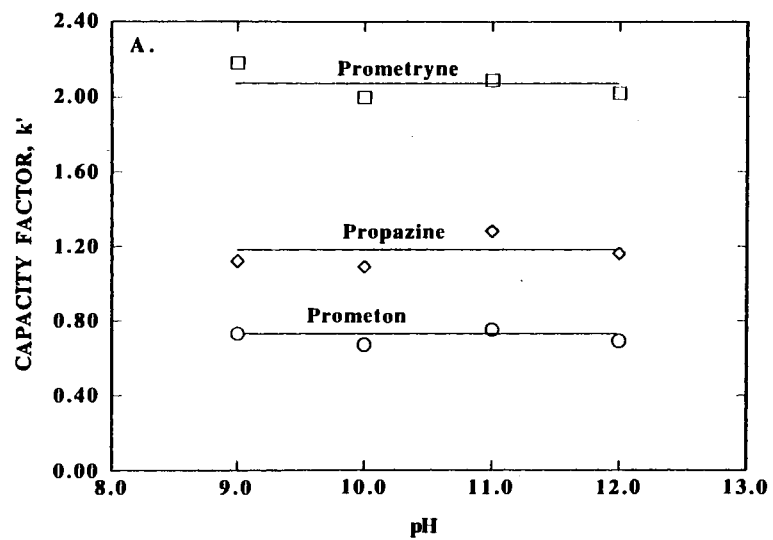


Figure 9. Capacity factor, k' , versus pH of the running electrolyte. Electrolytes, 100 mM borate containing 43 mM MEGA 9 at various pH; solutes: herbicides in (A) and alkylbenzenes and phenylhexanol in (B). Other conditions are as in Fig. 4.

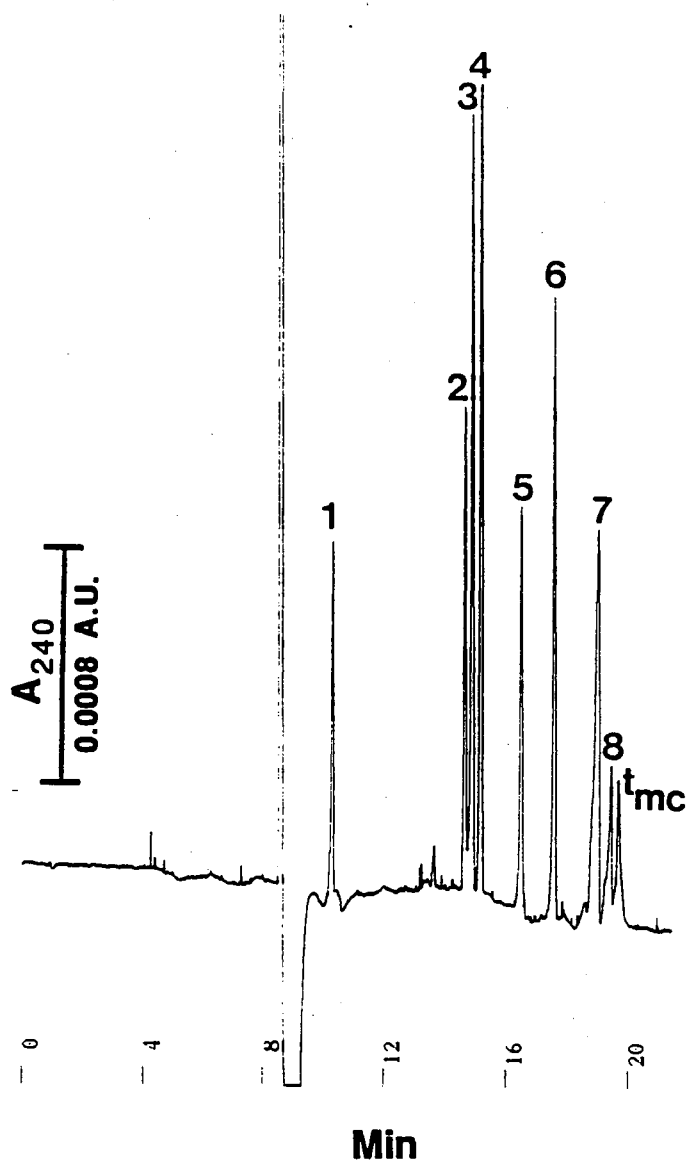


Figure 10. Electropherogram of herbicides (for structures of solutes, see text). Separation capillary, untreated fused silica, 50.0 cm (to the detection point), 80.0 cm (total length) x 50 μ m I.D.; electrolyte, 100 mM borate containing 100 mM MEGA 10, pH 10.0; running voltage, 15.0 kV; solutes: 1, aldicarb; 2, prometon; 3, silvex; 4, 2,4,5-T; 5, propazine; 6, prometryne; 7, diazinon; 8, butachlor.

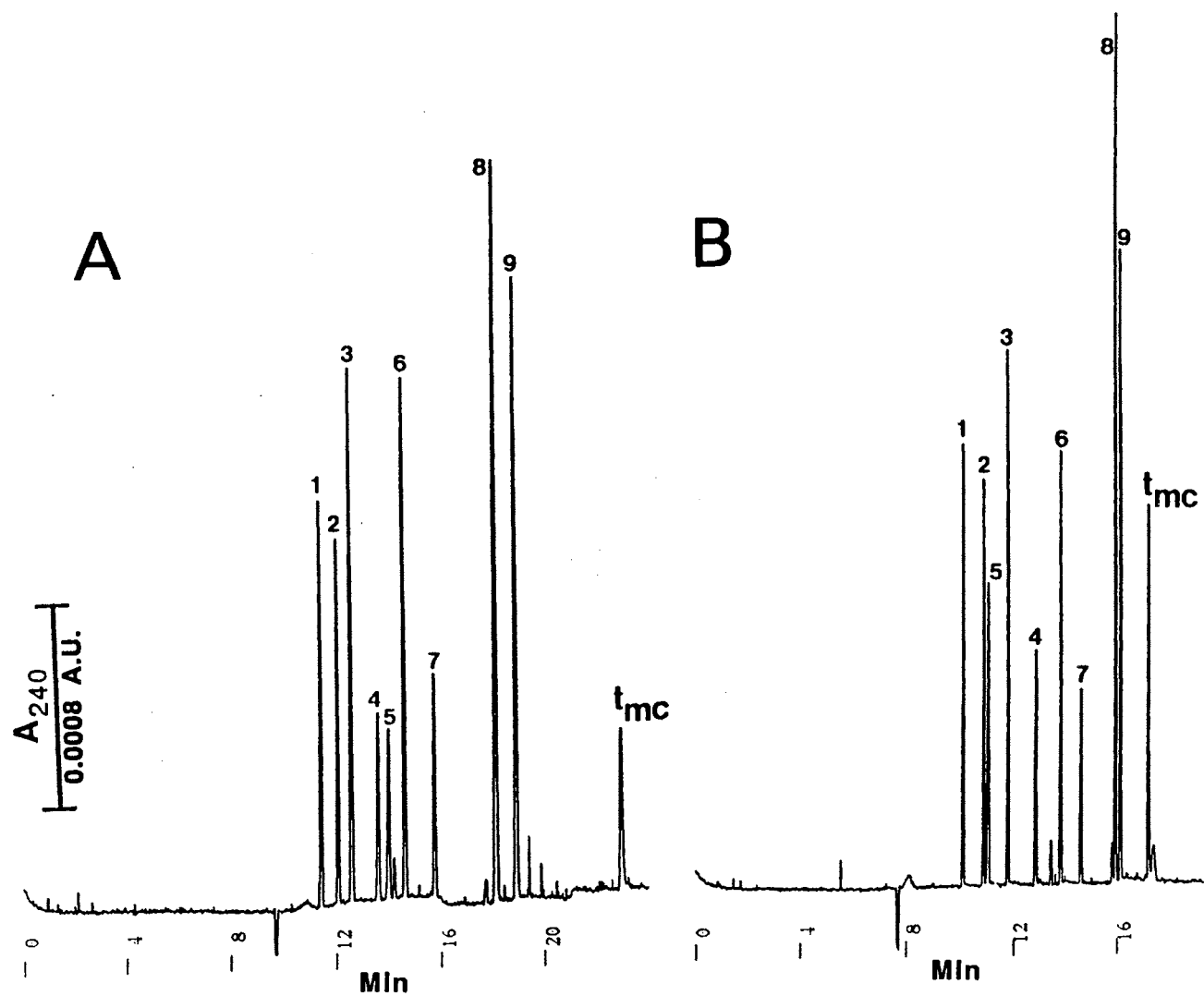
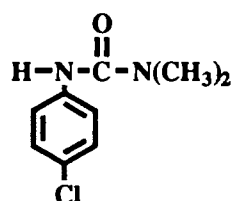


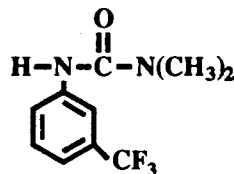
Figure 11. Electropherograms of urea herbicides (for structures of solutes, see text). Electrolytes: 125 mM borate, 100 mM MEGA 8, pH 10.0 in (A); 75 mM borate, 50 mM MEGA 10, pH 10.0 in (B). Solutes: 1, monuron; 2, fluometuron; 3, metobromuron; 4, siduron; 5, terbacil; 6, diuron; 7, linuron; 8, neburon; 9, chloroxuron. Other conditions are as in Fig. 12.

basis of retention is hydrophobic interaction. Moreover, neburon and chloroxuron having in their structures additional butyl and phenyl groups, respectively, eluted last. It should be noted that the elution order of terbacil changed when going from MEGA 8 to MEGA 10. This may be attributed to the weak ionization of terbacil at pH 10.0. The pK_a value of terbacil is not known, but in analogy with uracil ($pK_a = 9.45$) it may behave as a weak acid. Under this condition, terbacil may partially migrate by its own charge, and consequently would change elution order with respect to the other neutral solutes since MEGA 10 is more hydrophobic than MEGA 8.

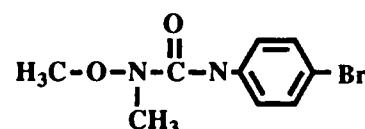
In a recent study from our laboratory with cationic micellar phases [20], only 6 of the urea herbicides could be resolved. This once again demonstrates the advantages of *in situ* charged MEGA micellar phases over traditionally used micelles. The bulky hydrophilic head group of MEGA-borate complexes affords more equitable distribution of hydrophobic and hydrophilic species between the aqueous and micellar phases, thus yielding higher resolution.



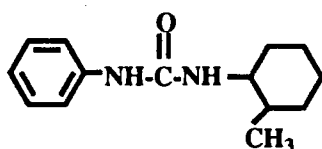
Monuron (1)



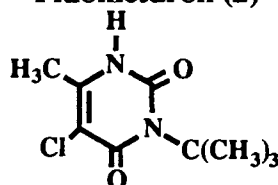
Fluometuron (2)



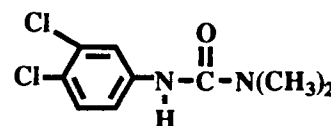
Metobromuron (3)



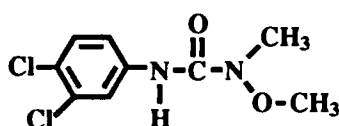
Siduron (4)



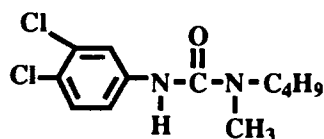
Terbacil (5)



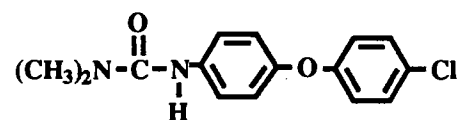
Diuron (6)



Linuron (7)



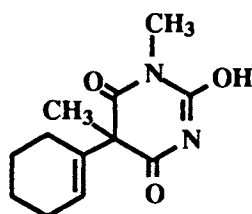
Neburon (8)



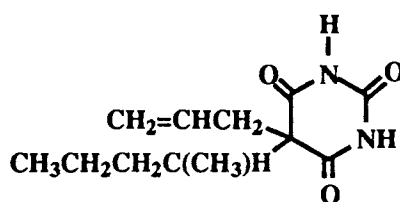
Chloroxuron (9)

Aromatics. The electropherogram depicted in Fig. 12 shows the separation of some aromatic compounds for up to three fused benzene rings. They eluted in the order of increasing number of fused benzene rings. The weak bases aniline and 2-naphthylamine having pK_a values of 4.6 and 4.11, respectively, are neutral at the pH of the experiment. The average plate count for these species is about 500,000 plates/m.

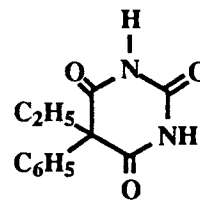
Barbiturates. Figure 13A and B depicts the electropherograms of four barbiturates, namely hexo-, seco- and phenobarbital and barbital. An average plate count of 424,000 plates/m is achieved using MEGA 10-borate micellar phase. These solutes are weak acids having pK_a values of 8.4, 7.9, 7.3 and 8.0 for hexobarbital, secobarbital, phenobarbital and barbital, respectively. Therefore, they are completely dissociated at the pH of the present experiment (i.e., pH 10.0), and consequently migrate mainly by their own charges in the opposite direction to the electroosmotic flow as the individual micelles. Barbital with higher charge-to-mass ratio eluted last, and secobarbital being more hydrophobic eluted after hexobarbital. Although the association of these species with the micelles was relatively weak, they were better resolved in the presence than in the absence of MEGA surfactant. In fact, when the surfactant was deleted but keeping other conditions the same, hexo- and secobarbital coeluted and the average plate count was 320,000 plates/m, see Fig 13B. Although small, the association of the solutes with the MEGA micellar phase can explain the higher separation efficiency obtained in the presence of surfactant. Because the micelle has a smaller diffusion coefficient, the solutes will undergo less longitudinal diffusion, and consequently sharper peaks are obtained [25].



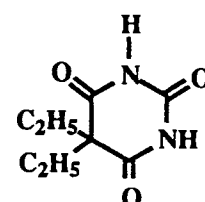
Hexobarbital



Secobarbital



Phenobarbital



Barbital

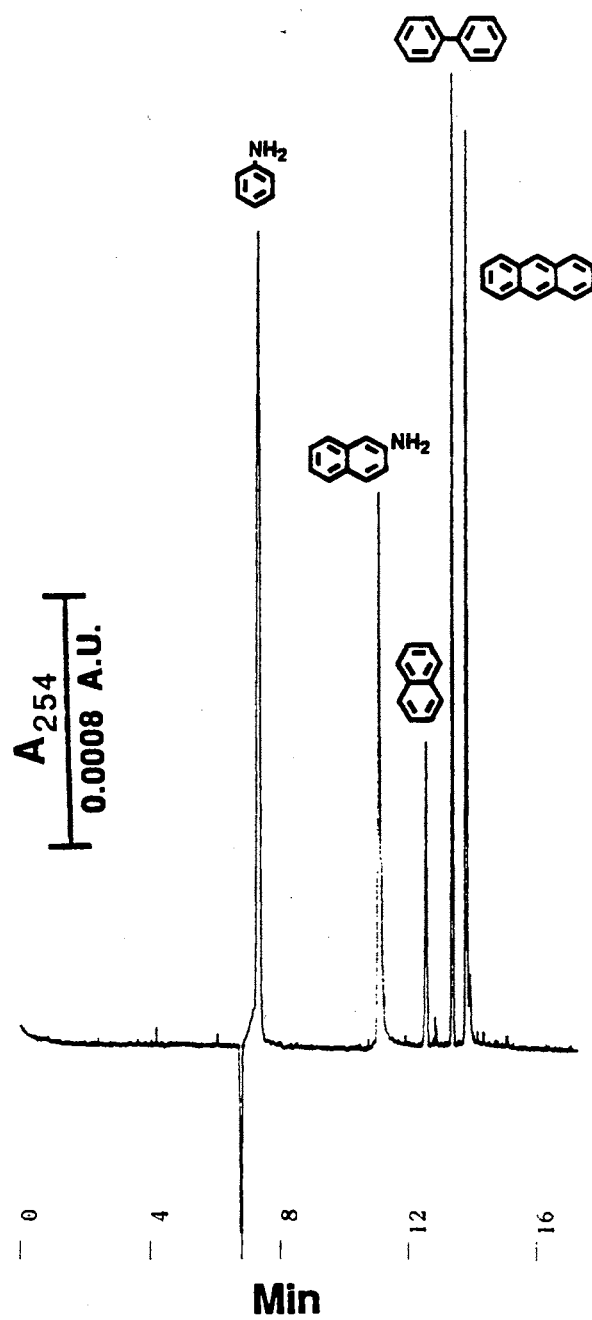


Figure 12. Electropherogram of some aromatics. Electrolyte, 50 mM borate, 50 mM MEGA 10, pH 10.0; solutes: (from left to right) aniline, 2-naphthylamine, naphthalene, biphenyl, anthracene. Other conditions are as in Fig. 10.

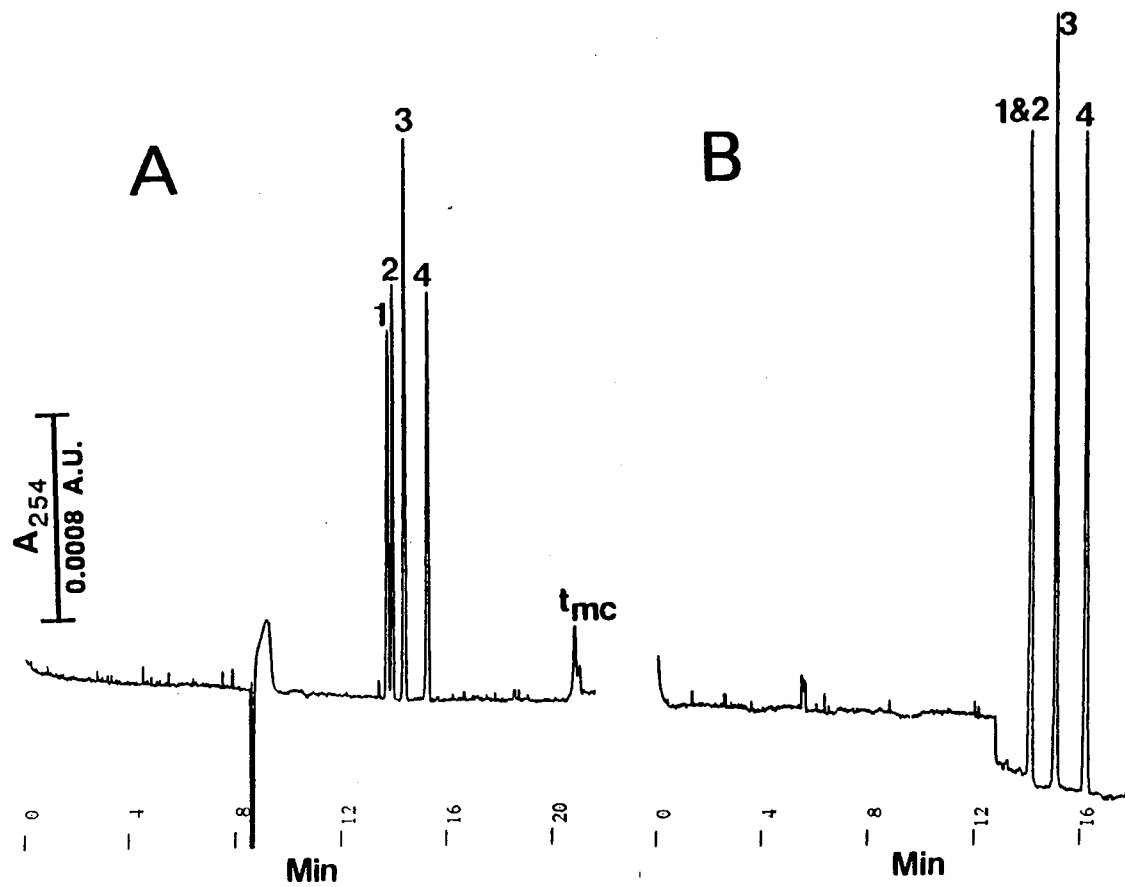


Figure 13. Electropherograms of some barbiturates (for structures of solutes, see text). Electrolytes, 100 mM borate containing 100 mM MEGA 10 in (A) or 0 mM MEGA 10 in (B), pH 10.0; solutes: 1, hexobarbital; 2, secobarbital; 3, phenobarbital; 4, barbital. Other conditions are as in Fig. 10.

Amino Acids. Fifteen dansyl amino acids (Dns-AA) were separated with 100 mM MEGA 10 containing 125 mM borate, pH 10.0, see Fig. 14A. The general chemical formula of the dansyl amino acids is $(\text{CH}_3)_2\text{NC}_{10}\text{H}_6\text{SO}_2\text{NH-AA}$, where NH-AA denotes the amino acid moiety of the derivatives. According to recent studies on the ionization of Dns-AA [55,56], the pK_a value of the dimethylamino group of Dns-AA, i.e., for the protonated form $(\text{CH}_3)_2\text{N}^+\text{HC}_{10}\text{H}_6\text{SO}_2\text{NH-AA}$, is between 3.0 and 4.0, and this value is largely independent of the ionic properties of the side chain of the amino acid. The amino group adjacent to the sulfonyl group of the dansyl moiety has a pK_a of 11.7, i.e., for the deprotonated form $(\text{CH}_3)_2\text{NC}_{10}\text{H}_6\text{SO}_2\text{N}^-\text{AA}$, and would dissociate only at extreme alkaline pH. At the pH of the experiment, the first amino group is uncharged while the ionization of second amino group is negligible. Therefore, the following Dns-AA: glutamine, asparagine, threonine, serine, valine, methionine, glycine, isoleucine, leucine, phenylalanine, and tryptophan will carry one negative charge each due primarily to the ionization of the carboxyl group of every amino acid. Glutamate, aspartate and cysteic acid are doubly negatively charged due to the ionization of the carboxyl group and to the side chain acidic group. Arginine with its guanidino side chain group ($\text{pK}_a = 12.5$), amino group linked to the dansyl function ($\text{pK}_a = 11.7$), carboxyl group ($\text{pK}_a = 2.2$) and the dimethyl amino group of the dansyl moiety ($\text{pK}_a = 3-4$) would have a pI value of 7.3-7.8, and is therefore negatively charged. The separation mechanism is rather complex involving hydrophobic interaction and electrophoretic migration of the various Dns-AA. Dansyl-asparagine and -glutamine each carrying a side chain acetamido group (polar groups) eluted first, while serine and threonine with a hydroxyl group side chain eluted thereafter. Although glycine is less hydrophobic than valine and threonine, this Dns-AA eluted later due to its higher charge-to-mass ratio. Isoleucine, leucine, phenylalanine and tryptophan were more retarded due to their stronger hydrophobic character. Arginine whose net charge is negative at the pH of the experiment may have formed ion pairs with the negatively charged micelles through its side chain guanidino group. As expected,

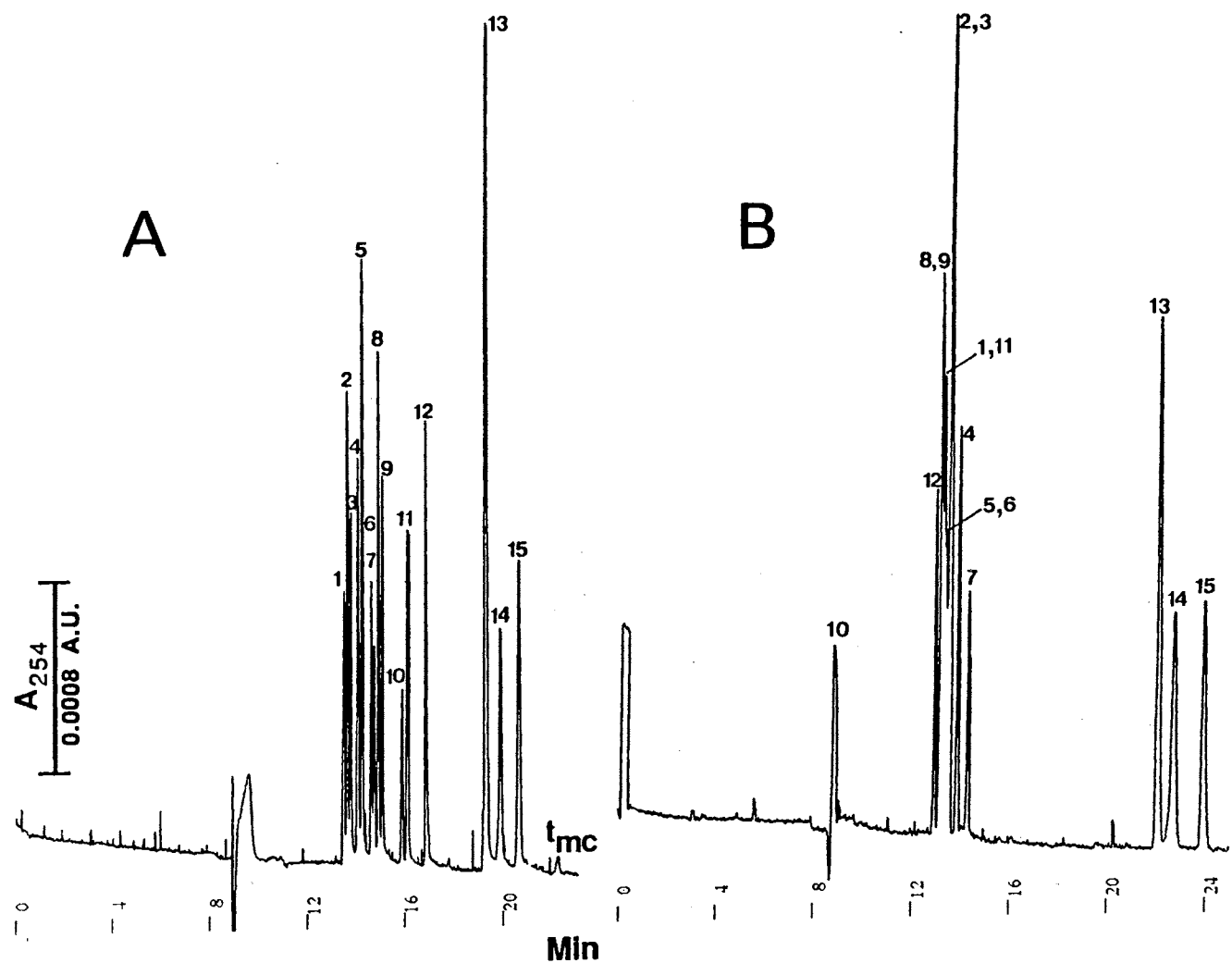


Figure 14. Electropherograms of dansyl amino acids. Electrolytes: 125 mM borate, 100 mM MEGA 10, pH 10.0 in (A); 125 mM borate, pH 10.0 in (B); solutes: 1, glutamine; 2, asparagine; 3, threonine; 4, serine; 5, valine; 6, methionine; 7, glycine; 8, isoleucine; 9, leucine; 10, arginine; 11, phenylalanine; 12, tryptophan; 13, glutamic acid; 14, aspartic acid; 15, cysteic acid. Other conditions are as in Fig. 10.

glutamate, aspartate and cysteic acid exhibited virtually no interaction with the micelles and eluted last because they are doubly negatively charged. The system allowed a high plate count with an average efficiency of about 580,000 plates/m. This again demonstrates the usefulness of MEGA-borate micelles in the separation of closely related charged species. In fact, in the absence of surfactant, most of the Dns-AA coeluted (see Fig. 14B) and some of the peaks are broader when compared to Fig. 14A. In the absence of surfactant, the solutes eluted more or less according to their charge-to-mass ratios.

We have also investigated the utility of the MEGA-borate micellar phases in the separation of D and L Dns-AA in the presence of small amounts of γ -cyclodextrin. A typical electropherogram is depicted in Fig. 15 where 810,000 plates/m are obtained. The addition of cyclodextrins to micellar solutions for the separation of enantiomers by MECC is a widely used approach [57].

Acknowledgement

This material is based upon work supported by the Cooperative State Research Service, U.S. Department of Agriculture, under Agreement No. 92-34214-7325. J.T. Smith is the recipient of a Water Resources Presidential Fellowship from the University Center for Water Research at Oklahoma State University. Finally, the authors acknowledge partial support by the NSF (CHE-8718150) and the Oklahoma Center for the Advancement of Science and Technology (No. 1506) for the upgrade of the NMR facility and the NSF (BSS-8704089) for the mass spectrometry laboratory.

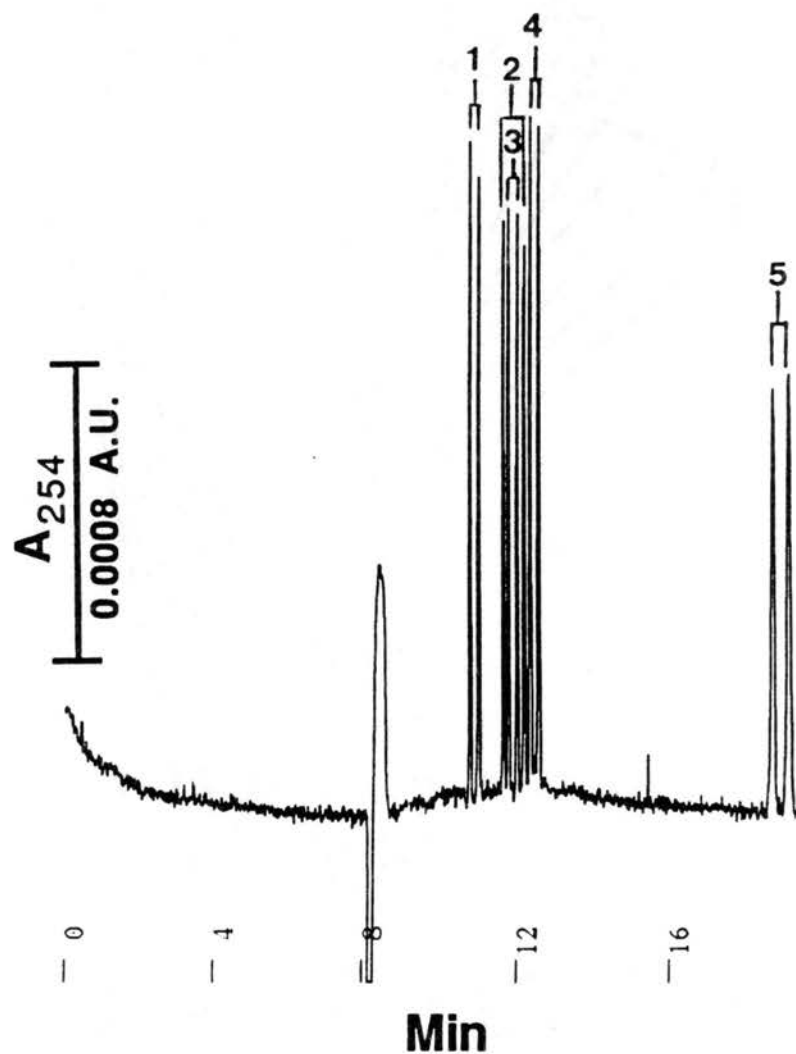


Figure 15. Electropherogram of D and L dansyl amino acids. Electrolyte, 150 mM borate, 75 mM MEGA 10, 15.0 mM γ -cyclodextrin, pH 10.0; solutes: 1, D,L phenylalanine; 2, D,L leucine; 3, D,L valine; 4, D,L methionine; 5, D,L aspartic acid. It should be noted that for all solutes D eluted before L. Other conditions are as in Fig. 10.

References

1. S. Terabe, K. Otsuka, K. Ichikama, A. Tsuchiya and T. Ando, *Anal. Chem.*, 56 (1984) 111.
2. S. Terabe, K. Otsuka and T. Ando, *Anal. Chem.*, 57 (1985) 834.
3. K. Otsuka, S. Terabe and T. Ando, *J. Chromatogr.*, 332 (1985) 219.
4. D. E. Burton, M. J. Sepaniak and M. P. Maskarinec, *J. Chromatogr. Sci.*, 24 (1986) 347.
5. A. S. Cohen, S. Terabe, J. A. Smith and B. L. Karger, *Anal. Chem.*, 59 (1987) 1021.
6. J. Liu, K. A. Cobb and M. Novotny, *J. Chromatogr.*, 519 (1990) 189.
7. M. G. Khaledi, S. C. Smith and J. K. Strasters, *Anal. Chem.*, 63 (1991) 1820.
8. M. M. Bushey and J. W. Jorgenson, *J. Microcol. Sep.*, 1 (1989) 125.
9. H. Nishi, N. Tsumagari, T. Kakimoto and S. Terabe, *J. Chromatogr.*, 477 (1989) 259.
10. P. Gozel, E. Gassmann, H. Michelsen and R. N. Zare, *Anal. Chem.*, 59 (1987) 44.
11. D. E. Burton, M. J. Sepaniak and M. P. Maskarinec, *J. Chromatogr. Sci.*, 25 (1987) 514.
12. S. Terabe, Y. Miyashita, O. Shibata, E. R. Barnhart, L. R. Alexander, D. G. Patterson, B. L. Karger, K. Hosoya and N. Tanaka, *J. Chromatogr.*, 516 (1990) 23.
13. R. O. Cole, M. J. Sepaniak, W. L. Hinze, J. Gorse and H. Oldiges, *J. Chromatogr.*, 557 (1991) 113.
14. S. Terabe, O. Shibata and Y. Miyashita, *J. Chromatogr.*, 480 (1989) 403.

15. K. Otsuka, J. Kawahara, K. Takekawa and S. Terabe, *J. Chromatogr.*, 559 (1991) 209.
16. S. Terabe, *Trends Anal. Chem.* 8 (1989) 129.
17. M. J. Sepaniak, A. C. Powell, D. F. Swaile and R. O. Cole, in *Capillary Electrophoresis, Theory and Practice*; Grossman, P. D.; Colburn, J. C., Eds.; Academic Press; New York, 1992; Chapter 6.
18. G. M. Janini and H. J. Issaq, *J. Liq. Chromatogr.*, 15 (1992) 927.
19. S. Terabe, H. Utsumi, K. Otsuka, T. Ando, T. Inomata, S. Kuze and Y. Hanaoka, *J. High Resolut. Chromatogr.*, 9 (1986) 666.
20. D. Crosby and Z. El Rassi, *J. Liq. Chromatogr.*, 16 (1993) 2161.
21. A. T. Balchunas and M. J. Sepaniak, *Anal. Chem.*, 59 (1987) 1466.
22. J. A. Lux, H. Yin, and G. Schomburg, *J. High Resolut. Chromatogr.*, 13 (1990) 145.
23. J. Gorse, A. T. Balchunas, D. F. Swaile and M. J. Sepaniak, *J. High Resolut. Chromatogr. Chromatogr. Commun.*, 11 (1988) 554.
24. A. T. Balchunas and M. J. Sepaniak, *Anal. Chem.*, 60 (1988) 617.
25. M. J. Sepaniak and R. O. Cole, *Anal. Chem.*, 59 (1987) 472.
26. J. Cai, and Z. El Rassi, *J. Chromatogr.*, 608 (1992) 31.
27. J. T. Smith and Z. El Rassi, *J. Chromatogr.*, *submitted*.
28. J. E. K. Hildreth, *Biochem. J.*, 207 (1982) 363.
29. J. Böeseken, *Adv. Carbohydr. Chem.*, 4 (1949) 189.
30. A. B. Foster, *Adv. Carbohydr. Chem.*, 12 (1957) 81.
31. H. Weigel, *Adv. Carbohydr. Chem.*, 18 (1963) 61.
32. V. Van Duin, J. A. Peters, A. P. G. Kieboom and H. Van Bekkum, *Tetrahedron*, 41 (1985) 3411.
33. M. Makkee, A. P. G. Kieboom and H. Van Bekkum, *Recl. Trav. Chim. Pays-Bas.*, 104 (1985) 230.

34. C. F. Bell, R. D. Beauchamp and E. L. Short, *Carbohydr. Res.*, 147 (1986) 191.
35. C. L. Christ, J. R. Clark and H. T. Jr. Evans, *Acta Cryst.*, 11 (1958) 761.
36. J. L. Frahn and J. A. Mills, *Aust. J. Chem.*, 12 (1959) 65.
37. H. B. Davis and C. J. B. Mott, *J. Chem. Soc. Faraday I*, 76 (1980) 1991.
38. G. R. Kennedy and M. J. How, *Carbohydr. Res.*, 28 (1973) 13.
39. R. J. Hunter, *Zeta Potential in Colloid Science*; Academic Press: London, 1981.
40. C. J. O. R. Morris and P. Morris, *Separation Methods in Biochemistry*, 2nd ed.; John Wiley and Sons: New York, 1976, p. 719.
41. R.M. Brito and W.L.C. Vaz, *Anal. Biochem.*, 152 (1986) 250.
42. J. P. Foley, *Anal. Chem.*, 62 (1990) 1302.
43. H. Nishi, T. Fukuyama, M. Matsuo and S. Terabe, *J. Microcol. Sep.*, 1 (1989) 234.
44. J. T. Smith and Z. El Rassi, *Electrophoresis*, 14 (1993) 396.
45. W. Nashabeh, J. T. Smith and Z. El Rassi, *Electrophoresis*, 14 (1993) 407.
46. M. J. How, G. R. Kennedy and E. F. Mooney, *Chem. Commun.*, 267 (1969) 267.
47. C. F. Bell, R. D. Beauchamp and E. L. Short, *Carbohydr. Res.*, 185 (1989) 39.
48. W. G. Henderson, M. J. How, E. F. Kennedy and E. F. Mooney, *Carbohydr. Res.*, 28 (1973) 1.
49. M.E. Rose, D. Wycherley and S. W. Preece, *Org. Mass Spectrom.*, 27 (1992) 876.
50. H. Colin, G. Guiochon, Z. Yun, J. C. Diez-Masa and J. Jandera, *J. Chromatogr. Sci.*, 21 (1983) 179.
51. W. R. Melander, J. Stovenken and Cs. Horváth, *J. Chromatogr.*, 199 (1980) 35.
52. Z. El Rassi and Cs. Horváth, *Chromatographia*, 19 (1984) 9.
53. J. Yu and Z. El Rassi, *J. Chromatogr.*, 631 (1993) 91.

54. M. J. Rosen, *Surfactants and Interfacial Phenomena*, 2nd ed.; John Wiley & Sons: New York, 1989.
55. I. M. Klotz and H. A. Fiess, *Biochim. Biophys. Acta*, 38 (1960) 57.
56. G. B. Gavioli, G. Grandi, L. Menabue, G. C. Pellacani and M. Sole, *J. Chem. Soc. Dalton Trans.*, (1985) 2363.
57. H. Nishi, T. Fukuyama and S. Terabe, *J. Chromatogr.*, 553 (1991) 503.

CHAPTER VII

MICELLAR ELECTROKINETIC CAPILLARY CHROMATOGRAPHY
WITH *IN SITU* CHARGED MICELLES II. EVALUATION AND
COMPARISON OF OCTYLMALTOSE AND
OCTANOYLSUCROSE SURFACTANTS
AS ANIONIC BORATE COMPLEXES
IN THE SEPARATION OF
HERBICIDES*

Abstract

This chapter is an extension to our previous work involving the development of *in situ* charged micellar phases with adjustable surface charge density for micellar electrokinetic capillary chromatography (MECC) of neutral and charged herbicides. The micelles evaluated here are basically alkyldisaccharide-borate complexes in which the surface charge density can be conveniently varied by changing the operating parameters such as borate concentration and/or pH of the running electrolyte. The two alkyldisaccharide surfactants (i.e., octyl- β -D-maltopyranoside and octanoylsucrose) differing in the length of the alkyl tail and the nature of the sugar polar head group, were compared and characterized over a wide range of conditions using neutral and acidic herbicides as model solutes. The effects of the operating parameters were discussed in terms of mobility, elution range parameter, capacity factor, peak capacity and separation

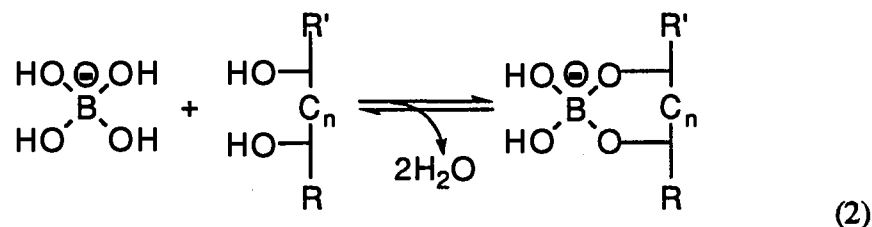
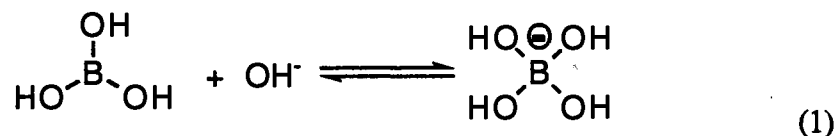
* J. T. Smith and Z. El Rassi, *J. Microcol. Sep.* 6 (1994) 127. Presented as a part of a poster at the 5th International Symposium on High Performance Capillary Electrophoresis (HPCE'93), Orlando, Florida, January 25-28, 1993.

efficiency. The retention energetics of the micellar phases were studied using two homologous series, alkyl phenyl ketones and alkylbenzenes. At constant micellized surfactant concentration, the two *in situ* charged micellar phases exhibited homoenergetic retention behavior toward the homologous solutes. On the other hand, even though the two surfactants have similar CMCs, the micelles exhibited different hydrophobic character, with octylmaltoside yielding higher retention.

Introduction

Micellar electrokinetic capillary chromatography (MECC), first reported in 1984 by Terabe *et al.* [1], has shown great promises in the separation of both neutral and charged species [2-5]. Very recently, we have introduced two different types of alkylglycoside-borate micellar phases, namely octyl- β -D-glucopyranoside and a series of three *N*-D-glucosyl-*N*-methylalkanamide (MEGA), as novel pseudo-stationary phases for MECC and investigated their fundamental characteristics [6,7]. These *in situ* charged micellar systems proved useful for the separation of neutral as well as charged solutes and provided several advantages over traditionally described micelles.

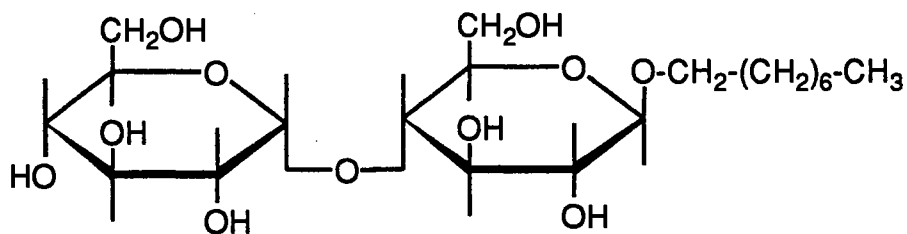
In situ charged micelles are dynamically charged entities *via* complexation of the polar sugar head group of alkylglycoside surfactants with borate ions at alkaline pH according to the following reactions:



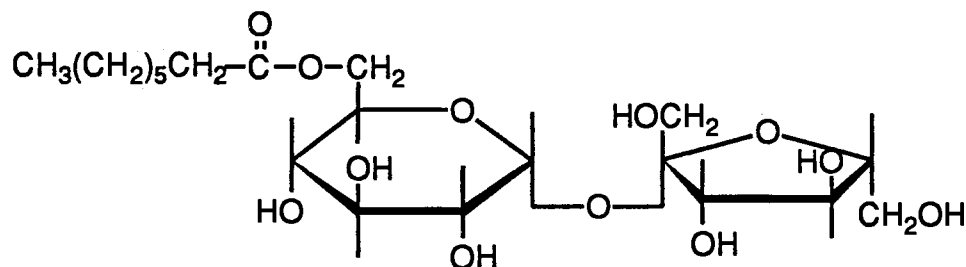
where equilibrium 1 represents the ionization of boric acid ($pK_a = 9.2$) to tetrahydroxy borate ion (i.e., borate), which is known to complex with polyhydroxy compounds including carbohydrates possessing vicinal diol groups of the proper geometry as shown in equilibrium 2 [8-11]. In equilibrium 2, n is either 0 or 1, which translates to 1,2- or 1,3-diol, respectively. According to equilibria 1 and 2, by altering the borate concentration, surfactant concentration, and/or the pH of running electrolyte, the surface charge density of the dynamically charged micelles can be easily manipulated, and as a result, the elution range of the *in situ* charged MECC system can be tailored to suit a given separation problem [6,7]. In addition, the balanced hydrophile-lipophile character of the micelles allows the separation of strongly hydrophobic solutes.

One of the important characteristics of these novel micellar systems is that while the surface charge density of the capillary changes very slightly in alkaline borate, the surface charge density of the micelle can be adjusted over a certain range through several operational parameters. For an in depth discussion of the equilibria involved with the charging of the micelle and the fundamental characteristics of *in situ* charged MECC systems, the reader is referred to previous reports from our laboratory [6,7].

This report, is concerned with the introduction of two new *in situ* charged micellar phases, the octyl- β -D-maltopyranoside- and octanoylsucrose-borate complexes. The structures of their surfactant monomers are shown below. The electrochromatographic properties of the two alkyldisaccharide-borate micellar phases were evaluated and compared under various operating conditions, and the results were discussed in terms of mobility, elution range parameter, capacity factor, retention energetic, peak capacity and separation efficiency.



Octyl- β -D-maltopyranoside (OM)



Octanoylsucrose (OS)

Experimental

Reagents and Materials

Octyl- β -D-glucopyranoside (OG) was obtained from Sigma Chemical Co. (St. Louis, MO, U.S.A.). Octyl- β -D-maltopyranoside (OM) and octanoylsucrose (OS) were purchased from Calbiochem Corp. (San Diego, CA, U.S.A.). All herbicides used in this study were purchased from Chem Service (West Chester, PA, U.S.A.). The series of alkyl phenyl ketones (APK) and alkylbenzenes (AB) were from Aldrich Chemical Co. (Milwaukee, WI, U.S.A.). Biphenyl, naphthylamine, and naphthalene were from Eastman Kodak Co. (Rochester, NY, U.S.A.). Anthracene (zone refined) purchased from TCI America (Portland, OR, U.S.A.) was used for the determination of the migration time of the micelles, t_{mc} . Methanol was obtained from EM Science (Cherry Hill, NJ, U.S.A.). All solutions were prepared with deionized water and filtered with 0.2 μ m Uniprep Syringeless filters from Fisher Scientific (Fair Lawn, NJ, U.S.A.) to avoid capillary plugging.

Instrument and Capillaries

The capillary electrophoresis instrument resembles that described previously [12]. It consisted of a 30-kV dc power supply Model EH30P03 of positive polarity from Glassman High Voltage (Whitehouse Station, NJ, U.S.A.) and a UV-Vis variable wavelength detector Model 200 from Linear Instrument (Reno, NV, U.S.A.) equipped with a cell for on-column detection. The detection wavelength was set at 240 nm for the detection of herbicides, and at 254 nm for the aromatics, alkylbenzenes and alkyl phenyl ketones. In all the experiments, the electric field strength was 187.5 V/cm. The electropherograms were recorded with a computing integrator Model C-R4A from Shimadzu (Columbia, MD, U.S.A.). Some portions of this work were performed on a capillary electrophoresis system Model HP^{3D}CE from Hewlett Packard (Waldbronn, Germany) equipped with a real time UV-visible diode array detector (DAD) and accompanying data analysis software. Both regular and HP extended light path capillaries were used with the HP^{3D}CE system. With the HP^{3D}CE system, the column temperature was maintained at 30 °C unless otherwise stated.

Fused-silica capillaries having an inner diameter of 50 µm and an outer diameter of 375 µm were obtained from Polymicro Technology (Phoenix, AZ, U.S.A.). In experiments using the in-house assembled instrument, the total length of the capillary was 80.0 cm with an effective separation distance of 50.0 cm, i.e., from the injection end to the detection point. With the HP^{3D}CE instrument, the total length was 64.0 cm with an effective length of 56.0 cm. The "bubble" capillaries used with the HP^{3D}CE instrument were supplied by Hewlett Packard (Waldbronn, Germany).

NMR Measurements

¹¹B NMR spectra were recorded at 25 °C on a Varian XL-400 fourier-transform spectrometer, using boron trifluoride etherate as an external standard. At this field

strength, the ^{11}B resonance is at 128 MHz. Samples were prepared in $\text{H}_2\text{O}:\text{D}_2\text{O}$ (80:20 v/v) while keeping the total borate concentration constant at 100 mM. The concentration of surfactant was varied and the pH was adjusted to 10.0 for all measurements. Quartz NMR tubes purchased from Wilmad Glass Co. (Buena, NJ, U.S.A.) were used in place of traditional pyrex tubes to reduce the background boron signal.

Procedures

The running electrolyte was prepared by dissolving proper amounts of boric acid and surfactant in water, and adjusting the pH to the desired value with sodium hydroxide. All stock solutions were made by dissolving pure compounds in methanol. Sample solutions were made by dissolving the proper amount of stock solution in the running electrolyte (*i.e.*, micellar solution) and adjusting the total volume of methanol in the sample to 20% (v/v).

Hydrodynamic sample injection mode, *i.e.*, gravity-driven flow, was used with the in-house assembled instrument. The sample reservoir was raised to a height of 20 cm above the outlet reservoir for 5 sec. The capillary was rinsed between runs with running electrolyte and was equilibrated for 5 min before sample introduction. With the HP $^{3\text{D}}\text{CE}$ system hydrodynamic injection was performed by pressurizing the sample reservoir for an appropriate amount of time (50-100 mbar \cdot s). Between runs, when using the automated system, the capillary was rinsed consecutively with water, 1.0 M NaOH, 0.10 M NaOH, water, and the running electrolyte.

In all calculations, the plate count was estimated from peak standard deviation taken as the half peak width at 0.607 of peak height (*i.e.*, the inflection point). In all cases, the reported plate count is the average of at least three runs.

Results and Discussion

Evaluation of OS, OM, and OG-borate complexation by Boron NMR

The stability of borate-polyol complexes have been studied using many approaches, including paper electrophoresis [9], infrared spectroscopy [13], pH measurements [14], calorimetric analysis [15], potentiometric studies [16], vapor pressure equilibrium studies [17], ^1H NMR [18], ^{13}C NMR [19], and ^{11}B NMR [20] analysis. Of these different approaches, ^{11}B NMR proved to be one of the most advantageous since it allows, among other things, simultaneous monitoring of the various components of the complexation equilibria. In our laboratory, very recently, we have used ^{11}B NMR to study complexation of borate with other polyol surfactants [7].

To assess the degree of complexation between borate and the polyol surfactants under investigation, a comparative study was performed between OM, OS, and OG. For these studies the borate concentration was kept constant at 100 mM and the concentration of alkylglycoside surfactant was varied. The pH was held constant at pH 10.0 where approximately 85% of the boric acid is ionized, i.e., equilibrium concentration of borate = [borate] \approx 85 mM. The peak due to the free borate, $\text{B}(\text{OH})_4^-$, at $\delta = 3.8$ ppm decreased gradually as other peaks at $\delta = 1.3$ (major) and $\delta = 2.0$ (minor) ppm increased upon increasing the concentration of the surfactant. The peak at $\delta = 1.3$ ppm corresponds to the borate complex with O-4 and O-6 of the terminal glucosyl residue present in all three surfactants as proposed by Foster [10]. The peak at $\delta = 2.0$ ppm was only observed with OM and OS, and is believed to correspond to complexation between hydroxyl groups of the two separate sugar moieties of the disaccharide polar head of the surfactants. This peak represented less than 5% of the total areas of the complexes. The peaks of the various spectra were integrated in order to estimate the extent of complexation between the different surfactants. The results of the integration are shown in Fig. 1 in terms of plots of the percentage of ^{11}B in free and complexed borate *versus* the surfactant:[borate] molar ratio

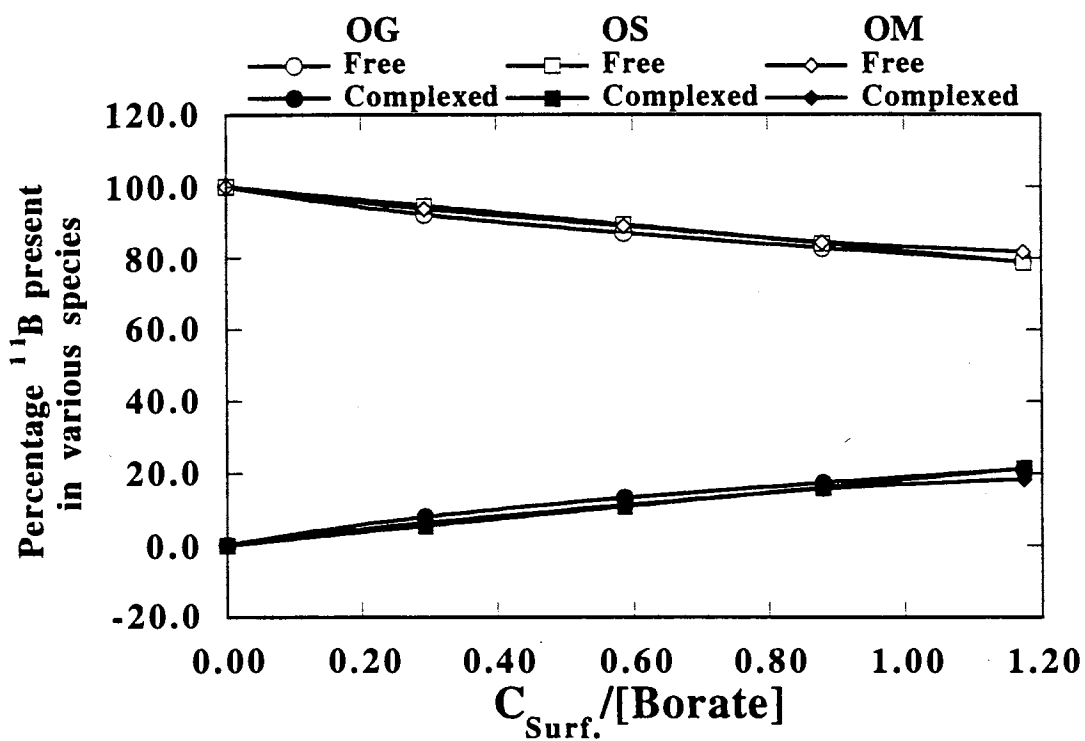


Figure 1. Plots of percentage of ^{11}B present in the free and complexed forms for OM-borate, OS-borate and OG-borate mixtures *versus* surfactant:[borate] molar ratio calculated using ^{11}B NMR integration data. Borate concentration, 85.2 mM ; concentration of surfactant was varied for the different measurements, pH 10.0.

($C_{\text{Surf}}/[\text{Borate}]$). As can be seen in Fig. 1, the extent of complexation between the different surfactants is practically identical. Under typical operating conditions in MECC, $C_{\text{Surf}}/[\text{Borate}]$ can range from 0.30 to 1.00 with fraction of complexed borate ranging from 8% to 20%, respectively.

Our previous ^{11}B NMR studies with MEGA-borate micellar phases [7] have shown that the MEGA surfactants have 3-5 fold higher affinity for borate ions than OG surfactant. Since OS and OM appear to have similar affinity for borate as that of OG, the extent of complexation of MEGA surfactants with borate ions is by far the highest among the various *in situ* charged micelles introduced and evaluated by our laboratory. This characteristic of the MEGA surfactants allow for relatively high surface charge densities to be achieved and consequently wider migration time windows under comparable operating conditions.

Effect of pH

Figure 2a illustrates the dependence of the migration time window on the pH of the running electrolyte at constant OM and borate concentrations. The width of the migration time window increases steadily with increasing electrolyte pH. As the pH increases, equilibrium 1 (see Introduction) shifts to the right which also results in a shift of equilibrium 2 in the same direction. The net effect is an increase in the surface charge density of the micelle with increasing pH. Moreover, changing the electrolyte pH changes the molar ratio of surfactant:[borate] which alters the percentage of complexed borate, see ^{11}B NMR data. Figure 2b shows the dependence of the effective electrophoretic mobility, μ_{ep} , on the pH of the running electrolyte. In MECC, the mobility of a neutral analyte results from its association with the micelle and is referred to as the effective electrophoretic mobility [24]. As can be seen in Fig. 2b, the electrophoretic mobility of the micelle, $\mu_{\text{ep}(\text{mc})}$, increased from $-0.438 \times 10^{-4} \text{ cm}^2/\text{V}^{-1}\text{s}^{-1}$ at pH 8.0 to $-1.430 \times 10^{-4} \text{ cm}^2/\text{V}^{-1}\text{s}^{-1}$ at pH 11.0. This represents a 3.3 fold increase in μ_{ep} by changing the pH from

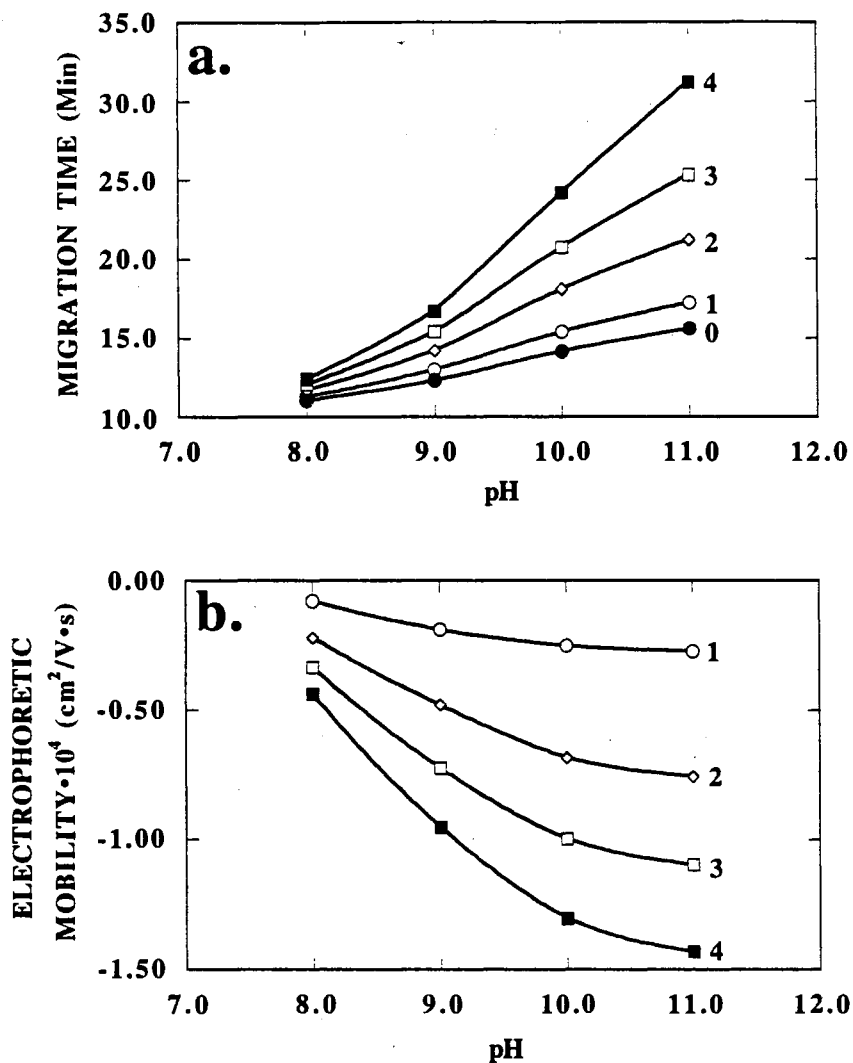


Figure 2. Effect of pH on (a) the migration time window and (b) electrophoretic mobility. Experimental conditions: running electrolytes, 50 mM OM and 200 mM borate at different pH; capillary, untreated fused silica, 50.0 cm (detection point), 80.0 cm (total length) x 50 μm I.D.; voltage, 15 kV. Solutes: 0, methanol (t_0); 1, nitrobenzene; 2, prometone; 3, prometryne; 4, anthracene (t_{mc}).

8.0 to 11.0. The negative sign for μ_{ep} is to indicate that the micelle is moving in the opposite direction to the electroosmotic flow (EOF). As expected, the μ_{ep} of the neutral species-micelle complexes also increased proportionally with increasing pH.

Table I lists the values of the elution range parameter, t_o/t_{mc} , as a function of pH. As seen in Table I, t_o/t_{mc} can be varied from 0.89 to 0.50 by changing the electrolyte pH by 3 units. This added flexibility offers the advantage of optimizing resolution while maintaining maximum throughput. Due to increasing the ionic strength and in turn the Joule heating with increasing pH, the separation efficiency decreased slightly (by ca. 12%) from 210,000 to 174,000 plates/meter with increasing the pH from 8.0 to 11.0. The substantial increase in the width of the migration time window coupled with the relatively high separation efficiencies allowed the peak capacity, n , to increase by almost 5 fold, i.e., from 14 to 66, with increasing the electrolyte pH from 8.0 to 11.0. As can be seen in Table I, the capacity factor, k' , is for all practical purposes constant as the pH is varied. This indicates that for neutral solutes the partitioning nature of the micelle is largely unaltered by pH. It should be noted that OS showed similar trends with respect to the migration time window, electrophoretic mobility, elution range parameter, and capacity factor (data not shown).

TABLE I. t_o/t_{mc} , and k' as a function of electrolyte pH. Experimental conditions: running electrolytes, 50 mM OM and 200 mM borate at different pH; capillary, untreated fused silica, 50.0 cm (to detection point), 80.0 cm (total length) x 50 μ m I.D.; voltage, 15 kV.

pH	t_o/t_{mc}	k' Nitrobenzene	k' Prometon	k' Prometryne
8.0	0.89	0.22	1.01	3.21
9.0	0.74	0.25	1.02	3.20
10.0	0.58	0.24	1.11	3.26
11.0	0.50	0.23	1.12	3.29

Effect of Borate Concentration

The dependence of the width of the migration time window on borate concentration is shown in Fig. 3a. These are typical plots of t_0 and t_{mc} versus the concentration of borate in the running electrolyte obtained with OS and OM at pH 10.0. In order to have a meaningful comparison, this study was performed at constant micellized surfactant concentration (i.e., $[S]-CMC = \text{constant}$, where $[S]$ is the total surfactant concentration and CMC is the critical micellar concentration) which ensures the presence of equal concentrations of surfactant to form the micelles. As expected, the migration time window increased with borate concentration. While t_0 increased only slightly in the concentration range studied, due primarily to the increase in the ionic strength of the running electrolyte, t_{mc} increased significantly. The larger increase in t_{mc} is due to an increase in the surface charge density of the micelle. This corroborates well with the results of ^{11}B NMR, which show that at a given surfactant concentration the amount of surfactant-borate complex increase with increasing the borate concentration. Both surfactants showed similar changes in the migration time window in the range of borate concentration studied.

Figure 3b illustrates $\mu_{ep(mc)}$ as a function of borate concentration for both OM and OS. By increasing the borate concentration from 100 to 400 mM, the $\mu_{ep(mc)}$ for OM increased from -1.25×10^{-4} to $-1.98 \times 10^{-4} \text{ cm}^2/\text{V}^{-1}\text{s}^{-1}$, while the $\mu_{ep(mc)}$ for OS increased from -1.64×10^{-4} to $-2.22 \times 10^{-4} \text{ cm}^2/\text{V}^{-1}\text{s}^{-1}$. At 100 mM borate, this represents a 23.8% higher in $\mu_{ep(mc)}$ for OS over OM. At 400 mM borate, the difference in $\mu_{ep(mc)}$ is only 11.1%. At first glance, the larger $\mu_{ep(mc)}$ may be attributed to a stronger affinity of OS to borate. However, ^{11}B NMR data indicates that the binding affinities of borate for OS and OM are practically the same. Therefore, a possible explanation could be that OS forms a slightly smaller micelle than OM due to the different nature of the disaccharide polar head groups of the surfactants. To the author's knowledge, there has been no reported data for

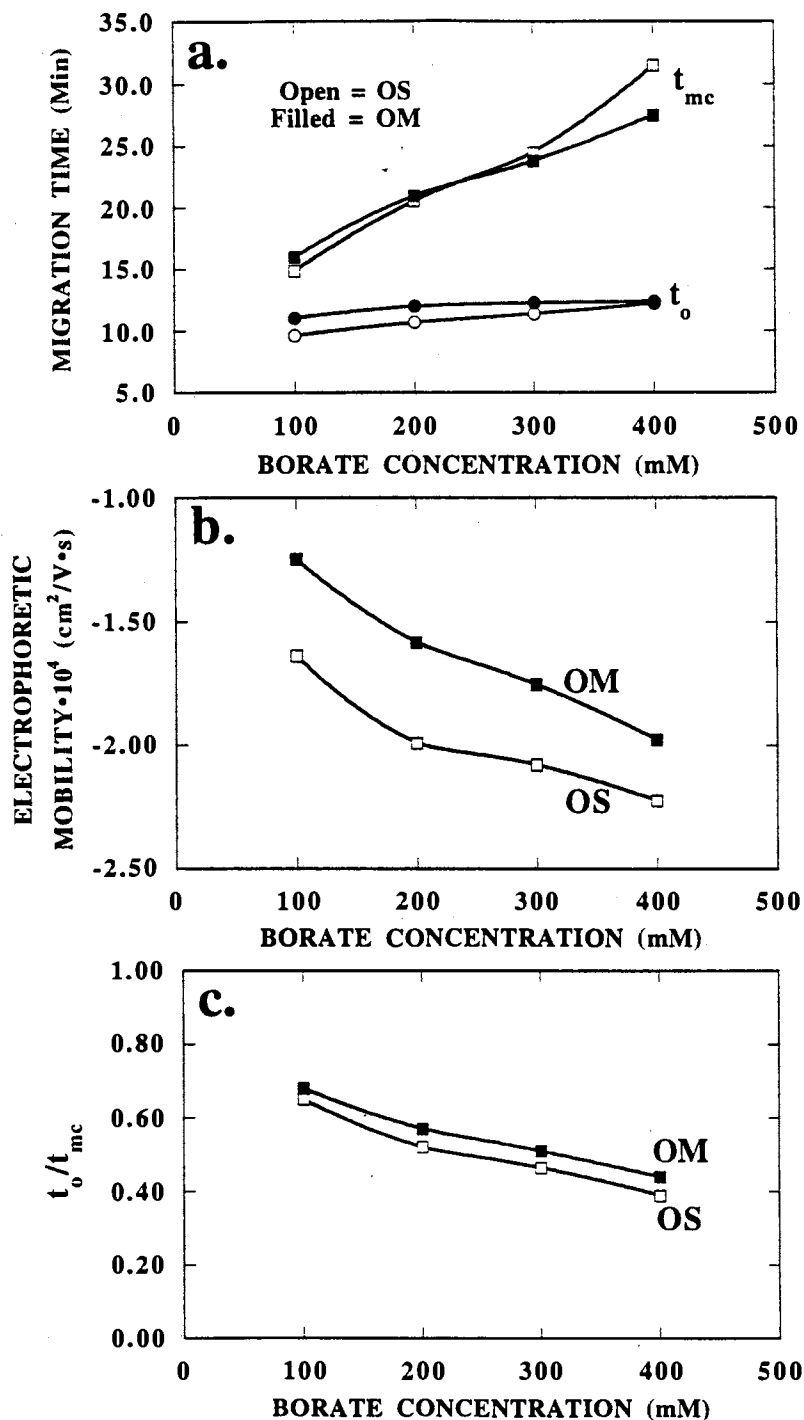


Figure 3. Effect of borate concentration on (a) the migration time window, (b) electrophoretic mobility of the micelle and (c) the elution range parameter for OM and OS. Experimental conditions: running electrolytes, 65.4 mM OM or 64.4 mM for OS at various borate concentrations, pH 10.0; other conditions as in Fig. 2. Solutes: methanol was used to determine t_o and anthracene for t_{mc} . Open symbols refer to OS and closed symbols refer to OM.

the aggregation number for these micelles, but they do possess slightly different CMCs in water, i.e., 24.4 mM for OS versus 23.4 mM for OM.

The elution range parameter is plotted in Fig. 3c as a function of borate concentration. With increasing the borate concentration from 100 to 400 mM, t_0/t_{mc} decreases from 0.68 to 0.44 for OM and from 0.65 to 0.39 for OS, respectively.

Table II lists the dependence of peak capacity, n , on borate concentration for both OM and OS. In both cases, n increased with increasing borate concentration, and its value was higher with OM surfactant may be due primarily to the greater plate number, N_{av} , observed with the OM (see Table II). The observed decrease in plate number with increasing borate concentration is due to the increased joule heating, see Table II.

The dependence of the capacity factor, k' , on borate concentration is shown in Table II. The general trend is that k' decreases slightly with increasing borate concentration due to the increase in heating at higher ionic strength. A noticeable difference between OS and OM is that with all analytes studied, OM always provided larger k' values than OS.

Table II. n , N_{av} (per meter), and k' as a function of borate concentration. Experimental conditions: running electrolytes, 65.4 mM OM or 64.4 mM for OS at various borate concentrations, pH 10.0; other conditions as in Table I.

[borate], (mM)	n		$N_{av} \cdot 10^{-3}$		k'_{Prometon}		$k'_{\text{Propazine}}$		$k'_{\text{Prometryne}}$	
	OM	OS	OM	OS	OM	OS	OM	OS	OM	OS
100	57	60	359.8	296.2	1.04	0.60	1.58	0.85	2.82	1.58
200	87	73	382.0	194.0	1.19	0.54	1.82	0.75	3.39	1.42
300	93	76	307.0	178.3	1.07	0.51	1.58	0.70	2.82	1.13
400	107	83	281.0	151.3	1.01	0.39	1.46	0.53	2.72	0.90

Effect of Surfactant Concentration

The dependence of the width of the migration time window on the surfactant concentration is illustrated in Fig. 4a. Also, Fig. 4a shows how the distribution of neutral species is affected by the concentration of the OM surfactant. Figure 4b portrays the dependence of the effective electrophoretic mobility, μ_{ep} , on the surfactant concentration. The μ_{ep} of the neutral species increases with increasing surfactant concentration due to increasing the phase ratio, and in turn k' . On the other hand, the $\mu_{ep(mc)}$ decreases with increasing surfactant concentration. This can be attributed to two factors. Foremost, at increased surfactant concentrations, the borate:surfactant ratio decreases (i.e., the amount of surfactant-borate complex decreases, see ^{11}B NMR data) thus lowering the surface charge density of the micelle. Secondly, at increased surfactant concentrations, the viscosity of the medium increases which in turn decreases the mobility of the micelle.

Figure 4c shows the effect of the surfactant concentration on the capacity factor of some herbicides. As expected, k' increases linearly with the surfactant concentration due to increasing the phase ratio, i.e., ratio of volumes of micellar phase to aqueous phase. The x-intercept of these lines is equal to the CMC of surfactant [21]. The average x-intercept of these lines is 20.6 mM. This is slightly lower than the reported value 23.4 mM, which was measured under conditions such that the micelle is nonionic.

The effect of the surfactant concentration of the elution range parameter, t_0/t_{mc} , is shown in Table III. The increase in t_0/t_{mc} is due to the fact that $\mu_{ep(mc)}$ decreases with increasing surfactant concentration (see discussion above). The peak capacity, n , is not significantly affected by the concentration of the surfactant, see Table III. This is due to the fact that the increase in t_0/t_{mc} is compensated for by an increase in plate number upon increasing surfactant concentration. The increased plate count may be attributed to higher k' because when the analyte spends more time in the micelle, its diffusion coefficient is decreased.

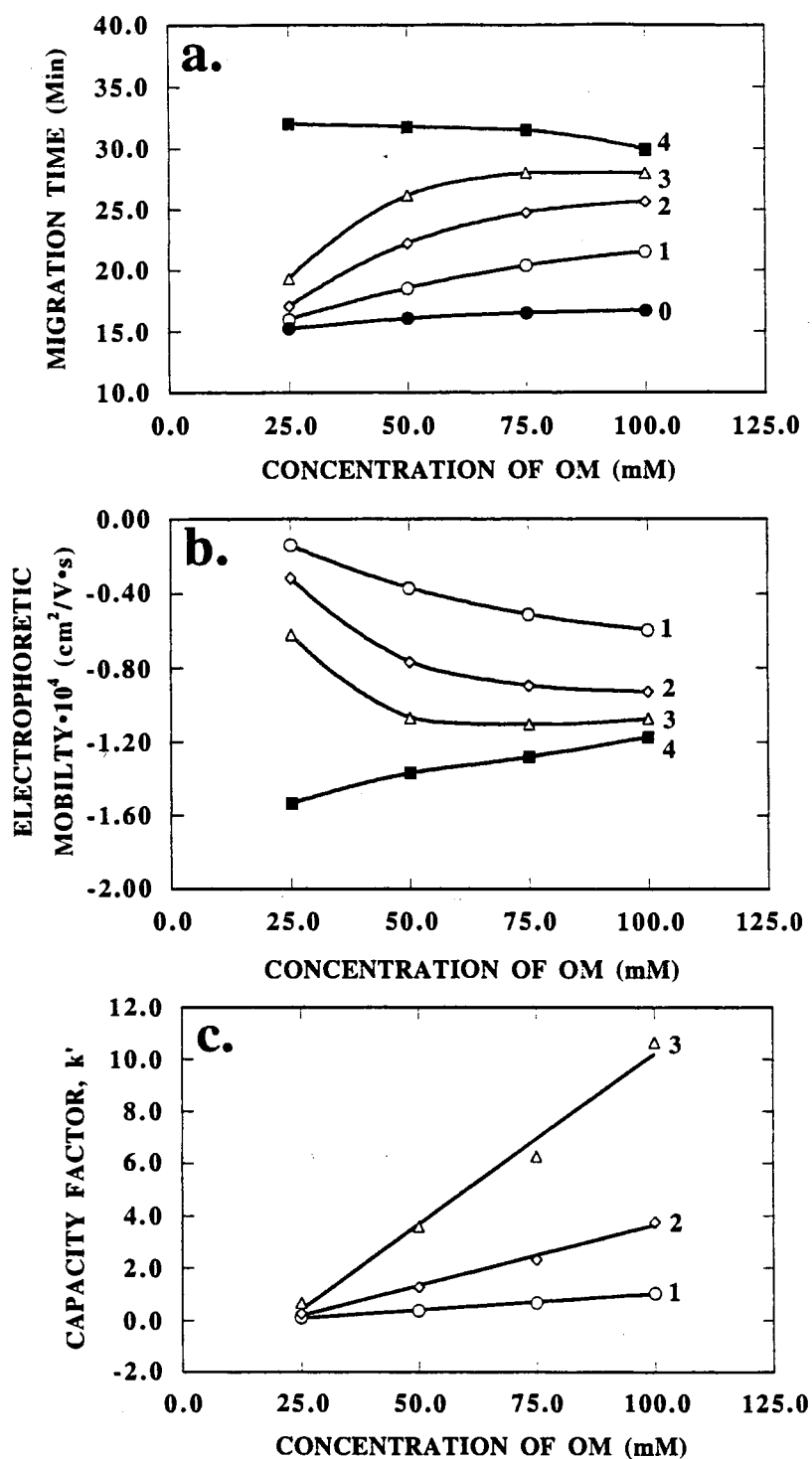


Figure 4. Effect of OM concentration on (a) the migration time window, (b) electrophoretic mobility and (c) capacity factor. Experimental conditions: running electrolytes, 200 mM borate, pH 10.0, at various OM concentrations. Other conditions as in Fig. 2. Solutes: 0, methanol (t_0); 1, nitrobenzene; 2, prometon; 3, prometryne; 4, anthracene (t_{mc}).

TABLE III. t_0/t_{mc} , n , and N_{av} (per meter) as a function of concentration of OM. Experimental conditions: running electrolytes, 200 mM borate, pH 10.0, at various OM concentrations; other conditions as in Table I.

[OM], (mM)	t_0/t_{mc}	n	$N_{av} \cdot 10^{-3}$
25	0.48	51	144.6
50	0.51	53	186.5
75	0.52	53	203.7
100	0.56	52	244.0

Comparison of Retention Energetics

To gain insight into the retention behavior of neutral solutes, two set of homologous series, namely alkylbenzenes (AB) and alkyl phenyl ketones (APK), were chromatographed with OM and OS micellar phases at constant micellized surfactant concentration. For these types of measurements, it is critical that the t_{mc} is determined accurately, especially when dealing with analytes possessing large capacity factors (i.e., greater than 10). Since homologous series were used in these measurements, t_{mc} was determined with the iterative method introduced by Bushey and Jorgenson [22]. Plots of the logarithmic capacity factors, $\log k'$, versus the number of carbon atoms, n_c , in the alkyl chain of the homologues yielded linear relationships with R values greater than 0.999. The two homologous series were chromatographed under different conditions. With alkylbenzenes, 100 mM borate containing 115.4 mM OM or 116.4 mM OS at pH 10.0 were used as the running electrolytes. Under these conditions where the surfactant concentration is greater than the borate concentration, t_0/t_{mc} was 0.75 for OM and 0.74 for OS. As a result of the narrow migration time window only four of the alkylbenzenes (AB) were fully resolved. With the alkyl phenyl ketones (APK), 200 mM borate containing 100 mM OS or OM was used as the running electrolyte. These conditions produced a wider migration time window and t_0/t_{mc} was 0.59 for OM and 0.65 for OS, allowing 6 of the homologous solutes to be easily resolved.

The slope of $\log k'$ vs n_c , i.e., $\log \alpha$, which represent the methylene or hydrophobic selectivity that characterizes nonspecific interactions, was practically the same for both homologous series regardless of whether OS or OM was used as the surfactant. In fact, with OS the $\log \alpha$ values are 0.349 and 0.334 for AB and APK, respectively, and with OM they are 0.357 and 0.334 for AB and APK, respectively. This may indicate that the physico-chemical basis of retention on OS and OM is practically the same. This finding corroborates our earlier observations with other types of surfactants [23].

As we reported previously [7,23], a plot of $\log k'$ for a given micellar phase versus the $\log k'$ for a reference micellar phase should give a straight line with an intercept equal to the logarithm of the quotient of the phase ratios. If the slope is unity, the difference in Gibbs retention energies of the two micellar phases is zero for all solutes and the retention is termed homoenergetic. If the slope is not unity, then the Gibbs retention energies are proportional by a constant that is equivalent to the slope of $\log k'$ - $\log k'$ plots, and the retention is termed homeoenergetic. Plots of $\log k'$ of AB and APK obtained with OM versus $\log k'$ of same homologous solutes obtained with OS yielded straight lines with R values of 1.000 and 0.999 for AB and APK, respectively. The slopes were 1.02 and 0.99 for AB and APK, respectively, thus indicating a homoenergetic retention behavior. The antilog of the intercepts ϕ_{OS}/ϕ_{OM} , i.e., the quotient of the phase ratios, were 0.64 and 0.52 for AB and APK, respectively. These results show that the phase ratio of OS micellar phase is almost one half that of OM. This shows again that the physico-chemical basis of retention with the alkyldisaccharide micellar phases is the same, and the only difference is the phase ratio.

Reproducibility

To examine the reproducibility of the micellar systems under investigation, repetitive injections were performed using 200 mM borate with 50 mM OS, pH 10.0, as the micellar phase. The analytes examined were urea herbicides, namely, linuron,

monuron, and chloroxuron. To compare the effects of adsorption of the surfactant onto the capillary wall, ten consecutive separations were performed with only flushing briefly with the running electrolyte between injections. Next ten consecutive separations were performed, but with a column reconditioning method consisting of flushing consecutively with water, 1.0 M NaOH, 0.10 M NaOH, water again, and the micellar phase between injections. Without the reconditioning step, the % RSD of migration times were 0.16, 0.04 and 0.21 for linuron, monuron and chloroxuron, respectively. With the reconditioning step, the % RSD values were 0.03, 0.06 and 0.34 for linuron, monuron and chloroxuron, respectively. These values correspond to excellent reproducibility in both cases, and indicate that the surfactant does not significantly adsorb to the capillary wall, building up a layer that could alter the EOF. When efficiency was examined, the reconditioning step prove to be critical. The plate counts were on the average 32% higher for ten injection with the reconditioning step than by only flushing with buffer. This indicates that for maximum performance, the capillary should be reconditioned before injection. Figure 5 overlays three electropherograms obtained with repetitive injections of 8 urea herbicides obtained with 200 mM borate containing 100 mM OM, pH 10.0, using the reconditioning method. The % RSD for peak area for each herbicide ranged from 1.6 to 9.6 % while the % RSD for peak height ranged from 1.7 to 4.6 % .

Limits of Detection

To evaluate the linear dynamic range that can be attained with the micellar phases under investigation, calibration curves were constructed for three urea herbicides using OM as the micellar phase and an extended path length capillary. Plots of peak areas versus the concentration injected were linear with R values of 0.996, 0.999 and 0.998 for fluometuron, diuron and chloroxuron, respectively. The peak area showed excellent linearity over two orders of magnitude. The limits of detection were determined to be $9.0 \times 10^{-6} M$, $7.0 \times 10^{-6} M$, and $5.0 \times 10^{-6} M$ for fluometuron, diuron, and chloroxuron,

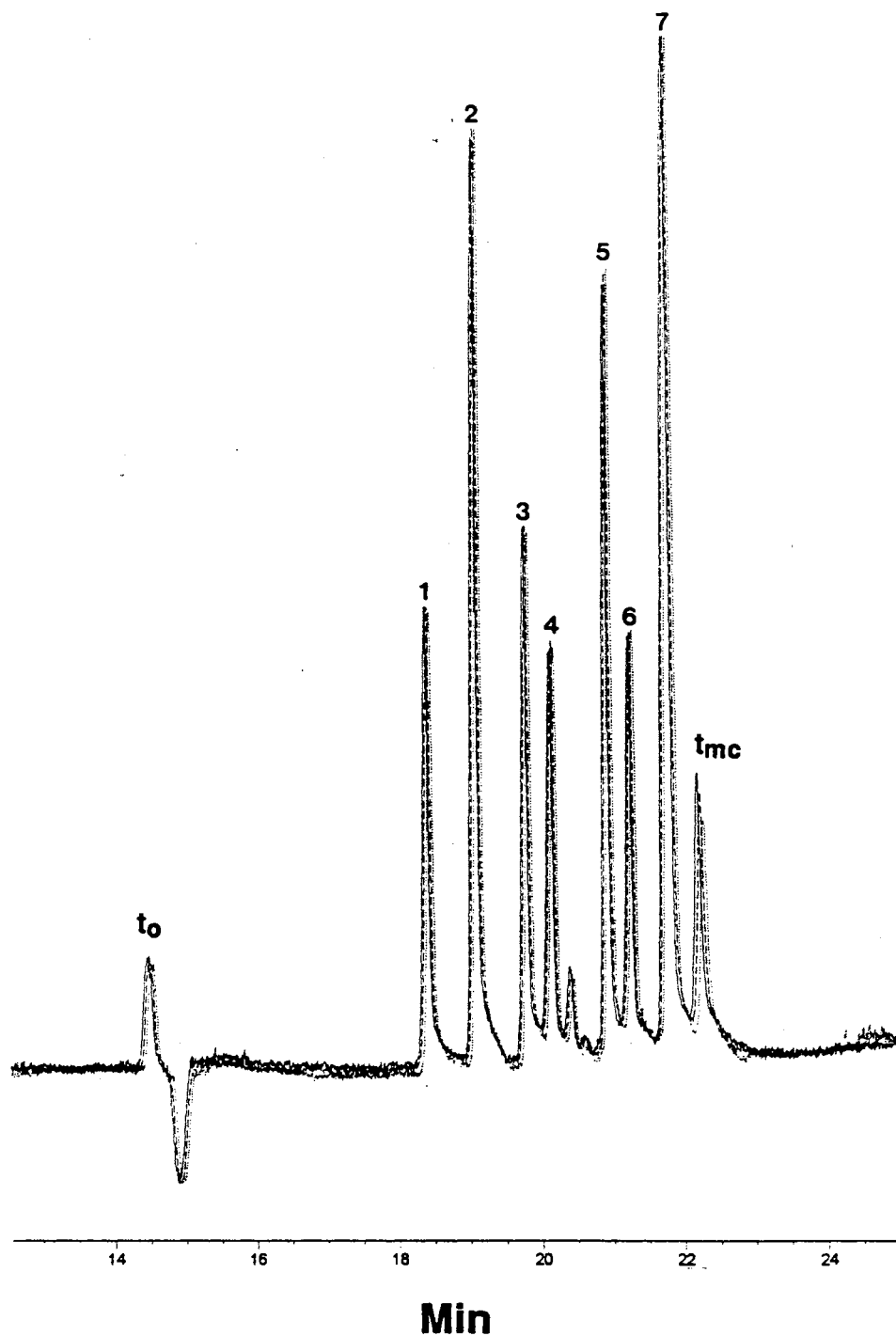


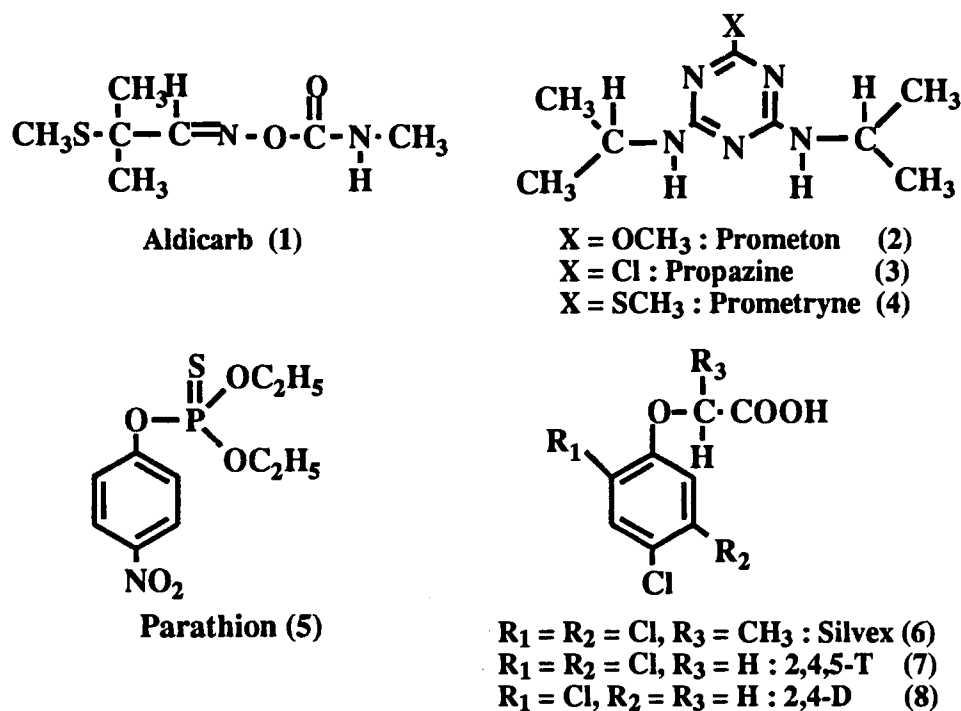
Figure 5. Electropherograms of three consecutive injections of urea herbicides. Experimental conditions: running electrolyte, 100 mM OM, 200 mM borate, pH 10.0; Capillary, untreated fused silica, 56.0 cm (to detection point), 64.0 cm (total length) x 50 μ m I.D.; voltage, 12.5 kV. Solutes: 1, monuron; 2, fluometuron; 3, metobromuron; 4, siduron; 5, diuron; 6, linuron; 7, neburon and chloroxuron. t_{mc} = anthracene.

respectively, which translate to ca. 18, 14 and 10 femtomoles (at $S/N = 3$). Assuming that the viscosity of the sample solution is identical to that of pure water, the volume injected as estimated from the Hagen-Poiseuille equation is approximately 2 nL when a hydrodynamic injection at a 100 mbar*s is used. Using this assumption, the above concentration detection limits translate to mass detection limits of 4.2 pg for fluometuron, 3.3 pg for diuron, and 2.9 pg for chloroxuron.

To determine the effectiveness of the extended pathlength cell, a comparison with regular capillaries was performed. The "bubble" cell provides approximately a three fold increase in effective pathlength. Figure 6 illustrates typical electropherograms obtained with the extended pathlength and regular capillaries of the same total length. The extended pathlength provides on average a 3.9 fold increase in peak area over regular capillaries with peak height being increased 3.2 on the average. The extended pathlength capillary produced notably lower plate numbers, $\approx 25\%$, than the regular capillary under the conditions studied. N_{av} was 564,000 plates/m for the regular capillary and 413,000 plates/m for the extended pathlength cell capillary with the three urea herbicides.

Applications of OM and OS

Figure 7 illustrates the separation of a mixture of 8 herbicides. The herbicides consist of three s-triazine herbicides (i.e., prometon, propazine, and prometryne), three chlorinated phenoxy acid herbicides (i.e., silvex, 2,4,5-T, and 2,4-D), one organophosphorous pesticide (i.e., parathion), and one sulfur-carbamate herbicide (i.e., aldicarb). The structures of these herbicides are shown below



The separation was carried out using 200 mM borate containing 100 mM of surfactant, pH 10.0. Under these conditions, silvex, 2,4,5-T, and 2,4-D, are fully ionized and experience little interaction with the negatively charged micelles, and therefore elute after the micelle. The other herbicides are neutral at this pH and elute in the order of increasing hydrophobic character. With OS, parathion and prometryne are only partially resolved, but with OM these two herbicides are baseline separated. This clearly illustrates how small changes in the structure of the surfactant can greatly affect the separation. Note the change in migration times of the last eluting herbicide, 2,4-D. Its effective μ_{ep} is $-1.82 \times 10^{-4} \text{ cm}^2/\text{V}^{-1}\text{s}^{-1}$ with OS and is $-1.54 \times 10^{-4} \text{ cm}^2/\text{V}^{-1}\text{s}^{-1}$ with OM, a 15 % difference in mobility. Since 2,4-D is fully ionized at the pH of the experiment, the herbicide is migrating primarily by its own electrophoretic mobility while experiencing slight interaction with the micelles. This weak interaction seems to be sufficient to produce significant changes in the effective mobility. OM exhibited stronger interactions with all of the acidic herbicides.

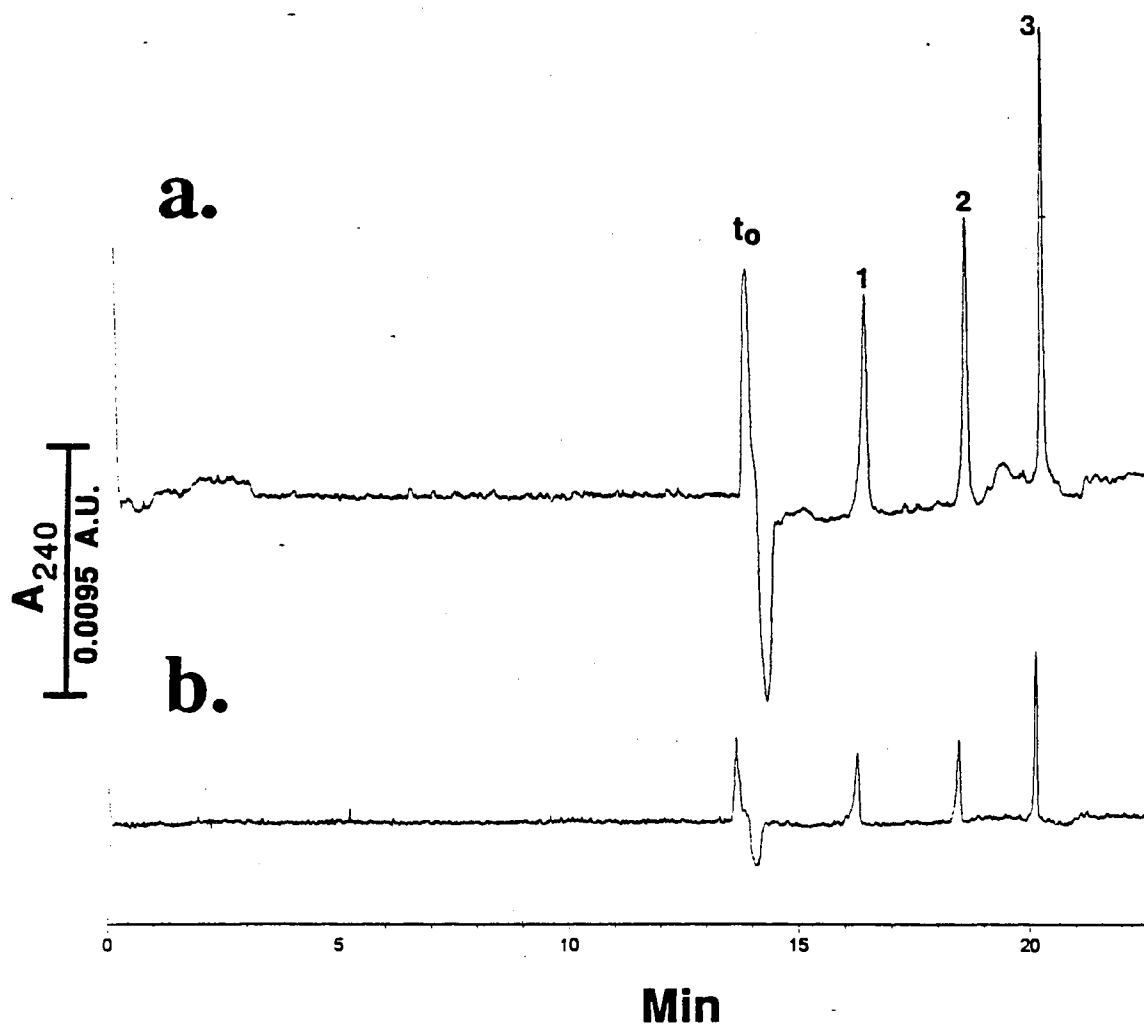


Figure 6. Electropherograms obtained with (a) a "bubble" cell capillary and (b) regular capillary. Experimental conditions: running electrolyte, 50 mM OM, 200 mM borate, pH 10.0; other conditions as in Fig. 5. Solutes: 1, fluometuron; 2, diuron; 3, chloroxuron.

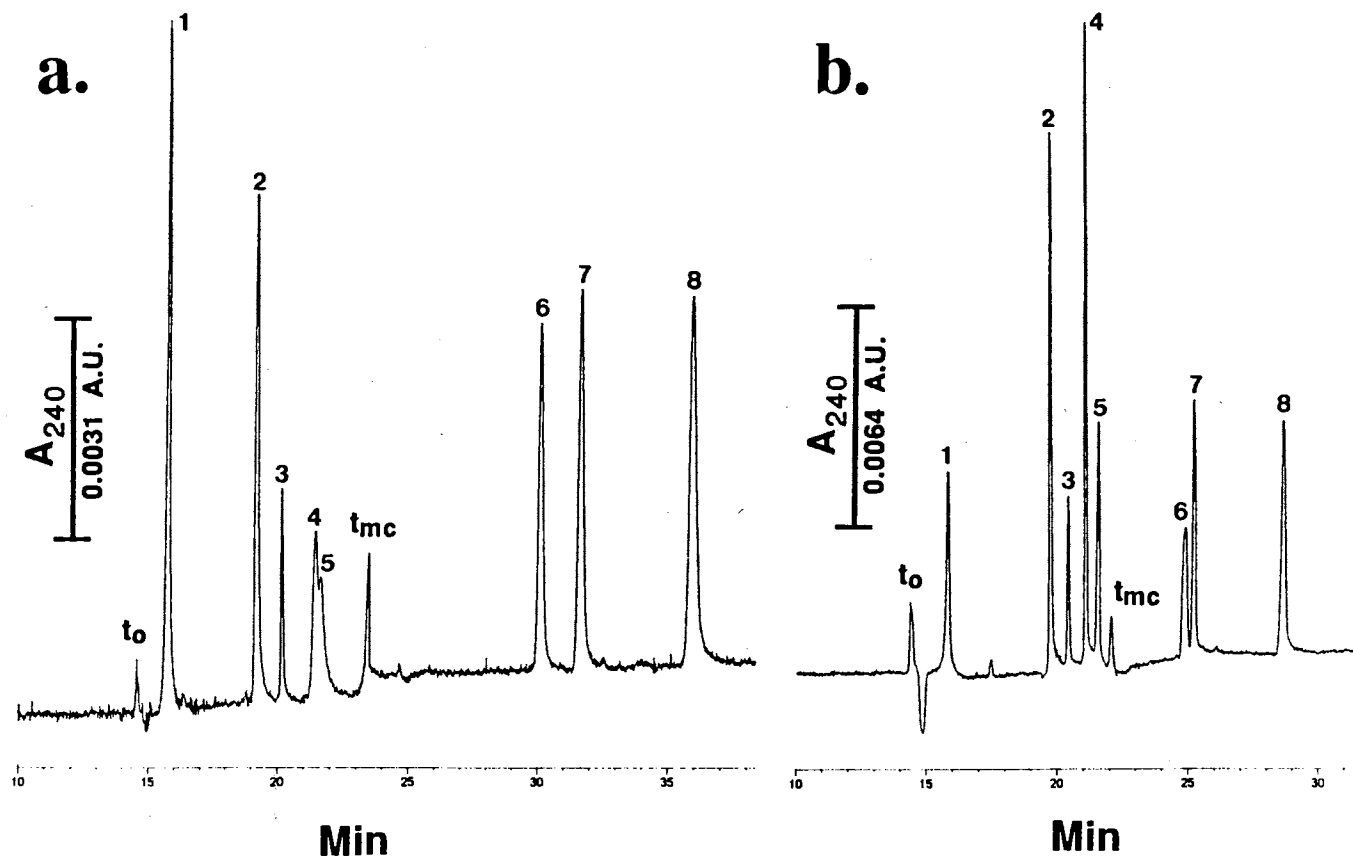
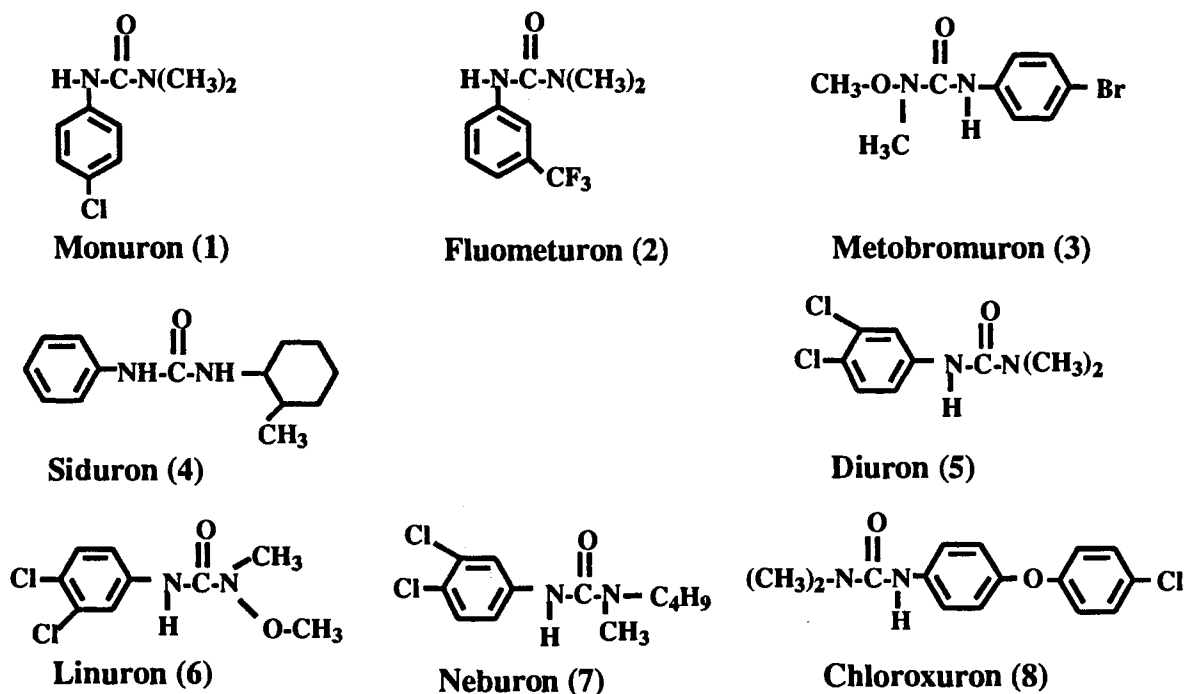


Figure 7. Electropherograms of herbicides obtained (a) OS and (b) OM. Experimental conditions: running electrolytes, 100 mM OS or 100 mM OM, 200 mM borate, pH 10.0. Other conditions as in Fig. 5. Solutes: 1, aldicarb; 2, prometon; 3, propazine; 4, prometryne; 5, parathion; 6, silvex; 7, 2,4,5-T; 8, 2,4-D. t_{mc} = anthracene.

To further illustrate the utility of these surfactants, a mixture of closely related urea herbicides (for structures, see below) were separated. Figure 8 portrays electropherograms obtained with 200 mM borate containing 50 mM OM or 100 mM OS at pH 10.0.



Using 50 mM OM as the micellar phase, all of the urea herbicides are clearly baseline resolved except the two most hydrophobic herbicides (i.e., neburon and chloroxuron). The average plate count was 376,000 plates/m (see Fig. 8a). Increasing the OM concentration to 100 mM OM the average plate count increased to 589,200 plates/m but the neburon and chloroxuron co-eluted under these conditions (see Fig. 5). Note that the effective separation distance was 50.0 cm with 50 mM OM and 56.0 cm with 100 mM OM.

To evaluate the effectiveness of OS in the separation of urea herbicides and compare its chromatographic behavior to that of OM, 200 mM borate, pH 10.0, containing 50 mM OS was used as the running electrolyte. Under these conditions, the strongly retained solutes neburon and chloroxuron were well resolved, but the early eluting peaks, i.e., monuron, fluometuron and metobromuron, were partially resolved (results not

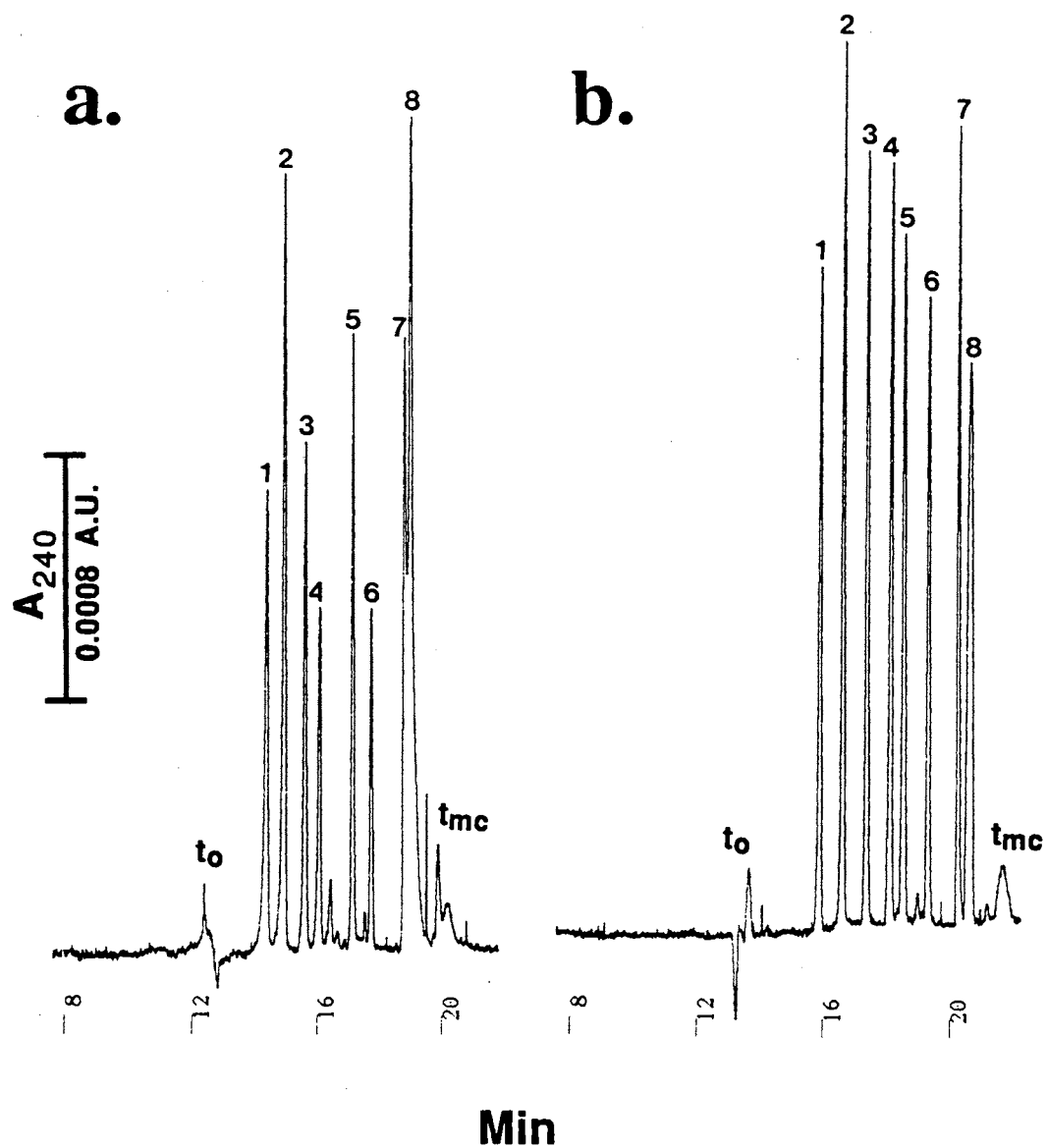


Figure 8. Electropherograms of urea herbicides. Experimental conditions: running electrolyte, 200 mM borate, pH 10.0, containing 50 mM OM in (a) or 100 mM OS in (b). Other conditions as in Fig. 2. Solutes: 1, monuron; 2, fluometuron; 3, metobromuron; 4, siduron; 5, diuron; 6, linuron; 7, neburon; 8, chloroxuron. t_{mc} = anthracene.

shown), and the efficiency was relatively low. This is due primarily to the fact that OS is more hydrophilic than OM. By increasing the concentration of OS to 100 mM while keeping other conditions the same, all peaks are baseline resolved (see Fig 8b) with a relatively high separation efficiency averaging 414,000 plates/m.

Figure 9 illustrates typical separations of some aromatic compounds for up to three fused rings. The electropherograms were obtained using 200 mM borate containing either 50 mM OM or OS at pH 10.0. These neutral aromatics elute in order of increasing hydrophobic character. This is a striking example of the differences in the hydrophobicity of the two micellar phases under investigation. With OM, the aromatics are distributed over a range of 2.9 min, but with OS, they are dispersed over a range of 6.0 min. The average plate counts is 372,000 plates/m for OM and 180,000 plates/m for OS. The differences in efficiency is due to changes in k' for the different micellar phases.

Conclusions

MECC shows promise for the determination of neutral and charged species. The *in situ* charged MECC systems offer micelles of adjustable surface charge density that allowed the precise control of the migration time window by altering one or more of the operational parameters. These novel micellar phases offer the additional flexibility to achieve desired resolution with maximum sample throughput. Because OM and OS surfactants possess different hydrophobic character, they exhibited different selectivity. OM is better suited for the separation of more polar compounds since it possess the greatest hydrophobic character, while OS being less hydrophobic will yield a more equitable distribution for highly hydrophobic species, and thus enhanced resolution. The detection limits were found to be in the femtomole range for the urea herbicides studied with UV detection. The theoretical plate counts were frequently over 300,000 plates/m.

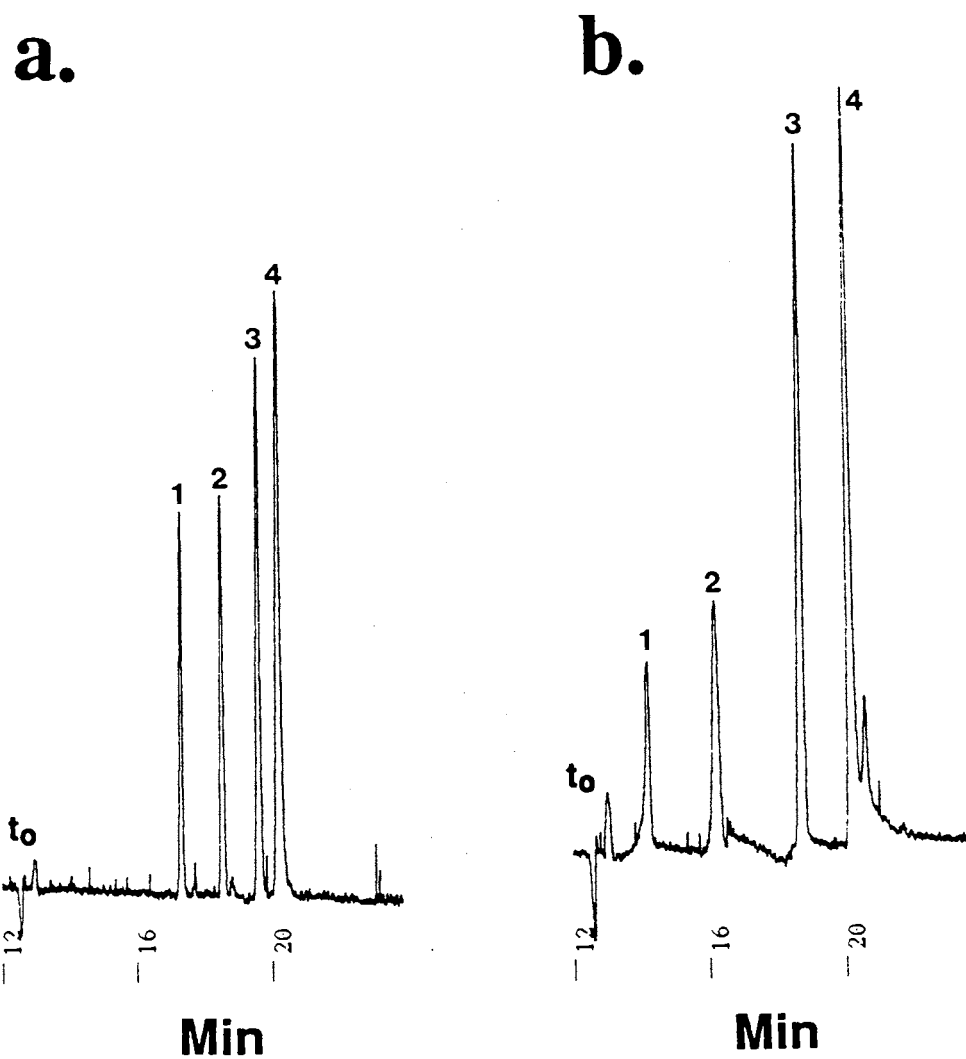


Figure 9. Electropherograms of aromatic compounds obtained with (a) OM and (b) OS. Experimental conditions: running electrolytes, 50 mM OM or 50 mM OS, 200 mM borate, pH 10.0. Other conditions as in Fig. 2. Solutes: 1, naphthylamine; 2, naphthalene; 3, biphenyl; 4, anthracene.

Acknowledgments

This material is based upon work supported by the Cooperative State Research Service, U.S. Department of Agriculture, under Agreement No. 92-34214-7325. J.T. Smith is the recipient of a Water Resources Presidential Fellowship from the University Center for Water Research at Oklahoma State University. Finally, the authors acknowledge partial support by the NSF (CHE-8718150) and the Oklahoma Center for the Advancement of Science and Technology (No. 1506) for the upgrade of the NMR facility. The loan of the capillary electrophoresis instrument from Hewlett Packard is greatly appreciated.

References

1. S. Terabe, K. Otsuka, K. Ichikama, A. Tsuchiya and T. Ando, *Anal. Chem.*, 56 (1984) 111.
2. K. Otsuka, S. Terabe and T. Ando, *J. Chromatogr.*, 332, (1985) 219.
3. D. Burton, M. J. Sepaniak and M. Maskarinec, *J. Chromatogr. Sci.*, 24 (1986) 347.
4. M.G. Khaledi, S.C. Smith and J.K. Strasters, *Anal. Chem.*, 63 (1991) 1820.
5. G. M. Janini and H. J. Issaq, *J. Liq. Chromatogr.*, 15 (1992) 927.
6. J. Cai and Z. El Rassi, *J. Chromatogr.*, 608 (1992) 31.
7. J. T. Smith, W. Nashabeh, and Z. El Rassi, *Anal. Chem.*, 66 (1994) 1119.
8. H. Weigel, *Adv. Carbohydr. Chem.*, 18 (1963) 61.
9. A. B. Foster, *Adv. Carbohydr. Chem.*, 12 (1957) 81.
10. A. B. Foster and M. Stacey, *J. Chem. Soc.*, (1955) 1778.
11. J. Böeseken, *Adv. Carbohydr. Chem.*, 4 (1949) 189.
12. J. Cai, J. T. Smith and Z. El Rassi, *J. High Resolut. Chromatogr.*, 15 (1992) 30.
13. R. Larsson and G. Nunziata, *Acta Chem. Scand.*, 24 (1970) 2156.
14. J. M. Conner and V. C. Bulgrin, *J. Inorg. Nucl. Chem.*, 29 (1967) 1953.
15. W. J. Evans, V. L. Frampton and A. D. French, *J. Phys. Chem.*, 81 (1977) 1810.
16. J. G. Dawber and D. H. Matusin, *J. Chem. Soc., Faraday Trans. 1*, 78 (1982) 2521.
17. M. Mazurek and A. S. Perlin, *Can. J. Chem.*, 41 (1963) 2403.
18. P. J. Garegg and K. Lindström, *Acta Chem. Scand.*, 25 (1971) 1559.
19. P. A. J. Gorin and M. Mazurek, *Carbohydr. Res.*, 27 (1973) 325.
20. W. G. Henderson, M. J. How, E. F. Kennedy and E. F. Mooney, *Carbohydr. Res.*, 28 (1973) 1.

21. S. Terabe, K. Otsuka and T. Ando, *Anal. Chem.*, 57 (1985) 834.
22. M. M. Bushey and J. W. Jorgenson, *J. Microcol. Sep.*, 1 (1989) 125.
23. D. Crosby and Z. El Rassi, *J. Liq. Chromatogr.*, 16 (1993) 2161.
24. K. Ghowsi, J. P. Foley and R. J. Gale, *Anal. Chem.*, 62, (1990) 2714.

CHAPTER VIII
MICELLAR ELECTROKINETIC CAPILLARY CHROMATOGRAPHY
WITH *IN SITU* CHARGED MICELLES III. EVALUATION
OF ALKYLGLUCOSIDE SURFACTANTS AS
ANIONIC BUTYLBORONATE
COMPLEXES*

Abstract

This chapter represents an extension to a new approach introduced very recently by our laboratory for the control of the surface charge density as well as the hydrophobic character of micellar phases used in micellar electrokinetic capillary chromatography (MECC). The approach is based on the complexation of polyolic surfactants, e.g., alkylglucosides, with butylboronate to form *in situ* branched, anionic surfactants. The butylboronate can also incorporate into the micelle *via* its alkyl tail and acts as a "class I" organic additive that mainly modifies the micelle by decreasing the critical micellar concentration, i.e., increasing the hydrophobic character of the micelle, while exhibiting little influence on the aqueous phase. The net result is an *in situ* charged micellar entity whose hydrophobic character is dynamically altered. The alkylglucoside-butyl boronate micellar phases yielded high separation efficiencies and proved useful in the separation of charged and neutral herbicides as well as the chiral separations of medicarpins and

* J. T. Smith and Z. El Rassi, *Electrophoresis*, submitted. Presented as a lecture at the 5th International Symposium on High Performance Capillary Electrophoresis (HPCE'93), Orlando, Florida, January 25-28, 1993.

precursors, and dansylated D and L amino acids in the presence of native or modified cyclodextrin chiral selectors.

Introduction

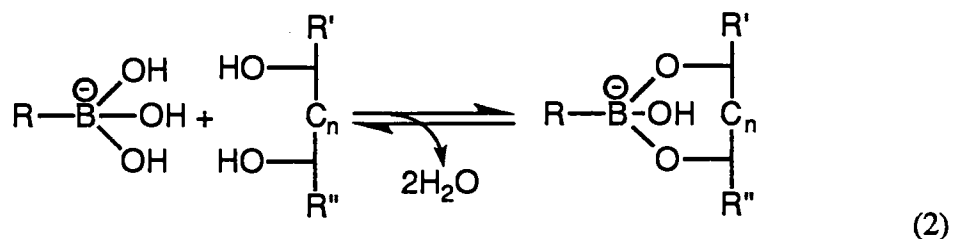
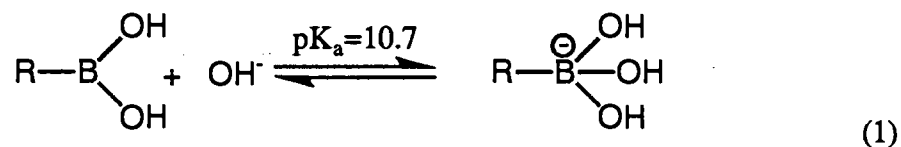
The concept of *in situ* charged micelles, which was introduced recently by our laboratory, proved to be a useful approach for micellar electrokinetic capillary chromatography (MECC) of neutral and charged species [1-3]. *In situ* charged micelles are based on the complexation of neutral alkylglycoside surfactants with borate or boronate ions. The dynamically charged micelles are characterized by an adjustable surface charge density, a condition that allows the manipulation of the width of the migration time window to suit a given separation problem. Thus far, we have introduced and characterized several different types of alkylglycoside-borate micellar phases, namely octyl- β -D-glucopyranoside [1], octyl- β -D-maltopyranoside, octanoylsucrose [3] and a series of three *N*-D-glucosyl-*N*-methylalkanamides (MEGA) [2]. Besides their tunable elution range parameter, these micellar systems are characterized by a balanced hydrophile-lipophile character that is imparted by the bulky carbohydrate head groups and the relatively short alkyl tails. These unique features of *in situ* charged micellar systems allowed the high resolution separation of various types of species widely differing in their hydrophobicity and ionic characters including s-triazine, urea and chlorinated phenoxy acid herbicides as well as barbiturates, polyaromatic compounds and dansyl amino acids including D and L isomers [1-3].

To further exploit the potentials of the concept of *in situ* charged micellar systems, this report is concerned with the introduction and evaluation of a series of dynamically charged micelles based on the complexation between a series of alkylglucoside surfactants and 1-butaneboronic acid (BBA). Due to its alkyl tail, the presence of BBA provides a means to dynamically change the hydrophobic character of the micellar system. The

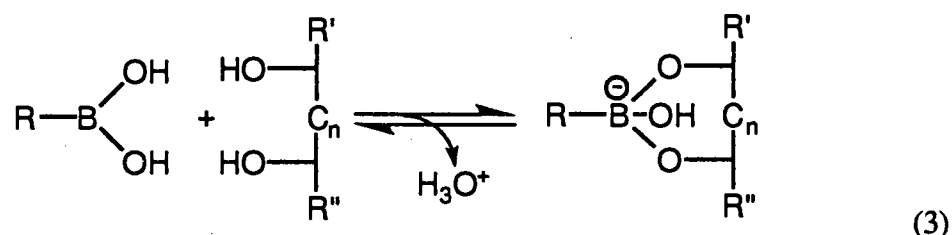
electrochromatographic properties of the different alkylglucoside-BBA micellar phases were evaluated and compared under various operating conditions, and the results were discussed in terms of mobility, elution range parameter, capacity factor, retention energetics and separation efficiency. The influence of BBA was studied under complexing as well as non complexing conditions. Applications towards the separation of both neutral and charged analytes are presented.

Some Aspects of Alkylglucoside-Boronate Micellar Phases

In this study, BBA was selected as the complexing agent for the charging of alkylglucoside surfactants. Two reaction mechanisms have been proposed for the interaction of boronic acids, such as BBA, with polyhydroxy compounds. In one case, the trigonal, coplanar boronic acid ionizes first to form a tetrahedral boronate anion as shown in equilibrium 1, see below. The ionization constant of BBA, K_a , is reported to be 1.8×10^{-11} for this equilibrium [4] which is about a factor of 35 lower than that of boric acid, $B(OH)_3$. This means that the pH must be approximately 1.5 units higher for BBA to have the same amount of ionized species. As shown in equilibrium 2, the boronate anion

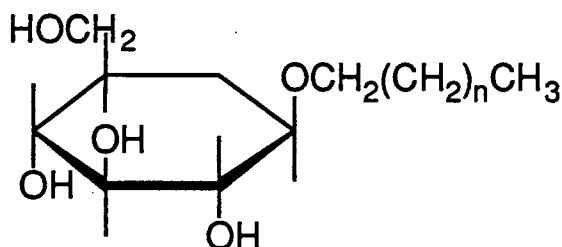


can then react with the polyhydroxy groups of a sugar to yield either a 5- or 6-membered cyclic boronate ester ring, which correspond to having either $n = 0$ (i.e., 1,2-diols) or $n = 1$ (i.e., 1,3-diols), respectively [4]. It is well known that 5-membered rings form a more stable complex [5], but the equilibrium is largely influenced by the geometrical arrangement of the diols. In the other proposed mechanism, a sequential nucleophilic attack of the diol oxygen atoms on the boronic acid causes the formation of the anionic species [6] as shown in equilibrium 3.



Recently, Pizer and Tihal [7] studied the reaction mechanism of methylboronic acid with diols and triols. Their studies indicated that boronates react more rapidly than trigonal boronic acids by factors of 10^3 - 10^4 which would mean that equilibrium 2 is primarily responsible for the formation of the charged complex.

As mentioned earlier, in this study we want to explore the potential of BBA with a series of alkyl- β -D-glucopyranoside the generalized structure of which is shown below

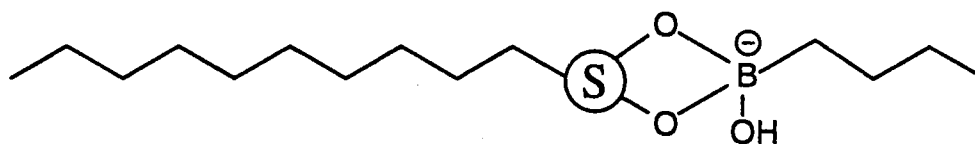


where $n = 5$ for heptyl- β -D-glucopyranoside (HG), $n = 6$ for octyl- β -D-glucopyranoside (OG), $n = 7$ for nonyl- β -D-glucopyranoside (NG) and $n = 8$ for decyl- β -D-glucopyranoside (DG). These surfactant possess CMCs of 79 mM, 25 mM, 6.5 mM, and

2 mM for HG, OG, NG and DG respectively [9]. It should be noted that these measurements were carried out under conditions where the micelle is nonionic.

According to equilibria 1 and 2 the surface charge density of the dynamically charged micelles can easily be adjusted by altering the BBA concentration, surfactant concentration, and/or the pH of the running electrolyte. As a result, the migration time window can be adjusted to a desired width that is best suited for a given separation problem. For an in depth discussion of the equilibria involved with charging of the micelle and the fundamental characteristics of *in situ* charged MECC systems, the reader is referred to previous reports from our laboratory [1,2].

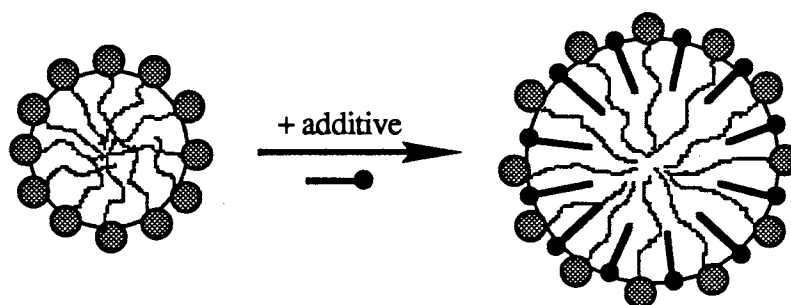
Another unique feature of BBA is that upon complexation with the surfactant, the resulting complex will be in the form of a branched surfactant, i.e., the polar head group has dynamically moved to a more central position, as follows



where S represents the sugar polar head group of the surfactant. The critical micellar concentration (CMC) of the dynamically branched surfactant-BBA complex will be lower than that of the original surfactant but higher than the CMC of an unbranched surfactant (i.e., all carbon atoms are in one tail) having the same number of carbon atoms [10]. In previous investigations, we have shown that small changes in the polar head group can dramatically shift the balance of the hydrophile-lipophile character of the micelle [3]. These changes can significantly affect the selectivity of the micellar system. Recently Tanaka *et al.* [8] explored the use of an anionic double chain surfactant, DBTD, as a micellar phase in MECC, and found that DBTD had significantly different characteristics when compared to SDS.

Besides complexing with the sugar head group of the surfactant, thus charging the micelle and altering its hydrophobic character by forming a branched surfactant, BBA can act as a micellar modifier by incorporating into the micelle which also alters the solubilizing power and hydrophobic character of the micelle. To realize the full benefit of the second role of BBA in MECC, the micelle must be charged by some other means. As will be seen later, this can be brought about by adding borate ions to the running electrolyte containing BBA and alkylglucoside surfactant. At certain pH (< 10), borate will complex preferentially with the polyol head group of the surfactant thus charging the micelle while BBA will predominantly incorporate into the micelle.

Butaneboronic acid as a micellar modifier can be viewed as a "Class I" organic additive which affects the micelle at relatively low concentrations where the additive has little influence on the aqueous phase. Members of class I additives with short alkyl tails are adsorbed mainly in the outer portion of the micelle close to the water-micelle "interface" and those with long alkyl tails are adsorbed mainly in the outer portion of the core, between the surfactant molecules [10]. Adsorption of class I additives results in decreasing the mutual repulsion of the ionic head groups of charged surfactants of the micelle by spacing the ionic groups and reducing unfavorable contact between the aqueous phase and the exposed hydrocarbon core. The incorporation of class I additives into the micelles can be described by the mechanism proposed by Winsor [11] as follows:



Recently, Aiken and Huie [12] have examined the effects of 1-alkanols on the performance of SDS micellar phase in MECC. These class I additives were used at low concentrations,

i.e., 50 mM, and produced increased capacity factors with little change in the EOF. Their data were consistent with the predications of Rosen [10] being that as the length of the alkyl tail of the additive approaches that of the surfactant, the more effective is the additive.

According to Schick [13], class I additives that have more than one group capable of forming hydrogen bonds with water in a terminal polar grouping, such as BBA, would produce greater depressions in the CMC, which in turn increase the hydrophobic character of the micelle. The explanation being that with one grouping capable of forming multiple hydrogen bonds with water helps counterbalance the lateral pressure tending to push the additive into the interior of the micelle and allows it to remain in the outer core between the surfactant molecules as shown in the illustration above. These modifications of the micellar surface would allow a decrease in surface curvature of the micelle and a subsequent increase in the capacity of the core to accommodate the additive [14]. The net effect is a larger micelle core possessing increased solubilizing capacity.

To reflect all conceivable ways by which BBA can associate with the alkylglucoside micellar phase under investigation, Fig. 1 visualizes our views towards the idealized structure of the alkylglycoside-BBA micelle. When BBA complexes with the sugar head group of the surfactant, indicated by the circled S, the butyl tail can be either pointed outwards, away from the hydrophobic core, or possibly two adjacent butyl tails could undergo nonpolar interactions and lie on the surface of the micelle. BBA can also (i) enter the micelle in the palisade layer (i.e., the layer between the sugar heads and the first few carbon atoms of the hydrophobic groups that comprise the outer core of the micellar interior), acting as a class I additive as discussed above and (ii) form hydrogen bonds not only with the surrounding aqueous phase but also with the hydroxyl groups of the surfactant. The net result is an *in situ* charged micellar entity whose hydrophobic character is dynamically altered.

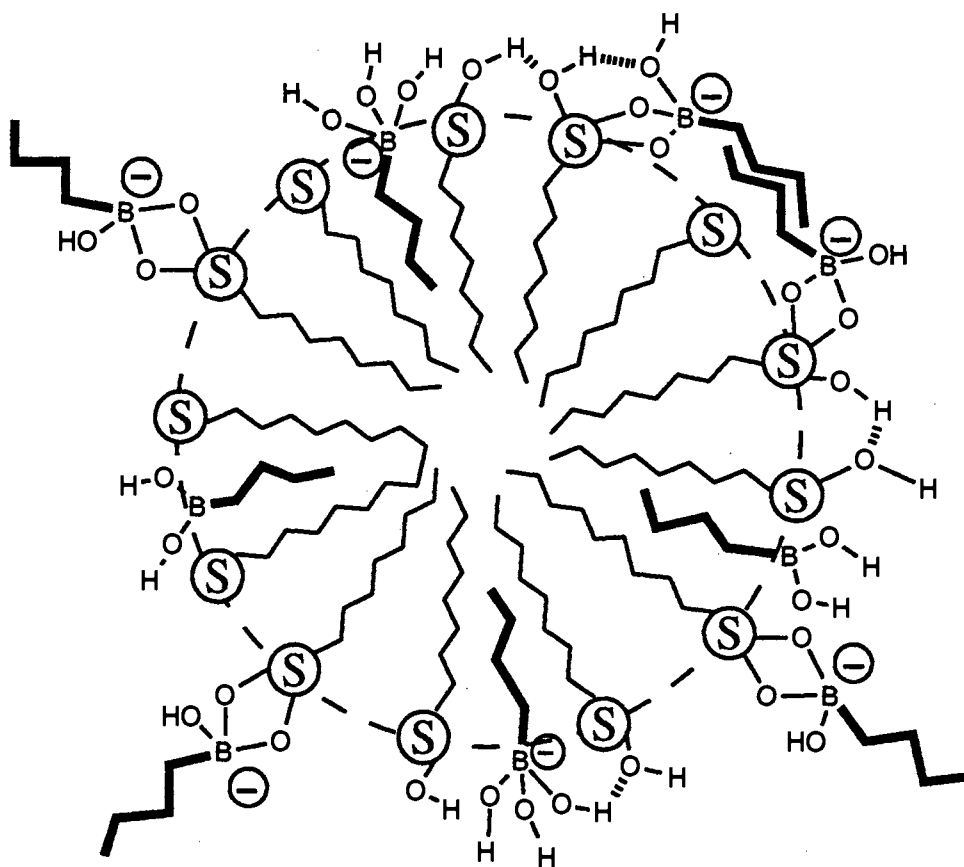


Figure 1. Idealized structure of the alkylglucoside-butyl boronate micelle.

Experimental

Reagents and Materials

Heptyl- β -D-glucopyranoside (HG), octyl- β -D-glucopyranoside (OG), nonyl- β -D-glucopyranoside (NG), decyl- β -D-glucopyranoside (DG), 1-butaneboronic acid (BBA), heptakis (2,6-di-O-methyl)- β -cyclodextrin, and dansylated amino acids were obtained from Sigma Chemical Co. (St. Louis, MO, U.S.A.). All herbicides used in this study were purchased from Chem Service (West Chester, PA, U.S.A.). The series of alkyl phenyl ketones (APK), alkylbenzenes (AB) and phenylalkyl alcohols (PAA) as well as boron trifluoride etherate were purchased from Aldrich Chemical Co. (Milwaukee, WI, U.S.A.). All chemicals for the preparation of the electrolyte solutions were purchased from Fisher Scientific (Pittsburgh, PA, U.S.A.). Methanol was purchased from EM Science (Cherry Hill, NJ, U.S.A.). The γ - and β -Cyclodextrin were gifts from American Maize-Products Co. (Hammond, IN, U.S.A.). Medicarpins and medicarpin precursors were donated by Dr. Paiva from the Samuel Roberts Noble Foundation, Inc. (Ardmore, OK, U.S.A.). All solutions were prepared with deionized water and filtered with 0.2 μ m Uniprep Syringeless filters from Fisher Scientific to avoid capillary plugging.

Instrument and Capillaries

The capillary electrophoresis instrument resembles that described previously [15, 16]. It consisted of a 30-kV dc power supply, Model CZE1000R of reversible polarity, from Spellman High Voltage Electronic Corp. (Plainview, NY, U.S.A.) and a UV-Vis variable wavelength detector Model 200 from Linear Instrument (Reno, NV, U.S.A.) equipped with a cell for on-column detection. The detection wavelength was set at 231 nm for the s-triazine and chlorophenoxy acid herbicides, 240 nm for urea herbicides, 254 nm

for ABs and APKs, and 210 nm for the PAAs. The medicarpins and related compounds were detected at 254 nm. In all experiments, the electrical field strength was maintained at 187.5 V/cm. The electropherograms were recorded with a computing integrator Model C-R4A from Shimadzu (Columbia, MD, U.S.A.). Fused-silica capillaries having an inner diameter of 50 μm and an outer diameter of 375 μm were obtained from Polymicro Technology (Phoenix, AZ, U.S.A.). In all experiments, the total length of the capillary was 80.0 cm with an effective separation distance of 50.0 cm, i.e., from the injection end to the detection point.

NMR Measurements

^{11}B NMR spectra were recorded at 25 $^{\circ}\text{C}$ on a Varian XL-400 fourier-transform spectrometer, using boron trifluoride etherate as an external standard at $\delta = 0.00$ ppm. At this field strength, the ^{11}B resonance is at 128 MHz. Samples were prepared in $\text{H}_2\text{O}:\text{D}_2\text{O}$ (80:20 v/v) while keeping the total borate or boronate concentration constant at 200 mM. The concentration of surfactant was varied and the pH was adjusted to 10.0 for measurements with borate and 11.0 for measurements using BBA. Quartz NMR tubes purchased from Wilmad Glass Co. (Buena, NJ, U.S.A.) were used in place of traditional pyrex tubes to reduce the background boron signal.

Procedures

The running electrolytes were prepared by dissolving proper amounts of BBA and surfactant in water, and adjusting the pH to the desired value with sodium hydroxide. All stock solutions of samples were made by dissolving pure compounds in methanol. Sample solutions were made by dissolving the proper amounts of stock solutions in the desired running electrolyte and adjusting the total volume of methanol in the sample to 20% (v/v). Sample injection was performed using the hydrodynamic mode, i.e., gravity-driven flow. The sample reservoir was raised to a height of 20 cm above the outlet reservoir for

an appropriate period of time, typically 5 sec. The capillary was rinsed between runs with running buffer and was equilibrated for 5 min before sample injection. In all calculations involving efficiency, the plate count was estimated from peak standard deviation taken as the half peak width at 0.607 of peak height (i.e., the inflection point) and was reported in all Tables as the average of at least three runs. Mobilities were determined from average migration times, and again a minimum of three runs were used to calculate the average.

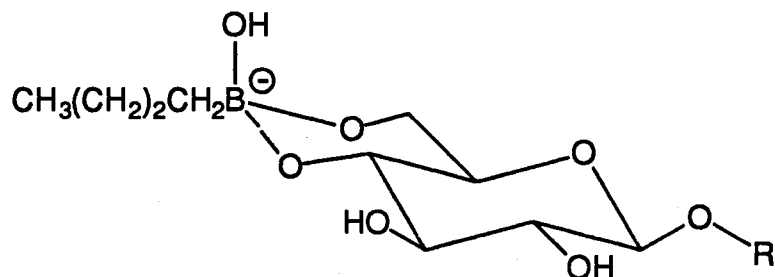
Results and Discussion

Boron NMR studies

In our laboratory, we have previously used ^{11}B NMR to evaluate the complexation between borate and various polyolic surfactants [2,3]. This technique allows the simultaneous monitoring of the various species involved in the complexation equilibria. The percentage of free and complexed borate or boronate can be determined by integrating the peak areas observed in the ^{11}B NMR spectrum. To compare the extent of complexation of BBA to that of borate with the alkylglucoside surfactants under investigation, a set of ^{11}B NMR experiments were performed using HG as a representative surfactant. For these studies the borate or boronate concentration was kept constant at 200 mM and the concentration of HG surfactant was varied. In the case of borate, the pH was held constant at pH 10.0 where approximately 85% of the boric acid is ionized in the form of borate ions, i.e., equilibrium concentration of borate = $[\text{borate}] \approx 170 \text{ mM}$. In the case of boronate, the pH was held constant at pH 11.0 where the $[\text{boronate}] \approx 129 \text{ mM}$. By using the equilibrium concentration of the ionized species, more accurate comparisons are made when considering equilibrium 2.

For the studies concerning boronate, the choice of pH 11.0 was well suited because the observed resonances for free and complexed boronate are well resolved and also depicts typical operating conditions in MECC. The peak due to the free butyl

boronate, i.e., butyl-B(OH)₃⁻, at $\delta = 13.7$ ppm decreased gradually as another peak corresponding to the boronate-surfactant complex appeared at $\delta = 4.2$ ppm upon increasing the concentration of surfactant. The peak at $\delta = 4.2$ ppm is believed to correspond to the glucopyranoside-4,6-butylboronate complex (shown below) as suggested by Ferrier [17, 18]



and matches well with reported values of other alkylboronate-polyol complexes [7]. The results of the integration are shown in Fig. 2 in terms of plots of the percentage of ¹¹B in free and complexed boronate *versus* the surfactant:[boronate] molar ratio ($C_{\text{Surf}}/[\text{Boronate}]$).

The borate system showed similar trends. The peak due to free borate, B(OH)₄⁻, at $\delta = 3.9$ ppm decreased gradually as another peak at $\delta = 1.3$ ppm increased upon increasing the concentration of the surfactant. This peak corresponds to the glucopyranoside-4,6-borate complex as described by Foster [5]. As can be seen in Fig. 2, the borate complexation is slightly favored over that of the BBA. This can be attributed in part to the fact that boric acid being more favored to undergo complexation *via* an equilibrium similar to that described in 3, i.e., where the unionized boric acid complexes with the sugar group. Under typical operating conditions in MECC, $C_{\text{Surf}}/[\text{Boronate}]$ can vary from ≈ 0.25 to ≈ 1.0 with the fraction of boronate complexed ranging from 4% to 13%, respectively, depending on the separation requirements.

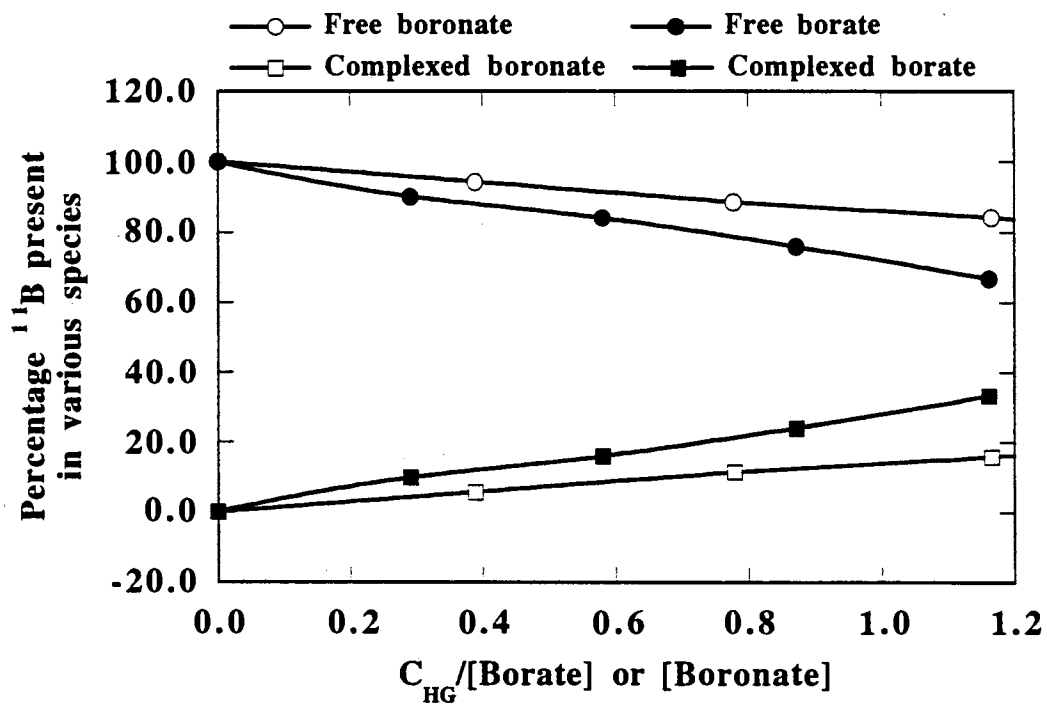


Figure 2. Plots of percentage of ^{11}B present in the free and complexed forms for HG-borate and HG-boronate mixtures *versus* surfactant:[borate] or surfactant:[boronate] molar ratio calculated using ^{11}B NMR integration data. Borate concentration ≈ 170 mM at pH 10.0; butyl boronate concentration ≈ 129 mM; concentration of surfactant was varied for the different measurements.

Electrochromatographic behavior

Influence of pH. The dependence of the migration time window on the pH of the running electrolyte for HG and NG micellar systems is illustrated in Fig. 3a. These typical plots were obtained with electrolytes containing 200 mM BBA and a constant micellized surfactant concentration (i.e., $[S] - \text{CMC} = \text{constant}$, where $[S]$ is the total surfactant concentration and CMC is the critical micellar concentration) which ensures the presence of equal concentrations of surfactant available to form micelles. As can be seen in Fig. 3a, the width of the migration time window increases steadily with electrolyte pH. Similar trends were observed with both OG and DG surfactants in terms of mobility as a function of pH. These behaviors are consistent with those observed with borate complexation of polyolic surfactants previously reported by our laboratory [1-3]. As the pH increases, equilibrium 1 shifts to the right which will result in shifting equilibrium 2 in the same direction, thus increasing the effective concentration of the HG-BBA complex. The net effect is an increase in the surface charge density of the micelle with increasing pH. This is illustrated clearly in Fig. 3b, where the electrophoretic mobility of the micelle is plotted versus electrolyte pH for HG and NG surfactants. The electrophoretic mobility of the micelle, $\mu_{\text{ep}(\text{mc})}$ increased by a factor of 2.75 and 2.40 for HG and NG, respectively, when going from pH 9.0 to 12.0. It should be noted that the $\mu_{\text{ep}(\text{mc})}$ increased with increasing the alkyl chain length of the surfactant, even though the micelle becomes bigger, see Fig. 3b for typical results. This discrepancy is due to the fact that as the chain length of the surfactant increased the molar ratio of BBA:surfactant also increased because in these experiments 200 mM BBA and constant micellized surfactant concentration were used. This leads to a greater surface charge density and consequently to increasing the electrophoretic mobility of the micelle as the alkyl chain length is increased. In fact, at pH 10.0, the electrophoretic mobility of HG, OG, NG and DG were -1.18, -1.56, -1.67 and $-1.78 \times 10^{-4} \text{ cm}^2\text{V}^{-1}\text{s}^{-1}$, respectively. A comparison of $\mu_{\text{ep}(\text{mc})}$ at similar surface charge

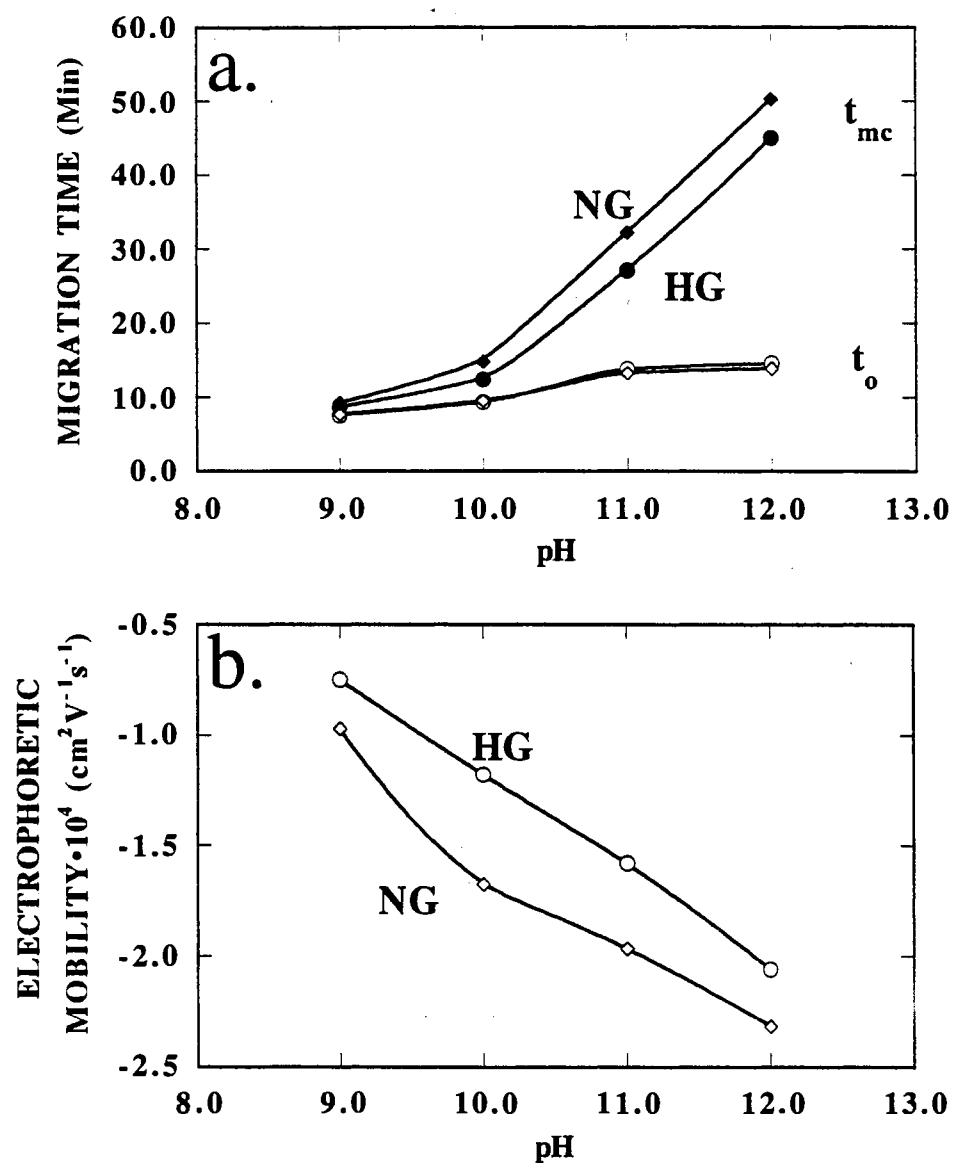


Figure 3. Effect of pH on (a) the migration time window and (b) electrophoretic mobility for HG and NG micellar phases. Experimental conditions: running electrolytes, 104 mM HG or 31.5 mM NG and 200 mM borate at different pH; capillary, untreated fused silica, 50.0 cm (detection point), 80.0 cm (total length) x 50 μm I.D.; voltage, 15 kV.

densities, using borate as the complexing agent, for the various micellar phases is provided in a latter section.

Effects of BBA concentration. Figure 4a illustrates the dependence of the migration time window on the concentration of BBA. These data were obtained using 50 mM OG with different concentrations of BBA at pH 11.0. At this pH, approximately 64 % of the BBA is ionized in the boronate form so that they can readily complex with OG to form a branched surfactant. As expected, the migration time window increased with BBA concentration. The increase in t_0 is primarily the result of increased ionic strength and viscosity with increasing BBA concentration. The increase in t_{mc} is caused by increasing the surface charge density of the micelle with increasing BBA concentration, which is reflected by the observed increase in the value of the $\mu_{ep(mc)}$ as shown in Table I. It should be noted that when going from 200 mM to 250 mM BBA there is a slight decrease in the value of $\mu_{ep(mc)}$. This decline in $\mu_{ep(mc)}$ is believed to arise from an increase in the size of the micelle since the amount of BBA complexed and/or adsorbed by the micelle becomes higher. Since t_{mc} increased at a greater rate than t_0 with increasing BBA concentration, the elution range parameter decreased from 0.73 to 0.45 when the BBA concentration increased from 50 mM to 250 mM, as indicated in Table I.

TABLE I. $\mu_{ep(mc)}$, t_0/t_{mc} and N_{av} (per meter) as a function of BBA concentration.^a

[BBA], mM	$\mu_{ep(mc)}$ (cm ² V ⁻¹ s ⁻¹)	t_0/t_{mc}	N_{av}
50	-1.47 x 10 ⁻⁴	0.73	309,000
100	-1.68 x 10 ⁻⁴	0.60	281,000
150	-1.73 x 10 ⁻⁴	0.54	299,100
200	-1.78 x 10 ⁻⁴	0.48	375,000
250	-1.69 x 10 ⁻⁴	0.45	353,000

^aExperimental conditions: running electrolytes, 50 mM OG containing various concentrations of BBA at pH 11.0; capillary, untreated fused silica, 50.0 cm (detection point), 80.0 cm (total length) x 50 μ m I.D.; voltage, 15 kV.

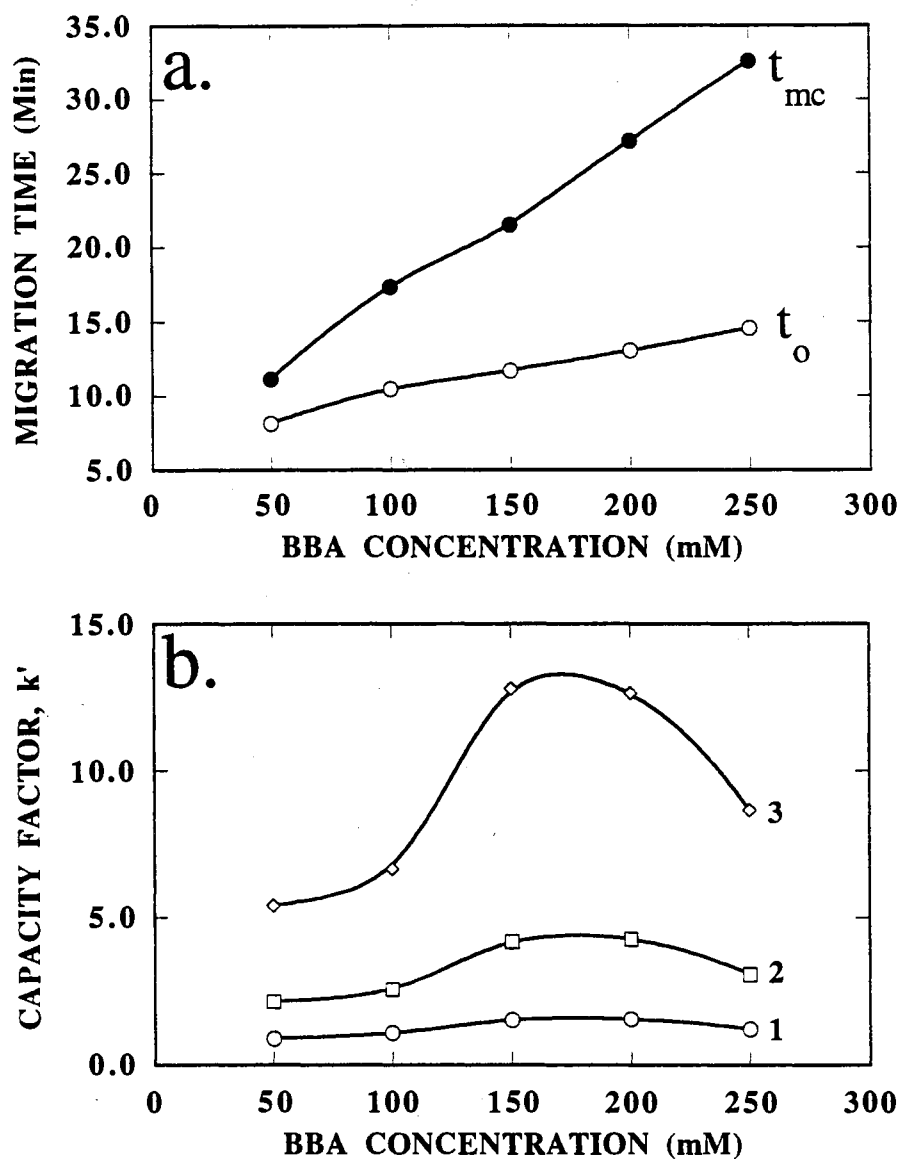


Figure 4. Effect of BBA concentration on (a) the migration time window and (b) capacity factor. Experimental conditions: running electrolytes, 50 mM OG at various BBA concentrations, pH 11.0; other conditions as in Fig. 3. Solutes: 1, toluene; 2, ethylbenzene; 3, propylbenzene.

As the concentration of BBA is increased, the hydrophobic character of the micelle would be expected to increase since more and more branched surfactant is formed and the amount of BBA incorporated into the micelle would also increase. Figure 4b illustrates the dependence of the capacity factor, k' , of three alkylbenzene homologous solutes on the concentration of BBA at pH 11.0. As expected, k' increased with increasing the concentration of BBA. The decrease in k' above 150 mM BBA can be attributed to increased column temperature at a higher ionic strength, i.e., higher BBA concentration. As the column temperature increases, the solubility of the solutes in the aqueous phase will increase resulting in a decrease in k' . The addition of 250 mM BBA to the electrolyte, which corresponds to only 2.5 % (w/v), would have little influence on the aqueous phase, and therefore the overall contribution of BBA as an organic modifier to decreasing k' of the solutes is rather negligible. Similar trends were observed with PAAs and three s-triazine herbicides, namely prometon, propazine and prometryne (data not shown). It could be envisioned that, if the experiments were carried out using a temperature controlled environment, k' would increase steadily with increasing BBA concentration and would be greater than observed in Fig. 4b since changes in solubility as a function of temperature would not be a factor. The efficiency of the three triazine herbicides was largely unaffected by the changes in BBA concentration, see Table I.

Effects of BBA concentration on the electrochromatographic behavior of alkylglucoside-borate micelles. To evaluate its effect as a "purely" class I organic additive, BBA was added to alkylglucoside-borate micellar solutions at a pH where the alkylglucoside surfactant would preferentially undergo complexation with borate ions. This was achieved by using 50 mM OG containing 200 mM borate and various BBA concentrations at pH 10.0. The borate serves to charge the micelle since it ionizes at a lower pH than BBA. At pH 10.0, less than 15 % of the BBA is ionized and this amount is overshadowed by the concentration of ionized borate. Table II lists the dependence of the

electrophoretic mobility of the micelle on the concentration of the BBA additive. As can be seen in Table II, the $\mu_{ep(mc)}$ was only slightly affected by the change in BBA concentration, but generally decreased as the amount of additive increased. This trend is in agreement with the enlargement of the size of the micelle upon the incorporation of BBA

TABLE II. $\mu_{ep(mc)}$, t_0/t_{mc} and k' as a function of BBA concentration.^a

[BBA], mM	$\mu_{ep(mc)}$ (cm ² V ⁻¹ s ⁻¹)	t_0/t_{mc}	k' Prometon	k' Propazine	k' Prometryne
0	-1.79 x 10 ⁻⁴	0.52	1.04	1.64	3.52
100	-1.86 x 10 ⁻⁴	0.50	1.37	2.03	4.44
200	-1.72 x 10 ⁻⁴	0.50	1.70	2.32	5.18
300	-1.69 x 10 ⁻⁴	0.44	2.40	3.11	7.05

^aExperimental conditions: running electrolytes, 50 mM OG containing 200 mM borate with various concentrations of BBA at pH 10.0; other conditions as in Table I.

into the micelle (see introduction). The elution range parameter decreased from 0.52 to 0.44 with the addition of 300 mM BBA even though $\mu_{ep(mc)}$ decreased only slightly, see Table II. This can be attributed to a slower EOF as a result of the addition of BBA, which decreased from 3.71 x 10⁻⁴ cm²V⁻¹s⁻¹ to 3.03 cm²V⁻¹s⁻¹ when going from 0 mM to 300 mM BBA.

Table II also lists the dependence of k' for the triazine herbicides on BBA concentration. The results show that k' can be doubled with the addition of 300 mM BBA. This is unique in that k' can be altered without changing the surfactant concentration. The increase in k' is consistent with enlargement of the micelle which will also increase the solubilizing power of the micelle.

Very recently, we have evaluated the correlation between capacity factor and the carbon number for homologous series as well as the associated energetics of retention [2, 3, 19]. These correlations provided a yard stick with which various micellar phases could be evaluated quantitatively. In the present study, we evaluated the retention behavior of

two sets of homologous series, namely, PAAs and APKs, where the carbon number (n_c) for the alkyl tail was 2 to 6 for the alcohols and 1 to 6 for the ketones. As was previously observed [2, 3, 19], plots of logarithmic capacity factor versus n_c yielded straight lines according to the following expression

$$\log k' = (\log \alpha)n_c + \log \beta$$

where the slope, $\log \alpha$, is a measure of the methylene group selectivity which characterizes nonspecific interactions, while the intercept $\log \beta$ reflects the specific interactions between the residue of the molecule and the aqueous and micellar phase. For an in depth discussion of this data treatment the reader is referred to previous reports from our laboratory [2, 19].

Table III lists the results of linear regression for plots of $\log k'$ versus n_c of the homologous solutes obtained with the various micellar phases containing fixed amount of alkylglucoside and borate but different concentrations of the BBA additive. The methylene group selectivity is not affected by the addition of BBA for either homologous series as reflected by the constancy of the values of the slopes, i.e., $\log \alpha$, thus indicating that the physico-chemical basis of retention on the various micellar phases is practically the same. On the other hand, the specific interactions, i.e., the values of $\log \beta$, are significantly increased by the addition of BBA. This is the result of the increase of the

TABLE III. Correlation between $\log k'$ and n_c of homologous series at various BBA concentration as an additive; solutes: PAA or APK homologous series.^a

[BBA], mM	$\log \beta$		$\log \alpha$		R	
	PAA	APK	PAA	APK	PAA	APK
0	-1.41	-1.08	0.31	0.39	0.9998	0.9992
100	-1.33	-0.95	0.32	0.38	0.9999	0.9995
200	-1.27	-0.87	0.33	0.38	0.9998	0.9995
300	-1.16	-0.74	0.34	0.38	0.9998	0.9997

^aConditions as in Table II.

hydrophobic character (i.e., phase ratio) of the micellar phase as the additive concentration is increased. The linear regression yielded excellent curve fits with all R values being greater than 0.999.

As we reported previously concerning the characterization of numerous micellar systems [2, 3, 19], plots of $\log k'$ of homologous solutes obtained with a given micellar phase *versus* $\log k'$ of the same solutes obtained with a reference micellar phase are usually linear. Using the linear $\log k'$ - $\log k'$ plots, the quotient of the phase ratios of the two micellar phases can be obtained from the antilog of the y-intercept. If the slope of the line is unity, the differences in Gibbs retention energies of the two micellar phases is zero for all solutes and the retention is termed homoenergetic. If the slope of the line is not unity, then the Gibbs retention energies are proportional by a constant that is equal to the slope and the retention is termed homeoenergetic. Figure 5 shows plots $\log k'$ for micellar phase B versus $\log k'$ of a reference micellar phase A for both PAA (Fig. 5a) and APK (Fig. 5b) homologous series. The addition of 300 mM BBA produced the most hydrophobic phase and was selected as the reference phase, i.e., micellar phase A, for comparison. The five data points for each line in Fig. 5a are the $\log k'$ obtained with the solutes of the PAA homologous series, whereas the data points for each line in Fig. 5b are obtained with the solutes of the APK homologous series. The slopes, intercepts and antilog of the intercepts of the $\log k'$ - $\log k'$ plots are listed in Table IV. The R values from the linear regression were all greater than 0.9999 (data not shown). The slopes of all $\log k'$ - $\log k'$ plots were either unity or very close to unity, thus indicating homoenergetic retention behavior with the addition of BBA to the borate-surfactant micellar phases. The effectiveness of BBA as a class I organic additive is realized by examining the quotient of the phase ratios, ϕ_B/ϕ_A . The phase ratio of the OG-borate micellar phase can be doubled by the addition of 300 mM BBA.

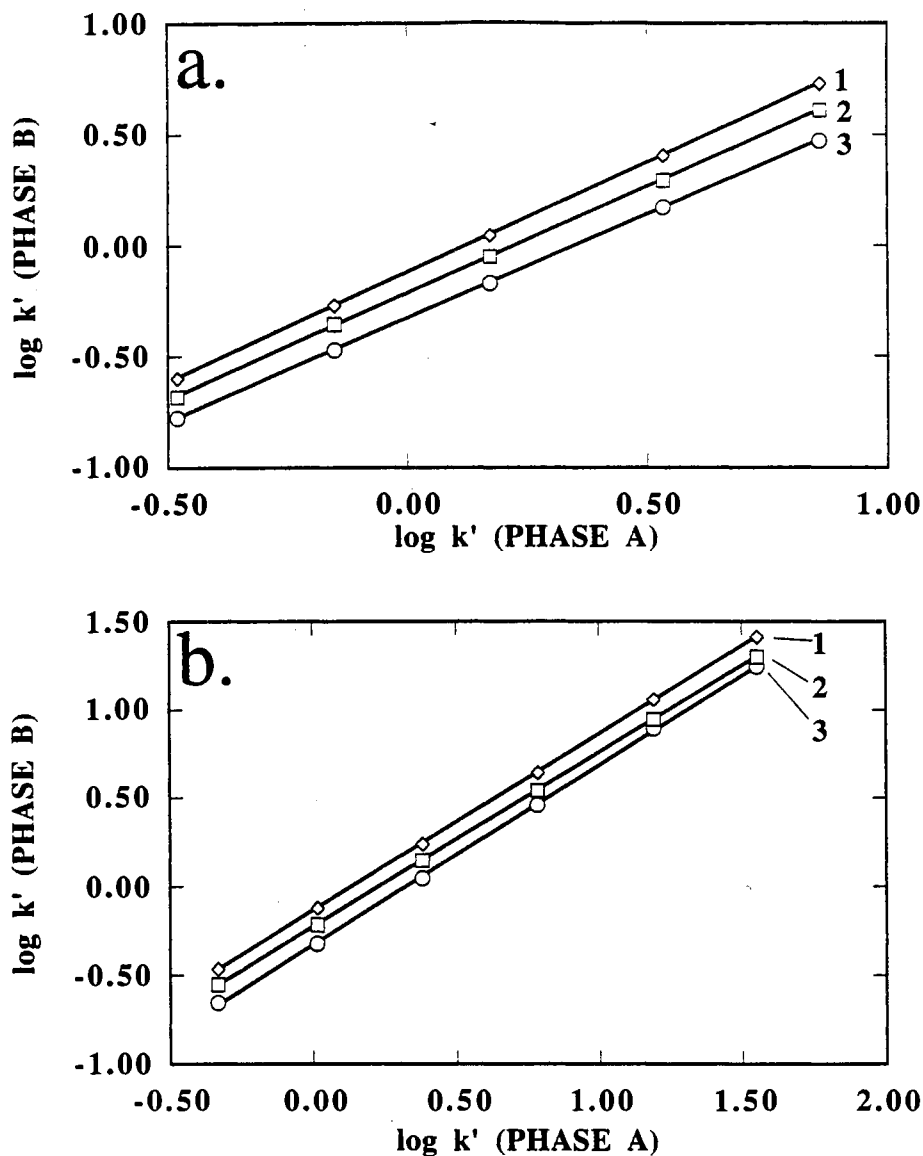


Figure 5. Plots of $\log k' - \log k'$ of (a) phenylalkyl alcohols homologous series and (b) alkyl phenyl ketones homologous series obtained on one micellar phase versus another reference micellar phase at constant micellized surfactant concentration. Lines: 1, HG micellar phase versus DG micellar phase; 2, OG micellar phase versus DG micellar phase; 3, NG micellar phase versus DG micellar phases. Experimental conditions: running electrolytes, HG phase: 129 mM HG, 258 mM borate; OG phase: 75 mM OG, 150 mM borate; NG phase: 56.5 mM NG, 113 mM borate; DG: 52 mM DG, 104 mM borate; pH 10.0; other conditions as in Fig. 3.

TABLE IV. Slopes, intercepts and antilog of intercepts (i.e., quotient of the phase ratios Φ_B/Φ_A) of $\log k' - \log k'$ plots for PAA and APK homologous series obtained with various concentrations of additive BBA.^a

Micellar phase A/ Micellar phase B	Slope		Intercept		Φ_B/Φ_A	
	PAA	APK	PAA	APK	PAA	APK
0 mM/300 mM	0.93	1.02	-0.33	-0.33	0.47	0.47
100 mM/300 mM	0.96	0.99	-0.22	-0.23	0.61	0.59
200 mM/300 mM	0.99	1.00	-0.12	-0.14	0.75	0.73
300 mM/300 mM	1.00	1.00	0.00	0.00	1.00	1.00

^aConditions as in Table II.

The above data treatment was also applied to the OG-BBA system described previously where the micelle is charged by the complexation with BBA thus forming a branched surfactant. The results in terms of slopes, intercepts and antilog of intercepts of $\log k' - \log k'$ plots for ABs are summarized in Table V where the OG-BBA micellar phase containing 150 mM BBA is considered as the reference micellar phase (micellar phase A)

TABLE V. Slopes, intercepts and antilog of intercepts (i.e., quotient of the phase ratios Φ_B/Φ_A) of $\log k' - \log k'$ plots for AB homologous series obtained with various concentrations of BBA.^a

Micellar phase A/ Micellar phase B	Slope	Intercept	Φ_B/Φ_A
50 mM/150 mM	0.84	-0.20	0.63
100 mM/150 mM	0.88	-0.14	0.73
150 mM/150 mM	1.00	0.00	1.00
200 mM/150 mM	0.98	0.01	1.03
250 mM/150 mM	0.92	-0.08	0.82

^aConditions as in Table I.

since above this BBA concentration k' starts to decline. The $\log k' - \log k'$ plots were linear with R values greater than 0.9998. As can be seen in Table V, the slopes are not as close to unity as in the case where BBA was used as class I organic additive, thus

indicating quasi homoenergetic retention. As in the case of plots of k' versus BBA concentration which showed a maximum at 150-200 mM BBA in the electrolyte, there is a maximum in the quotient of the phase ratios in the same concentration range. This is a temperature (i.e., Joule heating) induced behavior, see section on effect of borate.

Influence of the surfactant tail. Our previous investigations using *in situ* charged micelles revealed that in order to compare the retention energetics of different surfactants a few criteria must be met. First, a constant micellized surfactant concentration must be maintained. The ratio of surfactant:BBA should also be kept constant which allows the micelle to be charged in a unbiased fashion. Since retention energetics are thermodynamic parameters of the chromatographic process, excess Joule heating should be avoided such that the solubility of the analytes is not altered.

By adhering to the second criterion, i.e., keeping the ratio of surfactant:BBA constant, the hydrophobic characters of the various alkylglucoside-BBA micellar phases are altered to varying extents. Under these conditions, it is therefore important to evaluate the relative phase ratio of the various micellar phases as a function of the length of the alkyl tail of the surfactant. For the sake of comparison, it is useful first to evaluate the retention energetics of the alkylglucopyranoside surfactants in the presence of borate ions since this complexing agent does not alter the hydrophobic character of the various micelles. Again, the studies involving alkylglucoside-borate micellar phases were performed at constant micellized surfactant concentration and constant surfactant:borate, where $[S] + \text{CMC} = 50 \text{ mM}$, and $[\text{borate}] = 2 \times [S]$. The homologous series of PAA and APK were examined under the different micellar conditions. Table VI list the slopes, intercepts, and antilog of the intercepts obtained from the $\log k' - \log k'$ plots of both homologous series. Since DG should possess the most hydrophobic character, it was selected as the reference micellar phase. The slopes for most of the $\log k' - \log k'$ plots are close to unity, indicating quasi-

TABLE VI. Slopes, intercepts and antilog of intercepts (i.e., quotient of phase ratios Φ_B/Φ_A) of $\log k' - \log k'$ plots for PAA and APK homologous series obtained with different alkylglucoside-borate micelles.^a

Micellar phase A/ Micellar phase B	Slope		Intercept		Φ_B/Φ_A	
	PAA	APK	PAA	APK	PAA	APK
HG/DG	0.82	0.85	-0.17	-0.20	0.67	0.63
OG/DG	0.87	1.00	-0.06	-0.06	0.86	0.86
NG/DG	0.92	0.99	0.04	0.00	1.10	1.00
DG/DG	1.00	1.00	0.00	0.00	1.00	1.00

^a HG phase: 129 mM HG, 258 mM borate; OG phase: 75 mM OG, 150 mM borate; NG phase: 56.5 mM NG, 113 mM borate; DG: 52 mM DG, 104 mM borate; pH 10.0; other conditions as in Table I.

homoenergetic retention behavior among the various surfactants which differed in the tail length. This is similar to the trend observed with other *in situ* charged micelles, i.e., MEGA, evaluated previously by our laboratory [2]. It should be noted that the slope of the HG/DG is somewhat lower than unity (see Table VI), but since the borate concentration was 258 mM in HG phase, the increased Joule heating could be responsible for the deviations. The quotient of the phase ratios increased steadily as the alkyl tail length increased. The quotient of the phase ratios indicate that DG possess the higher hydrophobic character, 37 % and 33 % greater than HG with the PAAs and APKs, respectively.

An interesting point to mention was the variation in the electrophoretic mobility of the various alkylglucoside-borate micelles, $\mu_{ep(mc)}$ under the conditions used above. Assuming similar surface charge densities are present, it would be expected that as the size of the micelle increases, the $\mu_{ep(mc)}$ would decrease because of increasing frictional force. This trend was not observed. In fact, the $\mu_{ep(mc)}$ increased from $-1.71 \times 10^{-4} \text{ cm}^2\text{V}^{-1}\text{s}^{-1}$ to $-2.11 \times 10^{-4} \text{ cm}^2\text{V}^{-1}\text{s}^{-1}$ when going from HG to DG surfactants. The same trend of increasing mobility with size was observed with a different series of alkylglycoside:borate micelles introduced by our laboratory [2]. This observation could possibly be attributed to

changes in the viscosity for the different micellar phases or changes in zeta potential resulting from different ionic strengths.

Next, the experiments were carried out using the same conditions as described above with exception that BBA was used instead of borate and the pH was raised to 11.0. Table VII summarizes the results. Again, the systems appear to be quasi-homoenergetic as indicated by slopes close to unity. The R values from the linear regression were 0.999 or greater. In these systems, the concentration of BBA is varied over a wide range. The full potential of BBA as an additive and complexing agent is realized upon examination of the quotient of the phase ratios. Even though HG is three carbons shorter in the length of the

TABLE VII. Slopes, intercepts and antilog of intercepts (i.e., quotient of phase ratios ϕ_B/ϕ_A) of $\log k' - \log k'$ plots for PAA and APK homologous series obtained with different alkylglucoside-BBA micelles.^a

Micellar phase A/ Micellar phase B	Slope		Intercept		ϕ_B/ϕ_A	
	PAA	APK	PAA	APK	PAA	APK
HG/DG	0.86	0.85	0.06	0.02	1.16	1.03
OG/DG	0.86	0.96	-0.03	-0.03	0.93	0.93
NG/DG	0.91	1.01	-0.02	-0.01	0.95	0.98
DG/DG	1.00	1.00	0.00	0.00	1.00	1.00

^a HG phase: 129 mM HG, 258 mM BBA; OG phase: 75 mM OG, 150 mM BBA; NG phase: 56.5 mM NG, 113 mM BBA; DG: 52 mM DG, 104 mM BBA; pH 11.0; other conditions as in Table I.

alkyl tail than DG and possess a much higher CMC, the higher BBA concentration added to the HG micellar solution has transformed HG into a more hydrophobic micelle. It should be noted that with borate, HG possessed approximately 35 % lower phase ratio. With BBA, the phase ratio for HG is on the average 10% greater than that observed for DG. This feature gives the researcher the ability to significantly alter the hydrophobic character of the micelle to best achieve a given separation.

Effects of the surfactant concentration. In their initial work, Terabe *et al* [20] established the importance of the surfactant concentration in MECC by demonstrating that the capacity factor, k' , increases linearly with increasing the surfactant concentration in the running electrolyte. For a given surfactant whereby the distribution coefficient, K , is a constant, the linear relationship between k' and surfactant concentration would imply that the phase ratio i.e., the ratio of the volume of the micellar phase to that of the aqueous phase, increases linearly with increasing surfactant concentration. Figure 6a illustrates the dependence of k' of PAAs on the concentration of OG while keeping pH and BBA concentration constants. The x-intercept should correspond to the CMC of the surfactant-BBA complex. Linear regression yielded R values greater than 0.998 with an average x-intercept of 19.3 mM. The CMC values reported in the literature [9] range between 20 and 25 mM, but this under conditions where the micelle is nonionic and no additives are present.

Table VIII lists the electrophoretic mobility of the micelle, $\mu_{ep(mc)}$, at different OG concentrations using a fixed BBA concentration. The $\mu_{ep(mc)}$ decreases steadily as the OG concentration increases. This is because the viscosity of the medium increases and the surface charge density of the micelle decreases as less and less BBA is available for complexing with the micelle at elevated OG concentration. The elution range parameter, t_0/t_{mc} , is not significantly altered with the change in OG concentration. This is because the EOF is also decreased at higher OG concentrations. It should be noted, that the 200 mM is the highest practical concentration of OG that can be used. The viscosity at concentrations of 250 mM and above severely diminish the EOF yielding separations of extended analysis times.

One advantage of MECC is that when an analyte is partitioned in the micelle, its diffusion coefficient becomes that of the micelle. On this basis, it would be expected for the efficiency to increase as the concentration of surfactant is increased. Table VIII lists the efficiency observed as a function of OG concentration for the three s-triazine herbicides.

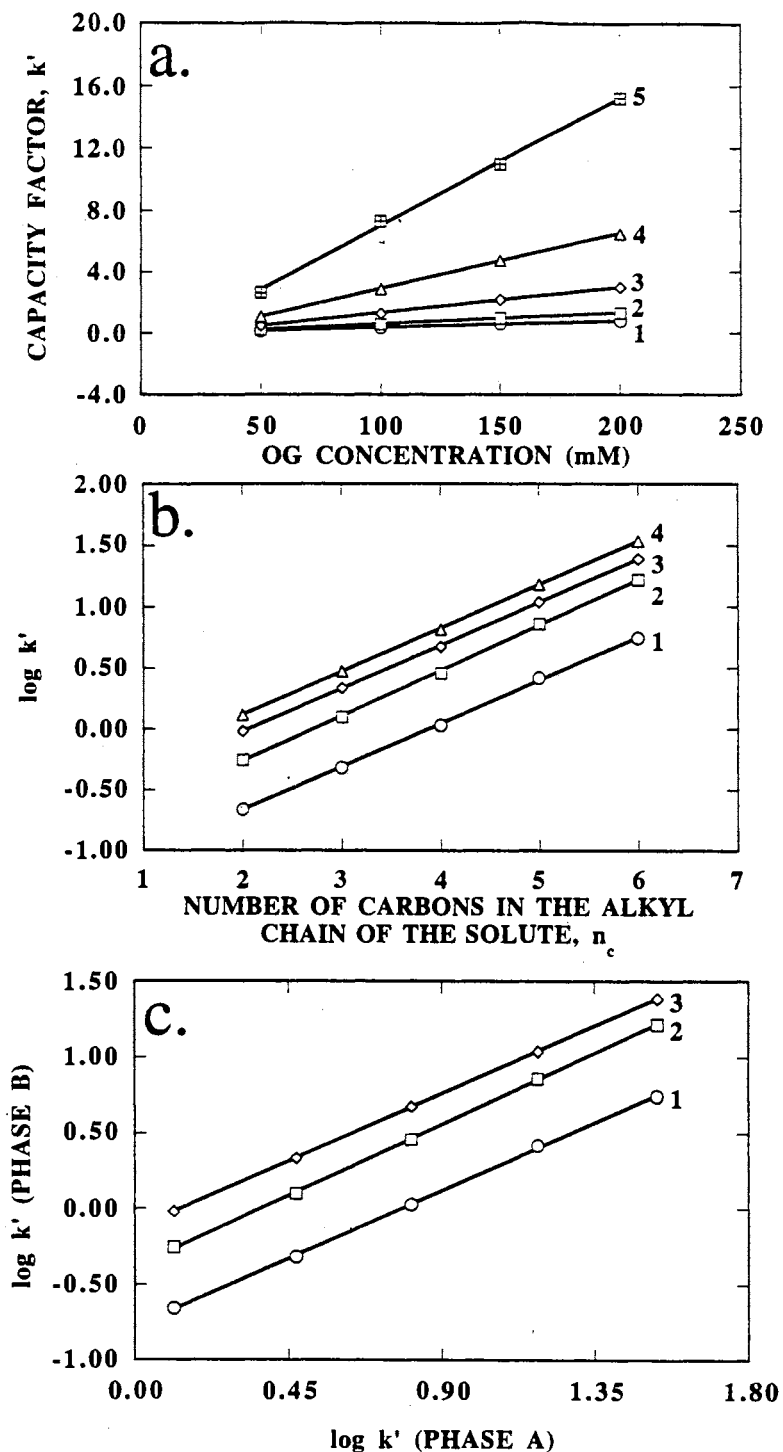


Figure 6. (a) Plots of the capacity factors of phenylalkyl alcohols versus concentration of OG. Experimental conditions: running electrolytes, 250 mM BBA at various OG concentrations, pH 11.0; other conditions as in Fig. 3. Solutes: 1, phenylmethanol; 2, 2-phenylethanol; 3, 3-phenyl-1-propanol; 4, 4-phenyl-1-butanol; 5, 5-phenyl-1-pentanol. (b) Plots of $\log k'$ versus carbon number of homologous series at various OG concentration. Lines: 1, 50 mM OG; 2, 100 mM OG; 3, 150 mM OG; 4, 200 mM OG. (c) Plots of $\log k' - \log k'$ for phenylalkyl alcohols series obtained on one micellar phase versus another reference micellar phase. Lines: 1, 50 mM OG versus 200 mM OG; 2, 100 mM OG versus 200 mM OG; 3, 150 mM OG versus 200 mM OG.

Table VIII. t_o/t_{mc} and N_{av} (per meter) as function of OG concentration.^a

[OG], mM	$\mu_{ep(mc)}$ (cm ² V ⁻¹ s ⁻¹)	t_o/t_{mc}	N_{av}
50	-1.80 x 10 ⁻⁴	0.48	187,000
100	-1.67 x 10 ⁻⁴	0.52	225,000
150	-1.64 x 10 ⁻⁴	0.51	356,000
200	-1.59 x 10 ⁻⁴	0.51	396,000

^aExperimental conditions: 250 mM BBA at pH 11.0 with various concentrations of OG; other conditions as in Table I.

The efficiency is more than doubled by increasing the surfactant concentration four fold.

Figure 6b plots $\log k'$ for the PAA homologous series versus n_c . The methylene group selectivity does not change with concentration of surfactant as indicated by the constant slope observed at each concentration. The slope averaged 0.36 with an RSD of less than 2.5 %. The R values from the linear regression were 0.999 or greater.

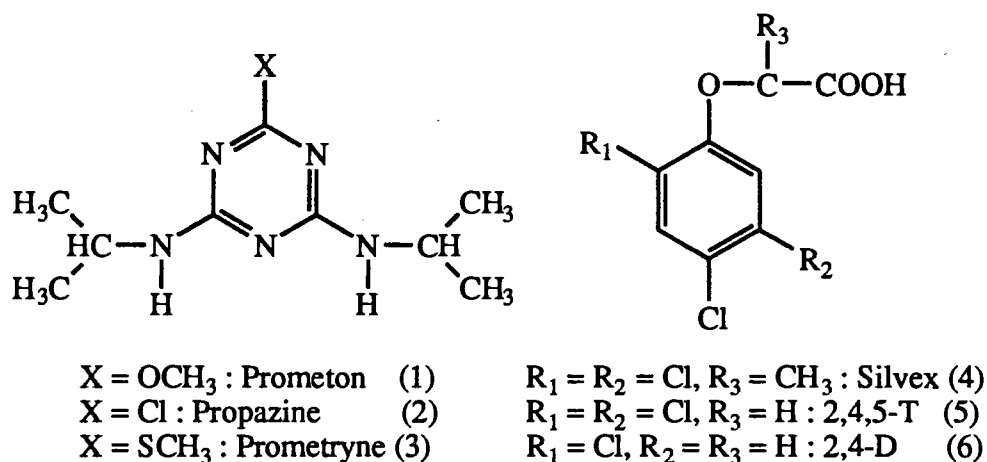
The retention energetics exhibited by OG-BBA micellar system at various surfactant concentration were examined through $\log k' - \log k'$ plots for the PAA homologous solutes. Figure 6c plots the $\log k'$ obtained with phase B (i.e., 50, 100 or 150 mM OG for lines 1, 2 and 3, respectively) versus $\log k'$ obtained with phase A (200 mM OG). The micellar phase containing 200 mM OG was selected as the reference phase since it is the most hydrophobic in character. The slopes for lines 1, 2 and 3 are 0.998, 1.045 and 0.991, respectively. Again, the linear regression yielded R values greater than 0.999. These slopes of unity indicate homoenergetic retention behavior among the different OG concentrations. The quotients of the phase ratios were found to be 0.166 for ϕ_{50}/ϕ_{200} , 0.413 for ϕ_{100}/ϕ_{200} , 0.737 for ϕ_{150}/ϕ_{200} , and 1.000 for ϕ_{200}/ϕ_{200} from the y - intercepts.

As discussed above, and according to the fundamental equations describing MECC, the phase ratio should increase linearly with the concentration of OG in a similar fashion to the trend observed with k' . To test the reliability of measuring retention

energetics using the $\log k' - \log k'$ plots, the quotients of the phase ratios obtained from the $\log k' - \log k'$ lines was plotted versus the concentration of OG. As expected, the quotient of the phase ratios increased linearly with OG concentration yielding a slope of 5.65×10^{-3} and a y-intercept of -0.13 with an R value of 0.999. This line has an x-intercept of 22.6 mM. At this point, the quotient of the phase ratios is equal to zero, which would correspond to the fact that the micelle is no longer existing and all the surfactant molecules are in the monomer form. In simple terms, the x-intercept, which is equal to 22.6, will correspond to the CMC of the surfactant. This value of 22.6 mM matches very well with that determined from the plots of k' versus concentration of OG and that reported in the literature [9]. This give confidence in the validity of the $\log k' - \log k'$ plots.

Applications

Figure 7 illustrates the separation of a mixture of neutral and acidic herbicides consisting of three s-triazine herbicides (i.e., prometon, propazine, and prometryne) and three chlorinated phenoxy acid herbicides. The structures of these herbicides are shown below.



These separations were carried out at pH 10.0 with either HG-BBA (Fig 7a) or DG-BBA (Fig. 7b). In both cases, the three acidic herbicides, which are fully ionized, eluted after the t_{mc} since at this pH the width of the migration time window is relatively narrow and the

species are migrating primarily by their own electrophoretic mobility. While the migration time window is 6.3 minutes for DG, that of HG is only 3.2 minutes because of the higher HG:BBA ratio. This results in the neutral herbicides being distributed over a 1.52 minutes span for DG and 0.66 minutes for HG. The fact that acidic and neutral solutes segregate into two separate locations on the electropherogram with the alkylglucoside-BBA micellar systems can be considered as an advantage since with micellar systems of wider migration time window, neutral and acidic species may elute over a narrow time frame, a condition that can lead in some cases to peak overlapping. The average separation efficiency for the herbicides is 755,000 plates/m for HG (Fig. 7a) and 341,000 plates/m for DG (Fig. 7b).

To further demonstrate the potentials of the alkylglucoside-BBA surfactants, a mixture of closely related urea herbicides (see structures below) was electrochromatographed.

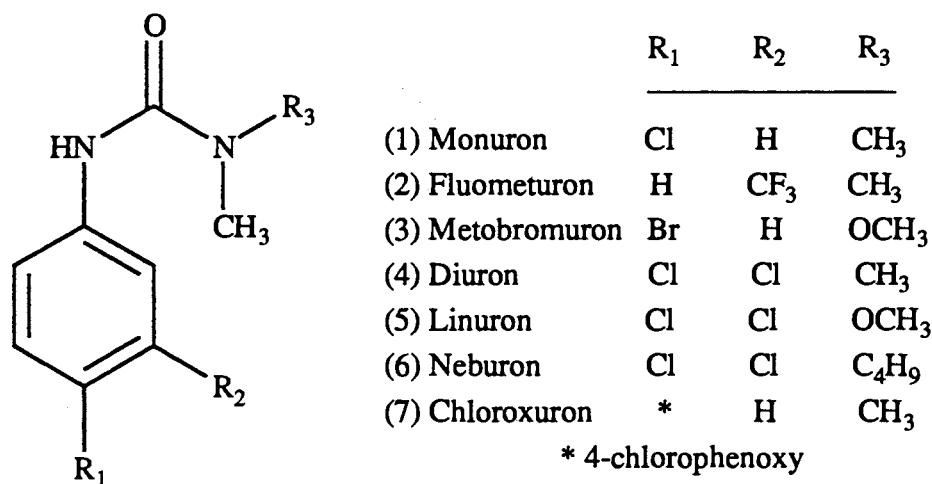


Figure 8 illustrates typical electropherograms obtained at pH 11.0 with HG-BBA and DG-BBA micellar systems. In both cases, the herbicides are all well resolved and high plate counts are observed reaching on the average 545,000 plates/m for HG and 760,000 plates/m for DG. It is important to note that the two micellar systems provided different selectivity. For instance, the values of the selectivity factor, α , for peaks 2 and 3 are 1.40 and 1.63 with HG and DG, respectively, and for peaks 6 and 7 are 1.52 and 1.41 for HG

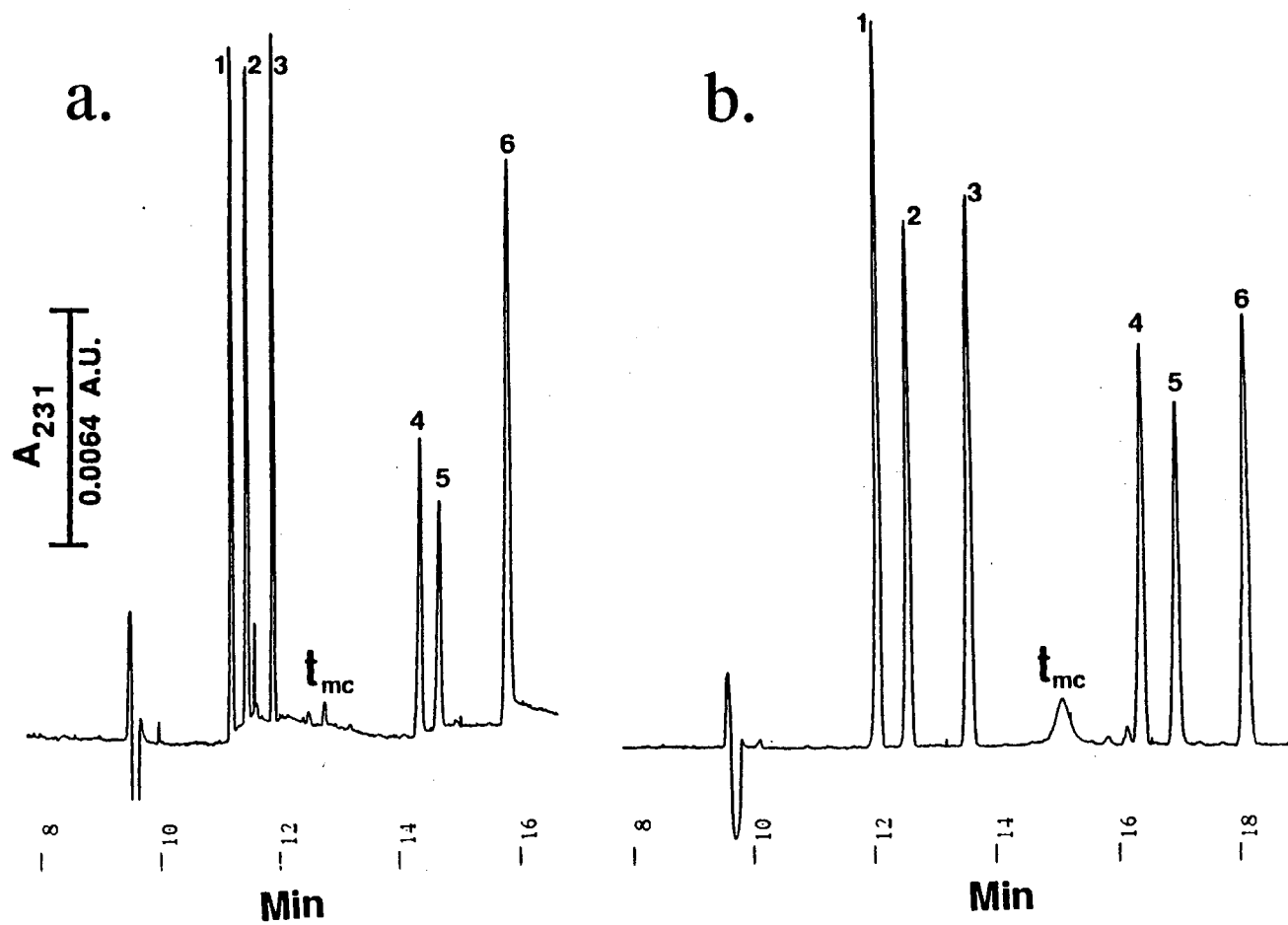
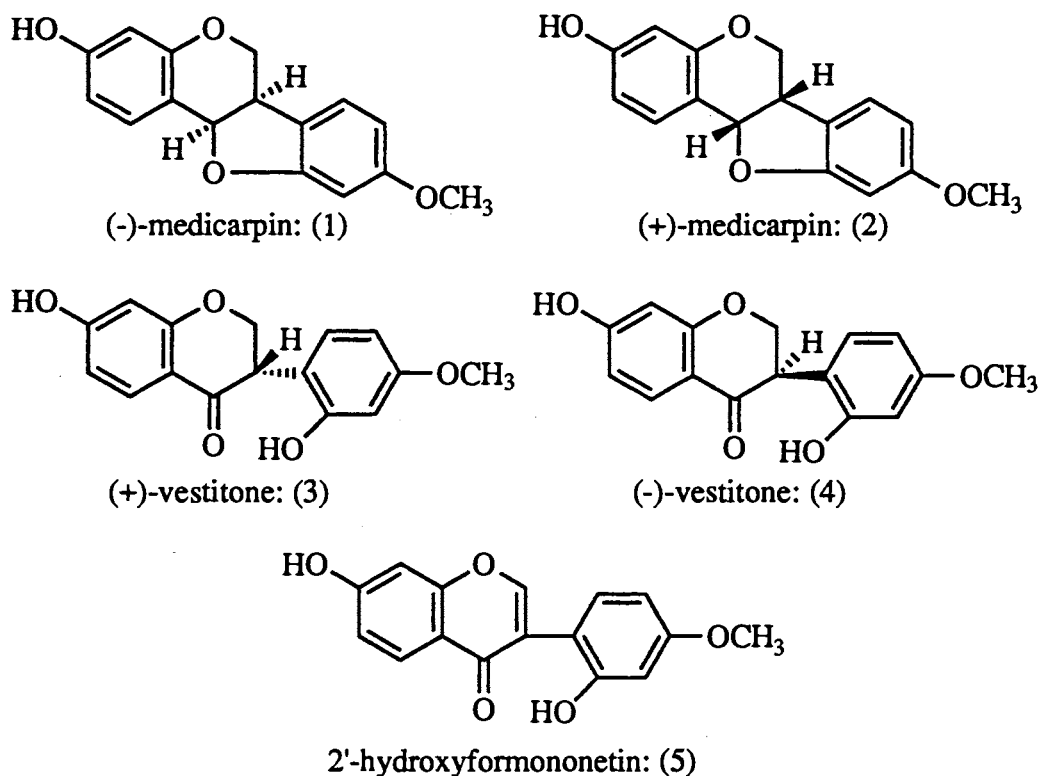


Figure 7. Electropherograms of neutral and acidic herbicides obtained with alkylglucoside-BBA micellar phases. Experimental conditions: running electrolytes, (a) 104 mM HG or (b) 28 mM DG, 200 mM BBA, pH 11.0. Other conditions as in Fig. 3. Solutes: 1, prometon; 2, propazine; 3, prometryne; 4, silvex; 5, 2,4,5-T; 6, 2,4-D, t_{mc} , anthracene.

and DG, respectively. Both micellar systems yielded much higher separation efficiencies (5 to 6 times higher) for the urea herbicides than previously reported [19] with traditionally used micelles, e.g., alkyltrimethylammonium halides, which are characterized by an invariable surface charge density.

To further illustrate the utility of the alkylglucoside-BBA micellar phases under investigation, a mixture of medicarpins and its precursors were electrochromatographed. Medicarpins are antifungal phytoalexins produced by leguminous plants, see structures below. The medicarpins are enantiomeric species, typically found in abundance in (-) or (+) forms depending on the plant.



Since chiral selectivity was necessary, native as well as modified cyclodextrins were evaluated with the alkylglucoside-BBA micellar phases. Figure 9a illustrates an electropherogram obtained using 50 mM DG and 150 mM BBA containing 15 mM γ -cyclodextrin at pH 11.0. The enantiomers of vestitone are resolved, but no separation between the medicarpin enantiomers is obtained. Figure 9b shows the separation obtained

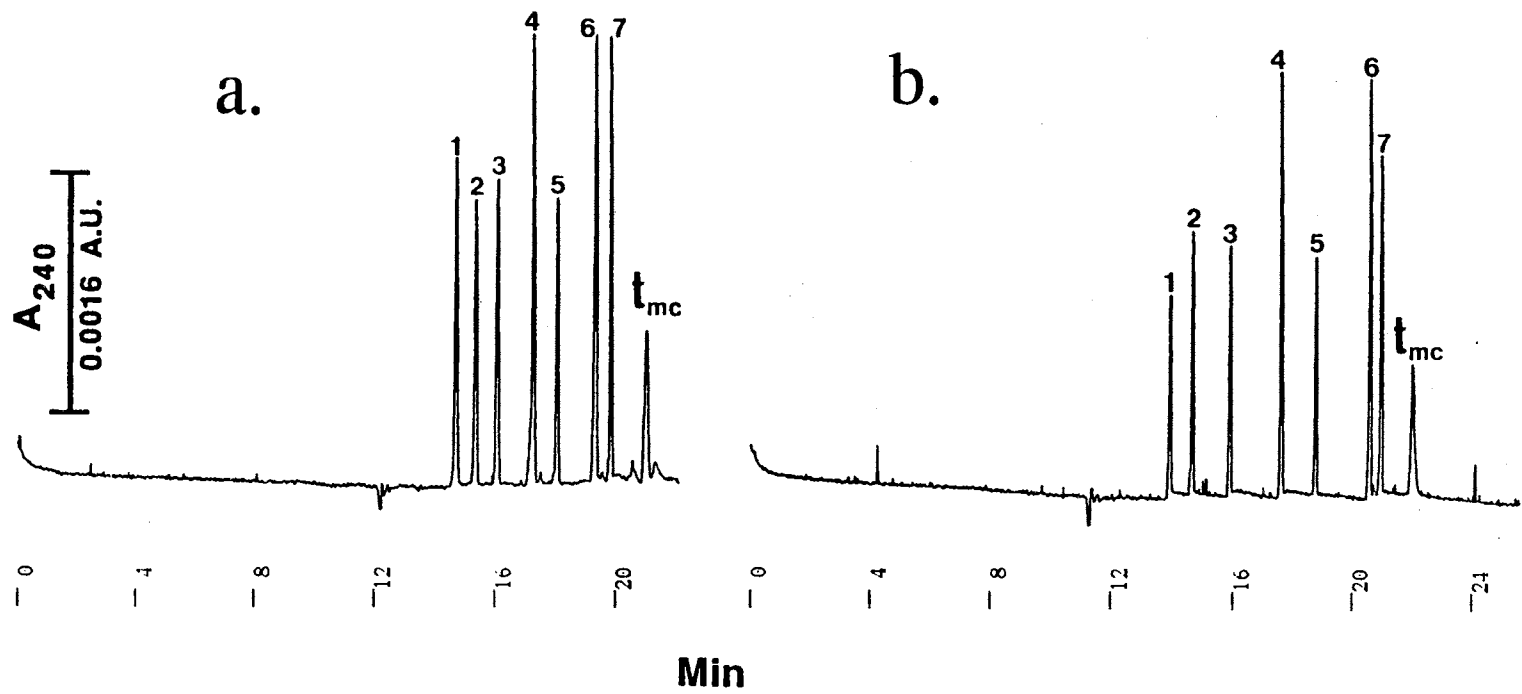


Figure 8. Electropherograms of urea herbicides obtained with alkylglucoside-BBA micellar phases. Experimental conditions: running electrolytes, (a) 125 mM HG or (b) 28 mM DG, 200 mM BBA, pH 11.0. Other conditions as in Fig. 3. Solutes: 1, monuron; 2, fluometuron; 3, metobromuron; 4, diuron; 5, linuron; 6, neburon; 7, chloroxuron; t_{mc} , anthracene.

using 150 mM OG and 250 mM BBA containing 20 mM hydroxypropyl- β -cyclodextrin at pH 11.0. As with γ -cyclodextrin, the vestitone enantiomers were well resolved, but still no resolution of the medicarpins was obtained. In addition, the analysis time is relatively high. Figure 9c illustrates the separation of the same mixture using 50 mM DG and 150 mM BBA containing 15 mM heptakis(2,6-di-O-methyl)- β -cyclodextrin at pH 11.0. Although some of the resolution between peaks 3 and 4 is lost when compared to the previous cases, the enantiomers of medicarpin are now resolved, and the overall quality of the separation is better than in the presence of γ -cyclodextrin and hydroxypropyl- β -cyclodextrin. In all cases, the alkylglucoside-BBA micellar phases supplied relatively high separation efficiencies.

As a final example of the utility of the alkylglucoside-BBA micellar phases is the separation of a mixture of dansylated-DL-amino acids shown in Fig. 10. The separation was obtained using 50 mM DG and 150 mM BBA containing 15 mM γ -cyclodextrin at pH 11.0. At this pH, the amino acids are migrating primarily by their own charges, but they possess enough hydrophobic character to undergo significant interaction with the *in situ* charged micelles. All the enantiomers are resolved and the average efficiency was 850,000 plates/m.

Conclusion

The *in situ* charged MECC systems described in the present study allow the surface charge density of the micelle to be adjusted for precise control of the migration time window. This can be achieved by altering one or more of the operational parameters such as pH, BBA concentration and surfactant concentration. In addition, BBA can act as a class I additive and as a complexing agent forming dynamically branched surfactant with adjustable hydrophobic character. These features offer additional flexibility to achieve the desired resolution with maximum sample throughput. Each of the alkylglucoside

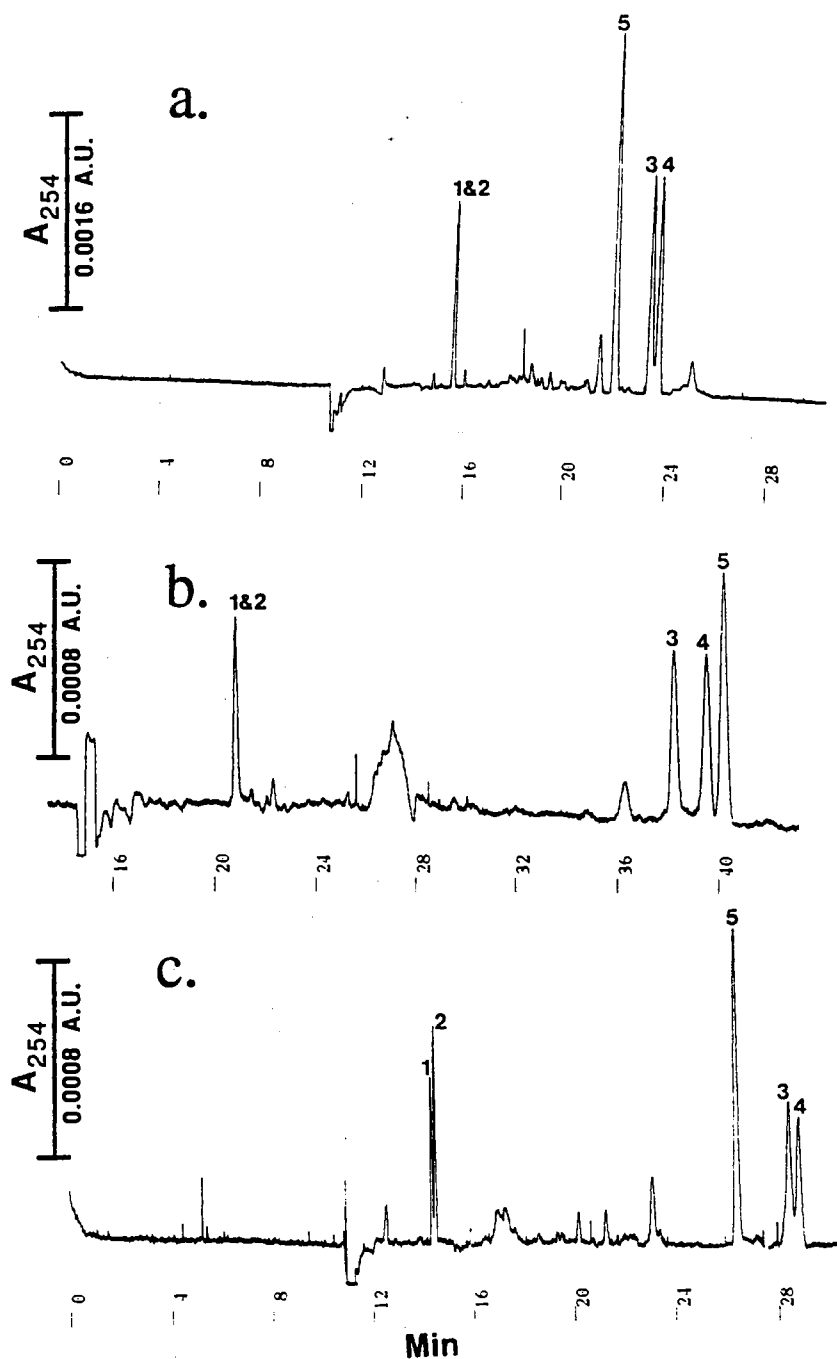


Figure 9. Electropherograms of medicarpins and precursors obtained with alkylglucoside-BBA micellar phases. Experimental conditions: running electrolytes, (a) 50 mM DG, 150 mM BBA, 15 mM γ -cyclodextrin; (b) 150 mM OG, 250 mM BBA, 20 mM hydroxypropyl- β -cyclodextrin; (c) 50 mM DG, 150 mM BBA, 15 mM heptakis(2,6-di-O-methyl)- β -cyclodextrin; pH 11.0. Other conditions as in Fig. 3. Solutes: 1, (-)-medicarpin; 2, (+)-medicarpin; 3, (+)-vestitone; 4, (-)-vestitone; 5, 2'-hydroxyformononetin.

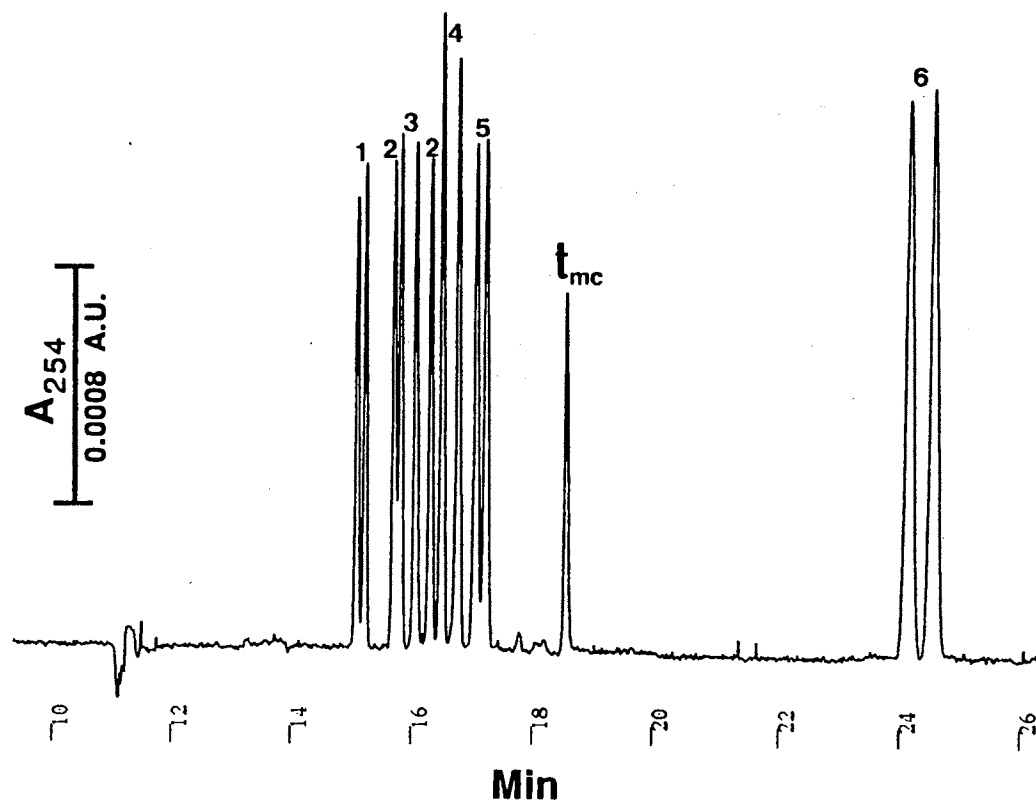


Figure 10. Electropherogram of D and L dansyl amino acids. Experimental conditions: running electrolytes, 50 mM DG, 150 mM BBA, 15 mM γ -cyclodextrin; pH 11.0. Other conditions as in Fig. 3. Solutes: 1, phenylalanine; 2, leucine; 3, valine; 4, methionine; 5, threonine; 6, glutamic acid; t_{mc} , anthracene.

surfactants demonstrated different hydrophobic character, which could be tuned to varying levels by simply changing the concentration of BBA in the running electrolyte.

Acknowledgments

This material is based upon work supported by the Cooperative State Research Service, U.S. Department of Agriculture, under Agreement No. 92-34214-7325. JTS is the recipient of a Water Resources Presidential Fellowship from the University Center for Water Research at Oklahoma State University. Finally, the authors acknowledge partial support by the NSF (CHE-8718150) and the Oklahoma Center for the Advancement of Science and Technology (No. 1506) for the upgrade of the NMR facility. Finally, we would like to thank Paul West for the writing of computer software that greatly simplified the calculation of t_{mc} using the iterative method.

References

1. J. Cai and Z. El Rassi, *J. Chromatogr.*, 608 (1992) 31.
2. J. T. Smith, W. Nashabeh and Z. El Rassi, *Anal. Chem.*, 66 (1994) 1119.
3. J. T. Smith and Z. El Rassi, *J. Microcol. Sep.*, 6 (1994) 127.
4. R. J. Ferrier, *Adv. Carbohydr. Chem. Biochem.*, 35 (1978) 31.
5. A. B. Foster and M. Stacey, *J. Chem. Soc.*, (1955) 1778.
6. S. A. Barker, A. K. Chopra, B. W. Hatt and P. J. Somers, *Carbohydr. Res.*, 26 (1973) 33.
7. R. Pizer and C. Tihal, *Inorg. Chem.*, 31(1992) 3243.
8. M. Tanaka, T. Ishida, T. Araki, A. Masuyama, Y. Nakatsuji, M. Okahara S. Terabe, *J. Chromatogr.*, 648 (1993) 469.
9. J. Neugebauer, *A Guide to the Properties and Uses of Detergents in Biology and Biochemistry*, 5th Printing, Calbiochem-Novabiochem Corp., San Diego 1994.
10. M. J. Rosen, in *Surfactants and Interfacial Phenomena*, 2nd ed., John Wiley and Sons, New York 1988, pp. 138-142.
11. P. A. Winsor, *Manufac. Chem.*, April (1956) 130.
12. J. H. Aiken and C. W. Huie, *J. Microcol. Sep.*, 5 (1993) 95-99.
13. M. J. Schick and F. M. Fowkes, *J. Phys. Chem.*, 61 (1957)1062.
14. D. Myers, in *Surfactant Science and Technology*, VCH Publishers, New York 1988, pp. 153-182.
15. J. T. Smith and Z. El Rassi, *Electrophoresis*, 14 (1993) 396.
16. J. T. Smith and Z. El Rassi, *J. High Resolut. Chromatogr.*, 15 (1992) 573.
17. R. J. Ferrier, *J. Chem. Soc.*, (1961) 2325.
18. R. J. Ferrier, W. G. Hannaford, W. G. Overend and B. C. Smith, *Carbohydr. Res.*, 1 (1965) 38-43.

19. D. Crosby and Z. El Rassi, *J. Liq. Chromatogr.*, 16 (1993) 2161.
20. S. Terabe, K. Otsuka and T. Ando, *Anal. Chem.*, 57, (1985) 834.

CHAPTER IX

MICELLAR ELECTROKINETIC CAPILLARY CHROMATOGRAPHY WITH *IN SITU* CHARGED MICELLES IV. INFLUENCE OF THE NATURE OF THE ALKYLGLYCOSIDE SURFACTANT*

Abstract

Four different *in situ* charged micellar phases were evaluated in micellar electrokinetic capillary chromatography (MECC) of neutral and acidic herbicides as well as aromatic compounds. *In situ* charged micelles refer to dynamically charged entities that are formed *via* the complexation of borate with surfactants having sugar head groups. These dynamically charged surfactants yield micelles with adjustable surface charge densities which can be conveniently manipulated by changing borate concentration and pH of the running electrolyte. The four surfactants, namely octanoylsucrose (OS), octyl- β -D-glucopyranoside (OG), octyl- β -D-maltopyranoside (OM) and nonanoyl-*N*-methylglucamide (MEGA 9), in the presence of alkaline borate yielded micelles characterized by migration time windows of varying width. The width of the migration time window was largely influenced by the nature of the sugar head group of the polyolic surfactant. The electrochromatographic behavior of OS, OM, OG and MEGA 9 was influenced by both the nature of the sugar head group and the length of the alkyl tail. Octanoylsucrose, which differed from the other surfactants by having an alkyl tail with one

* J. T. Smith and Z. El Rassi, *Electrophoresis*, submitted.

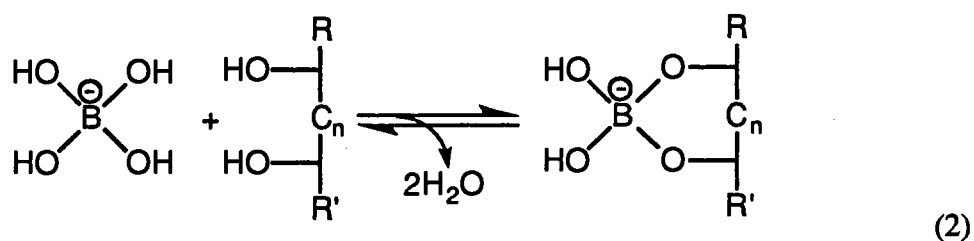
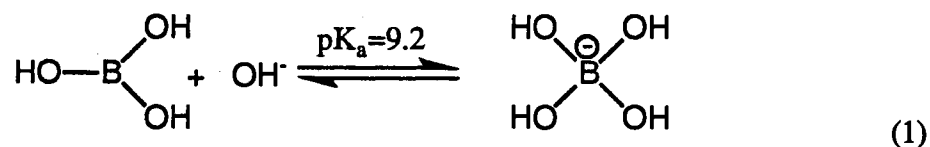
fewer carbon atom, exhibited the lowest retention. MEGA 9 with its acyclic sugar head group and the presence of a polar amide linkage between the sugar and the alkyl tail showed a medium retentivity towards the various solutes under investigation. Octyl- β -D-glucoside and OM, which differed from each other by the nature of the sugar head group, exhibited more or less similar retention behavior. Overall, due to differences in their migration time windows and retention behaviors, the four micellar phases afforded different selectivities toward charged and neutral solutes. The separation efficiencies achieved with *in situ* charged micelles, which exceeded 750,000 plates/m, appear to be superior to those achieved with traditionally used micellar phases.

Introduction

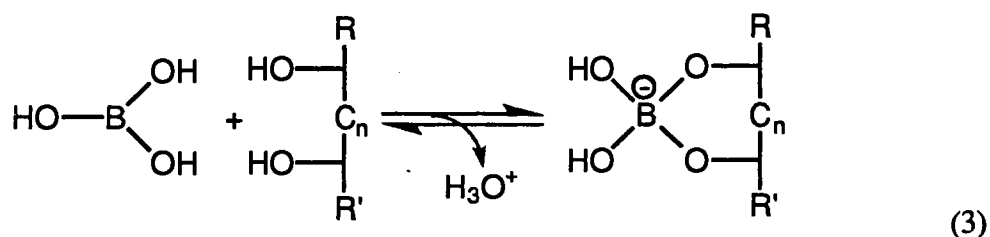
Over the last decade, capillary electrophoresis (CE) has developed rapidly and became an important analytical separation technique [1, 2] of unsurpassed resolving power. The technique has found applications in the separation of almost all types of compounds. This universal use of CE has been facilitated in part by the fact that a given separation can be performed in several modes thus permitting the achievement of different selectivities. An important development of CE has been the introduction of micellar electrokinetic capillary chromatography (MECC) by Terabe *et al.* in 1984 [3], a technique that allows the separation of neutral species under the influence of an electrical field. MECC has shown great promises in the separation of both neutral and charged species [4-8]. The separation is achieved *via* the differential partitioning of the analytes between an aqueous phase and a charged micellar phase. The basic operational principles and the applications of MECC have been recently reviewed [9, 10].

Recently, our laboratory has introduced the concept of *in situ* charged micelles [11-14] to MECC of neutral and charged species. *In situ* charged micelles are dynamically charged entities *via* complexation of a diol group of a polyol surfactant with borate or

boronate ion. The generalized reaction scheme of a diol with the borate ion is shown below.



Where equilibrium 1 represents the ionization of boric acid ($\text{pK}_a = 9.2$) to the tetrahydroxy borate ion, i.e., borate. Equilibrium 2 represents complexation between the borate ion and a diol. It is well known that a polyol possessing vicinal diols of the proper geometry can undergo complexation with borate to form an ionized complex upon the loss of two molecules of water [15-17]. In equilibrium 2, n is either 0 or 1, which corresponds to a 1,2- or 1,3-diol, respectively. The 1,2-diol forms a five membered ring upon complexation and is more stable than the 1,3 diol complex which forms a six membered ring. Boric acid, in the neutral form, can also complex with diols and is illustrated below in equilibrium 3.



In this reaction, the complex is formed upon the loss of one water molecule and a proton. It is well known that the stability constant of equilibrium 2 is much greater than that of equilibrium 3. The forward rate constant for the complexation (equilibrium 2) is at least 3 orders of magnitude greater than the rate constant for the trigonal boric acid (equilibrium 3)

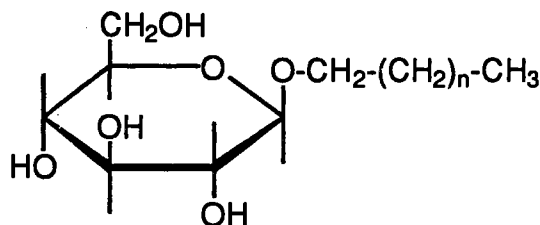
for some polyols [18]. Equilibrium 3, whose rate constants are largely dependent on the geometrical arrangement of diols, is currently being exploited in our laboratory with *in situ* charged micelles at neutral pH. At alkaline pH, the formation of diol-borate complex is primarily the result of equilibrium 2.

According to the above equilibria, the surface charge density of an alkylglycoside micelle can be easily manipulated by altering the borate concentration, the surfactant concentration, and/or the pH of the running electrolyte. As a result, the migration time window of the *in situ* charged MECC system can be tailored to suit a given separation problem.

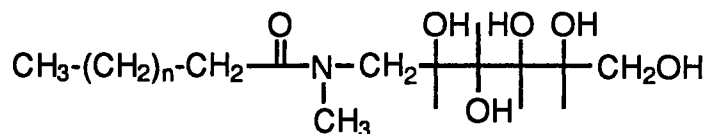
We have examined several polyol surfactants as possible *in situ* charged micellar phases including a series of four alkyl- β -D-glucopyranosides [12], a series of three *N*-D-glucosyl-*N*-methylalkanamides (MEGA) [14], octyl- β -D-maltopyranoside and octanoylsucrose [13]. The structures of these surfactants are listed in Table I. Figure 1 illustrates our views of the idealized structure of the alkylglycoside-borate micelle. The micelle consist primarily of the hydrophobic core with hydrophilic sugar residues facing outwards towards the aqueous phase. Borate can complex with the diols of the proper geometry at the surface of the micelle. Since the degree of complexation can be readily controlled, the surface charge density is therefore adjustable.

Due to the nature of the hydrophilic sugar head group, different surfactants have different affinities towards borate. ^{11}B NMR studies [13] have shown that the alkyl- β -D-glucopyranoside surfactants complex through O-4 and O-6 of the glucose residue as suggested by Foster [15]. Similarly, octanoylsucrose and octyl- β -D-maltopyranoside complex with borate primarily *via* the nonreducing glucose residue and have binding affinities very similar to that of the alkyl- β -D-glucopyranosides [14]. The MEGA surfactants possess an acyclic sugar residue which allows the hydroxyl groups to change their conformation freely. This freedom in changing conformation allows the MEGA surfactants to have a much higher affinity towards borate. Previous ^{11}B studies have

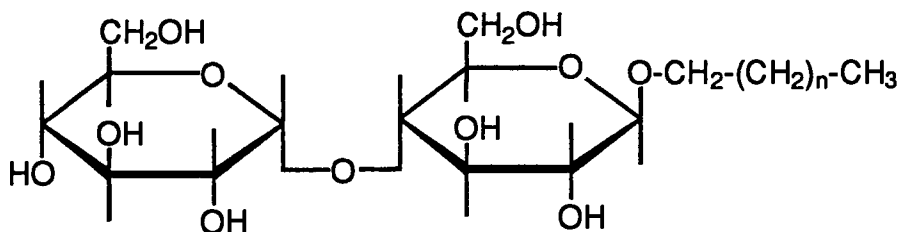
TABLE I. Structures and cmcs of surfactants used in our studies.

Alkylglucosides

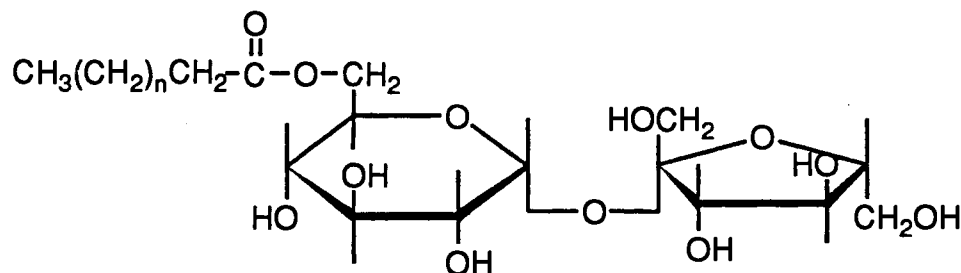
<u>identification</u>	<u>name</u>	<u>abbreviation</u>	<u>CMC*</u>
n=5	heptyl-β-D-glucopyranoside	HG	79 mM
n=6	octyl-β-D-glucopyranoside	OG	25 mM
n=7	nonyl-β-D-glucopyranoside	NG	6.5 mM
n=8	decyl-β-D-glucopyranoside	DG	2-3 mM

Alkylglucamides

<u>identification</u>	<u>name</u>	<u>abbreviation</u>	<u>CMC*</u>
n=5	octanoyl-N-methylglucamide	MEGA 8	58 mM
n=6	nonanoyl-N-methylglucamide	MEGA 9	19-25 mM
n=7	decanoyl-N-methylglucamide	MEGA 10	6-7 mM

Alkylmaltosides

<u>identification</u>	<u>name</u>	<u>abbreviation</u>	<u>CMC*</u>
n=6	octyl-β-D-maltopyranoside	OM	23.4 mM

Alkanoylsucrose

<u>identification</u>	<u>name</u>	<u>abbreviation</u>	<u>CMC*</u>
n=5	n-octanoylsucrose	OS	24.4 mM

* Obtained from Reference [24]

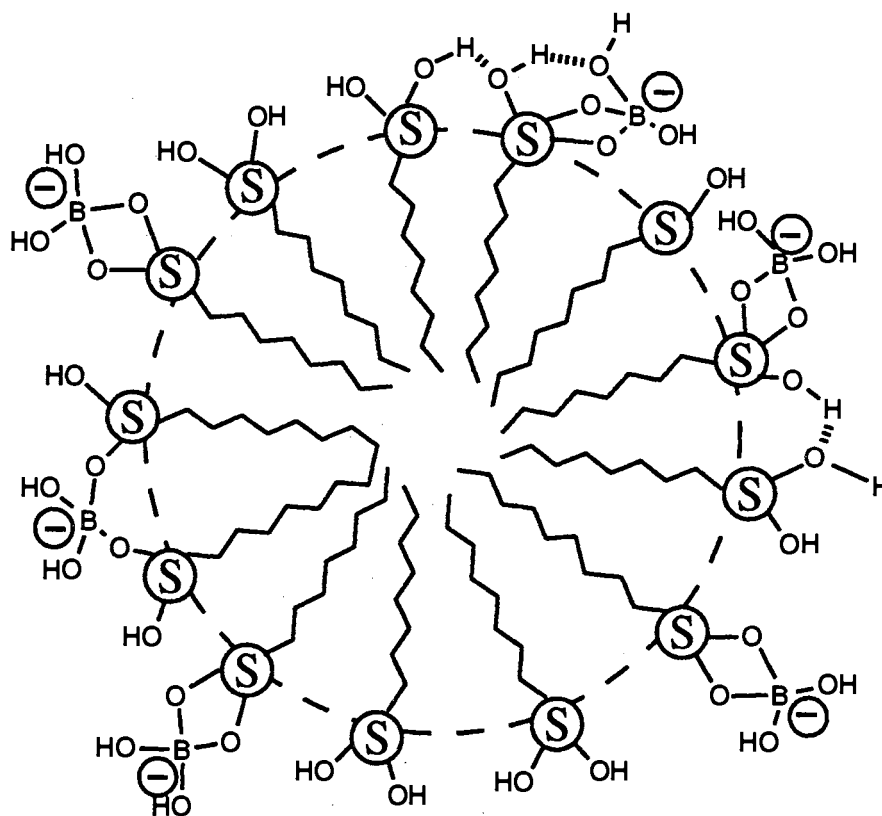


Figure 1. Idealized structure of alkylglycoside-borate micelle showing borate complexation and hydrogen bonding on the outer surface of the micelle. Circled-S stands for the sugar head group of the surfactant.

indicated that the surfactants with acyclic sugar head groups have at least a three fold higher affinity for borate than surfactants possessing a cyclic sugar head group [13]. This feature allows the MEGA micellar phases to form a larger migration time window under similar electrophoretic conditions.

As can be seen in Table I, the alkylglycoside surfactants under investigation possess a straight chain alkyl tail and a sugar polar head group. We have previously evaluated the influence of the length of the alkyl tail with various types of analytes [12, 13], and demonstrated that the differences in hydrophobic character among surfactants with different tails are useful in optimizing selectivity for a given separation.

The aim of this report is to investigate the influence of the nature of the alkylsaccharide surfactant on the electrochromatographic properties of the *in situ* charged micelles. To achieve this goal, surfactants having different types of sugar head groups and hydrocarbonaceous tails were evaluated, namely, octanoylsucrose (OS), octyl- β -D-maltopyranoside (OM), octyl- β -D-glucopyranoside (OG) and nonanoyl-*N*-methylglucamide (MEGA 9). As can be seen in Table I, all four of the surfactants have similar CMCs. Three of the surfactants differ in the nature of the sugar head group and have in common an eight carbon lipophilic tail (i.e., OM, OG and MEGA 9) while the fourth surfactant has a different alkyl tail (a seven carbon alkyl tail) and sugar head group, i.e., OS. The surfactants were compared in terms of the migration time window, peak capacity, efficiency, retention energetics and selectivity as a function of the nature of the surfactant. The micellar phases were applied to MECC of mixtures of both neutral and acidic herbicides as well as very hydrophobic aromatic compounds.

Experimental

Instrumentation

This work was performed on a capillary electrophoresis system Model HP 3DCE from Hewlett Packard (Waldbronn, Germany) equipped with a real time UV-visible diode array detector (DAD) and accompanying data analysis software. The column temperature was maintained at 30 °C. The detection wavelength was set at 240 nm for the detection of herbicides, and at 254 nm for the detection of aromatics and alkyl phenyl ketones. In all the experiments, the electrical field strength was 187.5 V/cm.

Fused-silica capillaries having an inner diameter of 50 μm and an outer diameter of 375 μm were obtained from Polymicro Technology (Phoenix, AZ, U.S.A.). The total length of the capillary was 64.0 cm with an effective length of 56.0 cm, i.e., from the injection end to the detection point.

Reagents

Octyl- β -D-glucopyranoside (OG) was obtained from Sigma Chemical Co. (St. Louis, MO, U.S.A.). *n*-Octanoylsucrose (OS), octyl- β -D-maltopyranoside (OM) and nonanoyl-*N*-methylglucamide (MEGA 9) were purchased from Calbiochem (San Diego, CA, U.S.A.). For the structures of the surfactants, see Table I. All herbicides used in this study were purchased from Chem Service (West Chester, PA, U.S.A.). The series of alkyl phenyl ketones (APK) was purchased from Aldrich Chemical Co. (Milwaukee, WI, U.S.A.). Aniline, 2-naphthylamine, naphthalene, biphenyl, 1-chloronaphthalene and anthracene were purchased from Eastman Kodak Co. (Rochester, NY, U.S.A.). All chemicals for the preparation of electrolytes were purchased from Fisher Scientific (Pittsburgh, PA, U.S.A.). Methanol was purchased from EM Science (Cherry Hill, NJ, U.S.A.). All electrolyte solutions were prepared with deionized water and filtered with 0.2 μm Uniprep Syringeless filters from Fisher Scientific to avoid capillary plugging.

Methods

The running electrolyte was prepared by dissolving proper amounts of boric acid and surfactant in water, and adjusting the pH to the desired value with sodium hydroxide. For all experiments, the running electrolyte was composed of 100 mM of the surfactant and 200 mM borate at pH 10.0. All sample stock solutions were made by first dissolving pure compounds in methanol. Sample solutions for injection were made by dissolving the proper amount of stock solution in the running electrolyte and adjusting the total volume of methanol in the sample to 20% (v/v). Sample injection was performed by pressurizing the sample reservoir for an appropriate amount of time (50-100 mbar•s). Between runs, the capillary was rinsed consecutively with water, 1.0 M NaOH, 0.10 M NaOH, water and the running electrolyte.

In all calculations involving efficiency, the plate count was estimated from peak standard deviation taken as the half peak width at 0.607 of peak height (i.e., the inflection point) and was reported as the average of at least three runs. Mobilities were determined from average migration times, and again a minimum of three runs were used to calculate the average. The migration time of an unretained species, t_0 , was determined by the deflection peak of methanol. The migration time of the micelle, t_{mc} , was determined by the iterative method of a homologous series [8]. Anthracene was used as a marker to visualize t_{mc} but was not used in the calculation of the capacity factor, k' .

Results and Discussion

Migration Time Window

As we have described in previous studies involving *in situ* charged micellar systems, i.e., alkylglycoside-borate or -boronate micelles [11, 13, 14], the migration time

window can be adjusted over a wide range by adjusting the pH, borate (or boronate) concentration and/or the surfactant concentration. This is because these parameters affect the surface charge density of the micelle.

To provide a meaningful comparison for the results pertaining to the migration time window, the four surfactants, OG, OS, OM and MEGA 9, were evaluated under conditions of constant micellized surfactant concentration. Constant micellized surfactant concentration [S] corresponds to keeping the concentration of surfactant minus the CMC constant, i.e., [S] - CMC = constant. Since the four surfactants all have similar CMC values, all electrolyte solutions used in the present studies contained the same surfactant concentration. All running electrolytes were composed of 100 mM surfactant and 200 mM borate at pH 10.0. Table II lists the migration times for the unretained species, t_0 , and those of the micelle, t_{mc} . The elution range parameters (t_0/t_{mc}) were calculated to be 0.65,

TABLE II. Comparison of migration time window, mobility, efficiency and peak capacity for the various micellar phases^{a)}

Micellar Phases	t_0 (min)	t_{mc} (min)	$\mu_{ep(mc)}$ (cm ² V ⁻¹ s ⁻¹)	N_{av}	n
OS	14.65	24.61	-1.38×10^{-4}	453,500	65
OM	14.27	21.97	-1.22×10^{-4}	602,200	63
OG	12.91	23.58	-1.75×10^{-4}	767,600	99
MEGA 9	12.47	40.77	-2.77×10^{-4}	538,400	163

a) Conditions: running electrolyte, 200 mM borate containing 100 mM surfactant, pH 10.0; capillary, untreated fused silica, 56.0 cm (to detection point), 64.0 cm (total length) x 50 μ m I.D.; voltage 15 kV.

0.60, 0.55 and 0.31 for OM, OS, OG and MEGA micellar phases, respectively. The width of migration time window was the smallest for OM-borate micelle (7.70 min) and the highest for MEGA 9 (28.30 min). The value of the width of the migration time window for OS (9.96 min) and OG (10.67 min) was slightly larger than that observed

with OM but much smaller than the one exhibited by MEGA 9. These results corroborate well those previously reported with ^{11}B NMR studies [13] in the sense that the MEGA surfactants have two to three fold greater affinity for borate than the alkylglucoside surfactants which translate into a greater electrophoretic mobility, $\mu_{\text{ep}(\text{mc})}$, for MEGA-borate micelle, and in turn to a wider migration time window. Moreover, the small differences in the width of the migration time windows among OS, OM and OG agree with ^{11}B NMR results which revealed that these surfactants have similar affinities for borate [14]. As can be seen in Table II, the values of t_0 were different among the various micellar phases which may due to slight differences in the viscosity of their running electrolyte solutions.

Furthermore, Table II lists the $\mu_{\text{ep}(\text{mc})}$ for the four surfactant-borate micellar phases under investigation. The $\mu_{\text{ep}(\text{mc})}$ is a direct indication of the degree of complexation between borate and the micelle. OS, OM and OG have a somewhat lower $\mu_{\text{ep}(\text{mc})}$ as reflected by the migration time window. The larger $\mu_{\text{ep}(\text{mc})}$ observed with MEGA 9 is a result of the acyclic nature of the sugar head group of the surfactant. This is because the hydroxyl groups of acyclic sugars, which are not held in a fixed position, are free to move into more favorable binding positions. Due to this conformational freedom found in acyclic sugars, they can possess up to a ten fold greater affinity for borate than cyclic sugars [19].

The differences in borate affinity for the different surfactants offer a variety of migration time windows. It should be emphasized that the $\mu_{\text{ep}(\text{mc})}$ for OS, OM and OG can be increased up to $\approx -2.5 \times 10^{-4} \text{ cm}^2\text{V}^{-1}\text{s}^{-1}$ by increasing the borate concentration and/or the pH because the surface charge density of the micelle is increased. The MEGA surfactants exhibit a relatively high $\mu_{\text{ep}(\text{mc})}$ that can be varied over a wide range with an upper limit approaching that achieved with SDS. A micellar phase consisting of 43 mM MEGA 9 and 400 mM borate at pH 10.0 produced an $\mu_{\text{ep}(\text{mc})}$ of $-3.6 \times 10^{-4} \text{ cm}^2\text{V}^{-1}\text{s}^{-1}$ [13] while that of 100 mM SDS is reported to be $-4.2 \times 10^{-4} \text{ cm}^2\text{V}^{-1}\text{s}^{-1}$ [20]. Many

separations do not require a large migration time window in order to completely separate all of the components of a given mixture. If a large migration time window is not required, OS, OM or OG could possibly provide the best results in terms of throughput, but if a complex sample is to be analyzed, a larger migration time window will probably be beneficial and the use of MEGA-borate is recommended in this case.

Efficiency and Peak Capacity

The separation efficiencies exhibited by the *in situ* charged micellar phases under investigation are listed in Table II in terms of average plate count per meter for the APK homologous series. OG offers the highest plate count averaging over 750,000 plates/m. The lowest plate count was observed with OS which on the average was 450,000 plates/m. According to Terabe *et al.* [21], the dominant intracolumn contributions to band broadening are longitudinal diffusion, sorption-desorption kinetics and electrophoretic homogeneity of the micelles. Since OS-borate micellar phase was the least retentive towards the APKs (see below), the solutes would spend less time associated with the OS micelle than with the other micelles, a condition that would lead to more longitudinal diffusion. This would explain in part the lower separation efficiency obtained with OS. With the other three alkylglycoside-borate micellar phases under consideration, the contributions to band broadening arising from longitudinal molecular diffusion or electrophoretic homogeneity can be considered to be similar. The observed differences in separation efficiencies among OM, OG and MEGA 9 suggest that the contributions to band spreading arising from sorption-desorption kinetics are different from one micellar phase to another. Davis [22] suggested that nonequilibrium band broadening can be reduced by decreasing the micelles mobility. In fact, the OM and OG micelles, having the lowest electrophoretic mobilities, yielded higher separation efficiencies than that exhibited by MEGA 9 which is characterized by a higher electrophoretic mobility. Overall, the *in situ*

charged micellar phases produced higher separation efficiencies than those reported with SDS [3, 21] or alkyltrimethylammonium halide micelles [23]. The conditions under which these measurements were made produced micelles with mobilities significantly lower than those obtained with SDS and alkyltrimethylammonium halide micelles which, among other things, could explain the higher efficiencies obtained with *in situ* charged micelles.

As a result of the high plate counts, the number of peaks that can be resolved in a certain time frame is very high as shown in Table II. The peak capacity, n , is defined as the number of peaks that will fit in a given elution time interval with a resolution of unity. The peak capacity can be calculated experimentally from the values of t_0 , t_{mc} and the average plate count [5]. Both OS and OM demonstrated peak capacities greater than 60, but these separations were achieved in a short time frame, i.e., less than 25 min. The peak capacities for OG approached 100 while that of MEGA 9 was in excess of 160. These peak capacities illustrate the tremendous resolving power of MECC in a short time period.

Retention Energetics

To evaluate the influence of the nature of the surfactant on the retention behavior of the various alkylglycoside-borate micellar phases, a series of alkyl phenyl ketone homologous solutes, ranging from acetophenone to heptanophenone, were electrochromatographed under the above mentioned conditions. In all cases, the six homologous solutes were well resolved, and typical electropherograms obtained with OG- and MEGA 9-borate micellar phases are illustrated in Fig. 2. The last peak is that of anthracene which was used to visualize the migration time window. Table III lists the capacity factors, k' , of the APK homologous solutes with each micellar phase. As expected, the k' values were the smallest for OS. This surfactant has one fewer carbon atom in its alkyl chain than the other three surfactants, see Table I. The k' values observed with MEGA 9 were significantly higher than those obtained with OS. Octylmaltoside showed higher retention than any of the other micellar phases for the first three solutes of

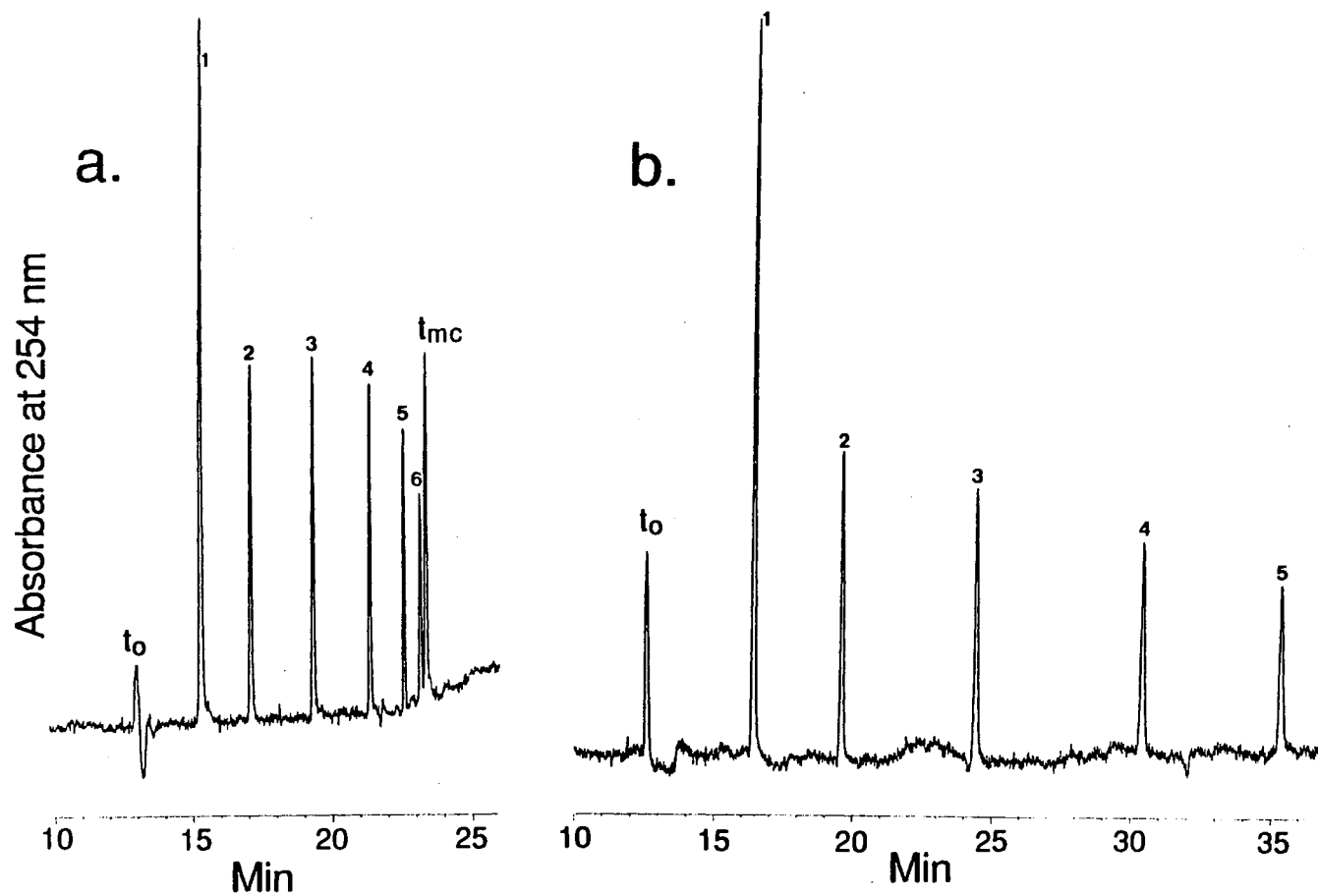


Figure 2. Electropherograms of APK homologous series. Experimental conditions: running electrolytes, 200 mM borate containing 100 mM OG in (a) or 100 mM MEGA 9 in (b), pH 10.0; capillary, untreated fused silica, 56.0 cm (detection point), 64.0 cm (total length) x 50 μ m I.D.; voltage, 15 kV. Analytes: 1, acetophenone; 2, propiophenone; 3, butyrophenone; 4, valerophenone; 5, hexanophenone; 6, heptanophenone; t_{mc} , anthracene.

the homologous series ($n_c = 1$ to 3, where n_c is the number of carbon atoms in the alkyl chain of the solute) while OG was the most retentive for the solutes having $n_c = 4$ to 6.

TABLE III. Comparison of capacity factors obtained with the various micellar phases^{a)}

Micellar Phase	$n_c=1$ k'	$n_c=2$ k'	$n_c=3$ k'	$n_c=4$ k'	$n_c=5$ k'	$n_c=6$ k'
OS	0.37	0.70	1.44	3.17	7.94	15.6
MEGA 9	0.52	1.08	2.37	5.67	14.1	30.4
OM	0.67	1.37	2.90	6.47	14.1	29.7
OG	0.51	1.14	2.69	6.65	16.1	37.2

a) Conditions in as Table II. Analytes: $n_c=1$, acetophenone; $n_c=2$, propiophenone; $n_c=3$, butyophenone; $n_c=4$, valerophenone; $n_c=5$, hexanophenone; $n_c=6$, heptanophenone.

The retention data of Table III were further exploited by plotting logarithmic capacity factor versus n_c for the homologous APKs which yielded a straight line on each micellar phase. This is in agreement with our previous studies [12-14, 23] in which we demonstrated that the relationship between $\log k'$ and n_c follows the expression normally found in reversed-phase chromatography:

$$\log k' = (\log \alpha)n_c + \log \beta$$

where the slope ($\log \alpha$) is a measure of the methylene group selectivity which characterizes nonspecific hydrophobic interactions, while the intercept ($\log \beta$) reflects the specific interactions between the residue of the molecule (i.e., benzaldehyde group) and the aqueous and micellar phase. For an in depth discussion of this data treatment the reader is referred to previous reports from our laboratory [13, 23].

Table IV lists the results of linear regression for plots of $\log k'$ versus n_c for the different micellar phases. The R values obtained with the four plots were either 0.999 or

1.000. The methylene group selectivity for the two surfactants having disaccharide head groups, i.e., OS and OM, are very similar. Both OG and MEGA 9 yielded higher methylene group selectivities, with OG being the highest. On the other hand, there is a significant difference between OS and OM in the magnitude of their specific interactions (i.e., $\log \beta$ values), whereas the specific interactions exhibited by OG and MEGA 9 are

TABLE IV. Correlation between $\log k'$ and n_c of APK homologous series for various micellar phases^{a)}

Micellar Phase	$\log \beta$	$\log \alpha$	R
OS	-0.805	0.333	0.999
OM	-0.517	0.332	1.000
OG	-0.681	0.375	1.000
MEGA 9	-0.673	0.359	0.999

a) Conditions as in Table II.

similar. OS showed the lowest specific interactions (i.e., the highest negative value for $\log \beta$) followed by OG and MEGA 9, while OM exhibited the highest specific interactions (i.e., the lowest negative value for $\log \beta$) with the APK series. These retention behaviors reflect the fact that OM is more retentive towards the smallest solutes in the homologous series (i.e., $n_c = 1$ to 3) where the specific interactions are predominant, and OG exhibits the highest retention toward the solutes with $n_c = 4$ to 6 where the effect of the hydrophobic chain of the solute becomes increasingly more significant.

To gain further insight into the retention behavior of the various micellar phases, the retention energetics of these phases were compared by plotting $\log k'$ of the APK homologous series obtained with a given micellar phase versus the $\log k'$ of the same solutes obtained with a reference micellar phase. Usually, such plots yield straight lines for homologous solutes. If the slope is unity, the differences in Gibbs retention energies of the two micellar phases is zero for all solutes and the retention is termed *homoenergetic*.

In this case, the intercept of the line is equal to the logarithmic of the quotient of the phase ratios of the two micellar phases. The quotient of the phase ratios can be then obtained from the antilog of the intercept. If the slope is not unity, then the Gibbs retention energies are proportional by a constant that is equivalent to the slope, and the retention is termed *homeoenergetic*. We have previously reported this approach in the characterization of numerous micellar systems [12-14, 23]. Figure 3 shows plots of $\log k'$ for micellar phase B versus $\log k'$ of a reference micellar phase A for the APK homologous series. In these plots, OM-borate system was chosen as the reference micellar phase, i.e., micellar phase A. The six data points for each line in Fig. 3 are the $\log k'$ obtained with the six APK solutes. The slopes, intercepts, and antilog of the intercepts of the $\log k' - \log k'$ of these plots are listed in Table V. The R values from the linear regression were all 0.999 or greater. The slope of $\log k' - \log k'$ plot for OS versus OM was close to unity, thus indicating *homoenergetic* retention behavior between the two micellar phases and is consistent with previously reported data [14]. The $\log k' - \log k'$ plots for MEGA 9/OM and OG/OM have slopes near unity indicating quasi-homoenergetic behaviors between these surfactants. The net influence of the nature of the surfactant (i.e., different hydrophilic sugar head groups and hydrocarbonaceous moieties) is realized by examining the quotient of the phase ratios, Φ_B/Φ_A . The phase ratio of the OM micellar phase is double that of the OS micellar phase. The phase ratios of MEGA 9 and OG micellar phases are 77% and 80%, respectively, of that obtained on the OM micellar phase.

TABLE V. Slopes, intercepts and antilog of intercepts of $\log k' - \log k'$ plots for APK homologous series obtained with different micellar phases^{a)}

Micellar phase A/ Micellar phase B	Slope	Intercept	R	Φ_B/Φ_A
OS/OM	1.005	-0.286	0.999	0.52
MEGA 9/OM	1.084	-0.112	1.000	0.77
OG/OM	1.132	-0.095	1.000	0.80
OM/OM	1.000	-0.000	1.000	1.00

^{a)} Conditions as in Table II.

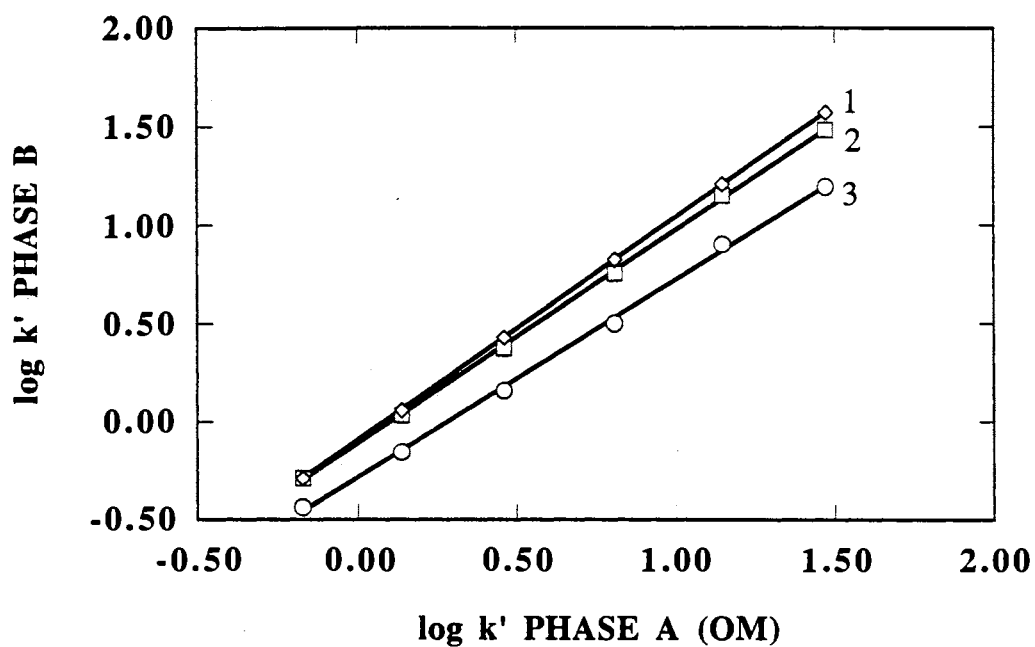
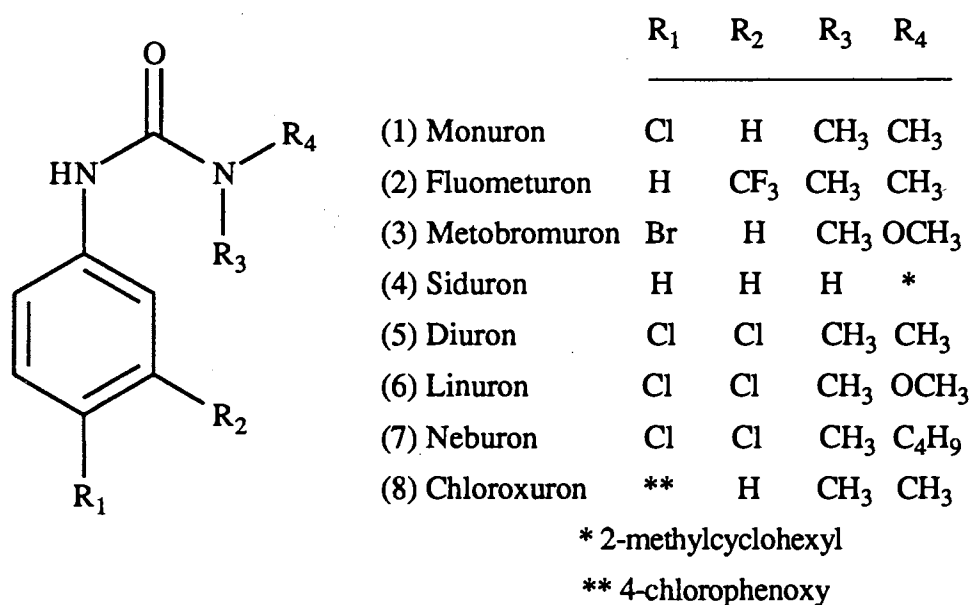


Figure 3. Plots of $\log k' - \log k'$ of APK homologous series obtained on one micellar phase versus another reference micellar phase at constant micellized surfactant concentration. Lines: 1, OG micellar phase versus OM micellar phase; 2, MEGA 9 micellar phase versus OM micellar phase; 3, OS micellar phase versus OM micellar phase. Experimental conditions: running electrolytes, 200 mM borate containing 100 mM surfactant, pH 10.0; other conditions as in Fig. 2.

This method of data treatment has proven to be very useful in the characterization of new micellar phases. The *in situ* micellar phases we have introduced differ significantly in hydrophobic character. These different characteristics are of great value when selecting a micellar system to perform a given separation. The difference in hydrophobic character allow each micelle to have slightly different selectivities as will be discussed in the following section.

Selectivity

Figure 4 illustrates the separation of a mixture of eight closely related urea herbicides obtained on each of the four micellar phases. The structures of the herbicides are listed below.



The average plate counts per meter were 531,000, 589,000, 693,000 and 507,000 for OS, OM, OG and MEGA 9 micellar phases, respectively. The distorted peak shape of neburon obtained with the OS micellar phase (Fig 4a) may be due to the presence of an impurity.

To examine the influence of the nature of the surfactant on the separation of these urea herbicides, the selectivity, $\alpha = k'_2/k'_1$, between adjacent peaks was calculated.

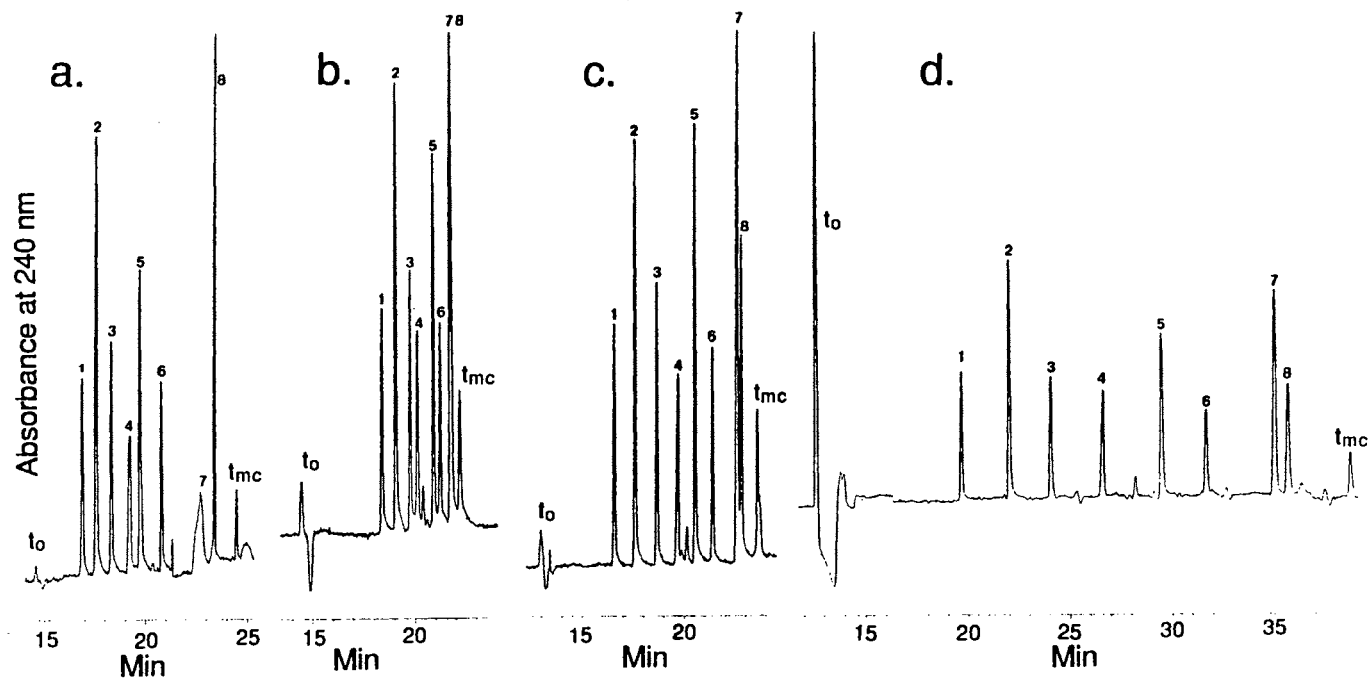


Figure 4. Electropherograms of urea herbicides obtained with each of the various micellar phases. Experimental conditions: running electrolytes, 200 mM borate containing 100 mM OS in (a) or 100 mM OM (b) or 100 mM OG (c) or 100 mM MEGA 9 in (d), pH 10.0. Other conditions as in Fig. 2. Solutes: 1, monuron; 2, fluometuron; 3, metobromuron; 4, siduron; 5, diuron; 6, linuron; 7, neburon; 8, chloroxuron; t_{mc}, anthracene.

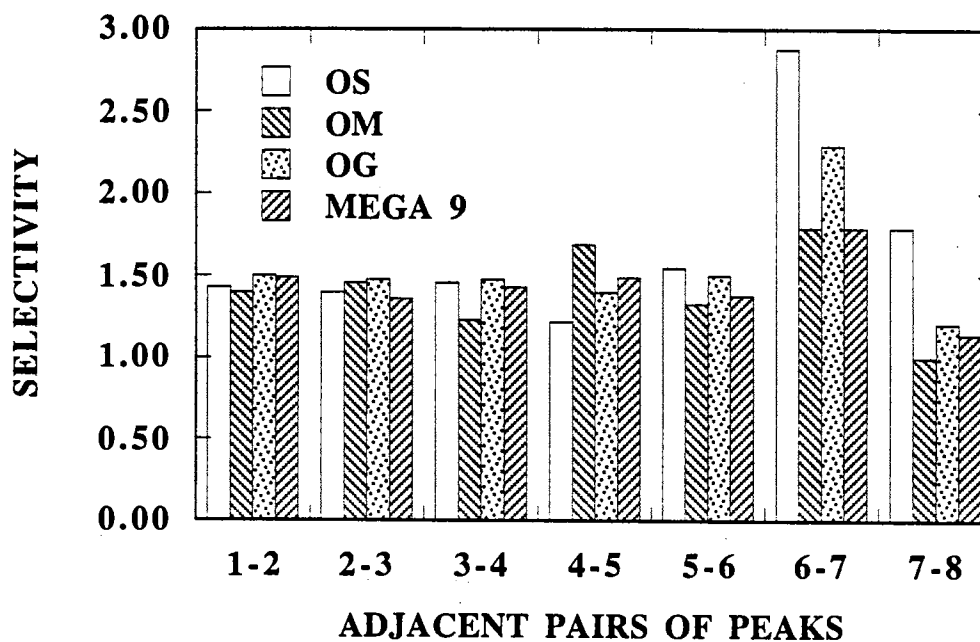


Figure 5. Bar graphs of the selectivity factor for the urea herbicides with each micellar phase. Experimental conditions as in Fig. 4.

Figure 5 shows bar graphs for the selectivity between each adjacent pair of urea herbicides obtained on each of the four micellar phases. The only case an adjacent pair of peaks is not resolved is with the OM micellar phase where the last two herbicides, neburon and chloroxuron, co-elute. This is attributed to the increased hydrophobic character of OM when compared to the other micellar phases. The selectivity of the first five adjacent pairs are very similar, but with the last two adjacent pairs OS provides notably higher selectivity. This is due to the weaker hydrophobic character of OS when compared to the other three surfactants.

To further illustrate the influence of the nature of the surfactant, a mixture of neutral and acidic herbicides were electrochromatographed. This mixture contained three s-triazine herbicides (i.e., prometon, propazine and prometryne), three chlorinated phenoxy acid herbicides (i.e., silvex, 2,4,5-T and 2,4-D), one organophosphorous pesticide (i.e., parathion) and one sulfur-carbamate herbicide (i.e., aldicarb). The structure of these herbicides are shown below.

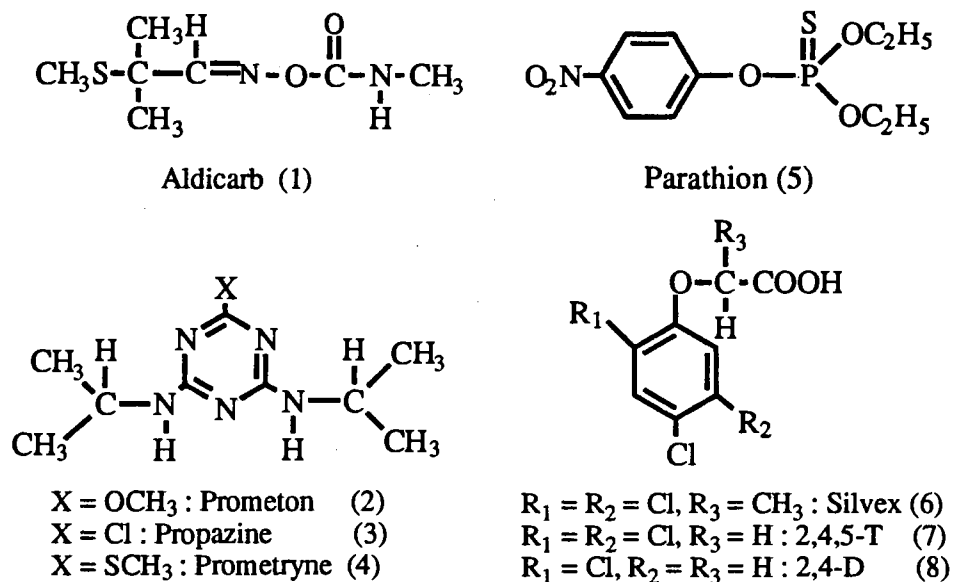


Figure 6 shows typical electropherograms obtained with 200 mM borate and 100 mM of surfactant at pH 10.0. At this pH, the acidic herbicides are fully ionized and are migrating primarily by their own electrophoretic mobility. These acidic herbicides elute after t_{mc} with

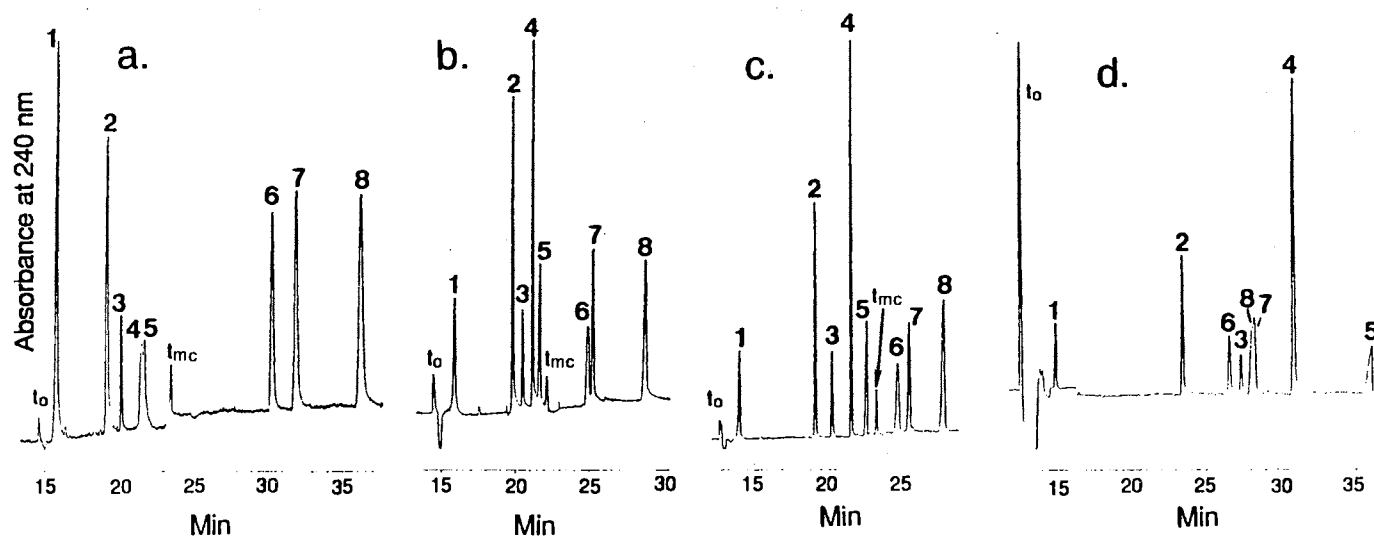


Figure 6. Electropherograms of neutral and acidic herbicides obtained with each of the various micellar phases. Experimental conditions: running electrolytes, 200 mM borate containing 100 mM OS in (a) or 100 mM OM (b) or 100 mM OG (c) or 100 mM MEGA 9 in (d), pH 10.0. Other condition as in Fig. 2. Solutes: 1, aldicarb; 2, prometon; 3, propazine; 4, prometryne; 5, parathion; 6, silvex; 7, 2,4,5-T; 8, 2,4-D, t_{mc} , anthracene.

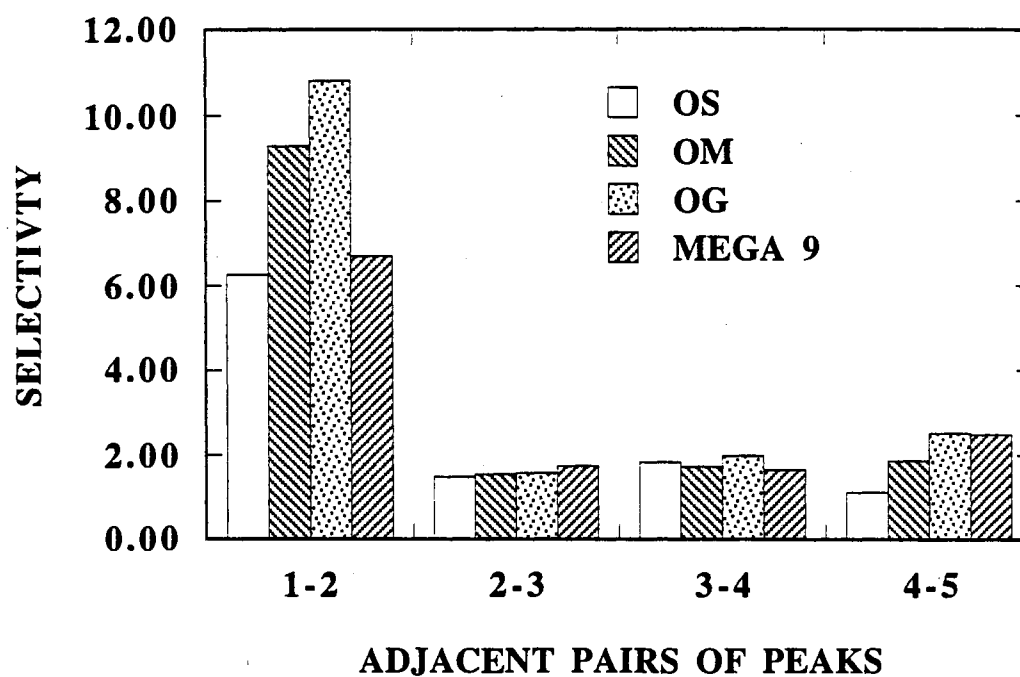


Figure 7. Bar graphs of the selectivity factor for neutral herbicides with each micellar phase. Experimental conditions as in Fig. 6.

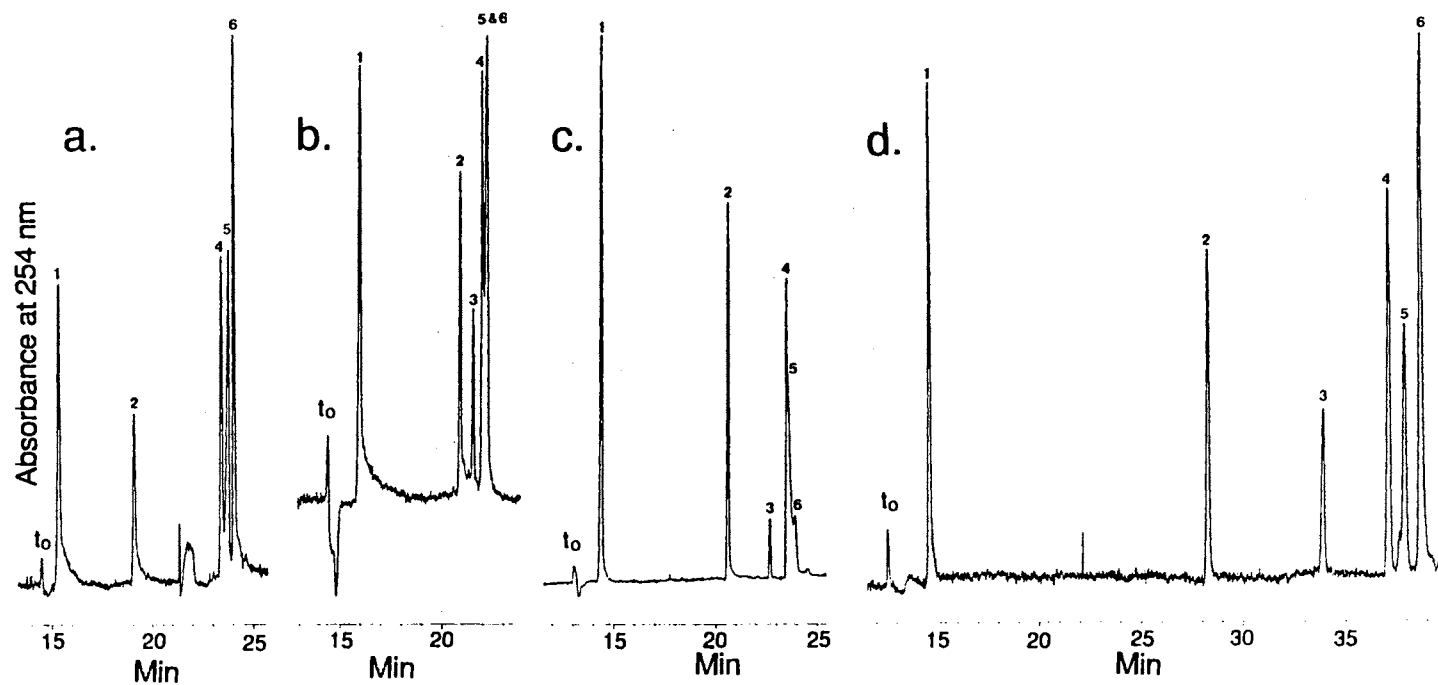


Figure 8. Electropherograms of aromatic species obtained with each of the various micellar phases. Experimental conditions: running electrolytes, 200 mM borate containing 100 mM OS in (a) or 100 mM OM (b) or 100 mM OG (c) or 100 mM MEGA 9 in (d), pH 10.0. Other condition as in Fig. 2. Solutes: 1, aniline; 2, 1-naphthylamine; 3, naphthalene; 4, biphenyl; 5, 1-chloronaphthalene; 6, anthracene.

OS, OM and OG micellar phases, but elute within the migration time window with the MEGA 9 micellar phase. In this aspect, the narrower migration time window is advantageous since the neutral components are removed from the acidic components. The average separation efficiencies were 315,000 plates/m for OS, 459,000 plates/m for OM, 507,000 plates/m for OG and 398,000 plates for MEGA 9. The lower average separation efficiencies arise from the much lower plate counts observed with the acidic species. This is because the acidic herbicides are not significantly partitioned in the micelle, a condition that leads to increased longitudinal diffusion.

Figure 7 shows plots of the selectivities between each adjacent pair of peaks for neutral herbicides (i.e., aldicarb, prometon, propazine, prometryne and parathion) for the various micellar phases. The selectivity for pairs 2-3 and 3-4 are very similar for all the micellar phases. The selectivity of the first adjacent pair, 1-2, is the highest with OM and OG micellar phases, whereas the selectivity for the last adjacent pair, 3-4, is greatest with OG and MEGA 9 micellar phases. For this mixture of herbicides, the OG micellar phase yielded the best separation in terms of resolution and separation efficiency.

As a final illustration of the different selectivities obtained with the different micellar phases, a mixture of hydrophobic aromatic compounds containing one, two or three fused rings were electrochromatographed, see Fig. 8. The OS micellar phase provides better separation than OM or OG micellar phases, but still the most hydrophobic species are only partially resolved. The wider migration time window of the MEGA 9 micellar phase allowed the best separation of the aromatic species, but at the cost of longer analysis time. The average plate counts were 417,000, 443,000, 513,000 and 440,000 plates/m for OS, OM, OG, and MEGA 9 micellar phases, respectively.

Conclusions

In situ charged micellar phases have proven very effective in the separation of both neutral and acidic species. These micellar phases offer an adjustable migration time window that is largely influenced by the nature of the hydrophilic sugar head group of the individual surfactants. The acyclic sugar head group present in the MEGA 9 micellar phase provides the widest migration time window due its increased affinity to borate. Retention energetic studies show that OM micellar phase possess the greatest hydrophobic character followed by OG and MEGA 9 micellar phases. Having one fewer carbon atom in its alkyl tail and possessing a disaccharide head group, the OS micellar phase displayed the least hydrophobic character making it most suitable for MECC of very hydrophobic species. In all cases, separation efficiencies ranged from 300,000 to 750,000 plates/m.

Acknowledgments

This material is based upon work supported by the Cooperative State Research Service, U.S. Department of Agriculture, under Agreement No. 92-34214-7325. JTS is the recipient of a Water Resources Presidential Fellowship from the University Center for Water Research at Oklahoma State University. The loan of the capillary electrophoresis instrument from Hewlett Packard is greatly appreciated.

References

1. B. L. Karger, *Am. Lab.*, October (1993) 23.
2. S. F. Y. Li, *Capillary Electrophoresis: principles, practice, and applications*, Elsevier, Amsterdam, 1992.
3. S. Terabe, K. Otsuka, K. Ichikama, A. Tsuchiya and T. Ando, *Anal. Chem.*, 56 (1984) 111.
4. A. S. Cohen, S. Terabe, J. A. Smith and B. L. Karger, *Anal. Chem.*, 59 (1987) 1021.
5. S. Terabe, K. Otsuka and T. Ando, *Anal. Chem.*, 57 (1985) 834.
6. K. Otsuka, S. Terabe and T. Ando, *J. Chromatogr.*, 332 (1985) 219.
7. D. Burton, M. J. Sepaniak and M. Maskarinec, *J. Chromatogr. Sci.*, 24 (1986) 347.
8. M. M. Bushey and J. W. Jorgenson, *J. Microcol. Sep.*, 1 (1989) 125.
9. S. Terabe, *Trends in Anal. Chem.*, 8 (1989) 129.
10. G. M. Janini and H. J. Issaq, *J. Liq. Chromatogr.*, 15 (1992) 927.
11. J. Cai and Z. El Rassi, *J. Chromatogr.*, 608 (1992) 31.
12. J. T. Smith and Z. El Rassi, *Electrophoresis*, submitted (1994)
13. J. T. Smith, W. Nashabeh and Z. El Rassi, *Anal. Chem.*, in press (1994)
14. J. T. Smith and Z. El Rassi, *J. Microcol. Sep.*, 4 (1994) 127.
15. A. B. Foster and M. Stacey, *J. Chem. Soc.*, (1955) 1778.
16. A. B. Foster, *Adv. Carbohydr. Chem.*, 12 (1957) 81.
17. J. Böeseken, *Adv. Carbohydr. Chem.*, 4 (1949) 189.
18. R. Pizer and C. Tihal, *Inorg. Chem.*, 31 (1992) 3243.
19. M. Makkee, A. P. G. Kieboom and H. van Bekkum, *Recl. Trav. Chim. Pays-Bas*, 104 (1985) 230.

20. T. Kaneta, S. Tanaka, T. Mitsuhiro and H. Yoshida, *J. Chromatogr.*, 609 (1992) 369.
21. S. Terabe, K. Otsuka and T. Ando, *Anal. Chem.*, 61 (1989) 251.
22. J. M. Davis, *Anal. Chem.*, 61 (1989) 2455.
23. D. Crosby and Z. El Rassi, *J. Liq. Chromatogr.*, 16 (1993) 2161.
24. J. Neugebauer, *A Guide to the Properties and Uses of Detergents in Biology and Biochemistry*, Calbiochem-Novabiochem Corp., San Diego, 1994.

VITA

JOEL TIMOTHY SMITH

Candidate for the Degree of

Doctor of Philosophy

**Thesis: DEVELOPMENT OF MICELLAR PHASES AND CAPILLARY COLUMNS
FOR HIGH PERFORMANCE CAPILLARY ELECTROPHORESIS**

Major Field: Chemistry

Biographical:

Personal Data: Born in Norman, Oklahoma, March 12, 1968, the son of Bobby Jack and LaWanda M. Smith.

Education: Graduated from Milburn High School, Milburn, Oklahoma in 1986; received Bachelor of Science Degree in Chemistry from the Southeastern Oklahoma State University, Durant, Oklahoma, in May, 1990; completed requirements for the Doctor of Philosophy degree at Oklahoma State University in July, 1994.

Professional Experience: June 1990 to present, graduate research and teaching assistant, Oklahoma State University.

Professional Organization: American Chemical Society, Phi Lambda Upsilon, American Society of Mass Spectrometry.